New electrochemical methods for the reduction of vat dyes

A dissertation submitted to the
Swiss Federal Institute of Technology (ETH), Zurich
for the degree of Doctor of Technical Sciences

presented by

Albert Roessler
Dipl.-Chem.-Ing. ETH
born on 23. Mai 1975
in Austria

accepted on the recommendation of

Prof. Dr. P. Rys, examiner
Prof. Dr. A. Baiker, co-examiner
Dr. O. Dossenbach, co-examiner

Zurich 2003

Diss ETH No 15120

New electrochemical methods for the reduction of vat dyes

A dissertation submitted to the
Swiss Federal Institute of Technology (ETH), Zurich
for the degree of Doctor of Technical Sciences

presented by

Albert Roessler
Dipl.-Chem.-Ing. ETH
born on 23. Mai 1975
in Austria

accepted on the recommendation of

Prof. Dr. P. Rys, examiner
Prof. Dr. A. Baiker, co-examiner
Dr. O. Dossenbach, co-examiner

Zurich 2003

Dedicated to the memory of my grandfather.

'Die Kunst des Färbens ist eine der nützlichsten und wunderbarsten Künste, die es gibt .... .'

J.A. Chaptal, *'Éléments de Chimie'*, 1789

'There are more things in heaven and earth, Horatio, than are dreamy of in your philosophy.'

W. Shakespeare, *'Hamlet'*, 1st act

Acknowledgments

I am very grateful to Prof. Paul Rys who gave me the possibility to do work on my PhD-thesis in his group. The freedom granted in the realisation of the project and the scientific support are greatly appreciated.

I thank also Prof. Alfons Baiker who kindly accepted to be the co-examiner. I am very much indepted for his help, the discussions and the possibility to use some apparatus in his group.

I want to express my sincere gratitude to Otmar Dossenbach who was my scientific teacher and who contributed significantly to this thesis in many fruitful discussions. I would like to thank him for teaching me how to, and sometimes how not to, do research and teaching! His confidence in my work was very supporting and encouraged me immensely.

Thanks are also due to many contributions from my industrial coaches Jacques and Pierre Bersier and Lars Carlsson (Electrocell AB, Sweden) and Walter Marte (Tex-A-Tec AG, Switzerland). I enjoyed their support and stories as well as the discussions with them. Their 'down-to-earth' contributions were decisive for finding an equilibrium between academia and industry.

I thank Roc Novi, David Crettenand, Evert Wipplinger and Michael Günther for their scientific collaboration during the course 'Praktikum Technische Chemie'. Especially to David I would like to express my gratitude, because his enthusiasm in his diploma thesis tremendously boosted my research.

I would like to acknowledge Prof. Arthur Schweiger, Walter Lämmler, Sabine van Doorslaer (Physical Chemistry, ETH) for the EPR-measurements. Many thanks are extended to Prof. Sotiris E. Pratsinis, Lutz Mädler and Markus Huber (Particle Technology Laboratory, Institute of Process Engineering, ETH) for assistance in measuring particle size distributions. Peter Wägli

X

Summary

In the attempt to increase the eco-efficiency of today's dyeing processes for vat dyes, in this thesis alternative electrochemical techniques for the vatting (= reduction) of such dyes, in particular of indigo, were investigated. The conventional, most used reducing agent, sodium dithionite, cannot be recycled and the disposal of dyeing baths and rinsing water is causing high costs and various problems with the effluent (high salt load, depletion of dissolved oxygen, problems with nasal nuisance, toxicity of sulphide, etc.). Therefore, modern economical and ecological requirements are not fullfilled yet with the conventional vatting techniques still applied today. But electrochemical reducing methods would be a valuable alternative because they do not require any reducing agent. Therefore, they offer tremendous environmental and economical benefits and have a vast potential in textile dyeing processes.

In the first part of this work (*chapters 3, 4, 5*), the application of direct electrochemical reduction of indigo was investigated. Here, the most challenging engineering task is to achieve a dyestuff reduction rate and a current efficiency which are high enough to make this electrochemical reduction industrially feasible. Obviously, the rate-limiting step of the electrochemical reduction is the electron-transfer from the cathode surface to the surface of the dispersed dye pigment by a solid-solid contact. Surprisingly, mechanistic studies by spectrophotometric and voltammetric experiments show a new autocatalytic reaction pathway. The process is based on a reaction mechanism according to which a radical anion is formed in a comproportionation reaction between the insoluble dye pigment and the water-soluble leuco dye and a subsequent electrochemical reduction of the formed water-soluble radical. The leuco dye (= reduced indigo), acting as an electron-shuttle between the electrode and the surface of the dye pigment, has to be generated first in a small amount to ini-

tiate the reduction. However, once the reactions have set in, the further process is self-sustaining. The experiments revealed that the reduction of the indigo radical is a diffusion controlled 1 H^+-1 e^- electrochemical process. If the mass transport to the electrode is enhanced, the radical formation as preceding chemical reaction can limit the electrochemical process. The determination of the industrial feasibility was performed with the aid of a laboratory-scale flow-cell system. However, although optimized conditions in the system were applied, the radical concentration is still low and, consequently, so is the reduction rate. Thus, it must be conceded that until now the reactor performance is too low for an industrial application.

Therefore, in a second part (*chapters 6, 7, 8*), the application of electrocatalytic hydrogenation (ECH) of several vat dyes was investigated by spectrophotometric and voltammetric experiments. This process is based on the electrochemical reduction of water producing adsorbed hydrogen which reacts chemically with indigo at the surface of a metal powder catalyst (*e.g.* Raney nickel). Here, platinum black proved to be the most active noble metal catalyst. The industrial feasibility of the process was studied in a divided flow-cell with indigo as the model compound. In addition, a kinetic model for the electrocatalytic hydrogenation of indigo with simultaneous hydrogen generation was developed and tested (*chapter 9*). In both the presence and the absence of indigo, the hydrogen evolution proceeds *via* a *Volmer-Heyrovský* mechanism.

The third part of this thesis (*chapter 10*) deals with the application of the direct electrochemical reduction of indigo on a fixed bed cathode consisting of graphite granules. This discovery seems to be of future interest both from an economical and ecological point of view for the industrial application of an electrochemical vatting process. The experiments in a laboratory-scale flow-cell system yield information about the kinetics, and they show the potential of this process. A special pre-treatment of the graphite (*e.g.* soaking with hydrogen peroxide, preanodization) can enhance the reduction rate by inducing the formation of redox-active functional groups. Especially the surface modification with quinones is successful and opens a rewarding field for further extended investigations.

Zusammenfassung

Im Bestreben, die Ökoeffizienz der heutigen Färbeprozesse mit Küpenfarbstoffen zu verbessern, wurden in der vorliegenden Arbeit alternative elektrochemische Verfahrenstechniken zur Verküpung (= Reduktion) von Farbstoffen dieses Typs, insbesonders von Indigo, erforscht. Das dabei hauptsächlich zum Einsatz kommende nicht recyclierbare Reduktionsmittel Natriumdithionit ($Na_2S_2O_4$) verursacht eine immense Kostenbelastung und verschiedenste Abwasserprobleme (Salzfracht, grosse Sauerstoffzehrung, Geruchsprobleme, Toxizität von Sulfiden, etc.). Die Entwicklung eines wirtschaftlichen und Chemikalien sparenden Reduktionsverfahrens lässt daher interessante ökonomische und ökologische Vorteile erwarten.

Im ersten Teil der Arbeit (*Kapitel 3, 4* und *5*) wurde die direkte elektrochemische Reduktion von Indigo untersucht. Auf den ersten Blick erwies sich dieses Verküpungsverfahren als nicht erfolgsversprechend, da angenommen werden musste, dass der Elektronentransfer über einen ineffizienten Fest-Fest-Kontakt zwischen dem unlöslichen Indigopigment und der Elektrodenoberfläche stattfinden muss. Mechanistische Studien mittels spektroskopischer und voltametrischer Methoden zeigten jedoch überraschend, dass die direkte elektrochemische Reduktion auch autokatalytisch über die wässrige Phase, d.h. über einen viel effizienteren Fest-Flüssig-Kontakt geführt werden kann. Dazu muss lediglich eine minimale Anfangsmenge an reduziertem Indigo (= Leukoindigo) vorhanden sein. Durch eine Komproportionierungsreaktion zwischen dem wasserlöslichen Leukoindigo und dem unlöslichen Indigopigment bildet sich das ebenfalls wasserlösliche Indigo-Radikalanion, das seinerseits an der Elektrode zum Leukoindigo reduziert wird. Dieser Zyklus findet solange statt, bis das gesamte Indigo reduziert ist. Die elektrochemische Reduktion des Radikalanions stellt

einen diffusionslimitierten $1\,H^+$-$1\,e^-$-Prozess dar. Eine Erhöhung des Stofftransports führt allerdings zu keiner wesentlichen Steigerung der Reaktionsgeschwindigkeit, da dann die Bildung des Radikals zum geschwindigkeitsbestimmenden Schritt im System wird. Trotz verschiedener reaktionstechnischer Massnahmen, wie z.B. Einsatz von Ultraschall, Variation der Temperatur, des pH-Wertes und der Strömungsgeschwindigkeit in der elektrochemischen Zelle, gelang es bisher noch nicht, eine industriell vernünftige Reaktorleistung zu erzielen.

Im zweiten Teil der Arbeit (*Kapitel 6, 7* und *8*) wurde die Verküpung über eine elektrokatalytische Hydrierung untersucht. Dieser Prozess beruht auf der Hydrierung des Indigos an einem Hydrierkatalysator (z.B. *Raney*-Nickel), welcher gleichzeitig als Elektrode zur elektrochemischen Erzeugung adsorbierter Wasserstoffatome aus Wasser wirkt. Platinschwarz hat sich dabei im Falle von Edelmetallen als aktivstes Elektrodenmaterial erwiesen. Es wurden der Mechanismus dieser Elektrokatalyse erforscht und in einer Laborpilotanlage die reaktionstechnischen Grundlagen in Hinsicht auf eine industrielle Verwendung des Verfahrens erarbeitet. Für die elektrokatalytische Hydrierung wurden kinetische Modelle aufgestellt und experimentell validiert (*Kapitel 9*). Dabei konnte gezeigt werden, dass die elektrochemische Entstehung von Wasserstoff aus Wasser nach dem *Volmer-Heyrovský* Mechanismus verläuft.

Der dritte Teil der Arbeit (*Kapitel 10*) befasst sich mit einer Entdeckung, welche den zukünftigen Einsatz einer elektrochemischen Verküpungs-technologie nicht nur ökologisch, sondern auch ökonomisch interessant erscheinen lässt. Es konnte gezeigt werden, dass für eine elektrochemische Reduktion von Indigo nicht notgedrungen eine teure Arbeitselektrode, die metall-beschichtet ist oder aus reinem Metall besteht, benötigt wird, sondern dass auch speziell vorbehandelter Graphit elektrokatalytische Aktivität besitzt. Diese lässt sich durch gezielte Modifikation des Graphits über bewusst erzeugte redox-aktive funktionelle Gruppen steuern.

Table of Contents

XX

Introduction

1.1 General aspects

Wet processing in textile dyeing and finishing can lead to effluents which have been subject to criticism for many decades. 40 years ago the dominant problems were large amounts of foam in river beds and effluent hazards sometimes leading to the extinction of fish populations and of other aquatic organisms. Due to the enforcement of environmental legislation the situation has changed considerably.

Nevertheless, there is a continuing need for improving the eco-efficiency of critical textile wet processes in dyeing and finishing. For example, dyestuffs such as sulphur and vat dyes, especially indigo, play an important role in today's dyeing industry (market about 120 000 t a^{-1}). Although only ten gramms of indigo are necessary for dyeing one pair of trousers, the world production of indigo is close to 14 000 t a^{-1} due to the vast annual sales of a billion blue jeans [1]. The present use of this dye category is based on the application of sodium dithionite to attain a water soluble form of the dye (= leuco dye) by reduction. The reduced dyestuff (*i.e.* the leuco dye) has an affinity to cellulosic fibers, will penetrate the fiber and will remain fixed inside after having been reoxidized back to the water-insoluble form (*Figure 1-1*).

$$(1.1)$$
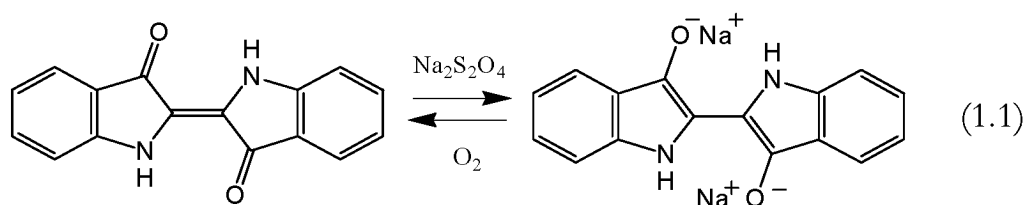
Fig. 1-1:   Vatting of indigo.

The disposal of dyeing baths and rinsing water is causing various problems, because the reducing agents necessary will finally be oxidized into species that can hardly be regenerated. Thus, sulphite, sulphate, thiosulphate and toxic sulphide heavily contaminate waste water from dyeing plants (worldwide approximately 180 000 t a^{-1}). In addition, as a result of the considerable excess of reducing agent required to stabilise the oxidation-sensitive dyeing baths, the waste water may contain excess dithionite which affects aerobic processes in waste water treatment.

Therefore, many attempts are being made to replace the environmentally unfavourable sodium dithionite by ecologically more attractive alternatives. Previous investigations were focused on:

- the conservation of dyes and chemicals by **optimization** of the **reaction** and the **dye fixation conditions** as well as by the use of **ultrasound** to accelerate the vatting procedure and to increase the conversion (*chapter 2.3.1*);
- the replacement of sodium dithionite by **organic reducing agents** (*e.g.* glucose, α-hydroxyketones) of which the oxidation products are biodegradable (*chapter 2.3.6*);
- the **catalytic hydrogenation** to produce pre-reduced vat dyes which can be added to the dye bath (*chapter 2.4.1*).

For ecological and economical reasons, the electrochemical reduction is an attractive alternative to vatting techniques employing chemical reducing agents [2], [3]. *Grotthuss* [4] was the first to discover that the electric current itself is capable to reduce indigo. Here, the most challenging engineering task is to achieve a dyestuff reduction rate and a current efficiency which are high enough to make this electrochemical reduction industrially feasible. Obviously, the rate-limiting step of the electrochemical reduction is the electron-transfer from the cathode surface to the surface of the microcrystal of the dispersed dye pigment. This is especially the case if the electrons have to be transferred directly between the solid surfaces. It is possible to reduce solid indigo microcrystals immobilized on the surface of several electrode materials in aqueous solution, and the results are very similar to those obtained for indigo dissolved

in various solvents [4]-[6]. However, if indigo is not immobilized but present as solid particles in an aqueous suspension, it shows a distinctly different behaviour. *Goppelsroeder* published an extensive series of experiments on the electrochemical reduction of indigo suspended in water [7]-[15]. This work was substantiated by *Wartha* [16], *Mullerus* [17] and *Nevyas* [18]. Unfortunately, it must be conceded from these investigations that it is not industrially feasible to reduce indigo electrochemically under dye bath conditions on a planar electrode. The current efficiency was in all experiments below 20% [19], [20]. Thus, the most limiting factor seems to be the poor contact between indigo particles and the electrode. It is therefore desirable to develop a reduction process by using a different reactor and/or process design based on the intensification of the contact between the dye particles and the electrode.

Chaumat has produced leuco indigo by electrolysis with a specially prepared cathode of finely divided indigo and graphite powder, in a solution of sodium carbonate [21], [22].

Recently the so-called precoat-layer-cell has been presented as a possible solution (*chapter 2.4.3*). In this technique the dyestuff particles are pressed through a filter consisting of an electrically conductive material (*e.g.* filter fabrics) with a cathodically polarized layer of *e.g. Raney* nickel formed on the filter *in situ* by precoat filtration. The severe drawback of this technique seems to be the large pressure drop built up during the filtration process and the persistent danger of blocking the reactor.

As a further alternative to improve the eco-efficiency of the vatting process an indirect electrochemical reduction process was developed to enhance the rate of the electron-transfer (*chapter 2.4.2*). This process employs a soluble redox mediator (complexes of iron with triethanolamine or gluconic acid). However, the mediator is expensive, and with triethanolamine as the complexing agent, toxicologically not entirely harmless. Furthermore, the specific reactor performance is low.

In view of the drawbacks of the latest electrochemical alternatives presented for the reduction of vat dyes, novel and eco-efficient alternatives for the application of vat dyes are still needed.

1.2 Aim and scope of this thesis

The aim of the work described in this thesis was to find and evaluate new biocompatible electrochemical alternatives for the reduction of vat dyes as part of the overall aim of developing a feasible full-scale industrial process. Three novel methods will be described:

- the **direct electrochemical reduction of the dye radical**, a process based on the formation of a radical anion in a comproportionation reaction between the dye and the leuco dye and the subsequent electrochemical reduction of this radical (*chapters 3 - 5*).
- the **electrocatalytic hydrogenation of vat dyes**, involving the *in situ* electrochemical reduction of water to produce adsorbed hydrogen which chemically reacts with the dye on the electrode surface (*e.g. Raney* nickel) (*chapters 6 - 9*).
- the **direct electrochemical reduction of the dye on graphite**, a process based on the quinoid structures at the surface of graphite (*chapter 10*).

This thesis presents results and conclusions from electrochemical experiments employing small-scale H-cells as well as laboratory-scale flow cells. The objective was a better understanding of the cathode reactions and their dependence on various significant parameters. The further aim was also to explore and discuss the technical implications of the knowledge gained from these investigations.

Chapter **2**

The chemistry and application of vat dyes

2.1 The general nature of vat dyes

In the coloration of cellulosic fibres vat dyes (including indigo) hold a large part of the dyestuff market (*Figure 2-1*) [28]. About 33 000 tons of vat dyes (including indigo) are being used annually since 1992 [23]. The situation will remain constant in the next years mainly because vat dyes yield coloured fibres with excellent colour fastness, particularly to light, washing and chlorine bleaching [23], [28]. The application of reactive dyes as the actual alternative has not yet reached the level of anthraquinone vat dyes invented a century ago [24]. Thus, at present, there is no true alternative to this class of dyes [23]-[27].
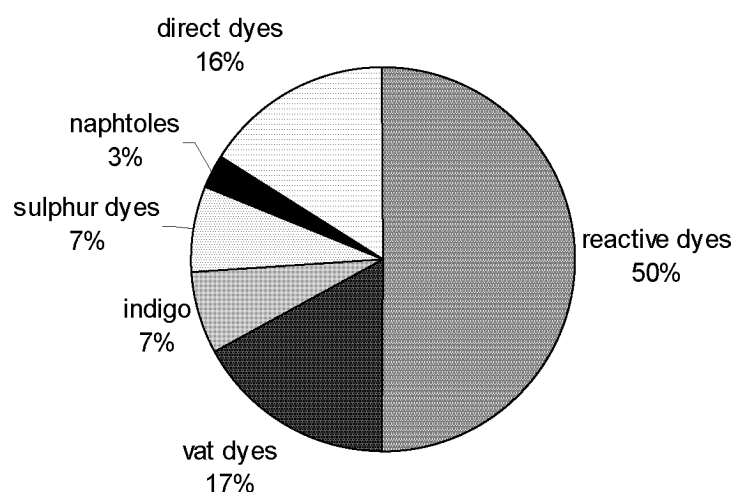
Fig. 2-1: Consumption of dyes for cellulosic fibres (in % on the base of the market value in 10^6 DM) [28].

Nevertheless, both vat and sulphur dyes require a somewhat complicated application procedure. Vat dyes are practically insoluble in water, but can be transformed by reduction (vatting) into a compound (leuco form) soluble in

aqueous alkali and can be applied in this form. Air oxidation will re-form the original dye on the fiber [27], [29]-[30] (*Figure 2-2*).

$$O= \overset{\overset{\displaystyle R^1}{|}}{C} \left[\overset{}{\underset{\underset{\displaystyle R^2}{|}}{C}} = \overset{\overset{\displaystyle R^3}{|}}{C} \right]_n \underset{\underset{\displaystyle R^4}{|}}{C} =O \quad \underset{-2\ e^-}{\overset{+\ 2\ e^-}{\rightleftharpoons}} \quad {}^-O- \overset{\overset{\displaystyle R^1}{|}}{C} \left[\overset{}{\underset{\underset{\displaystyle R^2}{|}}{C}} - \overset{\overset{\displaystyle R^3}{|}}{C} \right]_n \underset{\underset{\displaystyle R^4}{|}}{C} -O^- \qquad (2.1)$$
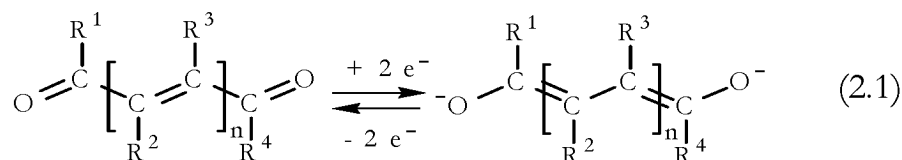
Fig. 2-2:   The redox equilibrium for vat dyes.

As a characteristic structure fragment vat dyes contain a chain of conjugated double bonds with two keto groups at the end position. As diols (vat acids) the leuco derivatives are very sparingly soluble in water, but, since the hydroxyl groups are of enolic character, they are acidic (pK_a = 9-11) and dissociate in alkaline media to form soluble enolates.

The mechanism of the reduction of vat dyes has been studied in detail over a long period of time [29]-[34]. Today, still some papers are published, especially presentig various novel kinetic models (*e.g.* shrinking core) [35], [36].

The dyeability of a fibre by a vat dye depends upon the fibre ability to adsorb the dye. Because vat dyes are not bound to the fibers but are rather trapped between the polymer chains that make up the fibre, the dye molecules must be able to enter the space between the polymer chains. Because of the open structure of cellulose, vat dyes are well adsorbed by cellulosic fibres such as cotton. In contrast to cotton, synthetic fibers have a packed structure with their polymer chains aligned tightly side by side. Thus, with a value of 1.78 g cm^{-3} polyester has a much higher density than cotton (with 1.05 g cm^{-3}) [37]. Therefore, vat dyes are traditionally used to dye cellulosic fibres and are hardly employed for synthetic fibres.

Typical structures of vat dyes are shown in *Figure 2-3*. The majority of vat dyes in use today are derivatives of anthraquinone, like Vat Blue 4 (**2**). A considerable number of vat dyes have a polycyclic structure with fused aromatic rings containing carbonyl functions (*Figure 2-3*, compound **4**). However, no account of vat dye chemistry would be complete without mentioning the indigoid dyes. *Figure 2-3* shows the structure of both anthraquinone (**3**) and indigo (**1**).

1   2

3   4
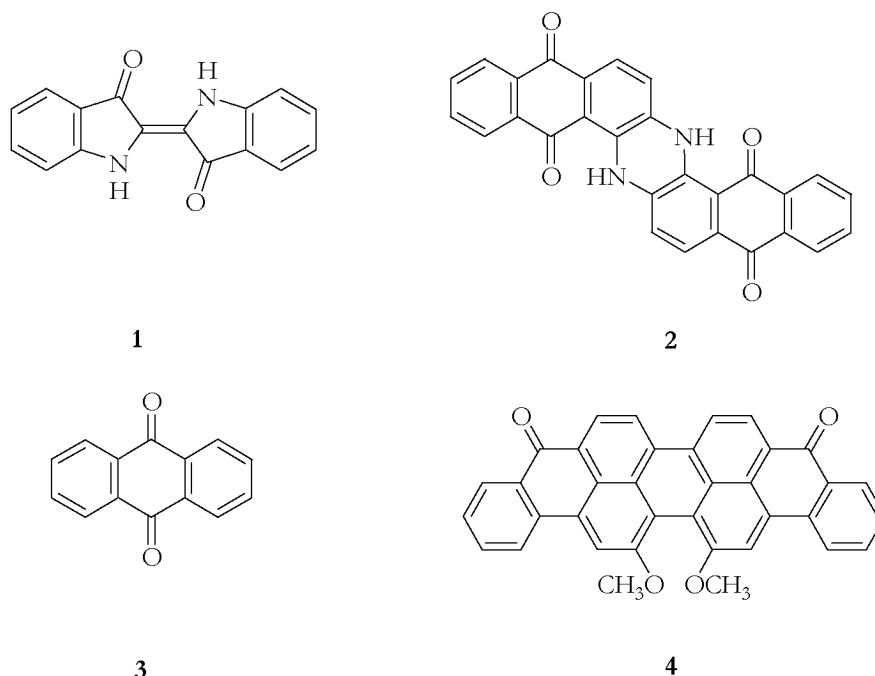
Fig. 2-3:   Typical structures of vat dyes.

In some ways, despite its long history and current importance, it is almost unfortunate that indigo must be classified as a vat dye, because the present application methods for indigo and the fastness properties of indigo dyeings are not typical of vat dyes as a whole. Since the discovery of *indanthrone* (now C.I. Vat Blue 4 (**2**)) by *René Bohn* in 1901, many vat dyes with no natural occurrence have been synthesized. *Bohn* actually obtained the first known anthraquinone vat dye, of which there are now approximately 200 in commercial use providing from yellow to black dyes. Dyeings of the products which have survived in the marketplace normally show outstanding colour fastness properties, particularly to light, washing and chlorine bleaching, while indigo dyeings have poor resistance to most of these and poor abrasive resistance as well [25].

However, the present importance of indigo, should teach a salutary lesson in marketing. Satisfying the needs of the customer is generally more important than achieving the highest levels of technical performance in dyed and finished goods, although the two sometimes coincide. Since the early 1970s, customers have wanted indigo blue denim[1] primarily for the appearance which can result

from the inferior fastness properties of the dyeings. This is exploited by garment dyers and finishers in stonewashing[2] and other wet processes [30], [38].

2.2 Indigo

2.2.1 History

The earliest evidence of the use of colour comes from cave paintings of Cro-Magnon man, which were painted between 10 000 and 30 000 BC. It is striking to note that blue (and consequently green) was not used in these paintings [39], [40]. However, long before the advent of systematic physical sciences and the growth of the chemical industry, as long as 5 000 years ago in India, dyeing methods were being used for the application of the water insoluble pigment, indigo, to natural fibers. In the early nineteenth century, between the first cotton gin and the Civil War, the value of natural indigo produced in South Carolina (USA) exceeded that of rice or cotton.

For textile dyeing with natural dyes, indigo has an almost unique position as the most important blue natural dye. Woad (*Isatis tinctoria L.*) and Dyer's Knotweed (*Polygonum tinctorium Ait.*) were cultivated in Europe for the production of indigo up to the 17th century. After this time indigo from the indigo plant (*Indigofera tinctoria L.*) was used because of the superior quality of the dyestuff. Indigo was recovered from the water-soluble glucoside of indoxyl (indican) present in the plants (*Figure 2-4*), and then the insoluble blue product was dissolved in wooden vats by a natural fermentation process later known as *vatting*. This was the origin of the name *vat* dyes [40], [44].

---

[1] Denim is an English corruption of the French phrase '*serge de Nime*', meaning a serge fabric from the town of Nimes in France. The term serge means a twill-weave fabric with a characteristic diagonal wale [41]-[43].

[2] Process in which pumice stones are added to the wash cycle to abrade denim and loosen color. Most jeans today are stonewashed, although they are not necessarily washed in actual stones as they were when this technique first became popular. Now, in addition to pumice stones, enzymes, sand, ceramic balls, and other solutions have been invented to give jeans that abraded, worn look [282], [283].
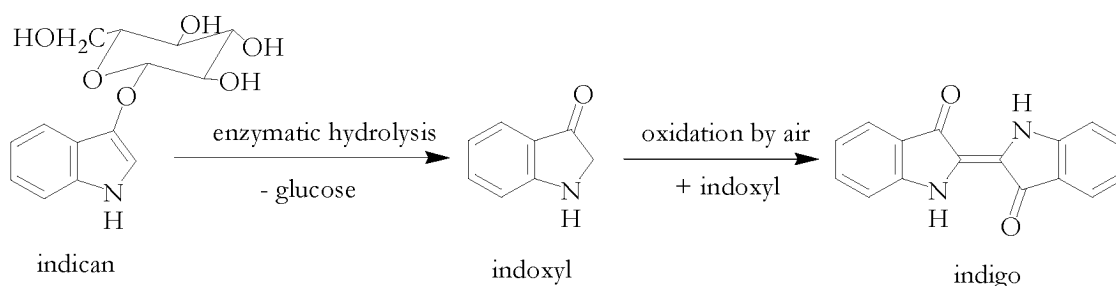
Fig. 2-4:   Indigo production from plants.

Under the right conditions, the known animal and vegetable (cellulosic) fibres accepted the greenish-yellow material dissolved in the vat, and on subsequent exposure of the dyed fibres to the oxygen in the air, the color was converted back to that of the original indigo pigment. Restoration of the indigo is an oxidation. Both oxidation and reduction will be discussed in detail later (*chapter 2.3*).

Since the massive growth of the production of indigoid denim, beginning in the 1970s, indigo is one of the most important single dyes in use today. At the end of the 19th century the synthetic indigo almost completely displaced natural indigo.

Another natural vat dye, a brominated derivative of indigo, was derived from the shellfish *Murex brandaris* found in small quantities at the eastern end of the Mediterranean. It was known as Tyrian Purple and was once important for its rarity and its hue. The Roman emperors practically monopolized it, which gave rise to the term 'royal purple' [25], [44].

2.2.2 Production

After the elucidation of its structure by *Adolf von Bayer* in 1883 [45], experiments culminated in 1897 in the commercialization and large-scale production of synthetic indigo by BASF, Germany. In the first BASF method, anthranilic acid, made from phthalic acid and phthalimide, was condensed with chloroacetic acid and alkali to give a salt of N-phenylglycine-o-carboxylic acid. This intermediate was then converted to indoxyl. Originally, the commercial method was devised at Zurich Polytechnic (which became later the ETH) by *Karl Heumann*

[40], [46]-[52]. This occurred during 1890 and to some extent it was inevitable, because there had also been a long tradition of dye making and innovations both in Zurich and Basle. Today, modifications of *Heumann's* original routes are still in use. After the observation by *Pfleger* in 1901 that the addition of sodium amide resulted in a high yield of indigo, this process was introduced at an industrial scale. The *Heumann-Pfleger* process provides indigo of adequate purity in yields up to 90%.
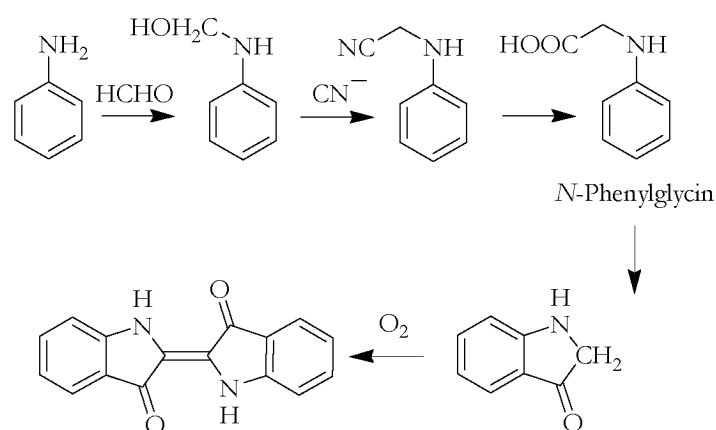
Fig. 2-5:   Indigo synthesis according to *Heumann-Pfleger*.

As the awareness of the need to preserve our natural resources is increasing, more and more researchers are becoming interested in finding renewable resources which can be used as alternatives. However, with the historical disappearance of indigo farming (especially in Europe) there is a considerable lack in knowledge about the simple production of natural indigo from plant material, even more if the ecological standards applied at present are considered. Recent work to evaluate whether it is possible to use plants as commercially viable sources of dyes has highlighted a significant resource, from which both industrial production and the consumer's choice could benefit. However, because of the multiplicity of products available, the expectation of the customers is very high. This means that in order to satisfy this demand for high quality and choice, the plants in question must be studied more closely to allow breeding of useful lines and to improve economic returns. Although it is unlikely that all dyestuffs will be produced solely from plants, it is an interesting and exciting prospect that one day a percentage of everyday colours could be produced naturally [53]-[58].

Due to the importance of indigo, considerable research has been done to replace the chemical synthesis also by applying biotechnological methods. Fermentation processes have been developed for the production of indigo from glucose using *e.g.* recombinant *Escherichia coli*. 'Biotech' indigo starts with tryptophane, which bacteria produce naturally. Tryptophane is ideal for the conversion to indigo because it already contains the ring-structure in the core of the indigo molecule. A few chemical alterations convert tryptophane into the dye. The bacteria was implanted an enzyme from another microbe that converts tryptophane into the ring-containing precursor indoxyl. Indoxyl spontaneously turns into indigo when exposed to air. The basis of this process derives from the pioneering work of *Gibson et al.* [59], [60], who showed that the naphthalene dioxygenase (NDO) of *Pseudomonas* could convert indole (the final intermediate in the tryptophane biosynthesis) to indoxyl. The commercial and environmental justification for developing such a process was reviewed by *Frost et al.* [61], [62]. However, a trace by-product renders jeans an unfashionable shade of red. *Weyler et al.* [63], [64] tweaked the genes of the bacterium *Escherichia coli* to eliminate the red pigment. The final colour is indistinguishable from the globally popular deep blue of the chemically made dye. Although this process was very appealing, recently an improvement has been achieved by a new enzyme (2-hydroxybiphenyl-3-monooxygenase), which can be employed in both types of biotechnological indigo production: the fermentation and the biotransformation [65].

In addition, a variety of several other processes not commented on in this work has been described in literature [66]-[69].

2.2.3 Physical and chemical properties

At ambient temperature and under normal pressure indigo [482-80-3], indigotin, 2-(1,3,-dihydro-3-oxo-2*H*-indol-2-ylidene)-1,2-dihydro-3*H*-indol-3-one, $C_{16}H_{10}N_2O_2$, M_r 262.27, C.I. Vat Blue 1, C.I. 7300 exists as dark blue-violet needles or leaves with a reddish bronze metallic appearance. It sublimes above 170°C (mp. 390-392 °C). Indigo is practically insoluble in water, aqueous acid, aqueous base and non-polar solvents, but slightly soluble in polar high-boiling solvents, (*e.g.* aniline, nitrobenzene, phenol, DMSO). The colour of

indigo is unusually intense, compared to conjugated molecules of similar size [70], and is influenced strongly by solvents. Despite the possibility of *cis-trans* isomerism about the central C=C double bond, only the *trans* isomer, stabilized by intra- and intermolecular hydrogen bonding, is observed [71]. This fact also explains the extremely low solubility, the high melting point and the vibrational and electronic absorption spectra of indigo. Bond orders and charge densities of the indigo chromophores have been investigated and calculated [72], and the X-ray crystal structure has been determined [73].

Indigo is very resistant to light and elevated temperatures, even in the presence of air. Reducing agents (*e.g.* sodium dithionite, hydroxyacetone, zinc or hydrogen) convert indigo to the leuco compound 'indigo white', which dissolves in sodium hydroxide solution to form the disodium salt. The action of oxidizing agents leads to dehydroindigo; oxidation with permanganate cleaves the molecule at the central double bond forming isatin. Substitution by electrophiles or nucleophiles is difficult; only sulphonation in concentrated sulfuric acid and halogenation in nitrobenzene are successful.

Concentrated alkali at elevated temperature leads to the decomposition of indigo with the formation of aniline, *N*-methylaniline and anthranilic acid.

In biological systems, indigo is extremely stable. For example, in the sludge of a waste water treatment plant, indigo is not degraded but simply adsorbed, probably as a result of its low solubility. This fact accounts for the low acute and chronic toxicity of indigo.

2.2.4 Toxicology

Despite the long use of indigo, only a few toxicological data were known until quite recently. Since 1962, however, the toxicological properties of indigo have been examined increasingly [74].

The low acute oral toxicity ($LD_{50} > 5\ 000$ mg/kg) has been confirmed in mammals. Subchronic and chronic feeding experiments with rats and dogs showed no serious negative effects other than the colouring of the organism. Similarly, no negative effects were found in rats in reproduction studies or in teratogenic investigations. Pure indigo is also negative in the *Ames* test.

2.2.5 Economic aspects

In view of steadily growing sales, the production capacities of larger producers (BASF, Buffalo Color, ICI, and Mitsui Toatsu) have been increasing during the past ten years. The annual capacity of indigo is estimated to 14 000 tons. With a market price of $ 6 - 10 per kilogramm indigo, this represents a significant share of the overall turnover in the textile industry [1]. U.S. manufacturers made 419 million pairs of denim jeans during 1997, with a value (at the consumer level) of about six billion dollars [75].

2.3 Reducing agents – state of the art

2.3.1 Sodium dithionite

a) General

To be useful in practice, solutions of reducing agents for vat dyes must have a level of reducing power (reduction potential) sufficient to reduce all commercial vat dyes to their water-soluble forms, economically and quickly, without converting the dyes to products from which the original pigments cannot be restored (over-reduction). The potential is usually in the range of approximately -600 to -1 000 mV $vs.$ NHE[3] [76]-[78].

In vat dyeing, the reducing agent of choice is sodium hydrosulphite, commonly known as 'hydro', but more correctly known as sodium dithionite, with the chemical formula $Na_2S_2O_4$. There is no reducing agent available today which can replace hydrosulphite in all areas of application. The dominant position of sodium dithionite is due to the particularly favourable relationship between its properties and its cost.

---

[3] -600 mV $vs.$ Ag/AgCl, 3 M KCl is sufficient for indigo

$$S_2O_4^{2-} + 4\,OH^- + \underset{R^2 \;\; R^4}{\overset{R^1 \;\; R^3}{O=C\!\!\left[C=C\right]_{n}\!\!C=O}} \longrightarrow \underset{R^2 \;\; R^4}{\overset{R^1 \;\; R^3}{{}^-O-C\!\!\left[C-C\right]_{n}\!\!C-O^-}} + 2\,SO_3^{2-} + 2\,H_2O$$
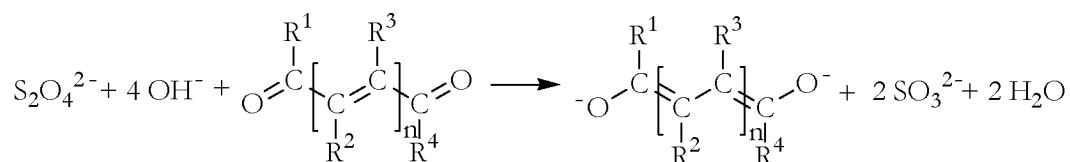
Fig. 2-6:   General scheme of the vatting process with sodium dithionite.

However, the disposal of dyeing baths and rinsing water is causing various problems, because the necessary amount of reducing agent will finally turn into sulphite, SO_3^{2-}, a species that can hardly be regenerated. In addition, the reduction process is accompanied by various undesirable side-reactions. Unfortunately, the oxygen in the air reacts with sodium dithionite to give sodium sulphite and sodium sulphate, Na_2SO_3 and Na_2SO_4 respectively. Moreover, thiosulphate, $Na_2S_2O_3$, is formed by the reaction of dithionite with sodium hydroxide [34]. In addition, the production of sulphide by sulphate-reducing bacteria is a well known phenomenon [79].

$$2\,Na_2S_2O_4 + 2\,NaOH \longrightarrow 2\,Na_2S_2O_3 + 2\,Na_2SO_3 + H_2O \qquad (2.3)$$

$$Na_2S_2O_4 + O_2 + 2\,NaOH \longrightarrow Na_2SO_3 + Na_2SO_4 + H_2O \qquad (2.4)$$
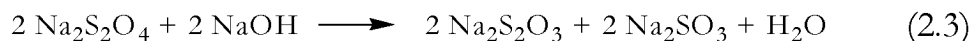
Fig. 2-7:   Undesired side-reactions of the vatting process with sodium dithionite.

Thus, sulphite, sulphate, thiosulphate and toxic sulphide heavily contaminate waste water from dyeing plants (worldwide approximately 180 000 t a^{-1}). An excessively high sulphate concentration in the effluent can cause damage to unprotected concrete pipes. In addition, as a result of the considerable excess of reducing agent required to stabilize the oxidation-sensitive dyeing baths, the waste water may contain excess dithionite which affects aerobic processes in the waste water treatment.

In the 60s and the early 70s, many attempts were made to reduce the hydrosulphite consumption by using additives in the dye liquor [80]-[84]. Unfortunately, the results were not satisfactory.

For various reasons, *e.g.* the increasingly severe environmental legislation and effluent problems, efforts are now being made to restrict the use of hydrosulphite and to find a better alternative.

b) State of the art technology, latest developments

Opportunities exist for conservation of dyes and chemicals through optimization of the concentrations of chemicals currently used and by improvements in dye fixation. Such efforts can result in significant money savings for the manufacturers, with an associated reduction of effluent load.

Recent developments in the field of indigo dyeing indicate that the consumption of sodium dithionite can be reduced to an almost stoichiometrical minimum of 1.1 (1.1 mol of dithionite used for 1 mol of indigo) [85], [86]. Since the degradation products of the excess dithionite can be acidic, and have to be neutralized by alkali, the hydroxide in the vatting mixture is also consumed during the process. Consequently enough hydroxide must be present initially to make certain that the bath remains strongly alkaline and reasonably stable during any desired dyeing process. The high basicity required for the vatting process is an important factor limiting the application of conventional vat dyes to the alkali-insensitive cellulosic fibres, although in special cases it is possible to dye other fibres with vat dyes as well.

It became clear now that the consumption of caustic soda in the vatting process is reduced compellingly with the reduction of the necessary amount of sodium dithionite. At the same time, due to the reduced salt load in the vatting mixture the dyestuff concentration in the stock solution can be increased considerably, up to 130 g l^{-1}. Thus, the process and the apparatus have the great advantage that a high colour yield is achieved and less environmental pollution is produced. However, a further reduction of the salt concentration which would increase the concentration of dissolved leuco indigo can be effected only with the electrochemical vatting technique or by hydrogenation.

A better dye fixation can be achieved by an almost absolutely oxygen free dye bath, a high concentration of the dye, a small amount of liquor (*e.g.* 200 l) and only a minimum number of dips of the yarn. In addition, a special fixation zone is used in front of the oxidation to enhance the dye uptake by 10-15% [85], [86]. Optimal concentrations and reaction conditions in the vatting reactor can be achieved on one hand by controlling the concentrations of the dye, the reducing agents and the caustic soda by appropriate modern analytical methods [82], [87]-[92]. On the other hand it could be demonstrated that

100% vatting can be accomplished in a few minutes in a completely oxygen free atmosphere in the vatting reactor and with the use of ultrasound [85], [86], [93]. Ultrasound enhances the vatting rate by disintegrating the dispersed water-insoluble dyestuff aggregates into smaller particles. Owing to the increase of the dyestuff surface, in addition to the simultaneous shortening of the diffusion path, the probability for collisions between molecules of the reducing agent and the indigo molecules increases and finally the reaction rate will be faster [35], [93], [94]. An apparatus for carrying out the process described above comprises a mixing vessel and at least one reactor with ultrasonic resonators. The dyeing solution is subsequently drawn off (*Figure 2-8*).
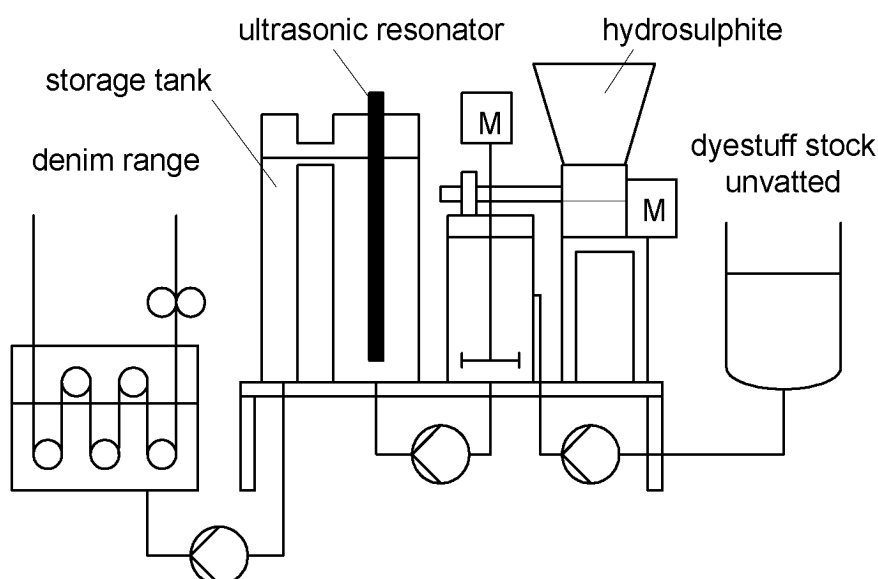
Fig. 2-8:   Dye stock preparation for the denim technology (vatting reactor VR3, Tex-A-Tec AG, Wattwil/Switzerland [85], [277]).

2.3.2 Hydroxyalkyl sulphinate (Rongalit)

Other reducing systems have been recommended for some years. However, it is only for special purposes (pad-steam processes and bath dyeings above 100°C) that combinations with hydroxyalkyl sulphinates − which are more stable to atmospheric oxygen − are employed. For textile printing, hydroxymethane sulphinate (Rongalit C) $HOCH_2-SO_2Na$ and a product based on hydroxyethane sulphinate (*e.g.* Rongalit 2PH) are preferred [95].

Unfortunately, the redox potential of the sulphinates depends strongly on the temperature which causes more or less the same problems of applications as the dithionite. A comparison between several reducing agents applied to textile printing has been published recently [96].

2.3.3 Thiourea

Another reducing agent receiving considerable attention is thiourea dioxide (THDO), formamidinesulphinic acid [27], [29], [95], [97].
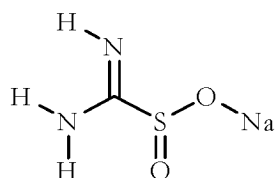
Fig. 2-9:   Thiourea or sodium formamidinesulphinate.

Its reducing effect is stronger than for dithionite and, therefore, problems due to over-reduction of vat dyes are frequent. In a normal pad-steam dyeing system or an exhaust dyeing process, this leads to completely unacceptable results, even at 50°C. In this case, the usual inhibitors, as *e.g.* sodium nitrite, have no effect [27], [29], [95]. Opinions differ with regard to the stability of the product to atmospheric oxygen in alkaline liquors. However, BASF investigations showed that formamidinesulphinate is apparently even more readily oxidized than dithionite. For this reason, the claimed ratio of one part thiourea dioxide to ten parts hydrosulphite is much exaggerated [30]. Depending on the dyeing procedure, the ratio one to two or one to three would seem to be much more realistic, but at current prices for thiourea dioxide it then appears less attractive. However, its relatively low sulphur content and the lower equivalent weight than that of hydrosulphite lead to better values for sulphite and sulphate in the effluent.

2.3.4 Two-component system

To a very limited extent, a two-component system consisting of a high alkaline solution containing 5% sodium borohydride and a powdered initiator of sodium formaldehyde sulfoxylate with 5% $Na_2[Ni(CN)_4]$ is now also being used. Here environmental concern relates to nickel and cyanide discharges from the dyeing mill [95], [97]-[100].

2.3.5 Iron(II)-salts

Iron(II) salts have been widely used since ancient times to reduce vat dyes by a technique known as 'copperas method' in which $FeSO_4$ and $Ca(OH)_2$ are used [101]-[104]. But the dye bath produced in this way results in bulky sediments due to the poor solubility of $Fe(OH)_2$. It has been found that $Fe(OH)_2$, produced *via* the reaction of iron (II) salts with NaOH, can be complexed (*e.g.* by gluconic acid) and brought into solution with the aid of gluconic acid to achieve the desired value for the reduction potential (Rongal TX5160). Successive elimination of gluconic acid takes place in the sewage tank by neutralization with a small amount of alkali. The free $Fe(OH)_2$ is then converted by areation to $Fe(OH)_3$, which acts as a flocculent. Hence, the basic problem associated with the use of sodium dithionite can be eliminated.

2.3.6 Organic reducing agents

It has been found that sodium dithionite can successfully be replaced by organic compounds such as hydroxyacetone (Rongal 5242), acetoin, glutaroin or adipoin [35], [85], [93], [105]-[107]. This class of α-hydroxyketones meets the requirements in terms of reductive efficiency and biodegradability. However, some substances are expensive and the use of hydroxyacetone is restricted to closed systems because it forms strong-smelling condensation products in alkaline solution.

The vatting process with α-hydroxyketones has proved to be extremely intricate. Hydratisation, keto-enol and acid-base pre- and side-equilibria determine the redox properties of these organic reducing agents and their corre-

sponding oxidation products. It is obvious that these equilibria also influence the effective concentration of the active reducing species and with it the rates of the redox steps and thus the reductive efficiency.

The exact knowledge of all the possible pre- and side-equilibria and of the rates at which they are established is not sufficient for a comprehensive understanding of the vatting process. Its complexity becomes evident, if one reflects on some experimental facts such as the observation that the reduction process is autocatalytic and exhibits an oscillatory reaction behaviour.
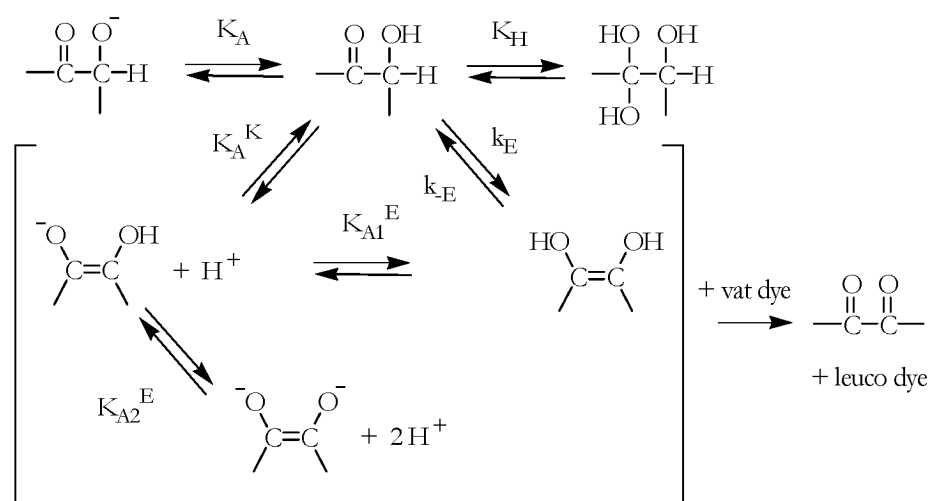
Fig. 2-10:   The ability of α-hydroxyketones to reduce vat dyes [35].

With the use of ultrasound the vatting rate can be increased by a factor of approximately four to five (*chapter 2.3.1*), [85], [93].

The role of reducing sugars for the reduction of vat dyes has also been studied [108], [101].

2.4 Other options for the reduction of vat dyes

2.4.1 Catalytic hydrogenation – pre-reduced dye

The catalytic hydrogenation of vat dyes has been suggested a long time ago by *Brochet* [109]. Although there are some problems with several vat dyes (*e.g.* overreduction, slow reduction rate), the preparation of the leuco indigo solutions by catalytic hydrogenation of indigo can be effected in a generally known manner. In particular by reducing an alkaline indigo paste (customarily from 10 to 35% by weight of indigo, from 2 to 10% by weight of sodium hydroxide) using *Raney* nickel as catalyst at a hydrogen pressure between generally 2 to 4 bar and at a temperature between generally 60° to 90°C.

However, it is impossible to use this technique on-site in the dye house due to the high explosion and fire risk. Thus, pre-reduced indigo is produced as commercial product in the indigo plant and shipped as 40% aqueous solutions. It can be used directly in the dye bath, which has only to be stabilized by reducing agents [110]. Therefore, this very young product has the advantage that in the dyeing process a considerable proportion of the chemical reducing agent, dithionite, can be dispensed with. Unfortunately, the eco-efficiency of this process is negatively affected by the high water content of the product (60%). However, transport costs are definitive influenced by the volume of the product and due to the low bulk density of indigo powder, the transport volume based on unit mass of indigo for pre-reduced aqueous solution is approximately the same as in case of indigo powder. Therefore, this product has the potential to conquer the denim market and lately a lot of companies are changing to this concept. Though, the dye houses get completely reliant on the dye supplier, because at present only DyStar is offering this technology [110].

2.4.2 Indirect electrochemical reduction (mediator technique)

Despite numerous attempts to optimize the use of reducing agents, the main disadvantage remains that it has as yet not been possible to regenerate these conventional agents. For ecological reasons, the electrochemical reduction is a most attractive alternative to vatting techniques employing chemical

reducing agents. The rate-limiting step of the electrochemical reduction is the electron-transfer from the cathode surface to the surface of the microcrystal of the dispersed dye pigment. This is especially the case if the electrons have to be transferred directly between the solid surfaces. Therefore, an indirect electro-chemical reduction process employing a soluble redox mediator was developed to enhance the rate of the electron-transfer [123]-[151].

This process is mediated by an electron-carrier, where the reduction is taking place between the separated surfaces of the electrode and of the dye pigment instead of a direct contact between both surfaces (*Figure 2-11*) [122].
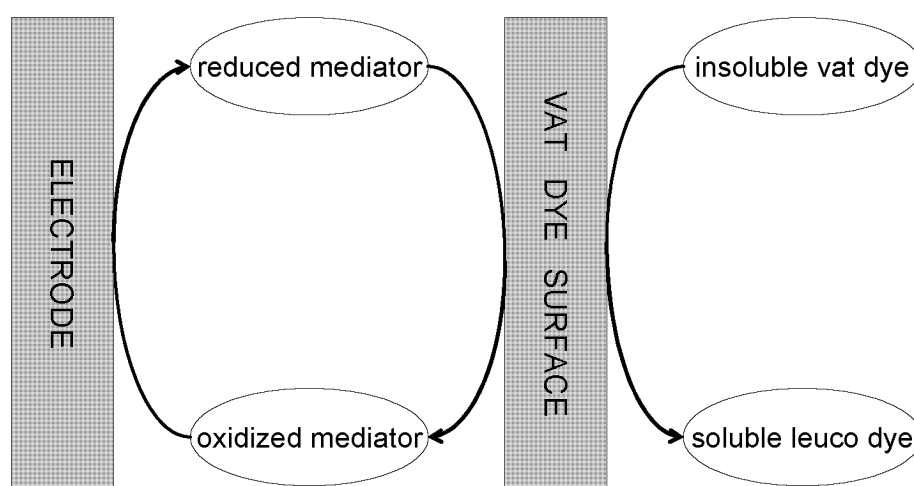
Fig. 2-11:   The mediator-enhanced electrochemical vatting process.

The mediators employed in this process are regenerable iron complexes with triethanolamine or gluconic acid as ligands (*Figure 2-12*). In a recent attempt complex mixtures of triethanolamine and D-gluconate have been investigated. They are of particular interest for the mediator process because it is possible to combine the advantages of both ligands [148], [149]. These mediators, however, are expensive and not entirely harmless from a toxicological point of view [152].

5   6
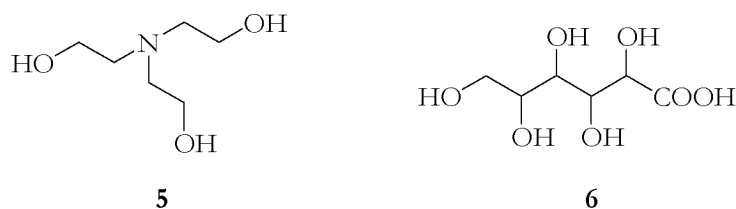
Fig. 2-12:   Complexing agents used for the formation of the mediator: triethanolamine (**5**) and gluconic acid (**6**).

A great advantage of this technique is the direct information about the state of reduction in the dye bath which is available by redox potential measurement and a control by adjustment of the cell current is possible. The reducing agents normally used cannot be monitored in a comparable manner [125]. Thus, often a distinct surplus of reducing agents has to be applied to guarantee stable dye bath conditions. An important property of the iron(II)-amine complex is the high rate of dye reduction, which is much faster than that with sodium dithionite [125]. However, as described in many publications, the cathodic reduction is running with low current density, because the electrochemical reduction of the complex is the rate-determining step and an increase of the concentrations of the electrochemically active iron-complexes is limited [123]-[126]. Therefore, to achieve a large cathode area with sufficient cell current, a novel electrochemical cell (especially a cathode construction) has been described [127]. In order to meet all requirements in an economical way, a multi-cathode cell with a large number of cathodes, electrically connected with one or two anodes, has been suggested [128]. This configuration allows the operation of the cell with a maximum cathode area and a minimum anode area [129], [130]. The process was tested successfully for continuous dyeing of cotton yarn on a full scale indigo dyeing range using a 1000 A multicathode electrolyzer [130]. However, still the huge electrode surface of 500 m^2 is necessary to attain a feasible reduction rate at an industrial scale. Thus, it is impossible to use this technique for the complete reduction of a stock solution in case of continuous dyeing, because the operating costs and the return on investment (ROI) are not attractive enough for an application in the denim-industry [28]. The indirect electrochemical reduction can only be used in discontinuous exhaust dyeing processes[4] and to stabilize the dye bath in continuous dyeing by diminishing the amount of leuco indigo oxidized during the dyeing process by contact with oxygen in the air passages and at the surface of the dye bath [110].

In addition, after the reduction and prior to the dyeing process the mediator has to be separated from the soluble leuco dye by ultrafiltration and the concentration of the mediator in the filtrate is increased by nanofiltration. This

---

[4] Exhaust dyeing is generally meaning the use of a dye bath of moderately large liquor to goods ratio, in which the fiber is immersed for some time, allowing the dye molecules to leave the bath and attach to the fibers. Exhaust dyeing is the typical process for most commercial fabric dyeing.

offers the possibility to restore the reducing power and to recycle water, the mediator (with losses of 15% [125]) as well as, textile auxiliaries. However, the filtration considerably increases the costs for this vatting process and induces several technical problems (*Figure 2-13*) [131], [132].

Therefore, this mediator-technique remains under development even after many years and at present production tests are performed only in one pilot plant coupled with a yarn-dyeing[5] machine (X-cones[6]) [133], [134].

dyestuff

```
                              dyestuff
                                 |
                                 v
   +--------------+        +----------------+
   |              | -----> |  electrochem.  |
   |   dye bath   |        |     cell       |
   |              | <----- |                |
   +--------------+        +----------------+
         |          dye bath circulation
         |                         ^
         v      dye bath           |   filtrate
   +--------------+ regeneration   |   mediator
   |  oxidation   |----------------+
   |  filtration  |
   +--------------+
    |
    v
 removed oxidized dyestuff, fibres, dust
```
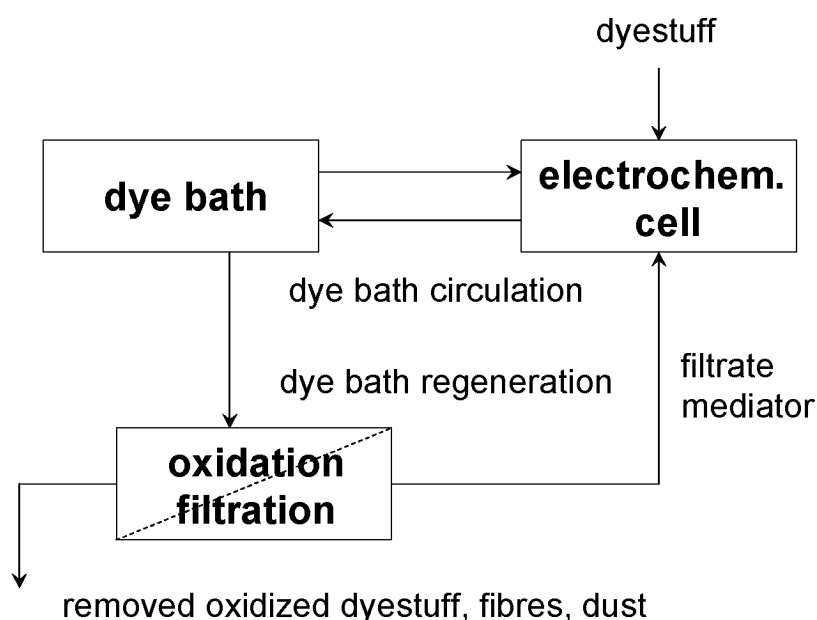
Fig. 2-13:   Flow scheme for the application of the indirect electrochemical reduction of vat dyes in package dyeing [124].

2.4.3 Direct electrochemical reduction in the precoat-layer-cell

The direct electrochemical reduction of indigo would be an elegant way, because it minimizes the consumption of chemicals. Unfortunately, it is impossible to reduce indigo present in an aqueous suspension on a planar electrode. However, it is possible to reduce solid indigo microcrystals immobilized on the surface of several electrode materials in buffered solution and the results are

---

[5] 'Yarn Dyeing' means that the yarn is dyed before it is woven into fabric. Yarn is a generic term for a continuous strand of textile fiber, filaments or material suitable for knotting, weaving, tufting, or otherwise intertwining to form a textile fabric.

[6] A 'cone' is a conical package of yarn, usually wound on a disposable core.

very similar to those obtained for indigo dissolved in solvents [5], [6]. The most limiting factor seems to be the poor contact between the indigo particles and the electrode. Therefore, it is desirable to develop a reduction process by using a different reactor design based on the intensification of the contact between the dye particles and the electrode. For this purpose the so-called pre-coat-layer-cell has been developed [153], [154]. The reactor is based on the filtration principle, *i.e.* by bringing the indigo into contact with a cathode, where the cathode is formed by a support of an electrically conductive material (*e.g.* filter fabrics) and a cathodically polarized layer (*e.g.* Raney nickel) formed on the filter *in situ* by precoat filtration (*Figure 2-14*). The severe drawback of this technique seems to be the big pressure drop built up during the filtration process and the persistent danger of blocking the reactor. In addition, the reactor performance is low. Thus, research and development has been abandoned [278].
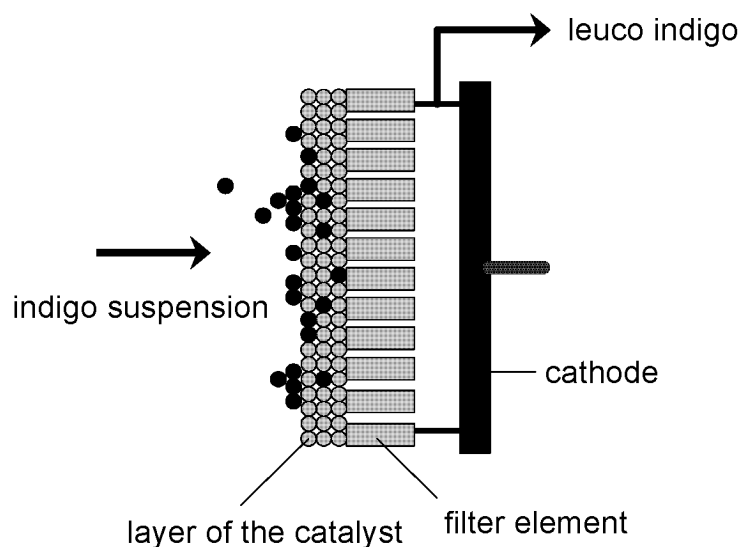
Fig. 2-14:   Concept of the precoat-layer-cell [153], [154].

2.4.4 Stabilization or regeneration of dithionite by electrolysis

It is obvious that another alternative could be based on the application of electrochemical techniques to the non-regenerable reducing agents. *Daruwalla* investigated the electrolysis of the dye bath [111]-[115]. He assumed that dithionite ions $S_2O_4^{2-}$ can be transformed to sulfoxylate ions SO_2^{2-} on an iron cathode. Thus, a very powerful reducing species with a redox potential higher

than that of dithionite itself is generated. This should reduce the dithionite consumption by 30%. However, until now no commercial realisation of the proposed process is known. Nevertheless, an electrochemical regeneration of the reducing agent from SO_3^{2-} and SO_4^{2-} would be an environmentally friendly way to solve the problems in the application of vat dyes. Electrolysis of a suspension of indigo in a warm solution of sodium bisulfite, $NaHSO_3$ has been successful [116]-[118]. In addition, several papers have been published about the electrochemical regeneration of dithionite [117]-[121]. Olin Corp. has recently brought electrosynthesis of dithionite to commercial scale. Unfortunately, the process is not feasible under normal dye bath conditions [120]-[121]. As a consequence, during the last few years investigations have been focusing on the electrochemical reduction of vat dyes.

2.5 Analysis of the eco-efficiency

The impact of textiles on both the environment and the consumers' health and sense of wellbeing is important. The public and the authorities pay increasing attention to this fact, and additional regulations and new labels are developed accordingly. Optimization is very often no longer sufficient to meet these requirements. New products, new procedures and new techniques are necessary [3], [156].

The eco-efficiency analysis has been used by BASF, Germany, as an instrument to identify the technology that will be the most promising manufacturing process for blue jeans in ecological and economical terms in the future [157]-[159].

Four alternative production methods, the extraction of indigo from the indigo plant, the chemical synthesis resulting in indigo granules (*chapter 2.2.2*), the biotechnological production process (*chapter 2.2.2*) and the synthesis variant likewise developed by BASF yielding a 40% aqueous solution of pre-reduced indigo (*chapter 2.4.1*), have been analysed. The latter, still very young product, has the advantage that in the dyeing process a considerable proportion of the chemical reducing agent, dithionite, can be dispensed with. The dyeing pro-

cesses examined were, on the one hand, the process most commonly used today (*chapter 2.3.1*), in which the indigo is converted to its water-soluble and hence colour-active form by addition of dithionite (*chapter 2.3.1*). On the other hand, an electrochemical process still under development was investigated, in which the electric current assumes the role of the dithionite (mediator-technique, *chapter 2.4.2*).

On the eco-efficiency portfolio the process exhibiting the highest eco-efficiency is that in which the 40% indigo solution and the electrochemical dyeing process were applied.
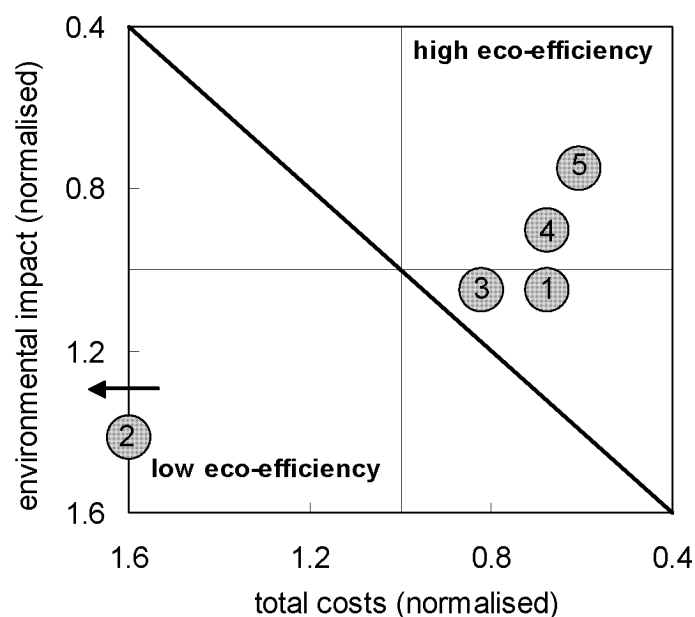
Fig. 2-15:   Analysis of the eco-efficiency of the denim manufacturing process (by BASF/ DyStar) [158]. BASF indigo (synthetic) (1); Indigo powder from plants (2); Biotechnologically produced indigo (3); BASF indigo vat solution 40% (dyed traditionally) (4); BASF indigo vat solution 40% (dyed electrochemically) (5).

Electrochemical reduction of indigo *via* the indigo radical
Part I: Preliminary experiments and mechanistic investigations

3.1 General aspects

The observation of a reddish or violet shade in the indigo dye bath or even in the coloured product is a well known phenomenon at very unsufficient controlled dye baths. This phenomenon is probably based on the formation of the known indigo radical, yielding a cherry-red solution [158]-[160].

The reaction could be due to the oxidation of leuco dye with the oxygen present in the system. However, in addition, it is well known that electron transfer can occur between a dianion and its original vat dye:

$$A^{2-} + A \longrightarrow A^{\bullet -} \qquad (3.1)$$

Russell et al. have described such reactions in literature also with indigo and its derivatives [161]-[163]. The indigo radical was generated when the molar ratio of reducing agent to indigo was smaller than stoichiometric. Therefore, it seems possible that the vat dye radical species are formed as long as both leuco dye and the dye molecules are present in the system.

Usually radicals are electrochemically active species. Previous studies on the electrochemistry of indigo dissolved in DMSO, DMF or pyridine revealed, that indigo can be reduced reversibly to its leuco form in two one-electron processes with the radical as an intermediate species [5]. In addition, the investigation of redox reactions with its soluble derivative indigo-carmine in aqueous solution led to comparable results [164], [165].

Therefore, the above-mentioned observations and results initiated a novel route for the reduction of indigo. The invention relates to a method for the direct electrochemical reduction of vat and sulphur dyes in aqueous solutions which does neither require a soluble reducing agent nor the permanent presence of a redox mediator [166]. The process is based on a reaction mechanism according to which a radical anion is formed in a comproportionation reaction between the dye and the leuco dye and a subsequent electrochemical reduction of this radical. In order to start the process, an initial amount of the leuco dye has to be generated by a conventional reaction, *e.g.* by adding a small amount of a soluble reducing agent. However, once the reactions have set in, it is not needed anymore and the further process is self-sustaining. *Figure 3-1* illustrates schematically the mechanism of the direct reduction under steady conditions.
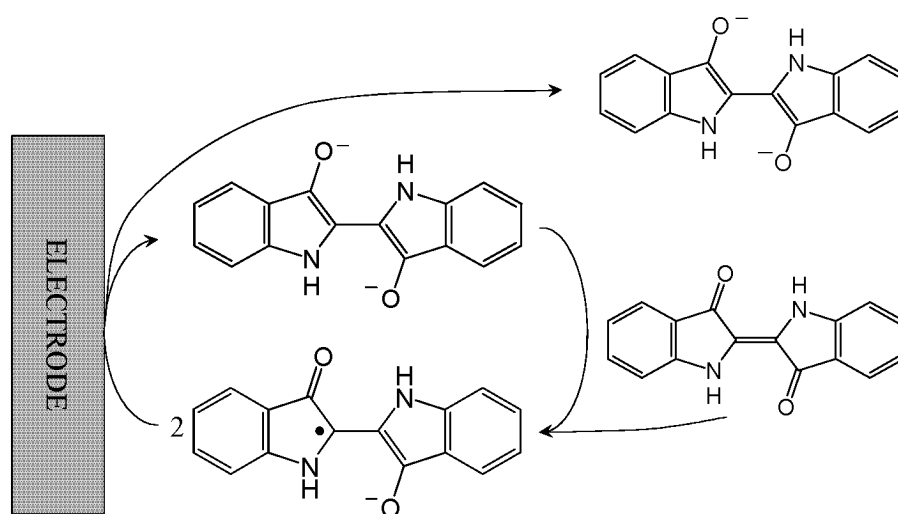
Fig. 3-1: Reaction mechanism of the direct electrochemical reduction of indigo *via* the indigo radical.

The goal of the present study is to get more insight into the mechanism of the electrochemical reduction of the radical and to show results from preliminary electrolysis experiments in small laboratory cells. These results provide basic information for the further development of the electrochemical process.

3.2 Experimental

3.2.1 Chemicals

All aqueous solutions were prepared with deionized water. Indigo and Set-amol WS was supplied from BASF, Ludwigshafen, Germany. Sodium hydroxide (Fluka, 71695, p.a.), sodium dithionite (Fluka, 71700, pract. 85%), sodium chloride (Fluka, 71379, p.a.) and argon 4.8 were used for the experiments.

3.2.2 Apparatus

A conventional two-compartment glass H-cell (each with a volume of 200 ml), separated by a Nafion-324 membrane (DuPont) was used both for the voltammetry and the small-scale preparative electrolysis. For online spectrophotometric measurement two glassfiber sensors were connected to a diode-array spectrophotometer (GMP, Jobin Yvon) and installed with tightness fittings. A potentiostat (Amel 549) was used both for galvanostatic and potentiostatic electrolysis experiments. Cell potential, cathode potential and current were measured with multimeters (Metex M 3610). In case of the voltammetric studies a computer controlled potentiostat (Radiometer Copenhagen DEA 332) was used together with the Radiometer rotating disc electrode model CTV101/EDI101. Cells were connected to a thermostat (Colora Messtechnik GmbH). A sieve-machine (AS 200, Fa. Retsch) with several sieves was used to obtain well defined fractions of indigo particles.

3.2.3 Electrodes

A three-electrode configuration consisting of different working electrodes, a reference electrode (Ag/AgCl, 3 M KCl, Metrohm) and a counter electrode (Pt/Ru) was used throughout the experiments. Polarisation curves were measured with small electrodes (16 cm^2) made of different materials like Ti, Ni, Cu, stainless steel (V2A) and Pb. A nickel rotating disc electrode (0.196 cm^2) in a Teflon housing was applied for voltammetric experiments. The electrode surface was carefully polished with fine abrasive paper, washed in destilled water

and in ethyl alcohol. For electrolysis experiments a 3D-electrode made of Ni-grid (100 mesh, G. Bopp + Co. AG) was used with an electrode surface between 100 - 400 cm^2.

3.2.4 Procedure

Cathodic solutions were composed of 10^{-4} M (0.0262 g l^{-1}) indigo (sieve fraction between 0.06 - 0.08 mm) suspended in 1 M NaOH. They were deoxygenated during at 2 h before the experiment and maintained under an argon atmosphere during the measurements. Various amounts of dithionite in aqueous solution (prepared after degassing the water for 2 h) were added by an injection needle through a septum to reduce the indigo. In all experiments the ratio of dithionite to indigo was smaller than stoichiometric in order to generate the red coloured radical solution. Anodic solutions consisted of 1 M NaOH. All reduction experiments were performed at 50°C. In case of different pH-values, the difference in ionic strength compared to 1 M NaOH (pH = 14) was compensated by adding NaCl.

3.3 Results and Discussion

3.3.1 Preliminary observations

VIS-spectra of indigo dispersions in aqueous solutions show a small absorption at about 700 nm corresponding to indigo particles in the system. After adding a reducing agent (*e.g.* dithionite) a peak is observed at 410 nm, which can be correlated to leuco indigo, the reduced form of the indigo pigment. If the molar ratio of dithionite to indigo is smaller than stoichiometric, additional peaks can be found at 540 and 495 nm. It is assumed that these peaks are due to the well known indigo radical [158]-[160], a species formed in a comproportionation reaction between leuco indigo and indigo and leading to a cherry-red coloured solution.

An EPR-spectrum, together with simulation, clearly showed that the structure of the radical species is in fact identical to the one assumed (*Figure 3-2* and *Table 3-1*) [158]-[160], [167].
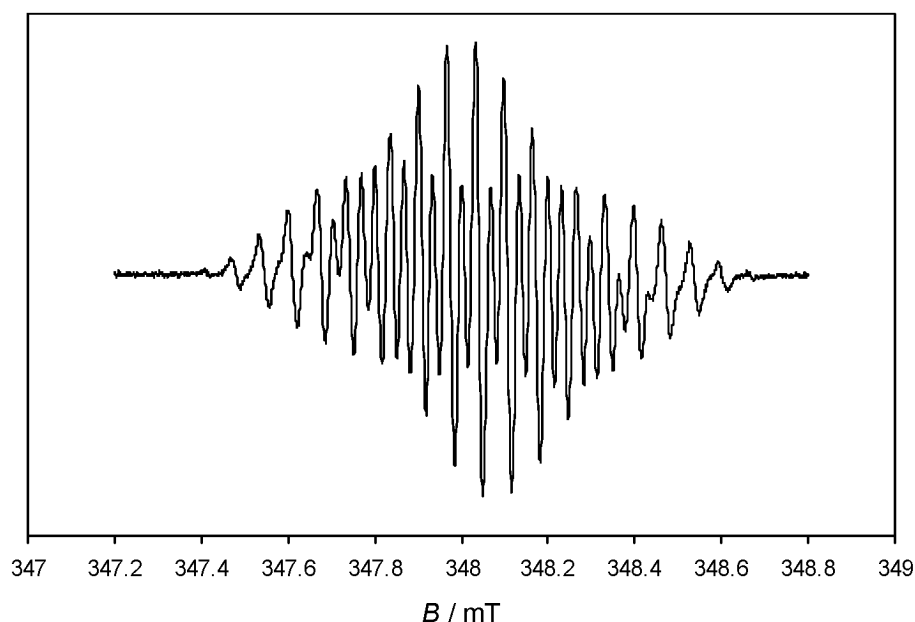
Fig. 3-2: X-band CW-EPR spectrum of the red coloured indigo radical at room temperature in 1 M NaOH, generated by sodium dithionite. The spectrum was recorded at room temperature on a Bruker ESP 300 spectrometer (microwave frequence 9.76 GHz) with the use of a flat cell. A microwave power of 2 mW, a modulation amplitude of 0.01 mT and a modulation frequency of 100 kHz was applied.

Table 3-1: Coupling constants measured by EPR-spectroscopy

related atoms	coupling / G
5,5' ^{1}H	0.66
7,7' ^{1}H	0.66
6,6' ^{1}H	1.98
4,4' ^{1}H	1.67
1,1' ^{14}N	0.66
1,1' ^{1}H	0.66

3.3.2 Voltammetric characterisation

Polarisation curves, obtained at Ni-electrodes, show that the radical can be easily reduced and that the reduction product – leuco indigo – is stable under these conditions (*Figure 3-3*). At potentials more negative than -1100 mV the current density increases due to the cathodic liberation of hydrogen. Starting at -900 mV (*vs.* Ag/AgCl, 3 M KCl) it appears that leuco indigo is also reduced to another substance, but this increase in current could be correlated to the cathodic wave of sodium dithionite at -1030 mV [168], [111]. In addition, after the vast majority of experiments a 100% mass balance of indigo was obtained by reoxidation and filtration of the electrolyte. However, in some experiments with a very high electrode surface (FIBREX Nickel Fiber Mat, National Standard Woven Product Div., 70% Fiber, 30% Powder) the total of the material balance amounted to only 70% due to the loss of material by adsorption on the electrode.

Copper turned out to be the most suitable of the materials tested so far in terms of the reaction rate. Titanium and iron give lower current densities and are therefore not useful materials for this process. Lead shows good catalytic properties for the radical reduction, but it is dissolved during the electrolysis, thus producing high background currents compared to other metals.
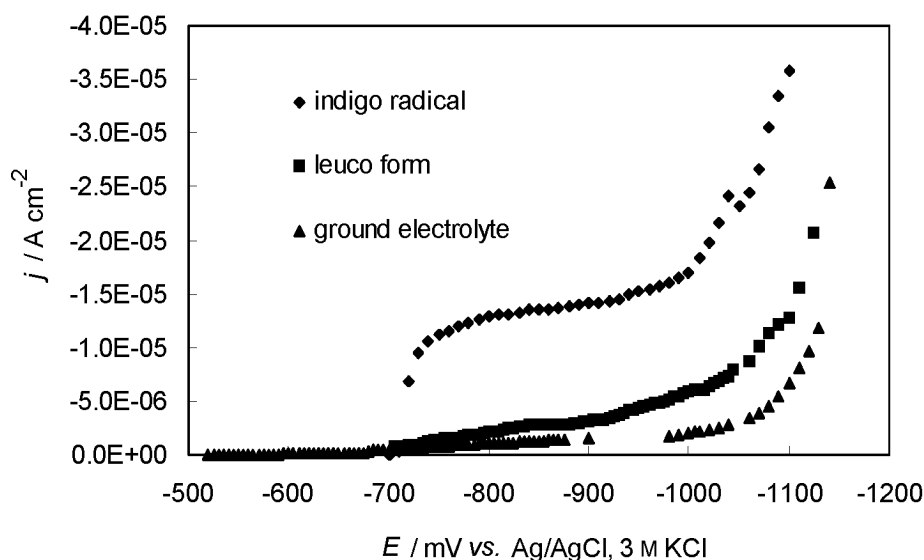
Fig. 3-3:   Voltammograms of different indigo derivatives (total indigo concentration $2 \cdot 10^{-4}$ M) in 1 M NaOH with 1 g l^{-1} Setamol at 50°C. Ni-electrode: 32 cm^2.

The limiting currents in the polarisation curves were found to be proportional to the square root of the rotation speed w of the disc-electrode indicating diffusion limitations (*Figure 3-4*). From these data the diffusion coefficient was found to be $D = (3 \pm 2) \cdot 10^{-9}$ m^2 s^{-1} (95%, N = 5) using the equation derived by *Levich* [169], [170]. At rotation frequencies higher than 2500 rpm the plot deviated from linearity suggesting a kinetic limitation by a preceding chemical reaction (*Figure 3-4*), most probably the step of the radical formation.
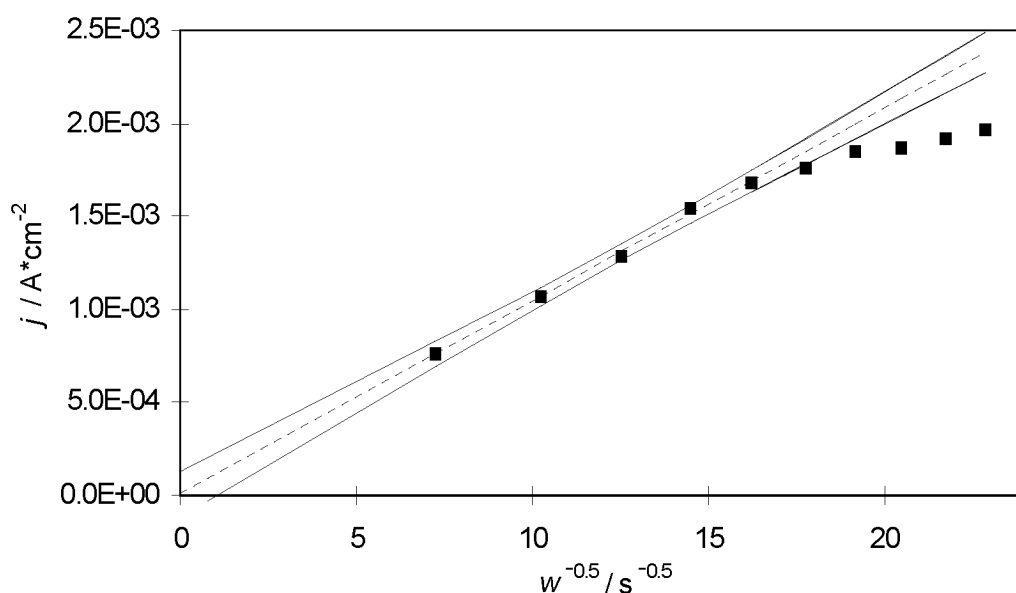
Fig. 3-4:   *Levich* plot for the electrochemical reduction of 10^{-5} mol l^{-1} indigo radical in 1 M NaOH at 50°C and -950 mV *vs.* Ag/AgCl, 3 M KCl. Ni-electrode: 0.2 cm^2.

The cyclic voltammograms[1] of all three important components − indigo, leuco indigo and indigo radical − were measured and compared to the one of the ground electrolyte (1 M NaOH). In contrast to indigo, which shows no electrochemical activity (*Figure 3-5 a*), the curve for the red-coloured radical

---

[1] Cyclic voltammetry (CV), a non-steady-state electroanalytical technique, is performed in an unstirred solution so that the measured current is limited by analyte diffusion at the electrode surface. The electrode potential is swept linearly to a more negative potential, and then swept in reverse back to the starting voltage. The forward scan produces a current peak for any analytes that can be reduced through the range of the potential scan. The current will increase as the potential reaches the reduction potential of the analyte, but then falls off as the concentration of the analyte is depleted close to the electrode surface. As the applied potential is reversed, it will reach a potential that will reoxidize the product formed in the first reduction reaction, and produce a current of reverse polarity from the forward scan. This oxidation peak will usually have a similar shape to the reduction peak [171]-[173].

solution shows four well defined peaks (*Figure 3-5 b*). The first reduction step with E_p = -1000 mV *vs.* Ag/AgCl, 3 M KCl corresponds to the reduction of the indigo radical. The signal of the according oxidation peak is small, indicating that the oxidation of leuco indigo to the radical is slow. The process was observed to be reversible in dimethyl sulfoxide (DMSO) as the solvent [5]. The observed i_{ox}/i_{red} ratio smaller than one is, therefore, probably based on the poor solubility of the mono-ionic radical species in water. The second reduction process with E_p= -1200 mV *vs.* Ag/AgCl, 3 M KCl can be identified as the reduction of α-Ni(OH)$_2$ to Ni. The anodic peak at -750 mV *vs.* Ag/AgCl, 3 M KCl correlates with the oxidation of the radical to indigo, because a layer of solid blue indigo could be observed at the electrode surface after some cycles. Certainly there should also be a signal due to the oxidation of Ni to α-Ni(OH)$_2$, for which in the literature for the peak potential a value of -700 mV *vs.* SCE can be found [175]-[177]. However, the intensity of the signals corresponding to the reactions of the Ni-electrode is small, suggesting that the peak is overlapping with the oxidation signal of the leuco dye. Additionally, it was observed that the signals correlated to the redox-chemistry of Ni became smaller after each cycle and sometimes are no longer detectable after 3 - 5 cycles.

The first sweep of the cyclic voltammogram of leuco indigo is shown in *Figure 3-5 c*. In addition to the signals of the interface between the Nickel electrode and the alkaline solution two peaks due to the oxidation of leuco indigo to the radical and subsequently to indigo can be detected at -960 mV and -640 mV *vs.* Ag/AgCl, 3 M KCl.

In order to obtain insight into the mechanism of the reduction reaction, a series of measurements was carried out at different scan rates. A significant increase of the cathodic peak current can be detected with increasing scan rate, and also the peak potential is shifted to a more negative value. The cathodic peak current (with background subtraction) is apparently linear to the square root of the scan rate. This is in agreement with the observed diffusion controlled process. A value of 0.59 $\pm$ 0.19 (95%, N = 5) for the charge transfer coefficient was calculated from the slope of the plot of log (j_p) versus log (v), which is almost linear.

a)

b)

c)
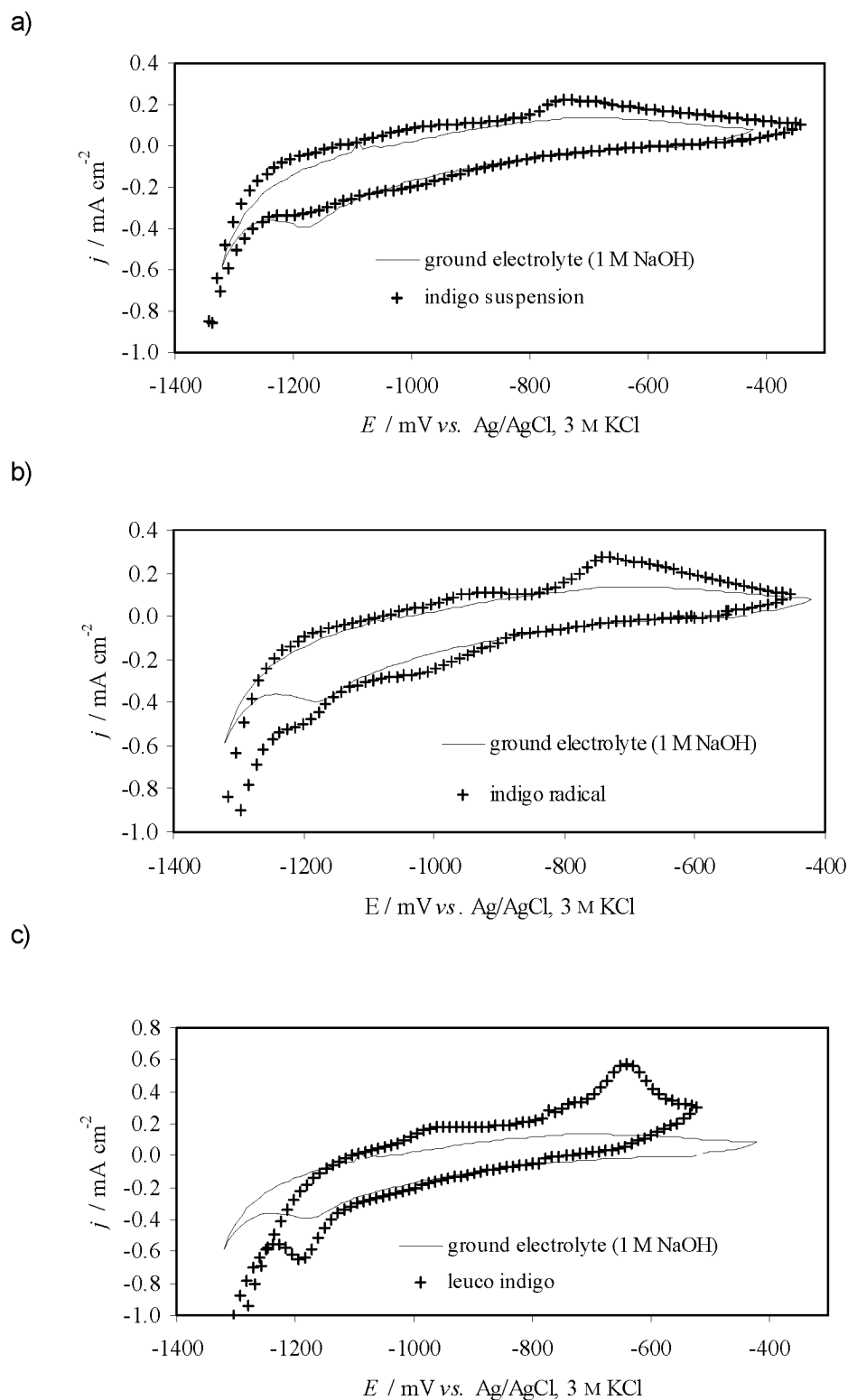
Fig. 3-5:   Cyclic voltammograms of the three indigo derivatives: a) $2 \cdot 10^{-4}$ M indigo, b) $2.5 \cdot 10^{-5}$ M radical and c) $2 \cdot 10^{-4}$ M leuco indigo in 1 M NaOH at a scan rate of 25 mV s^{-1} in the potential region of -400 to -1400 mV at 50°C (a, c) and 70°C (b). Ni-electrode: 0.2 cm^2.

The process observed in voltammetry is systematically affected by the pH of the aqueous solution. Peak potentials move towards negative values with increasing pH, indicating that it is more difficult to reduce the indigo radical at higher pH values. A plot of the peak potential E_p vs. the pH of the solution is shown in *Figure 3-6*. The slope of the curve is -64 mV ± 5 mV (95%, N = 5) per pH unit and is in agreement with the estimated Nernstian value for a one-electron one-proton transfer. However, at pH values higher than 13 the slope of the curve decreases. This suggests a change in the mechanism. It may be speculated that at these very high pH values the di-anionic form of the reduced indigo becomes stable and a transition to a one-electron zero-proton process is occurring. From these experimental data it might be deduced that the second acid-base equilibrium constant of leuco indigo in aqueous solution is approximately 13. This result is in good agreement with an estimated value of $pK_{a,2}$ = 12.7 published by *Etters* [178].
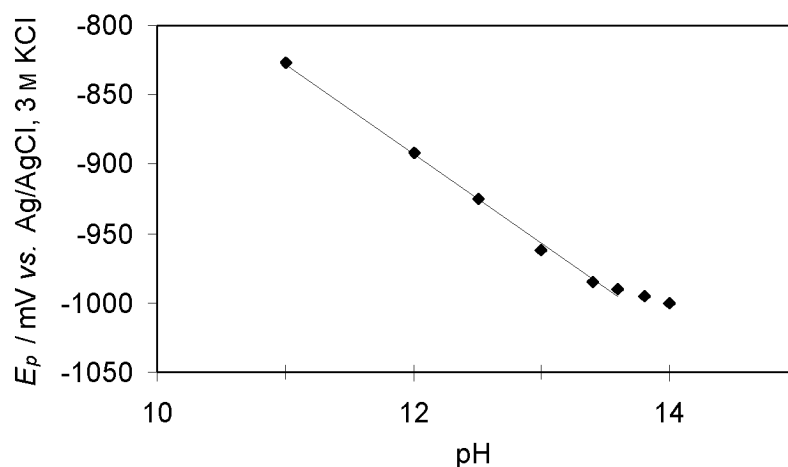
Fig. 3-6:   Plot of the peak potential E_p observed by cyclic voltammetry for the electrochemical reduction of 10^{-5} M indigo radical solution in 1 M NaOH at 50°C and at various pH values. Ni-electrode: 0.2 cm².

It is important to mention that the peak current at a certain radical concentration is practically independent of the pH. There might be a slight decrease of i_p with increasing pH, but the trend is really not significant. However, it was observed that the equilibrium between radical, indigo and leuco indigo moves to the radical side with higher pH. This stabilizing effect might be caused by the increasing amount of the more soluble dianionic form of leuco indigo and

the monoanion of the indigo radical, because non-ionic or 'acid' forms of reduced indigo are species of poor water-solubility [178].

3.3.3 Galvanostatic electrolysis experiments

The batch reactor (H-cell) served for a preliminary investigation of the macrokinetics. Nickel was chosen as the cathode material for a further characterisation of the process, because it is cheap, available in a defined purity and stable under the alkaline conditions of the process. As shown in the voltammetric studies, the system allows only low current densities and the experiments have to be done with a large electrode surface. Therefore, a 3D-Ni-electrode with a high surface area was used as cathode.

Online spectrophotometric monitoring of the reduction process provided more detailed information of the reduction products and the reaction kinetics. *Figure 3-7* shows typical UV spectra of the catholyte during a typical reduction run. The result is in perfect correlation with the suggested consecutive mechanism. The radical anion, a product of the comproportionation reaction between indigo and the leuco dye is continuously undergoing the secondary electrochemical reduction and is acting as an intermediate species only. The decline of indigo particles can be observed by the decreasing background absorption at 700 nm due to the continuously diminishing turbidity of the catholyte.

A series of galvanostatic runs was carried out in order to assess the effect of operating parameters such as current density and temperature on the electrochemical kinetics. *Figure 3-8* shows clearly the typical behaviour of the electrochemical batch reactor. The concentration decay is linear up to a current density of 2.5 μA cm^{-2} and approximately 40 min reaction time, the decrease in concentration can be described by a zero-order reaction. Further electrolysis results in an exponential decay.
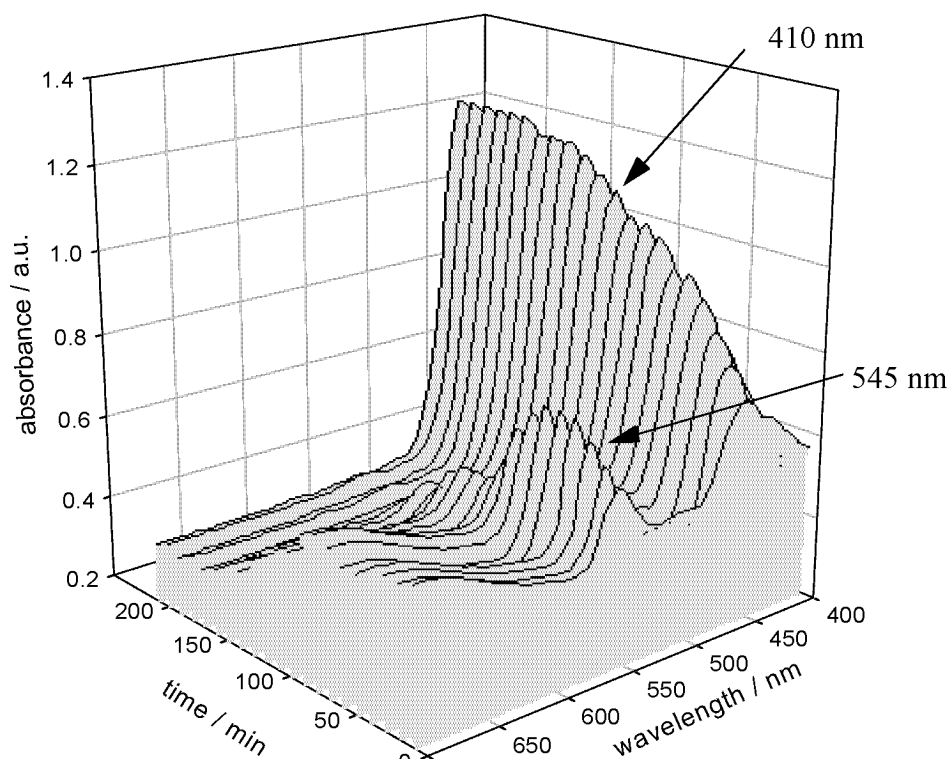
Fig. 3-7:   UV spectra af the catholyte during the reduction process. System parameters: 1 M NaOH, 1 g l^{-1} Setamol, total indigo concentration $2 \cdot 10^{-4}$ M, molar ratio indigo / moles dithionite (at t = 0): 8/1, current density 2.5 μA cm^{-2}, 50°C. Ni-electrode: 100 cm^2.

The time dependence of the current efficiency is shown in *Figure 3-9*. Only in case of the low current density of 1.0 μA cm^{-2} a region with a constant efficiency of approximately 80 % can be reached. In all other cases the efficiency is much lower and shows an exponential decrease with time. This is also the case at the low current density of 1.0 μA cm^{-2} after 40 min.

This behaviour is explained by the fact that – without adding further indigo pigment – after some time the concentration of the radical has become so small that the galvanostatic current density exceeds the limiting current density and the mass transport control becomes dominant. The electrode potential becomes more negative and a side reaction takes place at the cathode in the form of hydrogen liberation. This is also evident from the suddenly changing cell voltage.
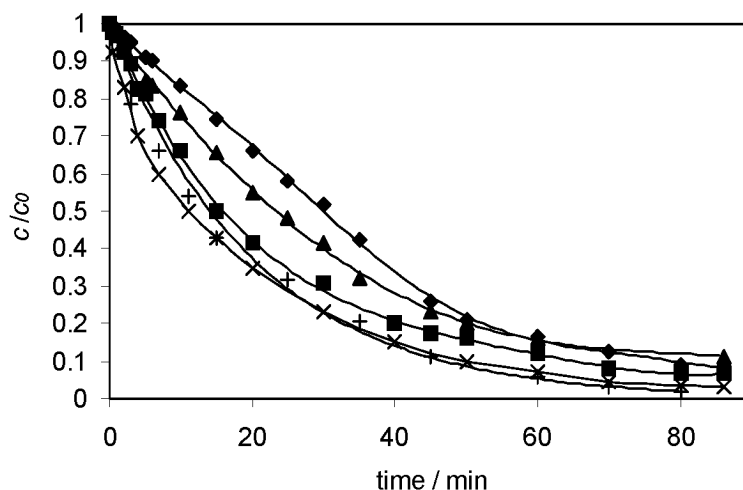
Fig. 3-8: Decline of indigo concentration *vs.* time for the galvanostatic reduction at different current densities. System parameters:1 M NaOH, 1 g l^{-1} Setamol, total indigo concentration 2·10^{-4} M, radical concentration at t = 0: 10^{-5} M, 50°C. Ni-electrode: 200 cm^2. Current density: (+) 0.1, (x) 0.01, (▲) 0.005, (■) 0.0025 and (◆) 0.001 mA cm^{-2}.
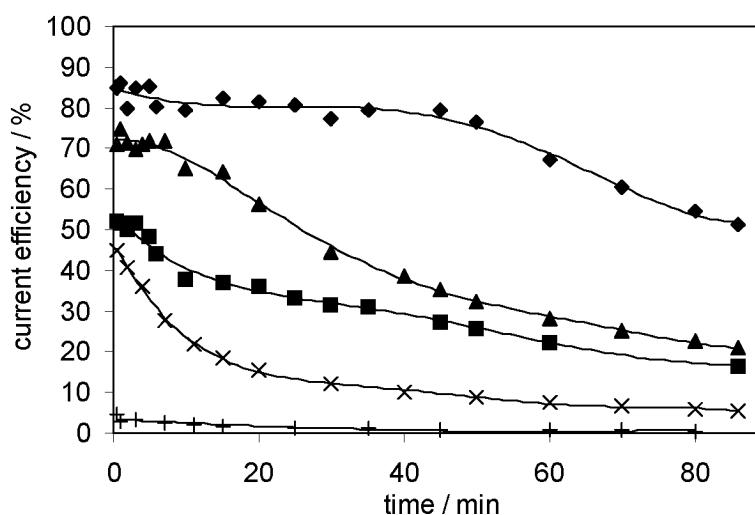
Fig. 3-9: Time dependence of the current efficiency for the galvanostatic reduction of the indigo radical. System parameters as in *Figure 3-8*. Current density: (+) 0.1, (x) 0.01, (▲) 0.005, (■) 0.0025 and (◆) 0.001 mA cm^{-2}.

In *Figure 3-10* the temperature dependence of the rate of the electrochemical reduction is shown. It can be observed that at higher temperatures the reaction is much faster. The results compares well with the apparent activation energy of 22.58 ± 1.18 kJ mol^{-1} (95%, N = 10) calculated from the relationship

between log (j) $vs.$ T^{-1} at a constant cathodic potential of -0.9 V $vs.$ Ag/AgCl, 3 M KCl. In addition, it has been observed that the equilibrium concentration of the radical is increasing with temperature.
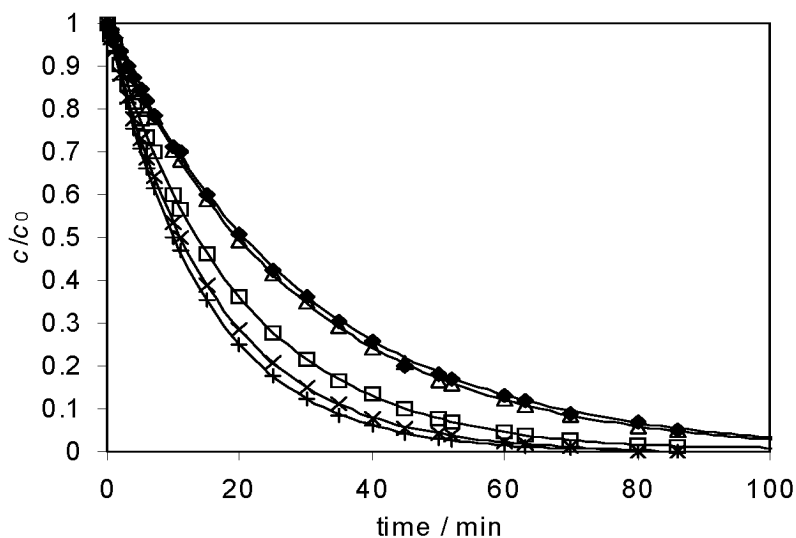
Fig. 3-10:   Decline of the indigo concentration $vs.$ time for the galvanostatic reduction of the indigo radical at different temperatures. System parameters:1 M NaOH, 1 g l^{-1} Setamol, total indigo concentration $2 \cdot 10^{-4}$ M, radical concentration at t = 0: $0.8 \cdot 10^{-5}$ M, current density 5.0 μA cm^{-2}. Ni-electrode: 250 cm^{2}. Temperature: (+) 80, (x) 70, (□) 60, (△) 50, (◆) 40 °C.
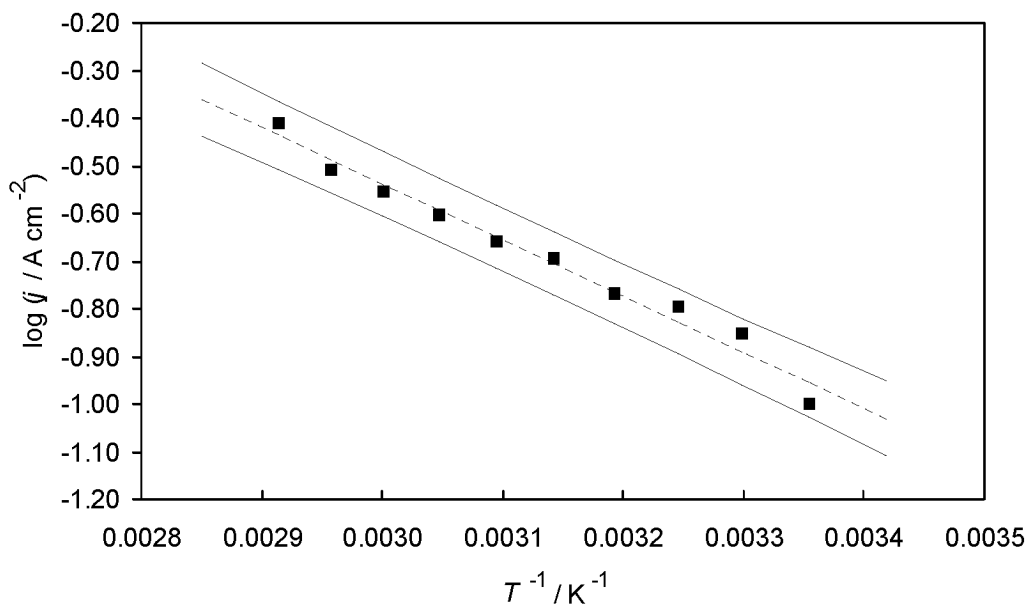
Fig. 3-11: $Arrhenius$ plot including 95% confidential intervall for determining the apparent activation energy ($E_{cathode}$ = -900 mV $vs.$ Ag/AgCl, 3 M KCl). System parameters as in $Figure\ 3\text{-}10$.

Moreover, the current efficiency was determined by the addition of a well defined amount of 30% H_2O_2 which simulated an oxidative load. Time was measured until more than 95% of conversion could be reached. This led to similar results as described above. However, this technique was also used to show the self sustaining effect of the process as long as not all leuco dye is reoxidized. It is obvious (*Figure 3-12*) that after complete reduction 90% of the leuco indigo are reoxidized by H_2O_2. Radical species are formed after some minutes in the resulting mixture of indigo and leuco indigo and the reduction process can be started again. Although *Figure 3-12* shows only two cycles, this was repeated several times without noticeable negative effects.
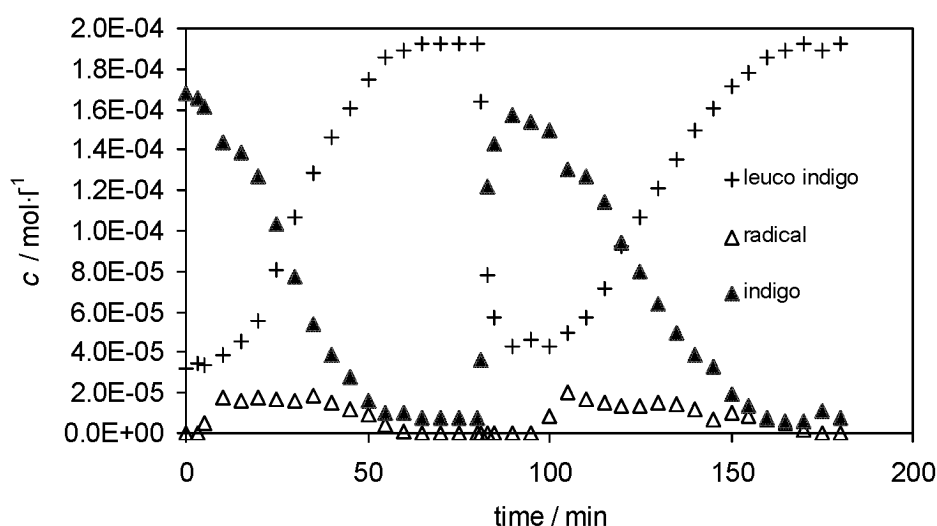
Fig. 3-12: Semi-batch experiments of direct electrochemical reductions and reoxidations with H_2O_2. System parameters as in *Figure 3-8*.

3.4 Conclusions

The novel route for the environmentally friendly production of water-soluble leuco indigo by direct electrochemical reduction of indigo suspended in aqueous solutions was confirmed by voltammetric experiments and electrolysis tests. The indigo radical anion can be easily reduced and the reaction product is stable under the applied conditions. At potentials more negative than

-1100 mV (*vs.* Ag/AgCl, 3 M KCl), the current density increases due to the cathodic liberation of hydrogen. It is shown that the reduction of the indigo radical is a diffusion-controlled 1 H^+-1 e^--electrochemical process at rotation frequencies smaller than 2500 rpm. If mass transport to the electrode is enhanced (> 2500 rpm), the radical formation as preceding chemical reaction is limitting the electrochemical process. The pH value has a large influence on the peak potential, whereas the reduction current is not highly affected.

However, the radical concentration is very low and, consequently, also the limiting currents and the reaction rates. Consequently, the current efficiency is limited to a maximum of only 80 % because hydrogen is liberated in a side reaction. Future work will include a more detailed study of the influence of the important parameters on the kinetics like pH, temperature, surfactant concentration and particle-size distribution in a flow-cell system. Therefore, these results are just the basis for further work towards scaling-up and optimizing an ecologically and economical compatible electrochemical process that can be employed in textile dyeing at an industrial scale (*chapter 4*).

Chapter 4

Electrochemical reduction of indigo *via* the indigo radical

Part II: Electrolysis in laboratory-scale flow cells

4.1 Introduction

Conventional H-cells were used in preliminary experiments (*chapter 3*). The results were then used as a guide in designing and operating the continuous flow cells. In the present work, direct electrochemical reduction of the indigo radical has been studied in a conventional divided flow cell to determine the industrial feasibility of the method and to optimize the electrolytic conditions.

However, the process is controlled by mass transfer (*chapter 3.3.2*). Thus, the reaction rate can be improved by increasing the electrode surface as well as accelerating the diffusion of the radical. Packed and fluidized bed electrodes are particularly suited to provide the large specific electrode area and the mass transfer coefficient required in such a case. Therefore, the cathodic reduction of the indigo radical has been investigated additionally in a packed and a fluidized bed electrode with the aid of an experimental circuit containing a flow channel cell with a particle-bed electrode.

4.2 Experimental details

4.2.1 Chemicals

All aqueous solutions were prepared with deionized water. Indigo and Set-amol WS was supplied from BASF, Ludwigshafen, Germany. Sodium hydroxide (Fluka, p.a.), sodium dithionite (Fluka, pract. 85%), and nitrogen 4.5 were used for the experiments.

4.2.2 Apparatus

a) Plate and frame cell

A small multipurpose plate and frame cell (EC Electro MP-Cell from Elec-troCell AB, Sweden) was chosen for the scale-up procedure. The cell permits the use of a combination of spacers and gaskets compressed (by a torque wrench to a value of 25 Nm) between two end plates. As working electrode configuration a flat nickel plate electrode plus an expanded mesh three-dimensional electrode made of nickel (100 mesh, G. Bopp + Co. AG) was used. The metal meshes were spot-welded to the plate to ensure good electrical conductivity and stacked with thin (about 0.2 mm) nickel strips at the edges and in the middle between the meshes in a vertical way. This provided equal access for the electrolyte to the whole surface of the meshes. The mesh was attached to both sides of a Ni-backplate so that the electrode is used double-sided (anode - membrane - mesh/Ni-backplate/mesh - membrane - anode). Nickel was also used as anode material and the cell was divided into two compartments by a Nafion-324 membrane (DuPont). The set-up of the pilot plant used in the experiments is given in *Figure 4-1*, *Figure 4-2* and *Figure 4-3*. Both electrolytes were pumped (D) from a reservoir (B, C) through the cell (A) in a flow-through pattern. In case of the catholyte, an additional circuit (bypass) was installed to circulate the suspension always independently from the flow rate through the cell to avoid sedimentation of the dispersed dyestuff. In this bypass a connection (E) for the online spectrophotometric measurement
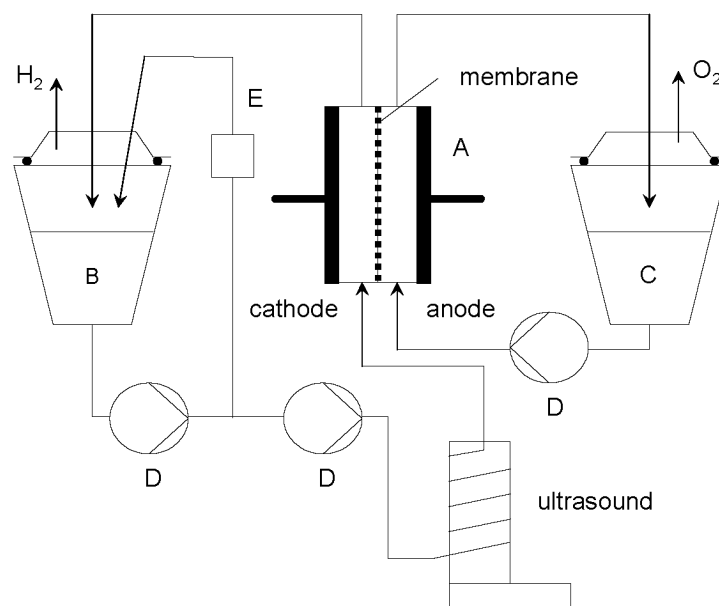
Fig. 4-1:   Laboratory flow-cell system. A: flow-cell (MP-Cell, ElectroCell AB), B: catholyte tank, C: anolyte tank, D: pump, E: online spectrophotometer.
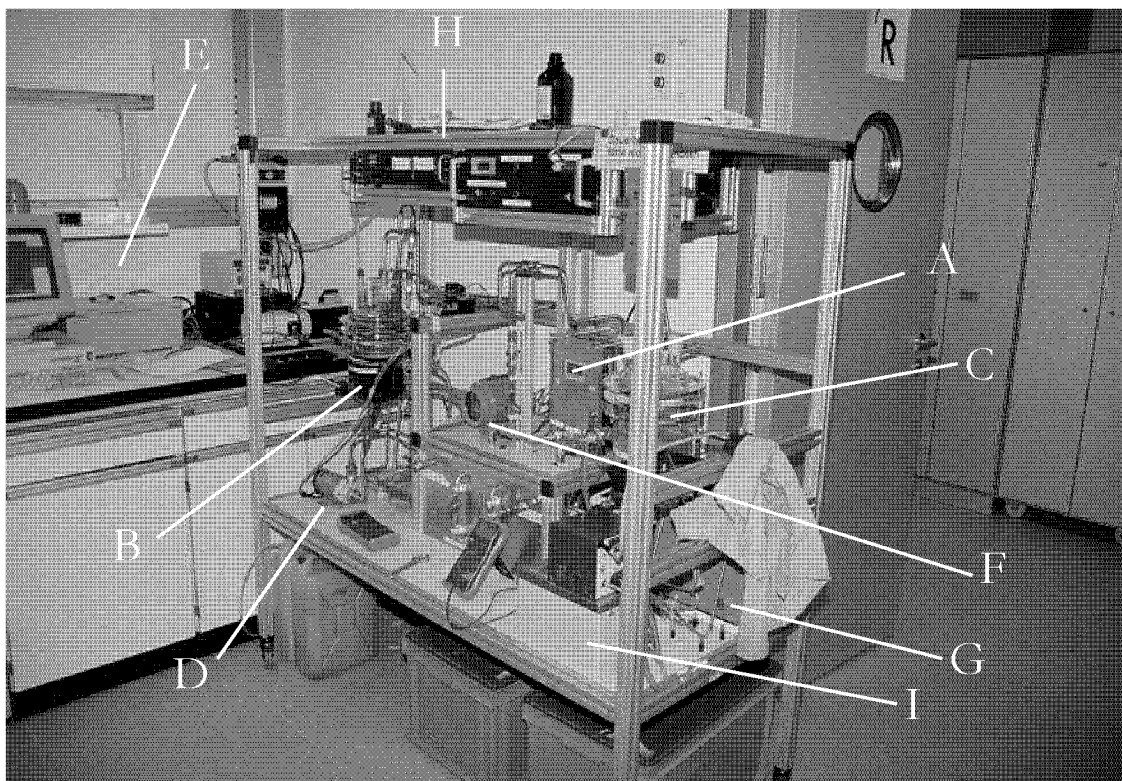
Fig. 4-2:   Picture of the whole laboratory-scale pilot plant. A: flow-cell (MP-Cell, Electro-Cell AB), B: catholyte tank, C: anolyte tank, D: pump, E: online spectrophotometer, F: flow meter, G: ultrasonic bath, H: power supply, I: thermostat.
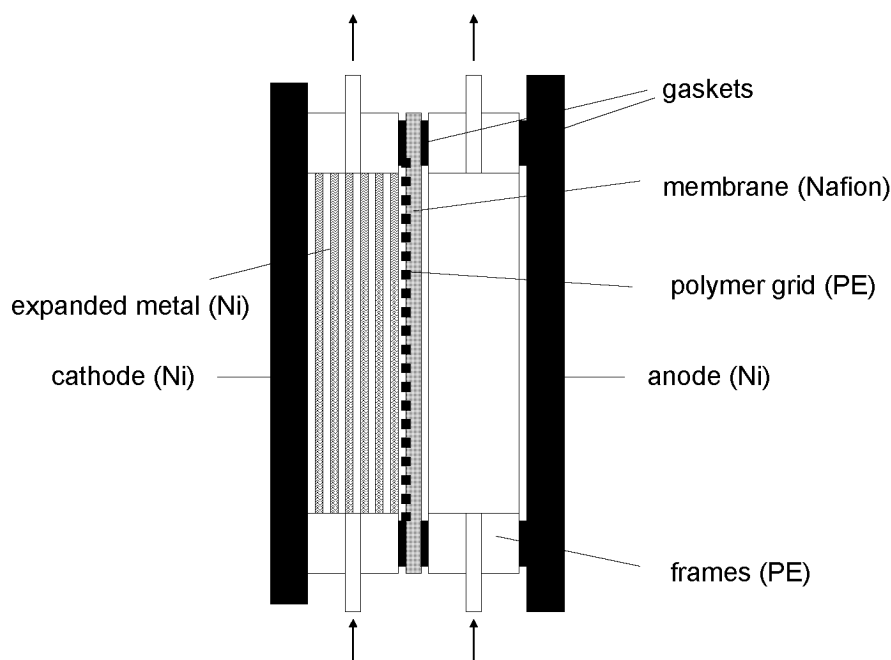
Fig. 4-3:   Schematic figure of the plate and frame reactor (Electrocell AB).

(Fibre Optical Spectrophotometer Avantes AVS-S2000) was implemented flow cell by Swagelok union cross tube fittings. Both electrolyte reservoirs were connected to a thermostat (Colora Messtechnik GmbH). A potentiostat (Soerensen, DCR 10-40B) was used both for galvanostatic and potentiostatic electrolysis experiments. Cell potential, cathode potential and current were measured with multimeters (Metex M 3610). To analyse the effect of ultrasound on the process, a spiral-shaped part of the catholyte-circuit was mounted in an ultrasonic bath.

b) Fixed- and fluidized bed

In addition, a small flow channel with a packed or fluidized bed was used for the experiments. Packed and fluidized bed electrodes are characterized by a bed of conducting particles functioning as an electrode, as opposed to the ordinary planar or structured electrodes, the current being fed in *via* a feeder electrode. This bed of particles is placed in a flow channel so that the electrolyte can flow between the particles. Thus, the working electrode consisted of a bed electrode made up of nickel spheres with 1 mm in diameter (Naegeli AG). A wire made of stainless steel (d = 1.5 mm) was fixed in the centre of the bed

and served as feeder electrode. This configuration, shown in *Figure 4-4*, has been suggested by *Crettenand* in his diploma thesis after optimisation of the cell construction [279]. Ru/Ta was used as anode material and the cell was divided into two compartments by a Nafion-324 membrane (DuPont). Current supplier was a potentiostat (Radiometer Copenhagen DEA 332, Electrochemical Interface IMT102, Software Voltamaster2).

c) Additional equipment

A sieve-machine (AS 200, Fa. Retsch) with several sieves was used to obtain well defined fractions of indigo particles. The particle size distribution was measured by laser diffraction (Sympatec Helos system H0702). The effect of ultrasound on the particle size distribution was investigated by the application of ultrasound on the sample reservoir of the particle size analyser.
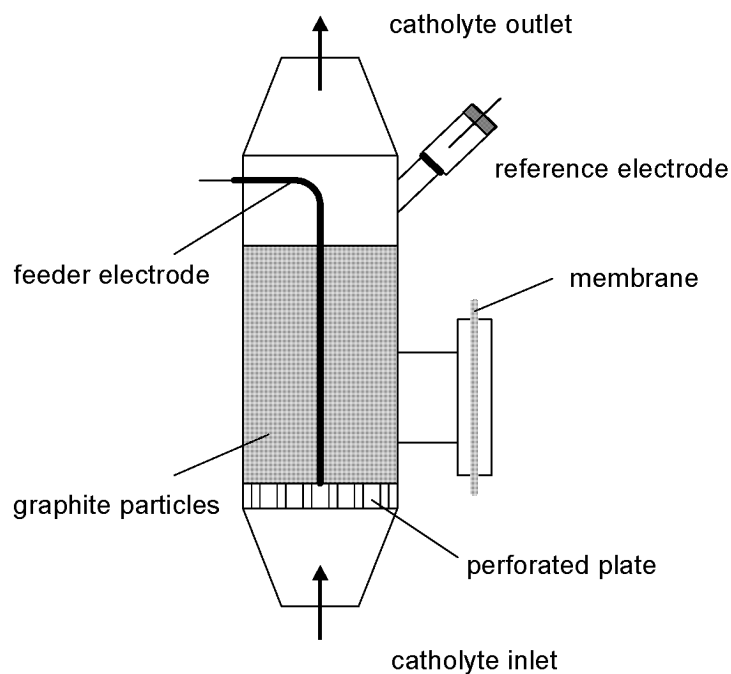
Fig. 4-4:   Schematic representation of the flow cell with a 3D-electrode used.

4.2.3 Procedure

Cathodic suspensions of indigo were composed of 1 M NaOH and 1 g l^{-1} of indigo (sieve fraction between 0.06 - 0.08 mm). They were deoxygenated

during at least 2 h before the experiment and maintained under a nitrogen atmosphere during the measurements. Various understoichiometric amounts of dithionite in aqueous solution (prepared after degassing the water for 2 h) were added by an injection needle through a septum to reduce indigo. In all experiments the ratio of dithionite to indigo was smaller than stoichiometric to generate the red coloured radical solution. Anodic solutions consisted of 1 M NaOH. All reduction experiments were performed at 50°C. In the case of different pH-values, the difference in ionic strength compared to 1 M NaOH (pH = 14) was compensated by adding NaCl.

4.3 Results and discussion

A series of galvanostatic runs was carried out in order to assess the effect on the electrochemical kinetics exerted by operating parameters such as current density, pH, temperature and flow rate of the catholyte.

4.3.1 Influence of the cathodic current density

Figure 4-5 shows clearly the typical behaviour of an electrochemical batch reactor. The concentration decay is linear up to a current density of 0.3 mA dm^{-2} and approximately 200 min reaction time. The reaction can be described by a zero-order kinetic law. Further electrolysis and reduction at a higher current density result in an exponential decay. The time dependence of the current efficiency is shown in *Figure 4-6*. A region with a constant efficiency of approximately 90 % can be reached in case of low current densities up to 0.25 mA dm^{-2}. In all other cases the efficiency is much lower and shows an exponential decrease with time. This is also the case at a current density of 0.1 mA dm^{-2} after 250 min reaction time. The results are in good agreement with previous work, indicating that the reduction of the radical species is controlled by mass transfer (*chapter 3.3.2*). Without adding further indigo pigment, after some time the concentration of the radical has become so small that the galvanostatic current density exceeds the limiting current density and the con-

trol by mass transport dominates. The electrode potential becomes more negative and at the cathode hydrogen is liberated in a side reaction.
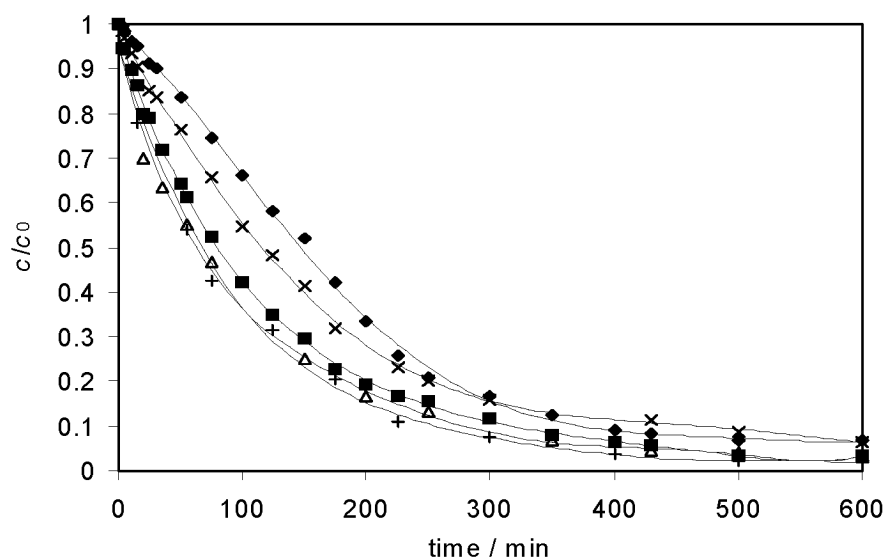
Fig. 4-5: Influence of the current density for the galvanostatic reduction of the indigo radical. System parameters:1 M NaOH, total indigo concentration 1 g l^{-1}, 10% of the indigo were reduced with dithionite at the beginning, 1 g l^{-1} Setamol, catholyte flow rate 20 cm^3 s^{-1}, 50°C. Ni-electrode: 600 cm^2. Current density: (+) 0.1, ($\triangle$) 0.01, (■) 0.005, (x) 0.0025, (◆) 0.001 mA cm^{-2}.
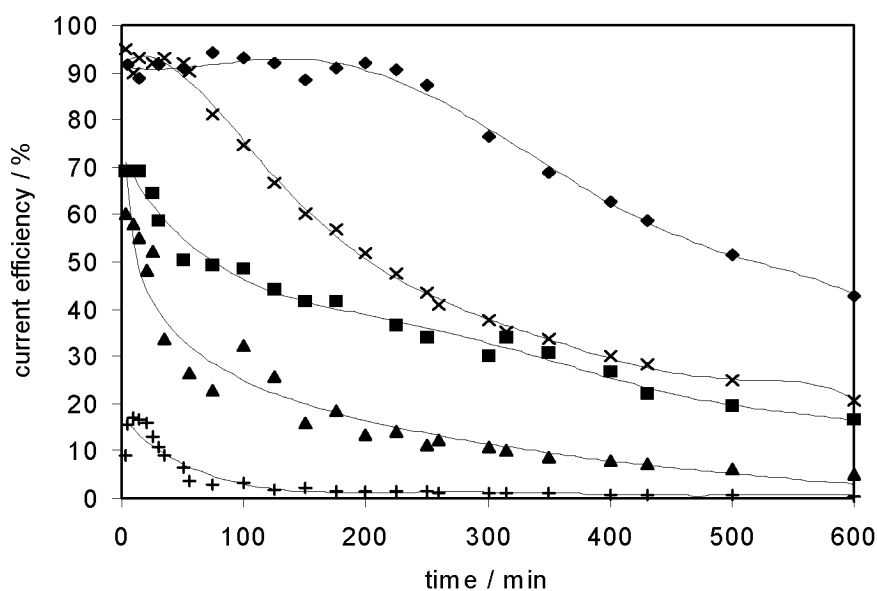
Fig. 4-6: Time dependence of the current efficiency for the galvanostatic reduction of the indigo radical. System parameters as in *Figure 4-5*.

4.3.2 Influence of the temperature

In *Figure 4-7* the temperature dependence of the reaction rate of the electrochemical reduction is shown. The reaction is much faster at higher temperatures and this is in good agreement with results presented previously (*chapter 3.3.3*). However, the curves shown in *Figure 4-7* were not measured at the same radical concentration, because the equilibrium concentration of the radical increases with temperature. Therefore, the higher reduction rate is based both on the enhanced electrode kinetics and the increasing radical concentration.

Fig. 4-7: Influence of the temperature on the galvanostatic reduction of the indigo radical. System parameters: 1 M NaOH, total indigo concentration: 1 g l^{-1}, 10% of the indigo was reduced with dithionite at the beginning, 1 g l^{-1} Setamol, current density 0.0025 mA cm^{-2}, catholyte flow rate 20 cm^3 s^{-1}. Ni-electrode: 600 cm^2. Temperature: (+) 80, ($\triangle$) 70, ($\square$) 60, ($\blacklozenge$) 50 °C.

4.3.3 Influence of the pH

The influence of catholyte-pH is shown in *Figure 4-8*. It is obvious that the reaction rate is clearly enhanced with increasing the pH. Only a slight increase in the reduction rate has been observed in previous studies (*chapter 3.3.2*). Therefore, this effect is mainly based on the higher radical concentration, because it has been observed that the equilibrium between radical, indigo and leuco indigo is shifted towards the radical side with higher pH. This stabilising

effect might be caused by the presence of the more soluble ionic forms of the indigo species, because non-ionic or 'acid' forms of the reduced indigo are of poor water-solubility.
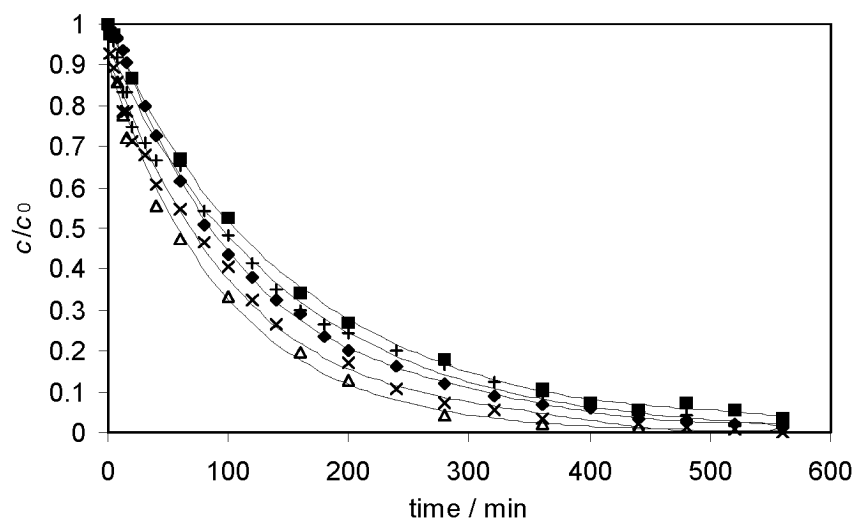
Fig. 4-8: Influence of the pH on the galvanostatic reduction of the indigo radical. System parameters: 1 M NaOH, total indigo concentration 1 g l^{-1}, 10% of the indigo were reduced with dithionite at the beginning, 1 g l^{-1} Setamol, current density 0.0025 mA cm^{-2}, catholyte flow rate 20 cm^3 s^{-1}, 50°C. Ni-electrode: 600 cm^2. pH: (■) 10, (+) 11, (◆) 12, (x) 13, (△) 14.

4.3.4 Influence of the catholyte flow rate

Figure 4-9 shows the influence of the catholyte flow rate on the limiting current. At higher velocities the mass transport of the radical species to the cathode is enhanced. This results in a higher limiting current and, therefore, a higher rate of decay of the concentration in the mass transfer controlled region.
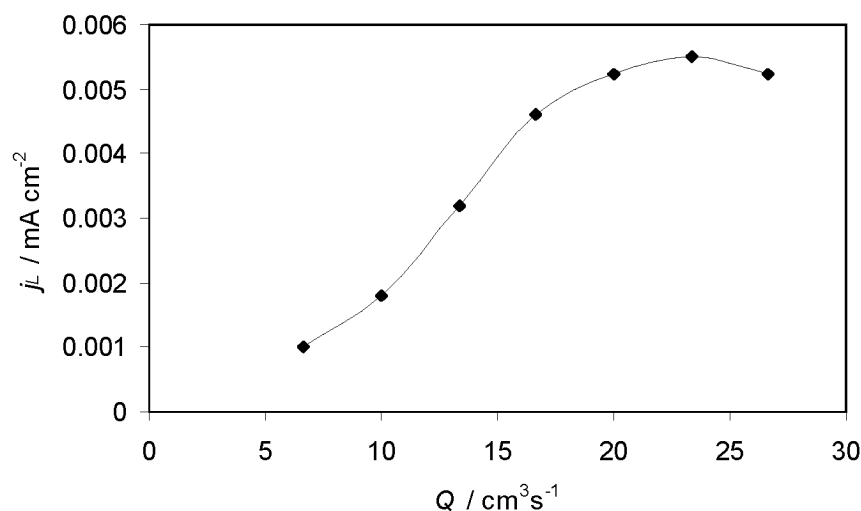
Fig. 4-9:   Influence of the catholyte flow rate Q on the limiting currents j_L of the electrochemical reduction of the indigo radical. System parameters: 1 M NaOH, total indigo concentration 1 g l^{-1}, 10% of the indigo was reduced with dithionite at the beginning, 1 g l^{-1} Setamol, current density 0.0025 mA cm^{-2}, 50°C. Ni-electrode: 600 cm^2.

4.3.5 Influence of the particle size and the use of ultrasound

Ultrasound was applied to the electrolyte before entering the reactor in order to influence the properties of the dye dispersion. It is obvious from *Figure 4-10* that in the presence of ultrasound the reaction rate of radical reduction is slightly enhanced.

Figure 4-11 shows the particle size distribution of a commercially available indigo (BASF AG, Ludwigshafen, Germany). The effect of ultrasound on the particle size distribution can be seen in *Figure 4-12*. It is obvious that larger particles or agglomerates of solid particles (> 100 µm) are efficiently broken down and smaller particles with a size between 1 and 10 m are created. This is in agreement with results obtained by *Lindley* [179] that ultrasound can reduce the particle size of non-metallic particles down to usually 1 - 10 µm. A longer application of ultrasound leads only to changes on the surface of the particles (*e.g.* cleaning), but no more smaller particles are generated [179]-[181]. Therefore, the positive effect is based mostly on the increase of the active reaction surface due to the reduction of the particle diameter. This can increase the production rate of the radical species, but on the other hand it is also possible that

more radicals will adsorb on the larger organic/water-interface and, therefore, the free bulk concentration of the radicals will be lower. However, it has never been observed in the UV/VIS-spectra that the radical concentration is decreasing after the application of ultrasound. Rather a slight increase was obtained, probably indicating that radicals can also be generated by ultrasound.

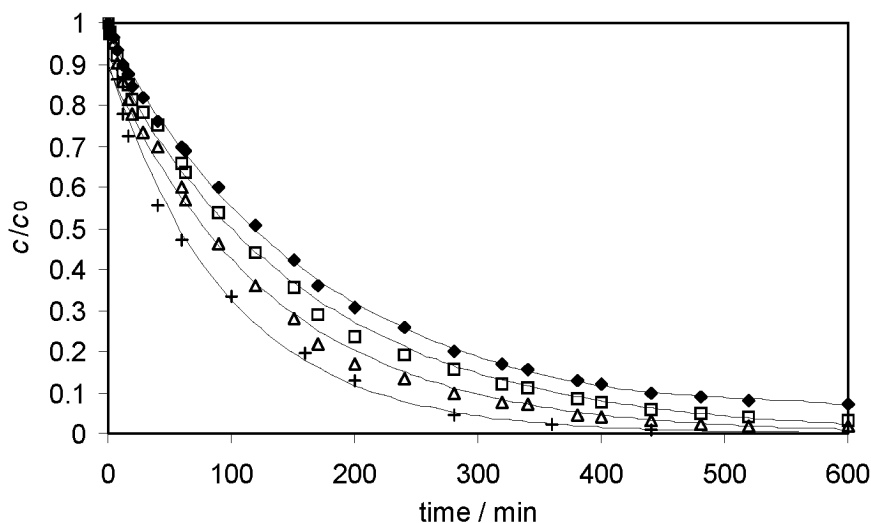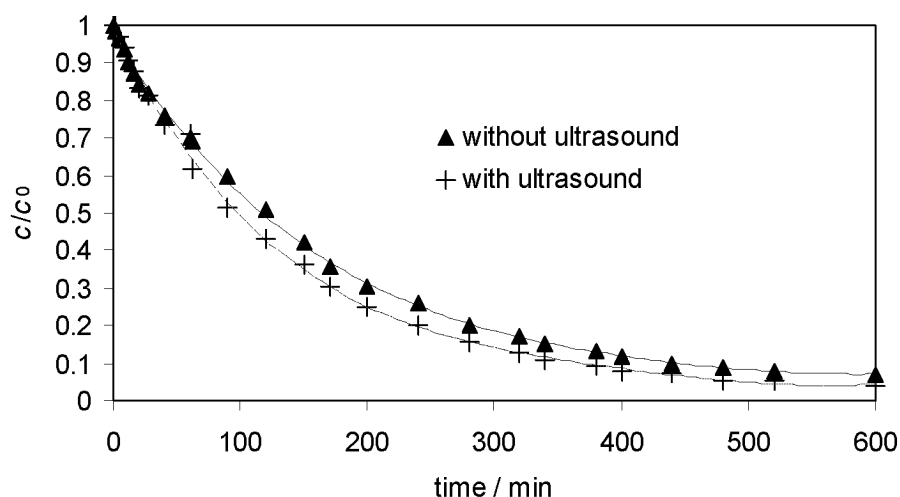**Fig. 4-10:** Influence of ultrasound on the kinetics of the galvaostatic reduction of the indigo radical. System parameters: 1 M NaOH, total indigo concentration 1 g l^{-1}, 10% of the indigo was reduced with dithionite at the beginning, 1 g l^{-1} Setamol, current density 0.0025 mA cm^{-2}, 50°C, catholyte flow rate 20 cm^3 s^{-1}. Ni-electrode: 600 cm^2.
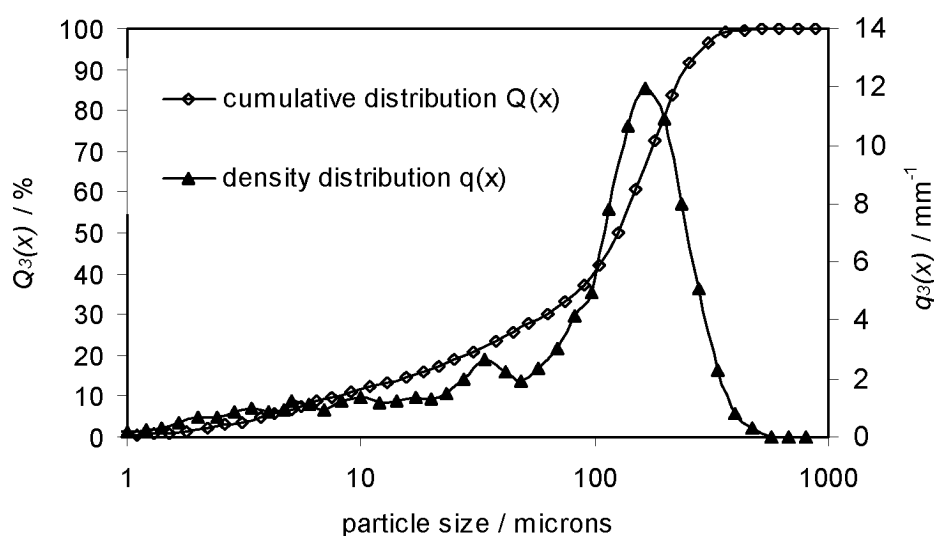
Fig. 4-11: Particle size distribution of BASF indigo.
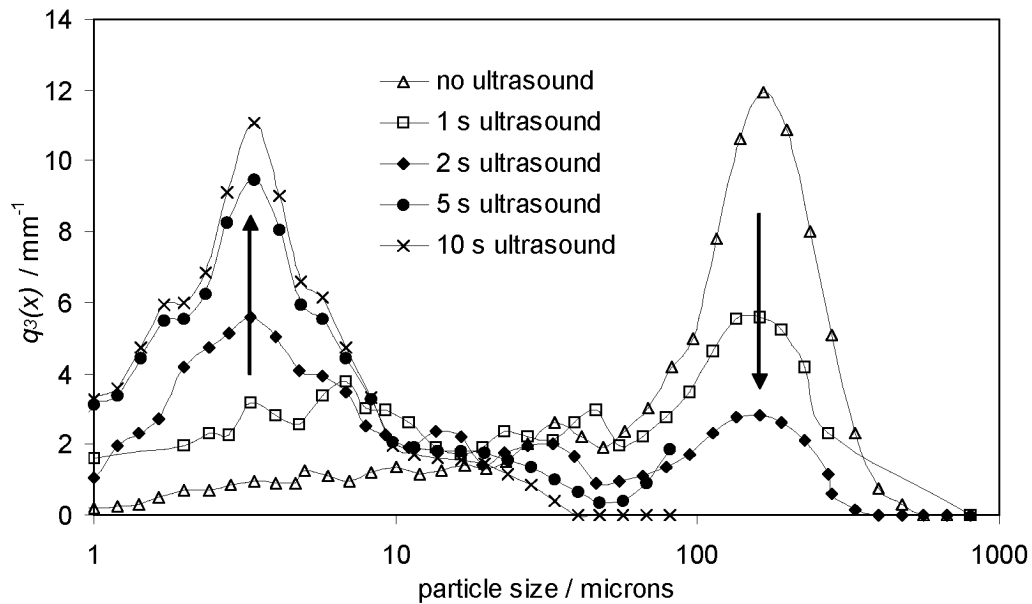
Fig. 4-12:   Influence of ultrasound on the particle size distribution.

4.3.6 Experiments with a packed and fluidized bed electrode

a) Determination of the fluidization point

Liquid fluidized systems are generally characterized by the regular expansion of the bed which takes place as the velocity increases from the minimum fluidisation velocity to the terminal falling velocity of the particles. The general relation between velocity and volumetric concentration or voidage is found to be similar to that existing between the sedimentation velocity and the concentration for particles in a suspension. The two systems are hydrodynamically similar, because in the fluidized bed the particles undergo no net movement and are maintained in suspension by the upward flow of liquid, whereas in the sedimenting suspension the particles move downwards and the only flow of liquid is the upward flow of the liquid being displaced by the settling particles.

Richardson and *Zaki* showed that for the sedimentation or fluidization of uniform particles [182], [183]

$$u_C = u_i \, \varepsilon^a = (1 - C)^a$$

where

u_c is the velocity of the empty tube fluidization

u_i is the corresponding value at infinite dilution

ε is the voidage of the system

C is the volumetric fractional concentration of solids and

a is an index.

If the voidage ε of the bed is plotted against the velocity of the fluid u_C (using logarithmic coordinates), the curve can be divided approximately into two straight lines joined by a short curve. At low velocities the voidage remains constant corresponding to the fixed bed. For the fluidized state there is a linear relation between log u_C and log ε. By extrapolation of the graph of log u over log ε in *Figure 4-13* to the packed bed voidage $\varepsilon_0 = 0.389$, a fluidization point of $u_C = 4.35 \pm 0.50$ cm s^{-1} (95%, N-1 = 11) is obtained.
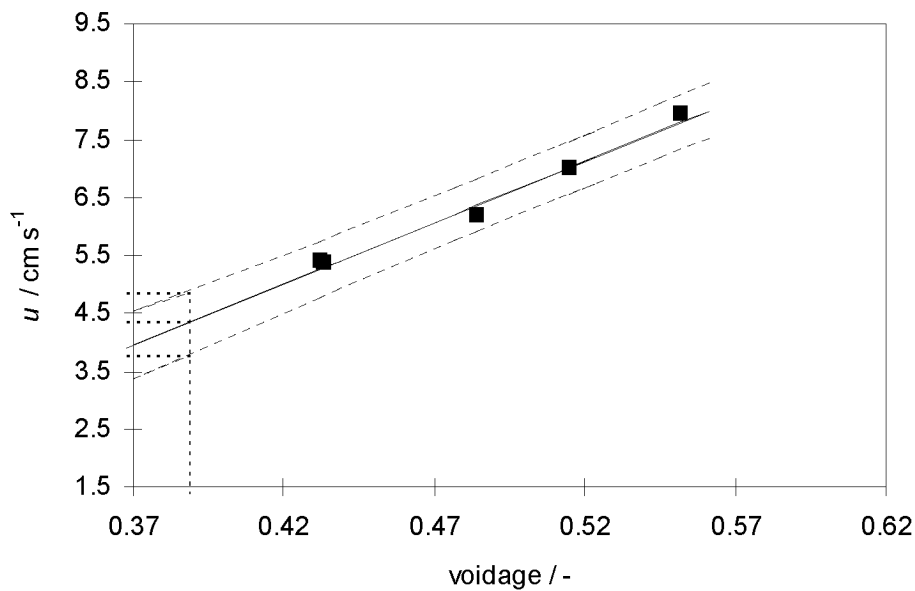
Fig. 4-13:   *Richardson-Zaki* plot for the dependence of the flow on the bed voidage.

b) Flow dependence of the macrokinetic bed current density

Figure 4-14 shows the relationship between the measured current density (based on the membrane area) and the flow rate, with an obvious peak near the fluidisation point. In the packed bed region the rise in current density is caused by the increase in the mass transfer coefficient and the corresponding increase in the limiting current density with increasing flow velocity. Above the fluidisation point the expansion of the bed causes a sharp rise in the effective resistance of the particle phase. The associated ohmic drop leads to a sharp decrease in the macrokinetic current density.

It has to be mentioned that due to the problem of non-uniform potential distribution, a loss of the well defined limiting plateaux on the current-potential curves has been observed. This is a well known phenomenon and is discussed in many references, but it is very complex to analyse [185]. Certainly, it cannot be assumed that all parts of the bed are operating near or on the limiting plateau. Some regions of the bed may propably operate even outside the region of cathodicity so that a local anodic oxidation can occur with the redeposition of indigo. In the limiting gradient region the upper part of the curve is in the region of the cathodic hydrogen evolution. Therefore, very often a true estimation of the limiting current is impossible [185].
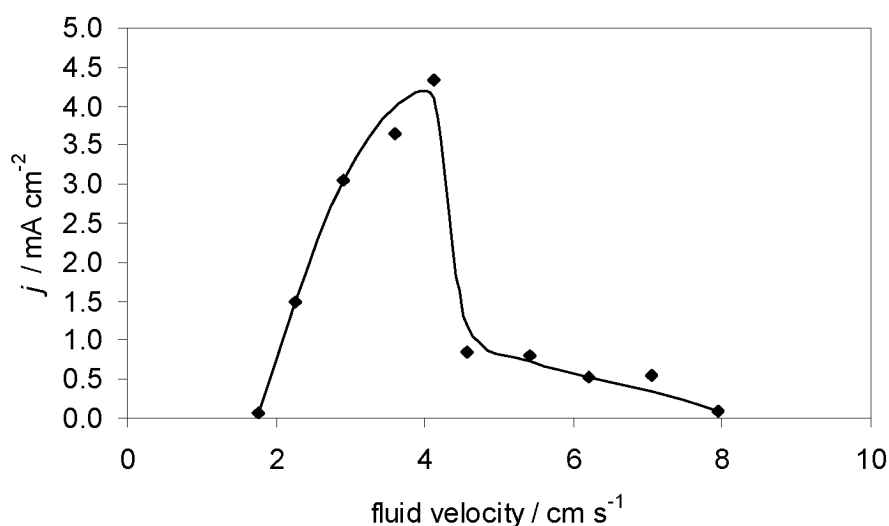
Fig. 4-14:   Flow dependence of the macrokinetic bed current density j (based on the membrane area) at -900 mV vs. Ag/AgCl, 3 M KCl. System parameters: 1 M NaOH, total indigo concentration 0.1 g l^{-1}, 10% of the indigo was reduced with dithionite at the beginning, 50°C.

4.4 Conclusions

The industrial feasibility of the novel route for the environmentally friendly production of the water-soluble leuco indigo by direct electrochemical reduction of indigo in aqueous solutions has been studied in a divided flow cell. Optimized conditions in the system were evaluated and a scale-up in indigo concentration up to 1 g l^{-1} was achieved. Increasing the pH and the temperature can enhance the reduction rate. A better mass transfer was achieved by higher flow velocities in the reactor. In the presence of ultrasound the reaction rate is slightly enhanced, based on the increased active reaction surface due to reduction in the particle diameter. In addition, the behaviour of a fixed-bed and a fluidized bed reactor for the electrochemical reduction of the indigo radical is described. Due to the enhanced mass transfer, higher reduction rates could be achieved. However, the reactor performance is still too low for an industrial application. The current efficiency is also limited to a maximum of 90 % at very low current densities.

The most ristricting factor is the low radical concentration. Therefore, future work must include a study of important parameters influencing the concentration of the radical species, like surfactants, and has to focus on the optimization of this novel electrochemical process (*chapter 5*).

Chapter 5

Electrochemical reduction of indigo *via* the indigo radical Part III: Effect of additives

5.1 General aspects

It was shown in several experiments that the kinetics of the direct electrochemical reduction of the indigo radical is very slow and controlled by mass transfer (*chapter 3* and *chapter 4*). In addition, it turned out that common engineering measures as *e.g.*, increasing the fluid velocity or the application of fixed- and fluidized beds do not suffice to reach a reduction rate which is high enough for an industrially feasible application (*chapter 4*). It is obvious, that an increase of the radical concentration accelerates the process. Therefore, it seems inevitable to find an additive as *e.g.*, cyclodextrins, organic solvents, surfactants which can stabilise the radical species in the aqueous environment without disturbing the electron transfer in a decisive way.

5.2 Experimental

5.2.1 Chemicals

Deionized water, indigo (synthesized, *cf. chapter 5.2.4*), NaOH (Synaopharm, puriss.), indole (Fluka, puriss. > 99% GC), acetic acid (Fluka, p.a.), molybdenum hexacarbonyl (Alfa Aesar, 98%), *tert*-butyl alcohol (Fluka, p.a.), cumene hydroperoxide (Aldrich, techn. 80%), cumene (Aldrich, 99% GC), Setamol WS, BASF), α-cyclodextrin (Fluka, >98% GC), β-cyclodextrin (Fluka,

> 99% GC), γ-cyclodextrin (Fluka, >98% GC), hexadecyltrimethylammonium chloride (HDTA) (Fluka, >98% NT), choline chloride ((2-hydroxyethyl)trimethylammonium chloride (Fluka, purum)), trimethyloctylammonium chloride (Fluka, puriss. > 98%), octadecyltrimethylammonium chloride (Fluka, puriss. > 98%), dodecyltrimethylammonium bromide (Fluka, purum > 98%), tetrahexylammonium bromide (Aldrich, 99%), methyltrioctylammonium bromide (Aldrich, 98%), tetraoctylammonium bromide (Aldrich, 98%), didodecyldimethylammonium bromide (Fluka), hexyltrimethylammonium bromide (Fluka, purum, > 98%), octyltrimethylammonium bromide (Fluka, purum, > 98%), benzyltrimethylammonium bromide (Aldrich, 50% in water), methyltributylammonium chloride (Aldrich, 75% (w/w) in water), 3-(N,N-dimethyloctylammonio)propane sulfonate (Fluka, assay > 97% (N)), sodium dodecyl sulphate (SDS) (Fluka, > 97% GC), dimethyl-n(C_{12}/C_{14})-alkyl benzyl ammonium chloride (Lutensit TC-KLC 50) (BASF, techn.), (2-hydroxyethyl)trimethylammonium chloride (Fluka, purum), Lutensol A8 (Alkylpolyethylenglycolether, BASF, techn.), Surfadone LP-300 (N-(n-octyl)-2-pyrrolidone, Fa. ISP Europe), Surfadone LP-100 (N-(n-dodecyl)-2-pyrrolidone, Fa. ISP Europe), N-benzyl-N,N-dimethyl-N-[4-(1.1.3.3-tetramethylbutyl)-phenoxyethoxyethyl] ammonium chloride (Hyamine 1622, Merck 112058), sodium dodecylbenzenesulfonate (Fluka, techn.), polyethyleneglycol 400 (Fluka, pract.), Setamol WS (BASF), methanol (Fluka, 99.8%), DMF (Fluka, p.a.), sodium dithionite, pract. (Fluka, 85%) were used as received. Argon 4.8 was used for degassing the solution employed for the experiments.

5.2.2 Apparatus

The experimental set-up is described in *chapter 3.2.*

5.2.3 Electrochemical experiments

Cathodic suspensions of indigo were composed of 1 M NaOH in several solvents, containing various amounts of additives and $2 \cdot 10^{-4}$ M of indigo. To reduce an initial part of the indigo, 1 ml of an aqueous solution of dithionite ($2 \cdot 10^{-4}$ M, prepared after degassing the water for 2 h) was added. Anodic solu-

tions consisted of 1 M NaOH. The catholyte was deoxygenated by stripping with argon for 2 h before the experiment and always maintained under an argon atmosphere. All reduction experiments have been performed at 50°C.

5.2.4 Synthesis of indigo

To a solution of indole (1.0 g), acetic acid (0.051 g) and molybdenum hexacarbonyl (2.25 mg) in *tert*-butyl alcohol (15 g), a 82 % (w/w) solution of 1-methyl-1-phenyl-ethylhydroperoxide (cumene hydroperoxide) in cumene was added. This mixture was warmed to 86°C and refluxed for 7 hours. Afterwards, the mixture was filtrated. The precipitate of indigo was collected, washed with methanol and dried under HV [188]. M.p. 380°C (Lit.: 390 - 392°C, subl. > 170°C [189]). EI-MS: 262.1 (100, [M$^+$]), 234.1 (13.12), 205.1 (12.56), 158.1 (6.73), 104.1 (11.43), 76.1 (6.12). Anal. calc. for $C_{16}H_{10}N_2O_2$ (262): C 73.27, H 3.84, N 10.68, O 12.20; found: C 73.27, H 4.02, N 10.47, O 12.30.

5.3 Results and discussion

5.3.1 Influence of organic solvents

It is well known that the addition of small amounts of methanol accelerates the vatting reaction. For example, the mixture for vatting indigo catalyzed by ultrasound contains 20 ml methanol per liter of the suspension [86]. The accelerating effect of methanol seems to be caused by its ability to partially dissolve indigo and its corresponding reduced species, *i.e.* the indigo radical and the leuco dye, better than water. And, organic species adsorbed on the indigo particles will be washed off into the bulk mixture.

Unfortunately, only concentrations higher than 20% (v/v) of the organic solvents (*e.g.* methanol, isopropanol, ethanol, DMF) are capable to stabilise the radical species lastingly. Of course, the use of such high amounts of solvents in the dye bath is not realistic at an industrial scale. Even the addition of N-meth-

ylpyrolidone which is capable to prevent the leuco species from being oxidized [194], [195], did not show a positive effect on the vatting process.

5.3.2 Effects of cyclodextrins

Cyclodextrins (α, β and γ–forms) are cyclic oligosaccharides having a hydrophobic internal cavity (*Figure 5-1*) [190]. They can form various inclusion complexes with organic molecules of different size, depending on the size of the cavity. Several research groups investigated the interaction between cyclodextrins and organic compounds like *e.g.* dye molecules [191]. *Okubashi et al.* [192] were especially interested in the effects of cyclodextrins on the electrolytic reduction of vat dyes like *e.g.* indigo. Unfortunately, their paper only describes electrochemical experiments with C.I. Acid Blue 25, an anthraquinone dye, whereas they do not report on experiments with indigo, probably because of its limited solubility. Nevertheless it seemed interesting for this work to evaluate the influence of cyclodextrins on the redox chemistry of the indigo radical.
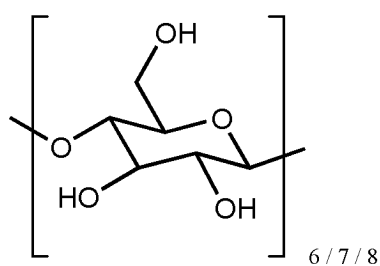
Fig. 5-1:   Structure of α– (6), β– (7) and γ–cyclodextrin (8).

Figure 5-2 shows a cyclic voltammogram for the indigo radical (10^{-5} M) in 1 M NaOH. Two cathodic peaks at -1000 mV and -1200 mV and an anodic signal at -750 mV *vs.* Ag/AgCl, 3 M KCl were observed. One cathodic and the anodic peak are attributed to the reduction and oxidation of the dye radical, respectively. The second cathodic peak can be correlated to the reduction of α-Ni(OH)$_2$ to Ni (*chapter 3.3.2*).

The peak potential E_p is shifted to more negative values in the case of β- and γ-cyclodextrin as additives, suggesting that both are interacting with the indigo radical. The potential did not change, regardless of the concentration of

α-cyclodextrin present, indicating that there is hardly any interaction between α-cyclodextrin and the indigo radical (*Figure 5-3*).

Fig. 5-2:   Cyclic voltammogram of 10^{-5} M indigo radical in 1 M NaOH at 50°C at a scan rate of 10 mV s^{-1} in the potential region of -400 to -1400 mV with 16 mM cyclodextrin (CDx) (= solid line). Ground electrolyte: 1 M NaOH (= dashed line).
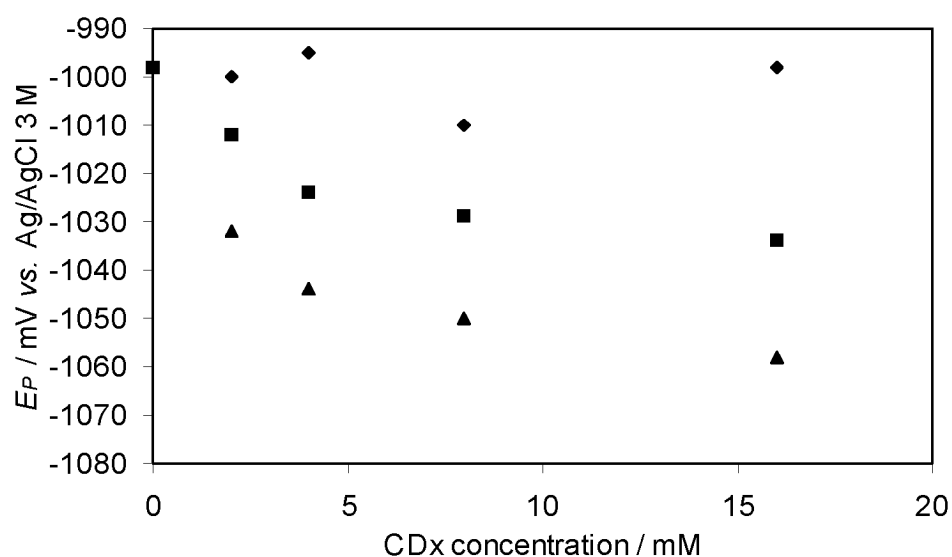
Fig. 5-3:   Plots of the peak potential E_P against the concentration of cyclodextrin (CDx) (10^{-6} M indigo radical in 1 M NaOH at 50°C, 10 mV s^{-1} scan rate). (◆) α-cyclodextrin, (■) β-cyclodextrin, (▲) γ-cyclodextrin.

As an additional evidence, spectrophotometric analyses corroborated an interaction between β- and γ-cyclodextrin and the indigo radical. *Figure 5-4* shows a UV/VIS spectrum of a 1 M NaOH solution containing a total amount of $2 \cdot 10^{-4}$ mol l^{-1} of indigo, indigo radical and leuco dye. The addition of α-cyclodextrin neither resulted in a significant shift in the λ_{max} of the radical (550 nm) nor in a significant change of the absorbances. In the case of β- and γ-cyclodextrin the absorbance was enhanced, whereas the position of the peak remained unchanged. From this it can be concluded that in the case of the β- and the γ-cyclodextrin the radical concentration might increase due to the stabilization of the radical species by the cyclodextrins. This would shift the equilibrium between indigo, leuco indigo and the radical towards the side of the radical. Although the mechanism of the interaction is not clear the interaction between the host molecule and the guest is generally dependent on the cavity size [193]. The internal diameters of the cavity are 0.45, 0.70, 0.85 nm in α-, β- and γ-cyclodextrin, respectively [190]. The size of the indigo molecule (distance between the two aromatic H's), including *van der Waals* radii, is estimated to be 0.74 nm (calculated by Dr. P. Skrabal, ICB, ETH: HyperChem 6.0, geometry optimized with PM3 (MNDO)). This suggests that the size of the indigo molecule (0.74 nm) is too large to interact with α-cyclodextrin (cavity of 0.45 nm).
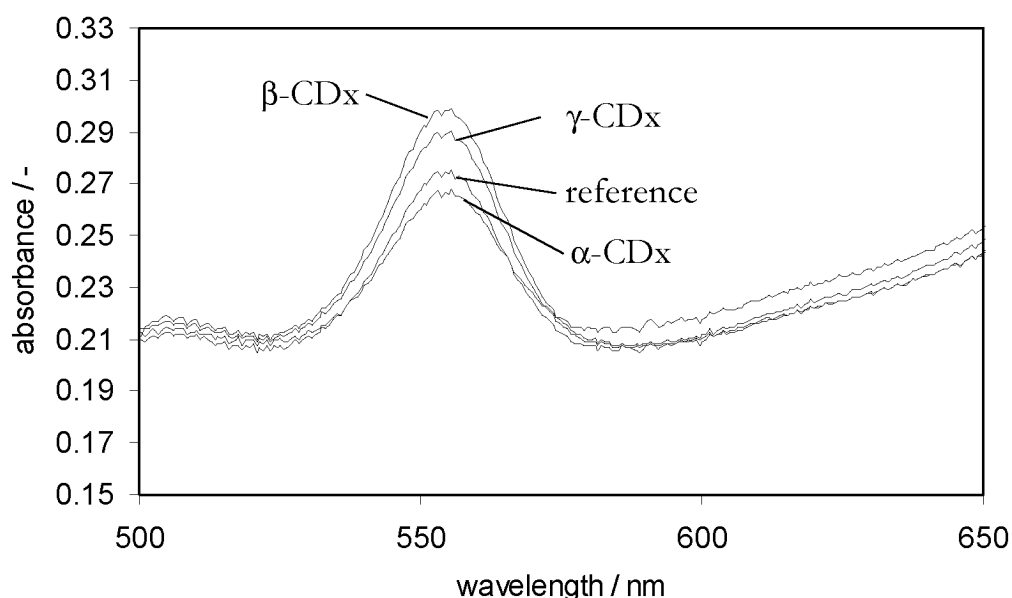
Fig. 5-4:   Absorption spectra of indigo radical in the absence and the presence of 16 mM cyclodextrin (CDx).

However, the addition of cyclodextrin changes the peak current to smaller values for all of the three cyclodextrins (*Figure 5-5*), indicating that the cyclodextrins prevent the indigo radical from diffusing to the electrode. In summary, cyclodextrins do not seem to be appropriate additives in the direct electrochemical reduction of indigo radical at an industrial scale.
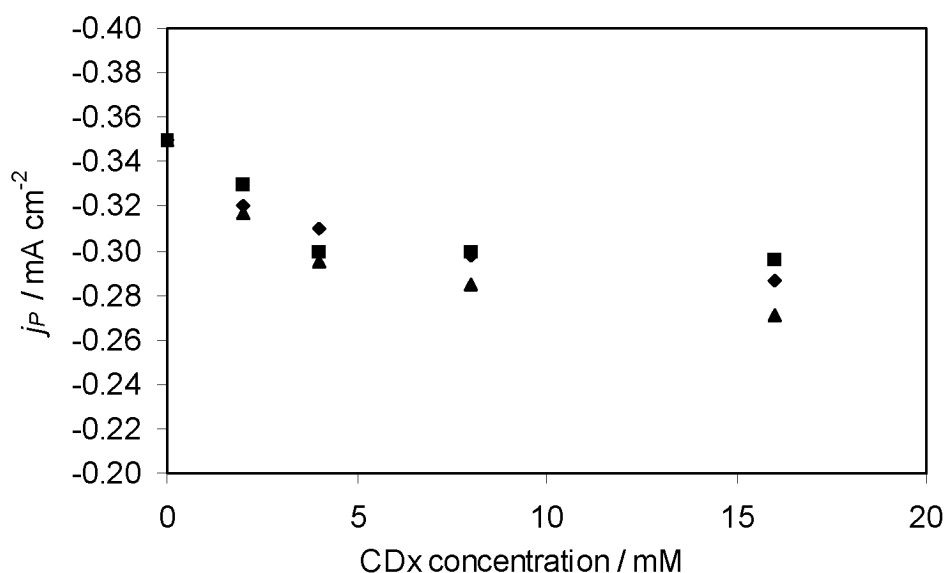
Fig. 5-5: Cathodic peak current density j_P *vs.* the concentration of cyclodextrin (10^{-6} M indigo radical in 1 M NaOH at 50°C, 10 mV s^{-1} scan rate). (◆) α-cyclodextrin, (■) β-cyclodextrin, (▲) γ-cyclodextrin.

5.3.3 Effects of surfactants

Surfactants play an important and interesting role in a wide variety of electrochemical systems [198]-[204]. In the present study, voltammetric experiments were performed to evaluate the effect of the surfactant type. Several surfactants were investigated as typical representatives for their classes, *i.e.*, for cationic surfactants: hexadecyltrimethylammonium chloride (HDTA); for anionic surfactants: sodium dodecyl sulphate (SDS) and sodium dodecylbenzenesulfonate; for non-ionic surfactants: alkylpolyethylenglycolether (Lutensol A8) and polyethyleneglycol 400. Additionally, also pyrolidone-type surfactants were investigated, because *N*-methylpyrolidone can prevent the leuco dye from being oxidized [194], [195]. However, the addition of Surfadone LP-100 (*N*-(n-

dodecyl)-2-pyrrolidone) and 300 (*N*-(n-octyl)-2-pyrrolidone) led to the formation of an oil layer on the water surface containing the whole indigo.

In the presence of non-ionic surfactants (Lutensol A8, polyethyleneglycol 400) the peak potential shifted slightly towards more positive values, but the peak current was dramatically diminished (for instance data of Lutensol A8 are shown in *Figure 5-6*). This effect is mainly based on a decrease of the radical concentration, because non-ionic surfactants destabilise this species. However, the peak current is also decreased during measurements with a constant radical concentration. From this it can be concluded that the surfactant is adsorbed on the electrode surface exerting a negative effect on the electron transfer kinetics.
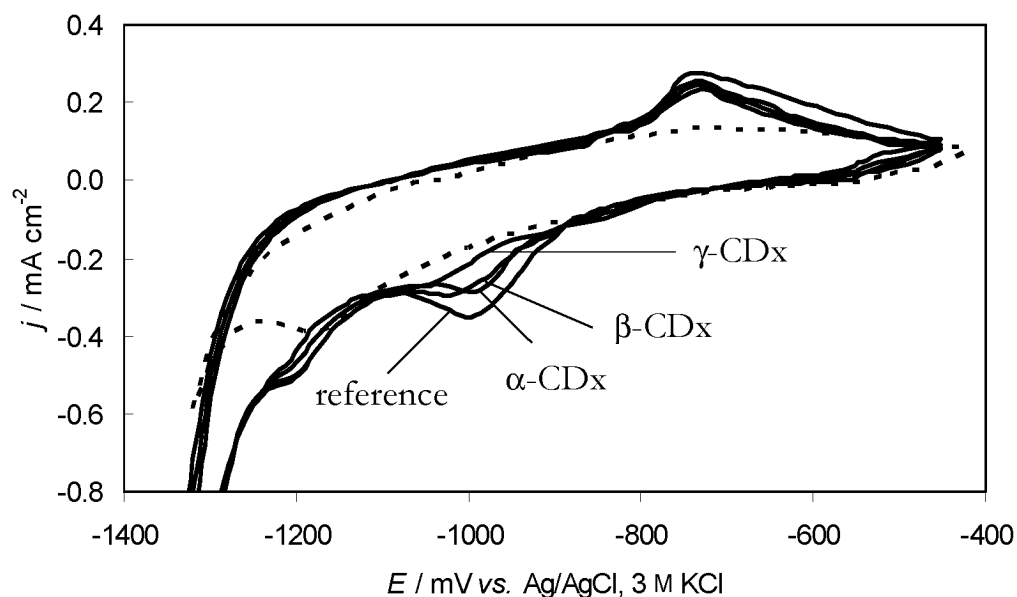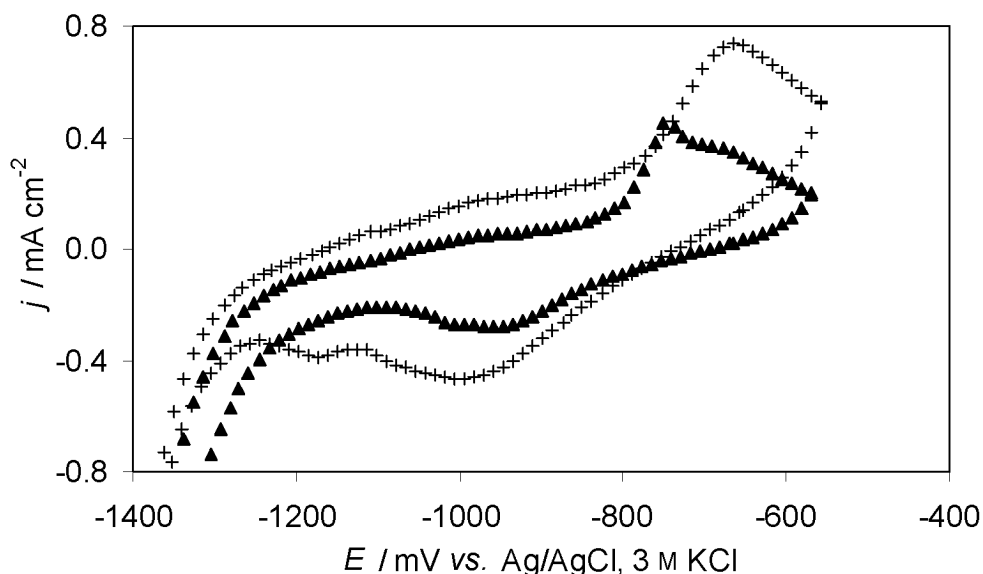

Fig. 5-6: Cyclic voltammogram of 10^{-5} M indigo radical in 1 M NaOH at 50°C at a scan rate of 10 mV s^{-1} in the potential region of -400 to -1400 mV with 10 mM Lutensol A8[1]. (+) without Lutensol A8, (▲) with Lutensol A8.

The same was valid for the anionic surfactants (SDS, sodium dodecylbenzenesulfonate) (for instance data of SDS are shown in *Figure 5-7*). These three surfactants can neither stabilise the radical nor sustain the electron transfer. On

---

[1] For Lutensol A 8 a critical micellar concentration *CMC* between $1 \cdot 10^{-5}$ and $10 \cdot 10^{-5}$ mol l^{-1} has been estimated due to data given by *Kosswig* [201].

the contrary, they suppressed the electroreduction by blocking the electrode [200].
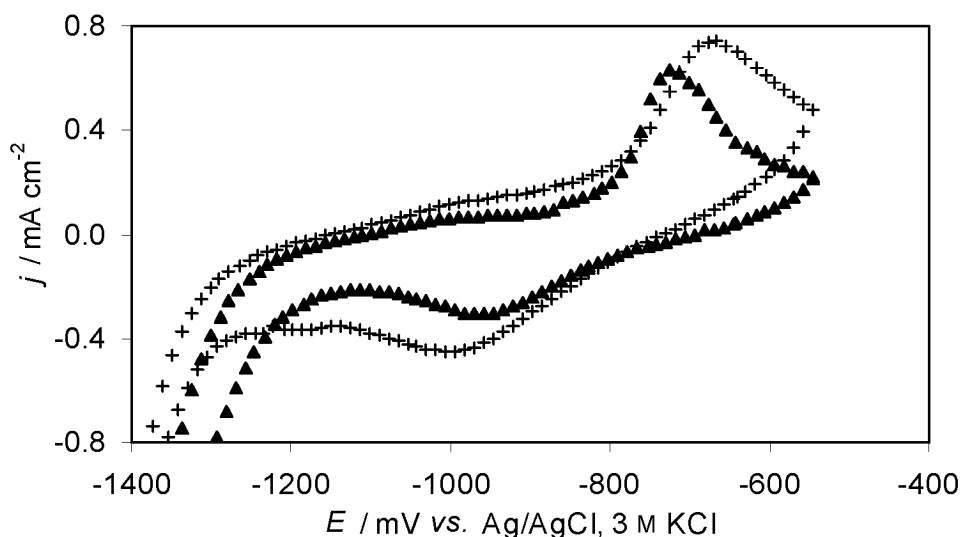
Fig. 5-7:   Cyclic voltammogram of 10^{-5} mol l^{-1} indigo radical in 1 mol l^{-1} NaOH at 50°C at a scan rate of 10 mV s^{-1} in the potential region of -400 to -1400 mV with 10 mM SDS^2. (+) without SDS, (▲) with SDS.

A completely different behaviour was observed with the cationic surfactants. Addition of this type of surfactants increased the radical concentration by a factor of 5 - 10 (*Figure 5-8*) and the electrode kinetics was influenced positively.

Increasing concentrations of the cationic surfactant (HDTA) shifted the peak potential to more positive values (from -1010 mV to -974 mV *vs.* Ag/AgCl, 3 M KCl with 2 mM HDTA), whereas the peak current remains more or less unchanged (*Figure 5-9*), (*Figure 5-10*). The dependence of j_p (at the same radical concentration) on the surfactant concentration in 1 M NaOH resembled the shape of a typical adsorption isotherm for the adsorption of polar surfactants on charged surfaces (*Figure 5-11*) [199], [205], [206]. Therefore, there appears to exist a direct relationship between the electroreduction of the indigo radical and the adsorption of the cationic surfactant on the cathode. Such interactions were also observed for other electrochemical syntheses (*e.g.*, the reduction of acetophenone or the reduction of oxygen to hydrogen peroxide

---

^{2} The critical micellar concentration *CMC* of SDS is approximately $8 \cdot 10^{-3}$ mol l^{-1} [202].

[205]). In *Figure 5-11* two regions could be identified. At low surfactant concentrations approximately up to 1 mM, the cationic surfactant had little effect on the peak current, whereas at concentrations close to 1 - 2 mM the peak current increases and reached a constant value at high concentrations. This result is in good agreement with the value of 0.0013 mol l^{-1} for the critical micellar concentration *CMC* published by *Rosen* [207].
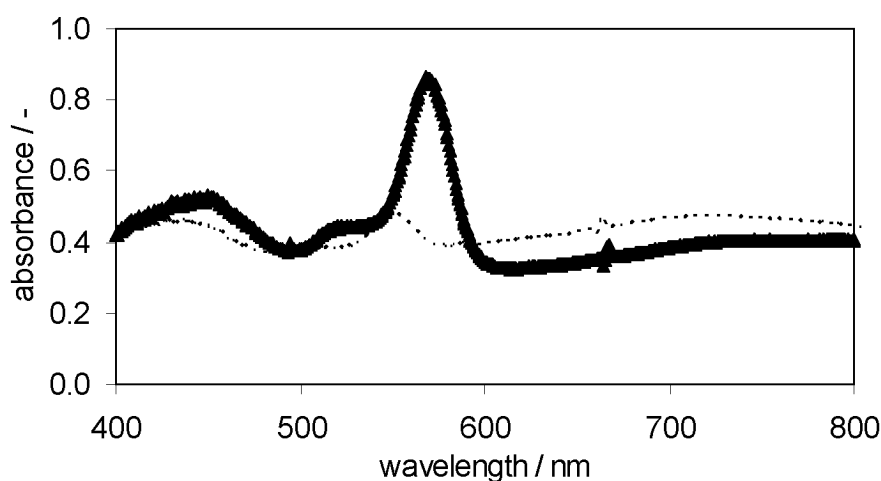
Fig. 5-8: UV/VIS-spectra of 1 M NaOH and a total amount of $2 \cdot 10^{-4}$ M indigo, leuco dye and radical at 50°C before and after the addition of HDTA (2 mM). With addition of HDTA (= solid line), reference (= dashed line).
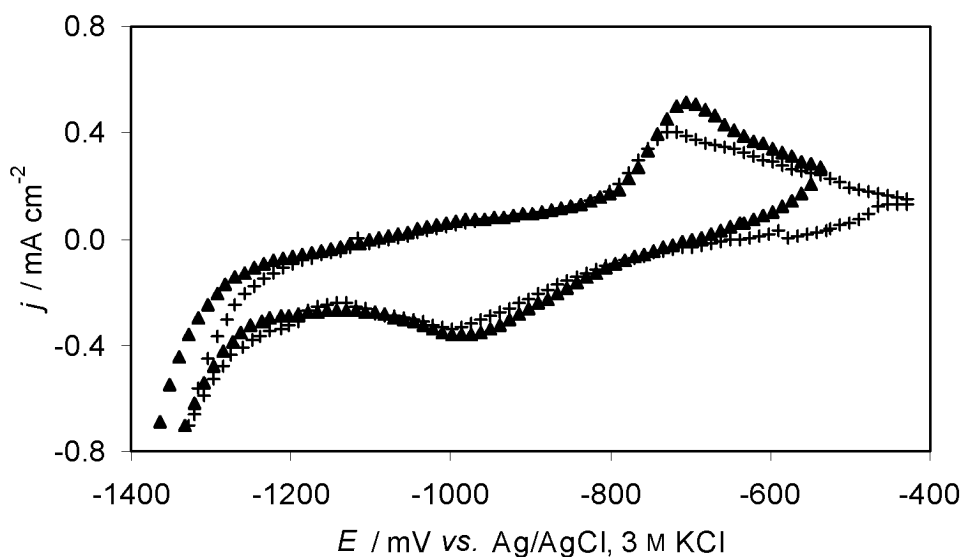
Fig. 5-9: Cyclic voltammogram of 10^{-5} M indigo radical in 1 M NaOH at 50°C at a scan rate of 10 mV s^{-1} in the potential region of -400 to -1400 mV with 2 mM HDTA. (+) without HDTA, (▲) with HDTA.
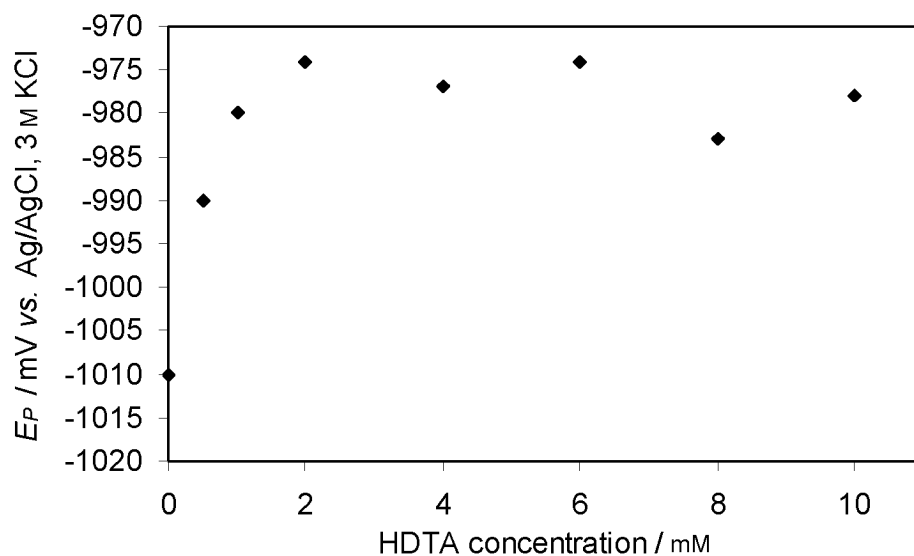
Fig. 5-10:   Peak potential E_p for the reduction of the indigo radical on the first scan *vs.* the HDTA concentration (10^{-5} M indigo radical, 1 M NaOH at 50°C at a scan rate of 10 mV s^{-1}).
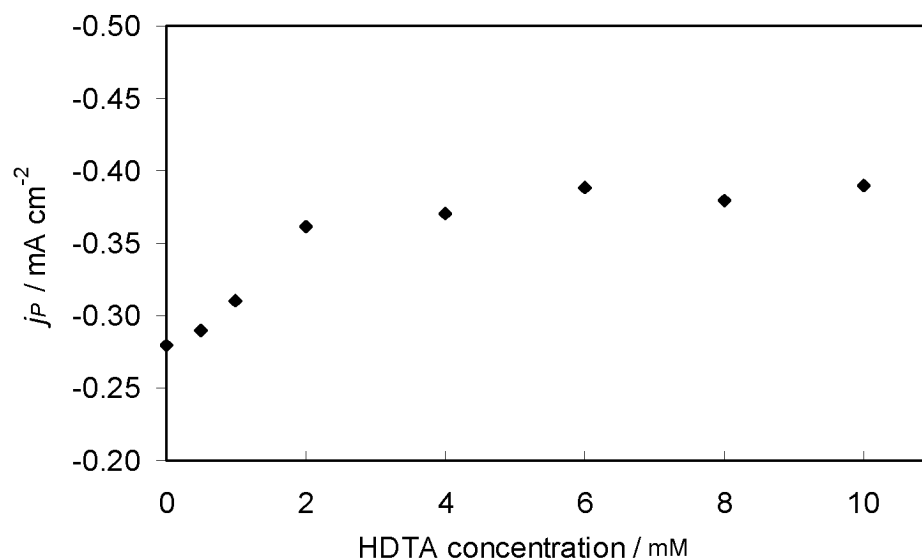
Fig. 5-11:   Peak current j_p for the reduction of the indigo radical on the first scan *vs.* the HDTA concentration (10^{-5} M indigo radical, 1 M NaOH at 50°C at a scan rate of 10 mV s^{-1}).

Unfortunately, it was observed that the leuco dye formed precipitates with the cationic surfactant. The yellow-coloured solid product cannot be reoxidized to indigo by air and it is impossible to dissolve it in EtOH or MeOH. Therefore, a screening was performed to find another cationic surfactant which can stabilise the radical and which does not precipitate with the reaction

product leuco indigo. The following list gives an survey about the tested substances:

hexyltrimethylammonium bromide
octyltrimethylammonium bromide
trimethyloctylammonium chloride
dodecyltrimethylammonium bromide
octadecyltrimethylammonium chloride
benzyltrimethylammonium bromide
didodecyldimethylammonium bromide
methyltributylammonium chloride
methyltrioctylammonium bromide
tetrahexylammonium bromide
tetraoctylammonium bromide
3-(N,N-dimethyloctylammonio)-propane sulfonate
Lutensit TC-KLC 50
Hyamine 1622

The addition of all these surfactants leads to precipitation, because obviously the hydrophobic chain is too long. It was tried to employ choline chloride ((2-hydroxyethyl)trimethylammonium chloride), which contains only a short hydrophobic chain with an hydroxyl group. No precipitation was observed, but unfortunately this molecule cannot stabilise the radical.

In addition, combinations of several surfactants were tested (*Table 5-1*), because in surfactant chemistry synergistic effects by mixing surfactants are well known. However, no mixture has been found so far which does not led to precipitation of an insoluble complex of surfactant and leuco dye.

Table 5-1:   Combinations of surfactants tested

cationic surfactant	additional surfactant
HDTA	SDS sodium dodecylbenzenesulfonate Lutensol A8 polyethyleneglycol 400
Hyamine 1622	SDS sodium dodecylbenzenesulfonate Lutensol A8 polyethyleneglycol 400
Lutensol KLC 50	SDS sodium dodecylbenzenesulfonate Lutensol A8 polyethyleneglycol 400

5.3.4 Effect of dispersing agents

Vat dyeing and printing processes involve the application of insoluble dyes in form of a dispersion [196], [197]. Therefore, dispersing agents are used in the application of these dyes for the following reasons [196]:

- As the air oxidizes the vat, insoluble dye particles form continuously and have to be maintained in a finely dispersed state to facilitate their rapid re-reduction.
- When the dyeings are oxidized at the end of the dyeing process, the dispersing agents ensure that the excess pigment remains in finely dispersed form so that it can be rinsed out rapidly.

For this application, condensation products of β-naphthalene sulphonic acid with formaldehyde (NCS products), lignin sulphonates and protein-fatty acid condensation products are used. NCS products belong to the oldest class of dispersing agents still being used in large amounts in the dyehouse.

Although these products, which became known as the *Tamol* types, have been used for a very long time, their constitution is not yet completely known. The following formula indicates schematically the assumed structure (*Figure 5-12*) [196].
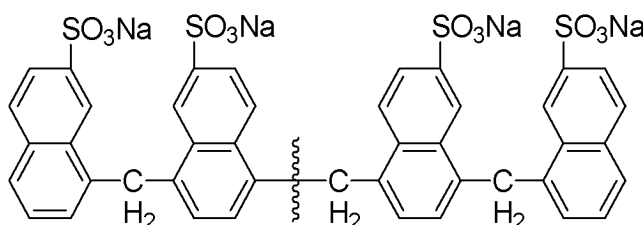
Fig. 5-12:   Condensation product of β-naphthalene sulphonic acid and formaldehyde (NCS product).

Voltammetric experiments were performed to evaluate the effect of Setamol WS. Unfortunately, it can neither stabilise the radical nor sustain the electron transfer. However, on the contrary to non-ionic and anionic surfactants, it did not suppress the electroreduction (*chapter 5.3.3*). Thus, the application of Setamol WS as a dispersing agent is still consistent with its general application in electrochemical processes for the reduction of vat dyes.

5.4 Conclusions

Organic solvents can increase the radical concentration and, consequently, the reaction rates, but lasting effects were only observed at non-viable concentrations of higher than 20% (v/v).

The interaction of cyclodextrins with the indigo radical has been investigated in view of the electrolytic reduction of the dye radical. The addition of β- and γ-cyclodextrin changed the peak potential in the cyclic voltammogram, whereas α-cyclodextrin did not. As an additional evidence, spectrophotometric analyse corroborated a stabilising interaction between β- and γ-cyclodextrin and the indigo radical. However, all the cyclodextrins suppressed the electrolytic reduction of indigo radical. In summary, the β- and the γ-cyclodextrin can

stabilise the indigo radical lastingly, but unfortunately the electrochemistry is influenced negatively.

The influence of surfactants (cationic, non-ionic and anionic) on the electroreduction of the indigo radical was investigated on Ni-electrodes. The non-ionic and anionic surfactant (*e.g.* Lutensol A8 and SDS) destabilised the indigo radical and, in addition, retarded the electroreduction by forming less organized surface aggregates, which block the access of the radical to the electrode. In contrast, cationic surfactants (*e.g.* HDTA) can stabilise the radical, and the electrode kinetics is influenced positively. However, several problems due to the precipitation of leuco dye with cationic surfactants were observed. Until now, no cationic surfactant molecule was found which does not precipitate with leuco indigo, the reaction product.

The application of Setamol WS as a dispersing agent is still consistent with its general application in electrochemical processes for the reduction of vat dyes, because it has no negativ effect on the electrochemical process.

Unfortunately, it must be conceded that until now the reactor performance is too low for an industrial application. Therefore, still new alternatives improving the eco-efficiency of the application of vat dyes have to be found.

Electrocatalytic hydrogenation of vat dyes Part I: Preliminary experiments and mechanistic investigations

6.1 General aspects

Many attempts are being made to replace in the vatting process the environmentally unfavourable reducing agent sodium dithionite by ecologically more attractive alternatives (*chapter 2*). For example, systematic electrochemical investigations of the indigo system led to a reduction process employing a redox mediator (*chapter 2.4.2*) as well as to a process based on the formation of the dye radical anion and the subsequent electrochemical reduction of this radical (*chapters 3 - 5*). However, in both cases the specific reactor performance is yet low and still some problematic chemicals have to be employed.

Based on this continuing demand for improving the eco-efficiency of the dyeing process and on the fact that the catalytic hydrogenation of indigo is a well known process [109], investigations in the present thesis were extended to a novel, environmentally friendly route for the reduction of vat dyes by electrocatalytic hydrogenation (ECH). This 'green' technology offers many advantages over conventional techniques including cost and energy efficiency, since it does not require any reducing agent. ECH involves the electrochemical reduction of water to produce adsorbed hydrogen (*Figure 6-1, reaction 6.1, Volmer* step) which reacts chemically with an organic substrate (*Figure 6-1, reaction 6.2*) at the surface of a metal powder catalyst (*e.g. Raney* nickel or platinum black) which is electrically conductive and exhibits a low hydrogen-overvoltage. The catalytic material serves both as the electrode (to generate the hydrogen) and as the catalyst for the hydrogenation. Thus, the process can be clearly

differentiated from an electron transfer process (electronation[1]-protonation-mechanism, EP-mechanism) where hydrogen is involved only in a protonation step after the electron transfer has occured [207]-[209].

For many years, ECH has been applied successfully to various substrates and it has several advantages over the catalytic hydrogenation. The kinetic barrier due to the splitting of the hydrogen molecule is completely bypassed. Thus, elevated temperatures and pressures can be avoided. Furthermore, the electrochemical production of hydrogen directly on the catalyst surface circumvents the compression, transportation and the storage of hydrogen [207]. An important limitation comes from the competition between the hydrogenation (*Figure 6-1*, *reaction 6.2*) and the formation of molecular hydrogen from adsorbed hydrogen (*Figure 6-1*, *reaction 6.3* and *6.4*), respectively the *Heyrovský* and *Tafel* steps of the evolution of hydrogen [211].

$$2\ H_2O + 2\ e^- \longrightarrow 2\ H_{ad} + 2\ OH^- \qquad (6.1)$$

indigo   leuco indigo

$$\qquad\qquad\qquad\qquad\qquad\qquad\qquad\qquad\qquad (6.2)$$

$$H_2O + H_{ad} + e^- \longrightarrow H_2 + OH^- \qquad (6.3)$$

$$2\ H_{ad} \longrightarrow H_2 \qquad (6.4)$$
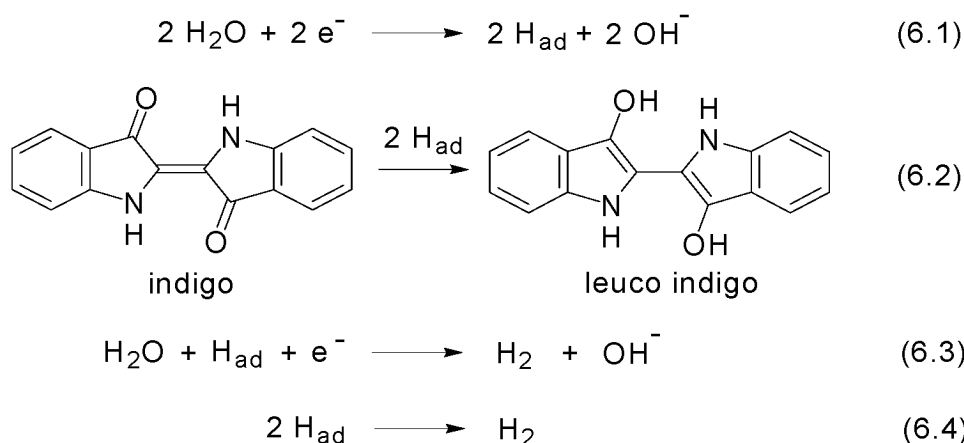
Fig. 6-1: Electrocatalytic hydrogenation of indigo

Recently this principle has been used in the so-called precoat-layer-cell (*chapter 2.4.3*) [151], [152]. The severe drawback of this technique seems to be the large pressure drop built up during the filtration process.

Therefore, these studies provide ECH of vat dyes on electrodes comprising a thin grid coated with a layer of metal in which fine particles of the catalyst are embedded.

---

[1] Electronation is the addition of an electron (or electrons) to an element or molecule [206].

6.2 Experimental

6.2.1 Chemicals

All aqueous solutions were prepared with deionized water. Indigo was supplied from BASF, Ludwigshafen, Germany. C.I. Vat Red 10 and C.I. Vat Green 1 were supplied from DyStar Textilfarben, Frankfurt, Germany. C.I. Vat Orange 9, C.I. Vat Orange 17, C.I. Vat Blue 21 and C.I. Vat Red 28 were supplied from BEZEMA AG, Montlingen, Switzerland. All other chemicals were analytical grade, purchased from Fluka and used as received without further purification.

6.2.2 Electrodes

The high surface area cathodes with a geometric area of 30 cm^2 were prepared in two different ways on a 100 mesh stainless steel grid (G. Bopp + Co. AG, Switzerland). Noble metal blacks were prepared by electrodeposition using literature procedures (platinum [212], palladium [213] and rhodium [214]). The convenient $Raney$-type electrodes were prepared by co-deposition of $Raney$ alloy particles with the electrodeposited nickel metal on the mesh followed by an activation step by immersing the electrode in a 30% (w/v) NaOH solution at 70°C for 10 h and washing it with deionized water [210], [211]. The cathodes were stored in a 5% (w/v) NaOH solution until used. Nickel was plated at a current density of 30 mA cm^{-2} (based on the geometric electrode area) and 70°C from a well stirred plating solution consisting of 300 g l^{-1} NiCl$_2$·6H$_2$O, 45 g l^{-1} NiSO$_4$·6H$_2$O and 30 g l^{-1} H$_3$BO$_3$ and 5 g l^{-1} of dispersed $Raney$ nickel alloy particles (Ni:Al 50:50 (w/w)). A piece of nickel was used as the anode. Both electrodes were mounted parallel in a vertical position. The current was applied for 30 min with one rotation (180°) of the cathode every 5 min to obtain a homogeneous distribution of the electrodeposition on both sides of the electrode. The amount of co-deposited Ni/Al-alloy before leaching was typically 8-12 mg cm^{-2} compared to 15.7 mg cm^{-2} for the electrodeposited nickel. Scanning electron microscopy studies have shown that the $Raney$ nickel particles are fixed in a porous layer of plated nickel (*Figure 6-2*). Elec-

trodes usually have a surface area of 8.57 ± 0.006 m^2 g^{-1} determined by the BET-isotherm. The content of aluminium could be reduced to very low contents by leaching.
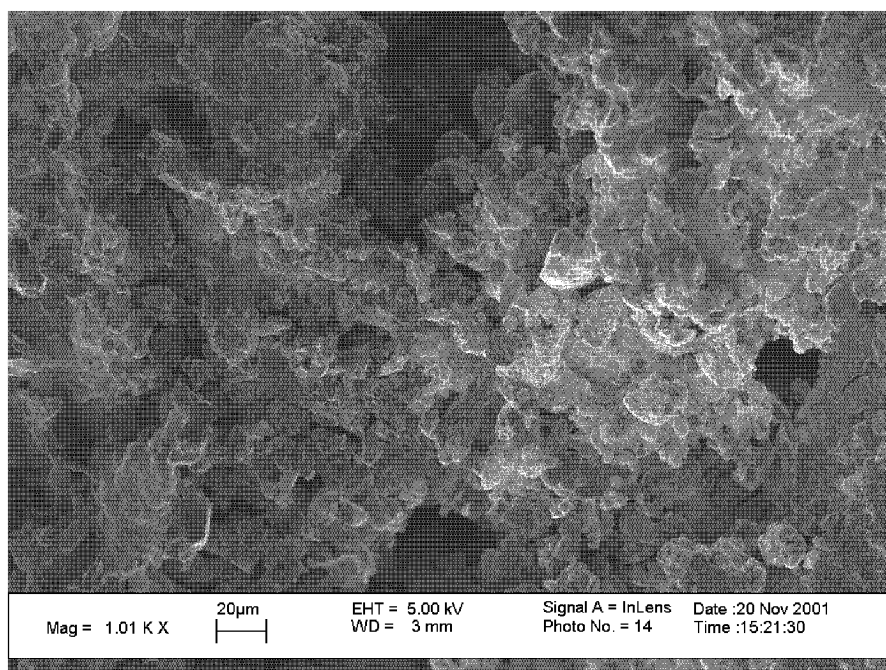
Fig. 6-2:   SEM micrograph of the *Raney* nickel composite-coated electrode.

Devarda copper has been prepared by a similar procedure by plating copper at 15 mA cm^{-2} and 70°C from a solution made of 200 g l^{-1} CuSO$_4$·5H$_2$O and 30 g l^{-1} H$_3$BO$_3$ with suspended 5 g l^{-1} *Devarda* copper alloy (Cu-Al-Zn 50:45:5 (w/w)) by using a copper anode. *Raney* cobalt was produced by co-deposition at 50 mA cm^{-2} and 70°C from a solution of 330 g l^{-1} CoSO$_4$·7H$_2$O and 30 g l^{-1} H$_3$BO$_3$ with suspended 5 g l^{-1} *Raney* cobalt alloy (Co-Al 31:69 (w/w)) by using a cobalt anode.

The preparation of *Raney* nickel electrodes mixed with small amounts of noble metals was achieved in the same way as mentioned before, but in addition different amounts of noble metal black were present in the plating electrolyte. Typical catalyst concentrations in the galvanic bath were in the region of 0.01 - 0.1 g l^{-1} and led to co-deposited amounts of 0.02 - 0.2 mg cm^{-2}.

6.2.3 Procedure

The electrohydrogenations were carried out at constant current densities (based on the geometric electrode area) in a two-chamber glass reactor in which the anode and cathode compartments were separated by a Nafion-324 cation-exchange membrane. In the 100 ml anodic cell compartment a Pt/Ru expanded mesh was used during the experiments as the counter electrode. The cathode compartment containing two glassfiber sensors for online spectrophotometric measurements (GMP, Jobin Yvon) also has a volume of 100 ml. Both cells were connected to a thermostat (Colora Messtechnik GmbH). A potentiostat (Amel 549) was used for the electrolysis experiments. Cathodic suspensions of indigo were composed of 1 M NaOH and 2 g l^{-1} of the vat dyes. They were deoxygenated during at least 2 h before the experiment and maintained under an argon atmosphere during the measurements. Anodic solutions consisted of 1 M NaOH solution.

6.2.4 Electrode characterization

The morphology of the obtained electrodes and the Ni/Al-relation was studied by scanning electron microscopy with EDX analysis (LEO C 1530) and the BET-isotherm (MICROMERETICS ASAP 2000).

6.3 Results and discussion

6.3.1 Electrocatalytic hydrogenation of indigo

ECH of indigo (C.I. Vat Blue 1) has been examined with various cathode materials, the leuco indigo being produced directly from the indigo suspension. The hydrogenation product was identified by spectrophotometric analysis (λ_{max} = 410 nm). In general, laboratory dyeing experiments show a dyeing behavior of the electrohydrogenated indigo similar to that of conventional reduction methods. In addition, in the vast majority of cases a 95% mass bal-

ance for indigo was obtained after the experiment by reoxidation to the insoluble product and filtration. Therefore, it is obvious that the reaction product is stable under the applied conditions and no other hydrogenation products are formed (*e.g.* by overreduction).

Table 6-1 summarizes the results of the influence of the electrode material. Palladium and rhodium are less active catalysts than platinum. In the case of *Raney*-type electrodes nickel is the most active catalyst, but with 3.5% current efficiency is very low. These results follow at least qualitatively the sequence established from catalytic hydrogenation [215]. Platinum and rhodium are well known to catalyse the hydrogenation of organic substrates at atmospheric pressure. Therefore, they are also effective under the applied electrochemical conditions. Palladium, which usually requires increased pressures and temperatures for normal hydrogenation, causes a lower electrocatalytic conversion. Nickel, which normally requires very severe conditions, shows very low electrohydrogenation. Instead, a large amount of hydrogen is evolved and both the current efficiency and the extent of hydrogenation are diminished. In the case of this reaction, the current efficiency is directly coupled to the conversion, because no side reaction (as, *e.g.*, overreduction) is taking place. Nevertheless, *Raney* nickel was chosen as the electrode material, because it is interesting from the standpoint of availability, costs and stability in alkaline media. The stability of platinum-black electrodes was shown to be poor, so that their industrial application does not seem feasible. Usually the *Raney*-type electrodes had a lifetime of 15 - 20 days in comparison to 1 - 2 days in the case of noble metal blacks. However, their activity was decreasing very fast after that time, because the *Raney* nickel particles just fell off the electrode, obviously because, due to the hydrogen evolution, the *Raney* nickel particles become rather crumbly.

A preliminary process optimization with *Raney* nickel electrodes was performed by analysing the effect of increasing the current density from 0.1 to 100 mA cm^{-2} (*Table 6-2*). Between 0.1 to 10 mA cm^{-2}, the small increase in cathodic polarization associated with the increase of current density favours the hydrogenation over the hydrogen evolution. This leads to an increase of both the current efficiency and the extent of hydrogenation. In turn, a further increase of the current density favours the hydrogen evolution over the hydro-

genation as shown by the diminution of the current efficiency and of the extent of hydrogenation.

Table 6-1:   Electrohydrogenation of indigo with different catalysts

Catalyst	Conversion[a] / %	Current efficiency / %
Pt-black	81.9	65.5
Rh-black	61.1	48.9
Pd-black	54.5	43.6
Raney nickel	4.4	3.5
Raney cobalt	2.9	2.3
Devarda copper	1.4	1.1

[a] The conversion or yield of the leuco compound was determined by spectrophotometric analysis. System parameters: 1 M NaOH, 2 g l^{-1} indigo, 50°C, current density 20 mA cm^{-2}, 32 cm^2 geometric electrode surface. Charge passed (Q) = 5 F mol^{-1}. Material balance > 95%.

Table 6-2:   Effect of the current density on the ECH of indigo at *Raney* nickel electrodes

Current density j[a] / mA cm^{-2}	Conversion[b] / %	Current efficiency / %
0.1	28.8	2.3
0.5	36.3	2.9
1	37.5	3.0
5	40.0	3.2
10	47.5	3.8
50	32.5	2.6
100	21.3	1.7

[a] Based on the geometric electrode area.

[b] The conversion or yield of the leuco compound was determined by spectrophotometric analysis. System parameters: 1 M NaOH, 2 g l^{-1} indigo, 50°C, current density 20 mA cm^{-2}, 32 cm^2 geometric electrode surface. Charge passed (Q) = 50 F mol^{-1}. Material balance > 95%.

6.3.2 Electrocatalytic hydrogenation of other vat dyes

To show the versatility of the new method, the electrocatalytic hydrogenation of various dye molecules has been studied at *Raney* nickel electrodes (*Table 6-3*), the variety basing on the following three classes of vat dyes: anthraquinone dyes, fused ring polycyclic dyes and indigoid dyes. It was possible to reduce C.I. Vat Green 1 (16,17-dimethoxyviolanthrone) with a current efficiency of 4.2 %, whereas all other dyes led to lower values. This is probably due to the higher solubility of C.I. Vat Green 1. In the case of two other dyes shown in *Figure 6-3* (C.I. Vat Red 10 (**7**) and C.I. Vat Orange 17 (**8**)), no conversion has been observed. However, it is important to mention that the dye molecules did not decompose either. This was also proved by the mass balance after reoxidation to the insoluble product and filtration of the electrolyte. The diminished mass balance of 90% is probably due to the loss of material by adsorption on the catalyst (*chapter 3.3.2*).
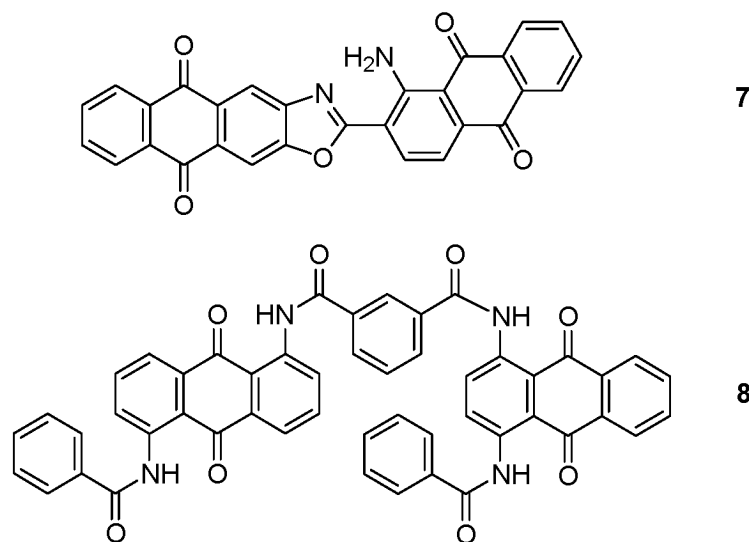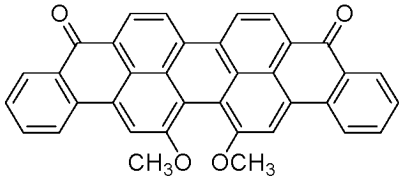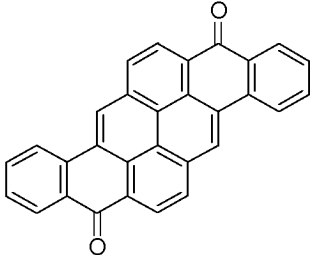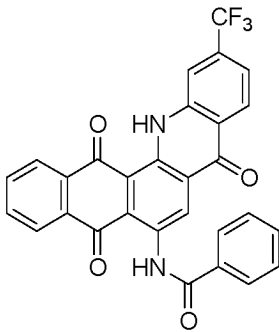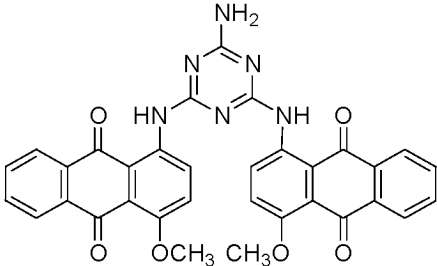
Fig. 6-3: Structures of the two dyes, C.I. Vat Red 10 (**7**) and C.I. Vat Orange 17 (**8**).

6.3.3 Results with doped electrodes

In all experiments the highest current efficiencies were obtained under a pH of 14, a current density of 20 mA cm^{-2} and 70°C in combination with the use of ultrasound and 10% (v/v) methanol as co-solvent. Under these conditions a current efficiency of 12.7% could be reached at 95% conversion. How-

Table 6-3:   ECH of different dye molecules at *Raney* nickel electrodes

Substrate	Formula	Conversion[a] / %	Current efficiency / %
C.I. Vat Green 1		52.5	4.2
C.I. Vat Orange 9		24.3	3.9
C.I. Vat Blue 21		26.2	2.1
C.I. Vat Red 28		20.0	1.6

[a] The conversion or yield of the leuco compound was determined by spectrophotometric analysis. System parameters: 1 M NaOH, 2 g l^{-1} indigo, 50°C, current density 20 mA cm^{-2}, 32 cm^2 geometric electrode surface. Charge passed (Q) = 50 F mol^{-1}. Material balance > 90%.

ever, this value is very small and should be improved. From previous studies it is known that electrodes made of noble metal blacks (*e.g.* platinum black) can

enhance the current efficiency of the ECH process up to 70%. These results can be compared at least qualitatively with the sequence established from the catalytic hydrogenation. Platinum is a well known hydrogenation catalyst at atmospheric pressure, but nickel normally requires more severe conditions. Therefore, platinum is also more effective than nickel under the applied electrochemical conditions. However, the stability of platinum-black electrodes is even worse than that with *Raney* nickel. Therefore, it was interesting to analyse as an alternative the effect of adding different contents of noble metal particles to the *Raney* nickel electrodes. The stability of these new electrodes was similar to that of *Raney* nickel, but their catalytic activity was enhanced significantly (*Table 6-4*).

Table 6-4:   Electrohydrogenation of indigo using *Raney* nickel electrodes doped with different noble metal catalysts

Catalyst[a]	Conversion[b] / %	Current efficiency / %
Raney nickel (reference)	4.4	3.5
Raney nickel with Pt	10.2	8.2
Raney nickel with Pd	8.6	6.9
Raney nickel with Pd/C[c]	4.7	3.8

[a] The amount of catalyst on the electrode was 0.2 mg cm^{-2}.

[b] The conversion was determined by spectrophotometric analysis. System parameters: 1 M NaOH, 2 g l^{-1} indigo, 50°C, current density 20 mA cm^{-2}, 32 cm^2 geometric electrode surface. Charge passed (Q) = 5 F mol^{-1}. Material balance > 95%.

[c] 5 wt.% Pd on activated charcoal (Fluka).

Increasing the amount of platinum in the electrode by using higher catalyst concentrations in the plating electrolyte was analysed in small-scale laboratory experiments in an H-cell (*Figure 6-4*). Obviously this can enhance both the conversion and the current efficiency, but significant effects could be observed only above at least 0.02 mg cm^{-2} platinum. This may be caused by the fact that small amounts of platinum particles are completely covered by plated nickel. If in the laboratory flow cell an electrode doped with 0.15 mg cm^{-2} platinum is

employed, under the optimized conditions mentioned above the current efficiency at 95% conversion could be increased up to 19.2%.
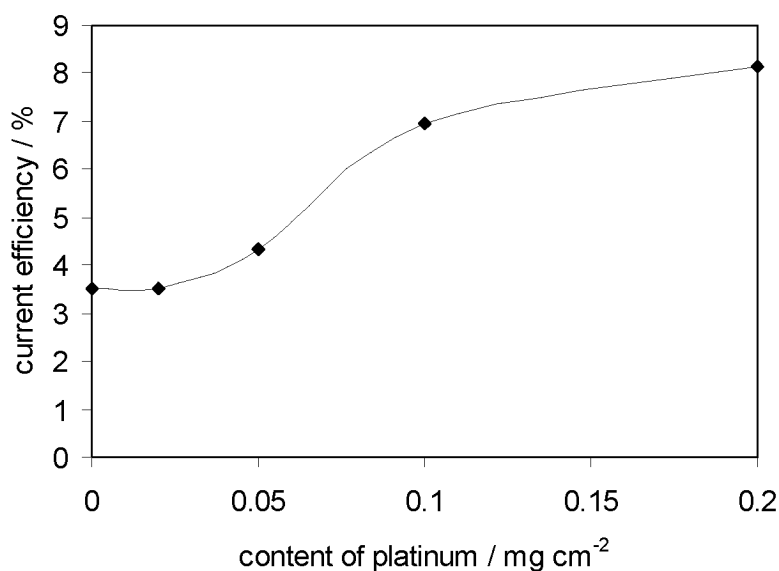
Fig. 6-4:   Influence of the platinum content in doped *Raney* nickel electrodes for the ECH of indigo after 5 F mol^{-1}, measured in an H-cell. System parameters: 1 M NaOH, 2 g l^{-1} indigo, 50°C, current density 20 mA cm^{-2}, 32 cm^2 geometric electrode surface.

6.3.4 Mechanistic investigations

The direct electrochemical reduction (EP-mechanism) of suspended indigo has never been observed at planar electrodes not exhibiting catalytic activity towards hydrogenation. However, the electrode surfaces are significantly increased by changing from planar metal sheets to porous *Raney* nickel electrodes. For this reason, the common electrochemical reduction by electron transfer (EP) cannot be excluded. Thus, a mechanistic proof for the hydrogenation process has been given with a method described by *De Hemptine* [208], [209], [216], [217]. The production rate of hydrogen was determined at a platinum-black electrode in electrolytes with and without indigo by a combination of a gas burette with the H-cell (*Figure 6-5*). Based on *Faradays* law, a straight line starting at the origin of the diagram was determined in the absence of indigo. In the presence of indigo the line shifts clearly to a certain current density - after which hydrogen gas (HER) is developed. Therefore, the process can

be identified with no doubt as the electrocatalytic hydrogenation (ECH), because an electrochemical reduction (EP) would end up in a nonlinear gas evolution behavior, starting in the origin of the diagram [216]. However, this test is only valid if no other electrochemical reaction is taking place at the electrode (as, *e.g.*, radical reduction). Therefore, platinum has been used as the electrode material. Due to its low hydrogen overpotential compared to nickel, even the electrochemical reduction of the indigo radical is suppressed before the hydrogen starts to evolve (*Figure 6-6*).
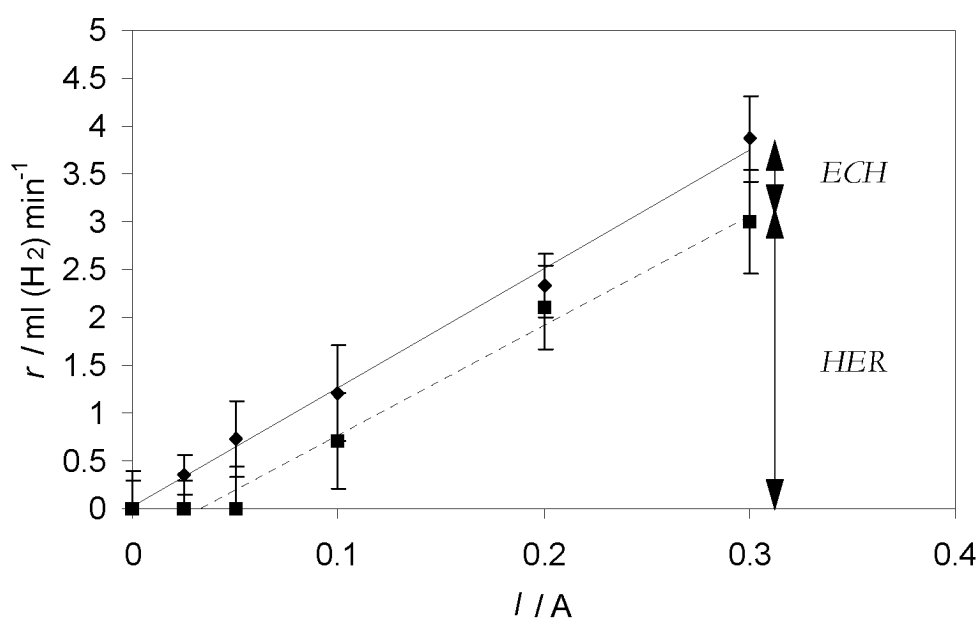
Fig. 6-5:   Hydrogen production rate r as a function of the current I at a platinum-black electrode with (= dashed line) and without (= solid line) indigo in the electrolyte. System parameters: 1 M NaOH, 1 g l^{-1} indigo, 50°C, 32 cm^2 geometric electrode surface. ECH: electrocatalytic hydrogenation; HER: hydrogen evolution reaction.
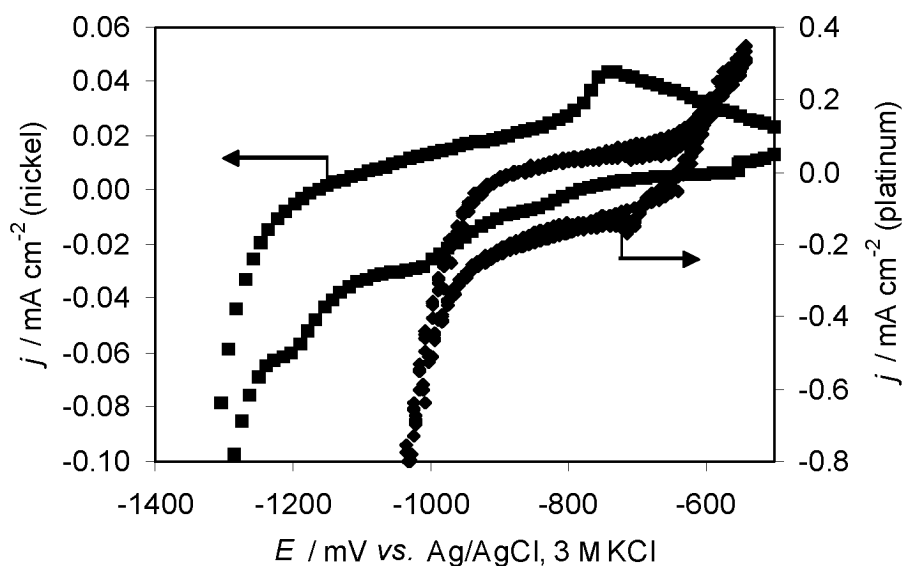
Fig. 6-6:   Cyclic voltammogram of a planar nickel and platinum-black electrode at a scan rate of 25 mV s^{-1} in the potential region of -200 to -1400 mV. System parameters: 1 M NaOH, 1 g l^{-1} indigo, 50°C, 0.2 cm^2 geometric electrode surface.

6.4 Conclusions

In summary, the feasibility of electrocatalytic hydrogenation as a new process for the reduction of vat dyes was shown. Important requirements of economy and ecology are fulfilled, because this process does not require any reducing agent.   Palladium and rhodium are less active catalysts than platinum. In the case of *Raney*-type electrodes − which are interesting from the standpoint of availability, costs and stability in alkaline media − nickel is the most active catalyst, but the current efficiency is much lower than with noble metal-black electrodes. Nevertheless, *Raney* nickel was chosen as the electrode material, because the stability of platinum-black electrodes was shown to be poor. However, the current efficiency could be increased to 19.2% by doping the *Raney* nickel electrodes with platinum particles.

The application has been investigated in small laboratory cells. Therefore, these results are just the basis for further work in scale-up and optimization studies (*chapter 7*).

Chapter *7*

Electrocatalytic hydrogenation of vat dyes Part II: Scale-up and optimization in laboratory-scale flow cells

7.1 General aspects

The results of the preliminary experiments with conventional H-cells (*chapter 6*) were used as a guide to design and operate continuous flow cells. Although platinum is the most active catalyst, *Raney* nickel was chosen as the electrode material for further work, because it is interesting from the standpoint of availability, costs and stability in alkaline media. In the present work, the electrocatalytic hydrogenation of an aqueous suspension of indigo was studied in a divided flow cell to determine the industrial feasibility of the method and to optimize the electrolytic conditions.

7.2 Experimental

7.2.1 Chemicals

All aqueous solutions were prepared with deionized water. Indigo was supplied from BASF, Ludwigshafen, Germany. Sodium hydroxide (Fluka, p.a.), nickel(II) chloride (Fluka, p.a.), nickel(II) sulphate heptahydrate (Fluka 72285, p.a.), boric acid (Fluka p.a.), *Raney* nickel alloy (Ni:Al 50:50 w/w, Fluka, purum) and nitrogen (99.99 %) were used as received without further purification.

7.2.2 Electrode preparation

The convenient *Raney*-type electrodes were prepared by co-deposition of *Raney* alloy particles with the electrodeposited nickel on a stainless steel mesh, followed by an activation step by immersing the electrode in a NaOH solution. The procedure is described in *chapter 6.2.2*.

7.2.3 Apparatus

A small multipurpose plate and frame cell (EC Electro MP-Cell from ElectroCell AB, Sweden) was chosen for the scale-up procedure. The cell and the set-up of the pilot plant used in the experiments are described in detail in *chapter 4.2.2*. As the working electrode a flat nickel plate electrode together with the above mentioned *Raney* nickel electrodes were used. The metal meshes were spot-welded to the plate to ensure good electrical conductivity and stacked with thin (about 0.2 mm) nickel strips at the edges and in the middle between the meshes in a vertical way.

7.2.4 Procedure

For flow-cell experiments, 10 g l^{-1} of indigo (sieve fraction between 0.06 - 0.08 mm, obtained with a sieve-machine AS 200, Fa. Retsch) were suspended in 1 M NaOH. In the case of H-cell experiments, only 0.1 g l^{-1} of indigo were used. The suspensions were deoxygenated during at least 2 h before the experiment and maintained under a nitrogen atmosphere during the measurements. Anodic solutions consisted of 1 M NaOH. In the case of varying the pH-values, the difference in ionic strength compared to 1 M NaOH (pH = 14) was compensated by the addition of NaCl.

7.3 Results and discussion

A series of galvanostatic runs was carried out in order to assess the effect of operating parameters such as current density, pH and temperature of the catholyte on the electrochemical kinetics. *Figure 7-1* shows a typical reaction profile of the ECH of indigo. Leuco indigo (λ_{max} = 410 nm) is produced directly from the indigo suspension and the red coloured radical species (λ_{max} = 565 nm) is produced after some time only in a very small amount by comproportionation of indigo with leuco indigo (*chapter 3.3*). Laboratory dyeing experiments proved a dyeing behavior of the electrohydrogenated indigo similar to that of conventional reduction methods.
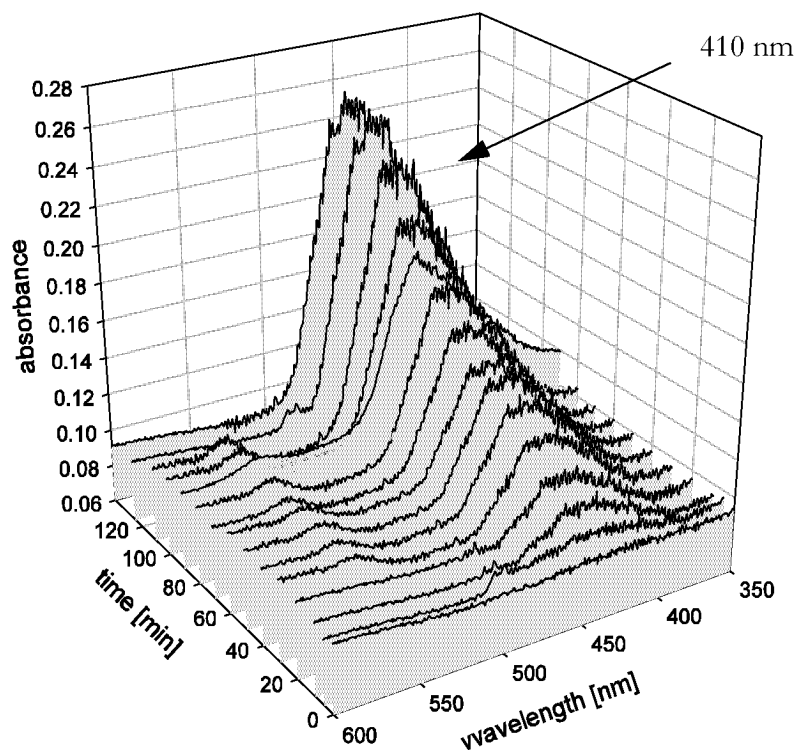
Fig. 7-1:   UV spectra of the catholyte during the reduction process. System parameters: 1 M NaOH, 10 g l^{-1} indigo, 50°C, current density 20 mA cm^{-2}, catholyte flow 10 cm^3 s^{-1}. Ni-electrode: 1200 cm^2.

7.3.1 Influence of pH

It is obvious from the reaction mechanism, that the ECH process produces hydroxide ions at the surface of the cathode. Therefore, the pH near the surface is most probably higher than that in the bulk solution and the pH of unbuffered electrolysis media increases as the electrolysis proceeds (*e.g.*, in case of pH = 10 at the beginning of the electrolysis, a final pH of 10.8 was reached). However, the effect of the initial pH of the bulk solution on the efficiency of the ECH of indigo was investigated. The results are reported in *Figure 7-2*. The conversion is clearly enhanced with increasing pH, but at higher values the conversion levels off and a maximum plateau is achieved at pH values above 13. This effect might be caused by the presence of the more soluble ionic forms of the indigo species, because non-ionic or 'acid' forms of reduced indigo are substances of poor water-solubility. In addition, this is in agreement with published values of the second acid-base-equilibrium constant $pK_{a,2}$ of leuco indigo in aqueous solution close to 13 (*chapter 3.3.2*) [178].
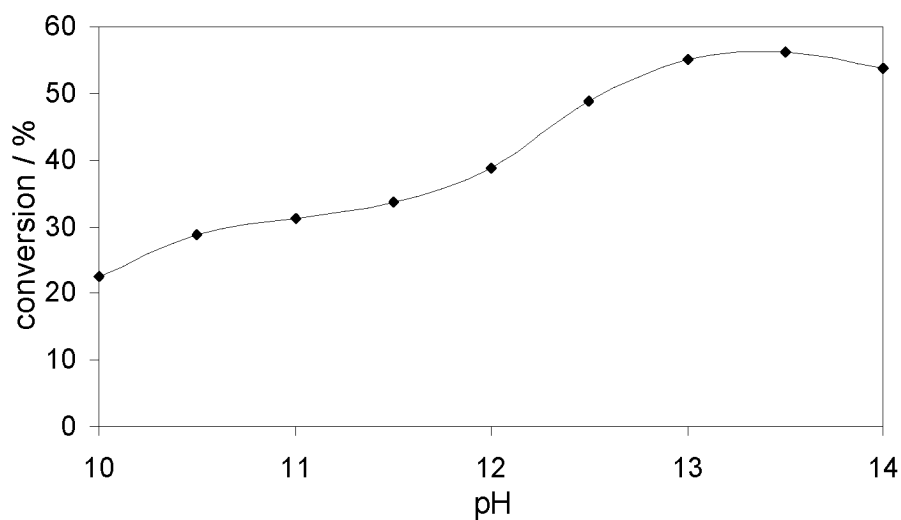
Fig. 7-2:   Influence of pH on the galvanostatic electrocatalytic hydrogenation of indigo after 50 F mol^{-1}. System parameters: 10 g l^{-1} indigo, 60°C, current density 20 mA cm^{-2}, catholyte flow 10 cm^3 s^{-1}. Ni-electrode: 1200 cm^2.

7.3.2 Influence of the current density and the temperature

For the ECH of vat dyes, the conversion passes a maximum upon increasing the temperature and also upon increasing the current density (*chapter 6.3.1*). Therefore, it seemed interesting to optimize the two other parameters simultaneously by measuring a response surface. A region of maximal conversion around the optimal values of temperature and current density at 70°C and 20 mA cm^{-2} can be seen in *Figure 7-3*.

In general, an increase of the temperature from 30 to 60 - 80°C caused an increase of the current efficiency, but at higher temperatures the current efficiency and the conversion were diminished significantly. In the case of *Raney* nickel, it was shown that the hydrogen evolution reaction involves a *Volmer-Heyrovský* mechanism [218]. Thus, by increasing the temperature up to 60-80 °C, the rate of hydrogenation (*Figure 6-1*, *reaction 6.2*) increases more rapidly than the rate of hydrogen desorption (*Figure 6-1*, *reaction 6.3*). At higher temperatures the situation appears to be reversed.
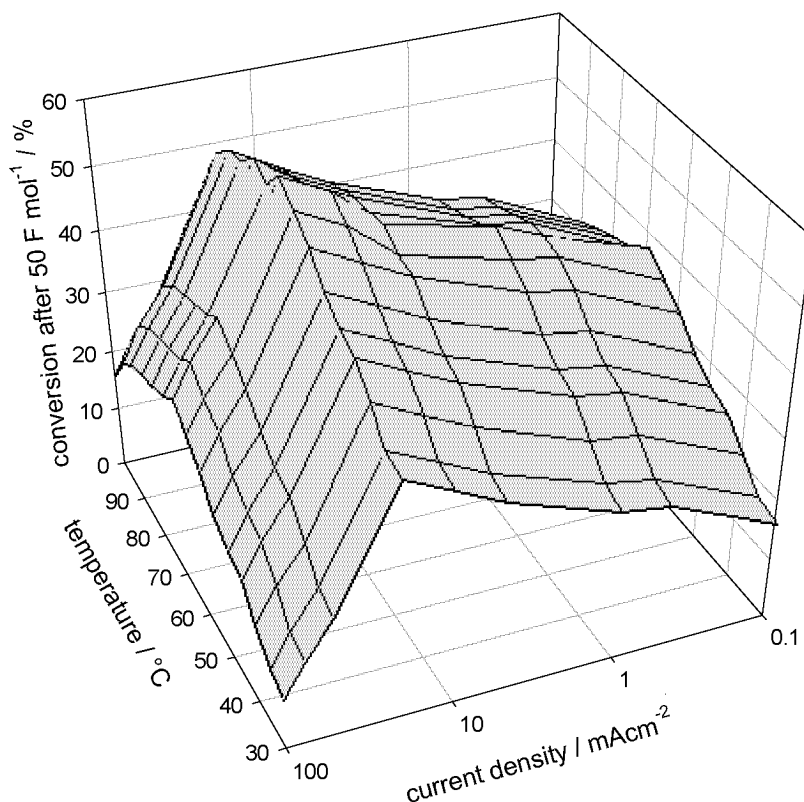
Fig. 7-3:   3D representation of the response surface for the ECH of indigo. System parameters: 1 M NaOH, 10 g l^{-1} indigo, catholyte flow: 10 cm^3 s^{-1}. Ni-electrode: 1200 cm^2.

The effect of increasing the current density from 0.1 to 100 mA cm^{-2} on the current efficiency shows a comparable behaviour. From 0.1 to 10 mA cm^{-2}, the small increase in cathodic polarization associated with the increase of the current density favours the hydrogenation (*Figure 6-1*, *reaction 6.2*) over the hydrogen desorption (*Figure 6-1*, *reaction 6.3*). This leads to an increase of both the current efficiency and the extent of hydrogenation. Further increase favours the hydrogen desorption (*Figure 6-1*, *reaction 6.3*) over hydrogenation (*Figure 6-1*, *reaction 6.2*) as shown by the diminution of the current efficiency and of the extent of hydrogenation.

7.3.3 Influence of ultrasound

Figure 7-4 shows the influence of ultrasound on the electrochemical reduction of the radical. It is obvious that in the presence of ultrasonic waves the reaction rate is clearly enhanced. It has been already analysed that larger particles or agglomerates of solid particles (> 100 μm) are effectively broken down and smaller particles with a size between 1 and 10 μm are created (*chapter 4.3.5*) [181]. Therefore, the positive effect is based mostly on the increase of the active reaction surface of indigo due to reduction of the particle diameter.
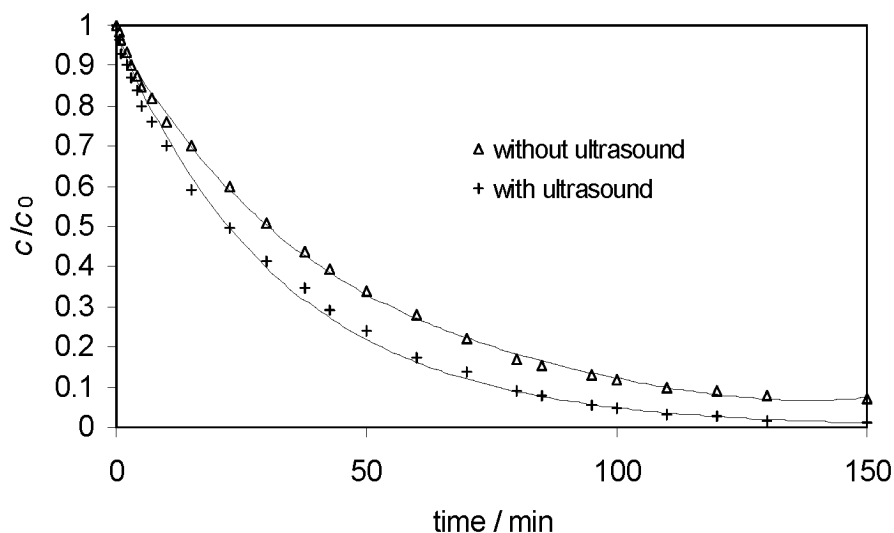
Fig. 7-4:   Influence of ultrasound on the reaction rate of the ECH of indigo. System parameters: 1 M NaOH, 10 g l^{-1} indigo, 70°C, current density 20 mA cm^{-2}, catholyte flow 10 cm^3 s^{-1}. Ni-electrode: 1200 cm^2.

7.3.4 Influence of organic solvents

First of all, a screening was performed in order to identify organic solvents that can enhance the electrocatalytic hydrogenation (*Table 7-1*). It is well known that the best organic co-solvents are those that are less organic [211]. For instance, very little hydrogenation was observed with diethylene glycol and ethylene glycol as co-solvent. This is most probably due to the adsorption of the organic solvent competing with the adsorption of the organic substrate [211]. Methanol is among the best solvents used so far and was used for further studies. The influence of increasing the methanol concentration on the conversion can be seen in *Figure 7-5*. 10% (v/v) of methanol can enhance the conversion after $Q = 5$ F mol^{-1} from 5.5 to 7%. Further addition up to 30% (v/v) approximately doubles the conversion up to 9%.

Table 7-1: Influence of 20% (v/v) co-solvents on the ECH of indigo at *Raney* nickel electrodes

Solvent	Conversion[a] / %	Current efficiency / %
methanol	43.1	6.9
ethanol	39.8	6.3
i-propanol	31.3	5.0
diethylene glycol	19.4	3.1
ethylene glycol	24.4	3.9
no solvent (reference)	26.9	4.3

[a] The conversion was determined by spectrophotometric analysis after 5 F mol^{-1} passed charge. Material balance > 95%. System parameters: 1 M NaOH, 10 g l^{-1} indigo, 50°C, current density 20 mA cm^{-2}, catholyte flow 10 cm^3 s^{-1}. Charge passed (Q) = 25 F mol^{-1}. Ni-electrode: 1200 cm^2.

It is well known that the addition of small amounts of methanol accelerates the vatting reaction (*chapter 5.3.1*). In case of the electrocatalytic hydrogenation the theoretical understanding is still in its infancy. Thus, so far we can only speculate about the mechanism. The poisoning effect of methanol

on the *Volmer-Heyrovský* mechanism has been found to be weak [211]. There-fore, the increase in the efficiency of the ECH in the presence of organic co-solvents would be due to an increase in the rate of hydrogenation. Both, (A) dissolution and transport of indigo to the electrode surface followed by hydride transfer and (B) hydride hopping across the solid/solid boundary layer, are plausible on a microscopic scale. However, the solubility of indigo in aque-ous media is very low. Therefore, probably solid dye particles are the active species and solid/solid contact is controlling the reaction. Methanol may enhance the solubility and might cause a change in mechanism, but also an activation of the surface by the solvent seems to be possible.
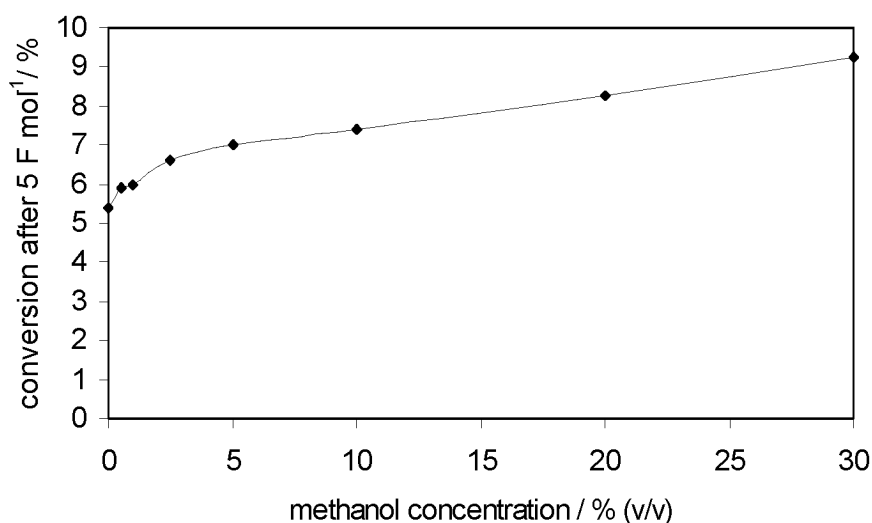
Fig. 7-5: Influence of the methanol concentration on the ECH of indigo at *Raney* nickel electrodes after 5 F mol^{-1}. System parameters: 1 M NaOH, 10 g l^{-1} indigo, 50°C, current den-sity 20 mA cm^{-2}, catholyte flow 10 cm^3 s^{-1}. Ni-electrode: 1200 cm^2 Ni-electrode.

7.4 Conclusions

The industrial feasibility of the novel route for the environmentally friendly production of water soluble leuco indigo by electrocatalytic hydroge-nation of indigo in aqueous solutions has been studied in a divided flow cell using *Raney* nickel electrodes. It was tried to establish optimized conditions in the system, and a scale-up in indigo concentration up to 10 g l^{-1} was achieved.

Increasing the pH can enhance the reduction rate. A maximum conversion has been found by optimizing the current density and the temperature. The reaction rate is clearly enhanced in the presence of ultrasonic waves. This might be due to the increase of the active reaction surface by the reduction of the particle diameter. Organic solvents can slightly increase the reaction rate. Methanol is the best co-solvent used so far and is used in concentrations of 10% (v/v).

Using the obtained optimized conditions, a very low current efficiency of 12.7% could be reached at 95% conversion. This value would be much higher with electrodes made of noble metal blacks. Nevertheless, *Raney* nickel was chosen as electrode material, because it is interesting from the standpoint of availability, costs and stability in alkaline media. The stability of platinum-black electrodes was shown to be poor. Therefore, their industrial application seems to be not feasible.

Until now, the most limiting factor is the poor contact between the indigo particles and the *Raney* nickel. Therefore, further work will focus on investigations with packed and fluidized bed reactors. *Raney* nickel will be fixed on spheres with diameters, large enough for the suspension not to block the reactor. In addition, other types of electrodes (*e.g.* bounded with lanthanum phosphate) should be tested (*chapter 8*), because the stability of *Raney*-type electrodes was shown to be poor.

Chapter **8**

Electrocatalytic hydrogenation of vat dyes Part III: Investigations with other types of *Raney* nickel electrodes

8.1 Introduction

The potential of the electrocatalytic hydrogenation (ECH) as a reduction method for vat dyes has been evaluated in *chapters 6 - 7*, while especially indigo as a model substance was investigated. These results showed that the reactor performance is yet to low and, in addition, the lifetime of the electrodes is very short, which would not yet make the ECH a feasible process at an industrial scale. However, the results would make a solid basis for an improvement of the process efficiency by a different reactor design and/or by employing different electrode materials.

The electrode material used for the electrohydrogenation of organic molecules is of paramount importance since the kinetics of the electrohydrogenation process depends substantially on the nature of the electrode material. Electrodes made from metallic powder particles generally exhibit weak mechanical strengths when no binding material is used (*chapter 6.3.1*) [220]. Pressure-molded, rigid electrodes with high surfaces, low electrical resistance and good mechanical strength are good alternatives. They consits of non-dissolving, electrically-conducting metal particles with high specific surfaces and fractal structure with lanthanum phosphate as the binding material [220].

For the ECH process composite metallic powders can be employed as follows: the powder particles are trapped within the pores of a porous electrode material which is practically inactive for the evolution of both molecular and adsorbed hydrogen when it is cathodically polarized. Electrodes of this type are constructed by inclusion of composite powder particles containing nano-

deposits of a catalyst metal on the surfaces. Reticulated Vitreous Carbon (RVC) is particularly attractive as the electrode material since it is an excellent electronic conductor and it is electrochemically stable and exhibits a well developed three-dimensional-network of large pores (*Figure 8-1*). It is also practically inactive with respect to the generation of hydrogen under cathodic polarization. The specific RVC surface is 66 cm^2 cm^{-3} for a 100 pore-per-inch (ppi) matrix with a void volume of 97% [221]. The high porosity of the RVC offers a great number of large pores accessible to the catalytic powder particles. The electrolyte penetrates the RVC by forced convection and the catalytic particles suspended in the electrolyte are trapped within the pores [220], [221]. This kind of electrode has been already employed in flow-through cells [223].
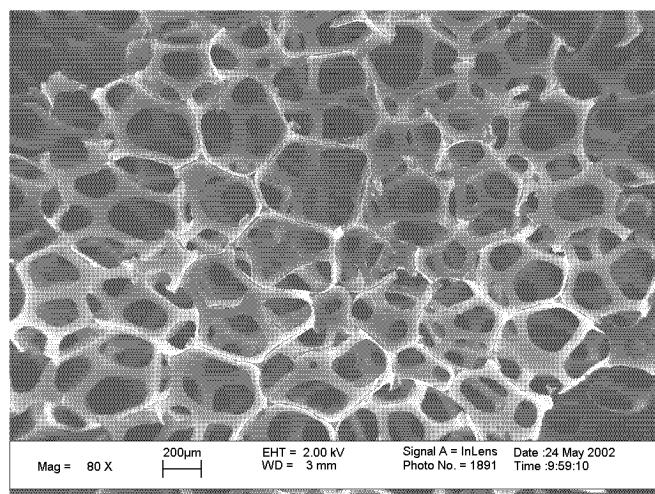
Fig. 8-1:   SEM-picture of the RVC foam without *Raney* nickel.

In addition to evaluations of different electrode materials, the investigations were focused on a different reactor design. Packed and fluidized bed electrodes are particularly suited to provide the large specific electrode area and the intensive contact between the dye particles and the electrode. Therefore, the electrocatalytic hydrogenation (ECH) of indigo was investigated with different electrode materials with a packed and fluidized bed electrode reactor with the use of an experimental circuit containing a flow channel cell with a particle bed electrode.

8.2 Experimental

8.2.1 Chemicals

All aqueous solutions were prepared with deionized water. Indigo was supplied from BASF, Ludwigshafen, Germany. All other chemicals were of analytical grade and used as received from Fluka without further purification.

8.2.2 Apparatus

a) Plate and frame flow cell

A small multipurpose plate and frame cell (EC Electro MP-Cell from ElectroCell AB, Sweden) was chosen for the scale-up procedure. The cell and the set-up of the pilot plant used for the experiments is described in detail in *chapter 4.2.2*. As the working electrode a flat nickel plate electrode together with above mentioned *Raney* nickel electrodes were used. Electrodes consisting of metal meshes were spot-welded to the plate to ensure good electrical conductivity and stack with thin (about 0.2 mm) nickel strips at the edges and in the middle between the meshes in a vertical way. In case of RVC the foam was pressed into the frame of the catholyte chamber and contacted just by pressure.

b) Fixed bed reactor

A small flow channel with a packed or fluidized bed was used for the experiments. The cell and the set-up of the pilot plant used for the experiments is described in detail in *chapter 4.2.2*.

8.2.3 Electrode characterisation

The morphology of the obtained electrodes was studied by scanning electron microscopy with EDX analysis (LEO C 1530).

8.2.4 Electrode material

a) RVC electrodes

The RVC electrodes consisted of a 5 x 5 x 0.5 cm^3 piece of a commercial RVC foam (ERG Materials and Aerospace Corporation, Oakland, USA, 100 ppi) into which 1.0 g of catalyst was embedded. This physical incorporation of the *Raney* nickel particles into the reticulated structure of the vitreous carbon ocurred spontaneously when the powder was stirred in the catholyte solution for about one hour in the presence of the vitreous carbon matrix. The particles remained in contact with the carbon matrix despite vigorous stirring, provided that there was no sudden perturbation [225].

b) Lanthanum phosphate bound Raney nickel electrodes

Lanthanum phosphate bound *Raney* nickel electrodes were made by mixing and grinding 45% of *Raney* alloy, 45% of *Raney* nickel catalyst powder and 10% of lanthanum phosphate.

The lanthanum phosphate was prepared by combining acid lanthanum phosphate and lanthanum hydroxide [220], [226]. Two reactions are involved in the formation of acid lanthanum phosphate La(H$_2$PO$_4$)$_3$ and its subsequent transformation into LaPO$_4$, namely:

$$0.5 \ La_2O_3 + 3 \ H_3PO_4 = La(H_2PO_4)_3 \cdot 1.5 \ H_2O \qquad (8.1)$$

$$La(H_2PO_4)_3 + 2 \ La(OH)_3 = 3 \ LaPO_4 + 6 \ H_2O \qquad (8.2)$$
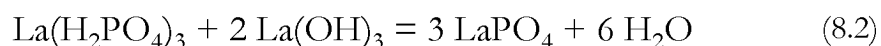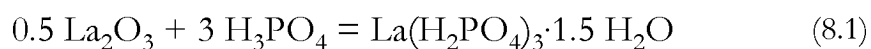
La(H$_2$PO$_4$)$_3$ was synthesized by adding 48.88 g (0.15 mol) La$_2$O$_3$ to 103.7 g (0.90 mol) H$_3$PO$_4$ (85%) in a Teflon beaker, since reactive intermediates react with glass rather than Teflon [227]. The reaction product, a viscous silicon-like paste, was heated for 24 h in an oven at 150°C and vacuum dried to remove traces of the water generated by the reaction [228]. The reaction is very fast, strongly exothermic and autocatalytic, even when the components are mixed at

room temperature. Therefore, the La_2O_3 must be completely incorporated within a few minutes.

Powders of acid lanthanum phosphate and lanthanum hydroxide were mixed throroughly with the *Raney* nickel powders. The addition of 0.883 g $La(OH)_3$ per 1 g of $La(H_2PO_4)_3$ made it easier to crush and mix the two components in a ball mill. The mixture should be stored in a dry atmoshere before the final polymerisation can take place, because the polymerisation is very slow at room temperature.

The polymer and the catalyst are mixed and about 40 g of this powder was pressed into a plate of 5 mm thick with about 1000 kg cm^{-2} into a 5 x 10 cm mould from which 2 x 25 cm^2 plates were cut. These plates were heated at 800°C for 4 h under an argon atomsphere to achieve the polymerisation. The electrical contact was made with a nickel stripe. The plates were leached in NaOH 30% at 75°C for 24 h to remove the aluminium.

c) Commercial Raney nickel extrudates

Two granulated *Raney* metal catalysts were used as received (*Degussa* 1678 Typ B and *Metalyst Alpha*).

d) Self-made Raney nickel spheres

Convenient self-made *Raney* nickel electrodes were prepared by co-deposition of *Raney* alloy particles with the electrodeposited nickel metal on stainless steel spheres.

50 g spheres (stainless steel, d = 1 mm, *Naegeli AG*, Güttingen, Switzerland) were plated at 70°C and with a current density of 30 mA cm^{-2} in a well stirred plating solution consisting of 300 g l^{-1} $NiCl_2 \cdot 6H_2O$, 45 g l^{-1} $NiSO_4 \cdot 6H_2O$, 30 g l^{-1} H_3BO_3 and 5 g l^{-1} of dispersed *Raney* alloy particles (Ni:Al 50:50 (w/w)). A piece of nickel was used as the anode. The cathode consisted of a jigging screen made of stainless steel with the spheres on it. The continuous oscillation of the sieve garantee a homogeneous deposition on the

surface of the spheres and prevents of the spheres from sticking to the grid. The catalyst was activated in 30% NaOH at 70°C over night.

8.2.5 Procedure

Cathodic suspensions of indigo were composed of 1 M NaOH and 0.1 g l^{-1} of indigo (sieve fraction between 0.06 - 0.08 mm). They were deoxygenated during at least two hours before the experiment and maintained under a nitrogen atmosphere during the measurements. Anodic solutions consisted of 1 M NaOH. All the reduction experiments were performed at 50°C and a fluid flow velocity of 1.68 cm s^{-1}.

8.3 Results and discussion

8.3.1 RVC carbon

The morphology of the electrodes was investigated with SEM, because it was interesting to know how the *Raney* nickel particles are trapped in the foam (*Figure 8-2* and *Table 8-1*). The catalyst particles just stick to the surface rather than forming agglomerates within the pores.

| Mag = 10.00 K X | 1µm | EHT = 3.00 kV WD = 3 mm | Signal A = InLens Photo No. = 1899 | Date :24 May 2002 Time :10:52:04 |
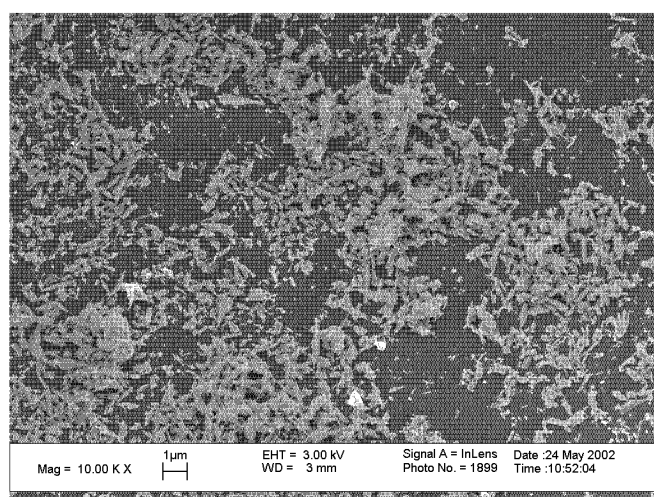
Fig. 8-2:   SEM picture of the RVC foam after pre-treatment with *Raney* nickel.

Table 8-1: SEM pictures of the RVC foam (ERG Materials and Aerospace Corporation, Oakland, USA, 100 ppi) (left side) and of the RVC foam after pre-treatment with *Raney* nickel (right side) at different magnitudes
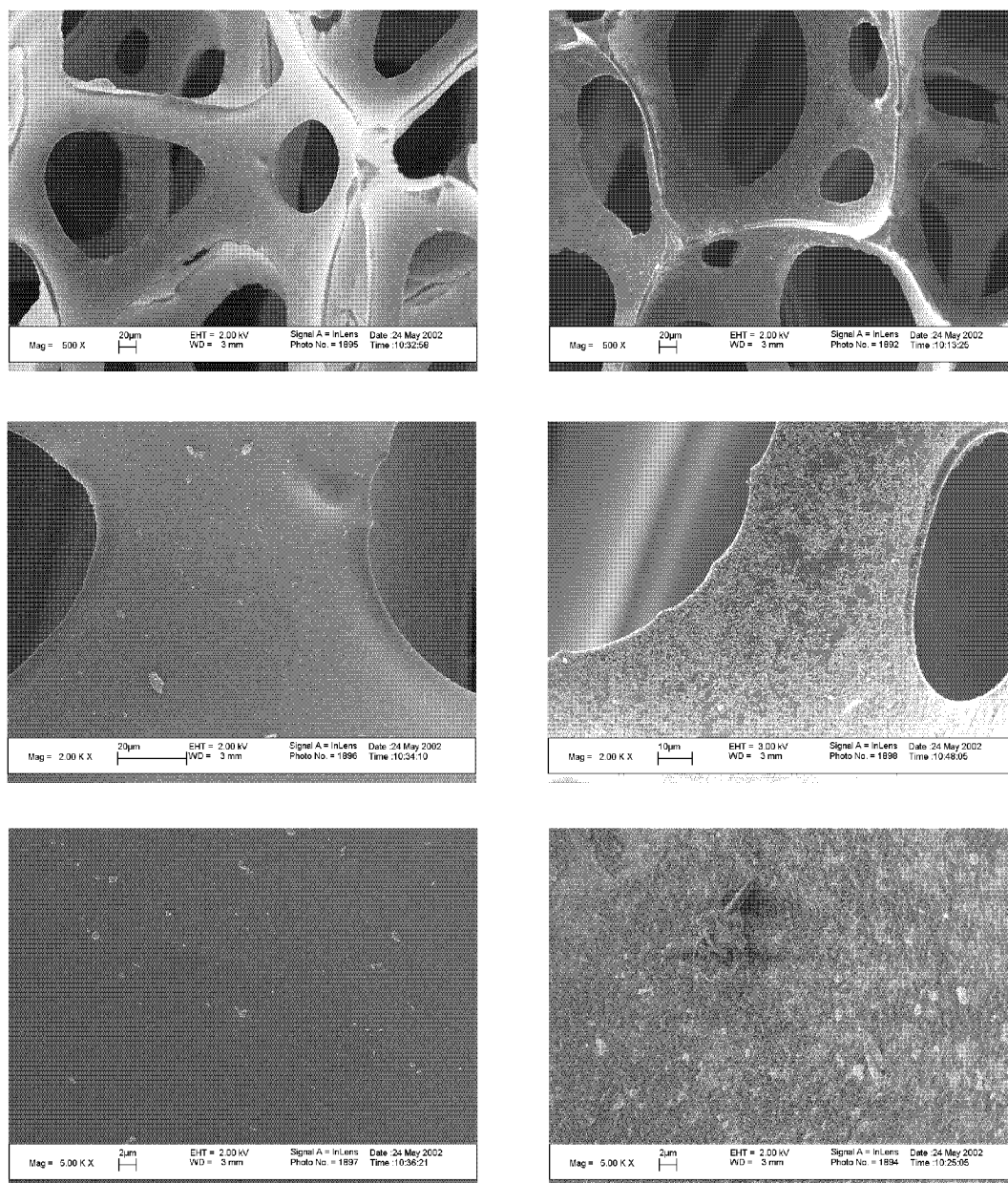
The electrodes were examined with indigo reduction experiments. In the case of implemented *Raney* nickel the reaction rate reached fair values of $0.4\ \mu mol\ min^{-1}\ g^{-1}$ RVC. However, to intensify the contact between indigo and

the electrode, a flow-through pattern had to be employed. With this process, the filtration of indigo could not be avoided. During the experiment a great pressure drop is built up across the filtration layer and, in addition, the reactor was blocked very often at higher indigo concentrations. Therefore, the same problems occured as in the case of the precoat-layer cell (*chapter 2.4.3*).

However, it is important to mention that it was possible to use the RVC foam itself as the electrode material for the reduction of indigo. The reaction rate of 0.08 μmol min^{-1} g^{-1} RVC is quite high. This could be a rewarding field of investigation, because graphite is a very cheap and stable material. Thus, on the basis of the results presented, it should be possible to improve the efficiency by a different reactor design (*e.g.* fixed bed of graphite granules, see *chapter 10*) where the blocking of the reactor can be circumvented.

8.3.2 Lanthanum phosphate bounded electrodes

This type of electrode was used in small H-cell as well as in the flow through cell of the pilot plant. The electrodes are much more stable than in the case of electrodeposited *Raney* electrodes and they are very convenient.

However, because of the binder the active surface is not as high as in case of freshly prepared electrodeposited *Raney* electrodes. Therefore, although the activity is lower, still reduction rates of 0.09 g min^{-1} and 100 cm^2 (geometric area) could be reached.

8.3.3 Experiments with commercial *Raney* nickel extrudate

Several batch electrolysis experiments were performed with *Raney* nickel granulate. However, no conversion at all could be observed. This result is inevitable to some extent, because it is well known from catalytic hydrogenation that the *Metalyst* range from *Degussa* is not nearly as active as the supported nickel catalysts. In addition, morphological studies were performed by electron microscopy. The catalyst is built up of very coarse material and the inner as well as the outer surface is very low compared to that of the self-made *Raney* nickel electrodes (*Figure 8-3*).

10μm   EHT = 0.60 kV   Signal A = InLens   Date :3 Apr 2002
Mag = 1.00 K X |———| WD = 2 mm   Photo No. = 1263   Time :9:16:53
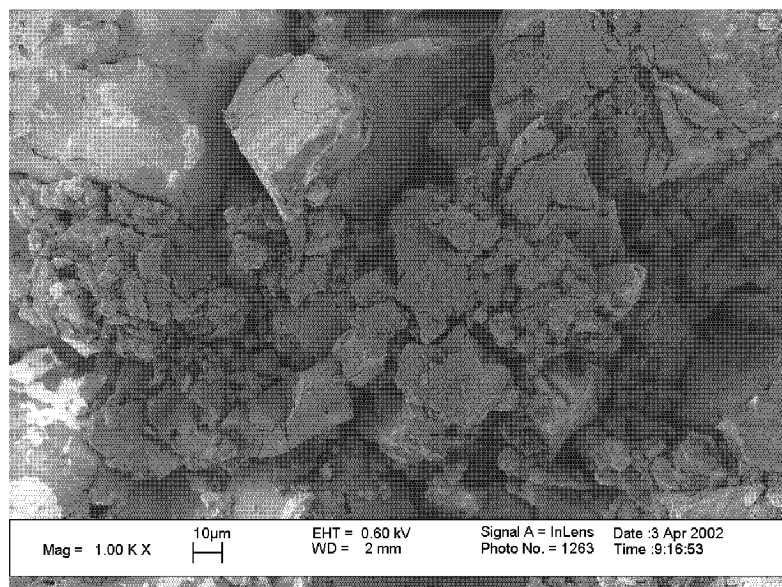
Fig. 8-3:   SEM-picture of the Degussa *Metalyst* catalyst.

8.3.4 Experiments with self-made *Raney* nickel spheres

A completely different behaviour was observed with self-made electrodes. In this case the indigo could be reduced quite efficiently. However, it was never possible to reach the reactor performance of the planar plates in the filter-press cell. This is not surprising, because it was very difficult to prepare the spheric catalysts by electrodeposition. In *Table 8-2* the porous electrodeposited layer of nickel can be seen on the surface of the sphere. The surface morphology can be described by the typical cauliflower-like structure, characteristic for the electrodeposition of nickel at high current densities. It is important to mention that the whole surface of the sphere is covered with the *Raney* catalyst.

Figure 8-4 shows the typical behaviour of the electrodes. The leuco indigo concentration is increasing linearly with time (0.01 μmol min^{-1} g^{-1} *Raney* nickel catalyst). After switching off the current, the leuco indigo is still produced for a short time (30 min), probably due to the hydrogen stored in the porous nickel structure. This might be also interpreted as a proof for the ECH, because in the case of an EP mechanism the storage of hydrogen should not have any influence. A maximum current efficiency of 20% could be reached at an electrode potential of -1000 mV *vs.* Ag/AgCl, 3 M KCl. At higher potential the

hydrogen evolution increases and the current efficiency is diminished to very
fast values below 5%.
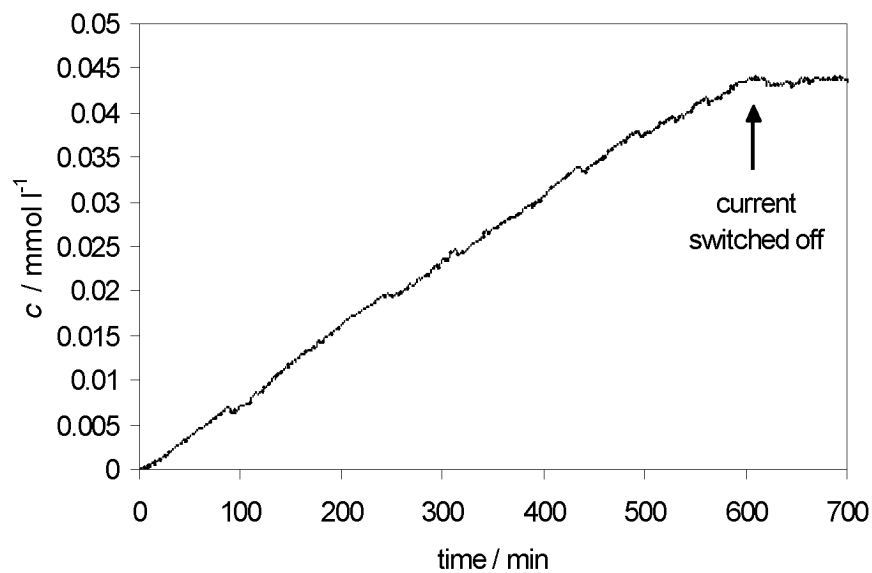
Fig. 8-4:   Leuco indigo concentration c *vs.* time, measured at -1000 mV *vs.* Ag/AgCl,
3 M KCl.

Table 8-2:   SEM-pictures of the self-made electrodes

a)	b)
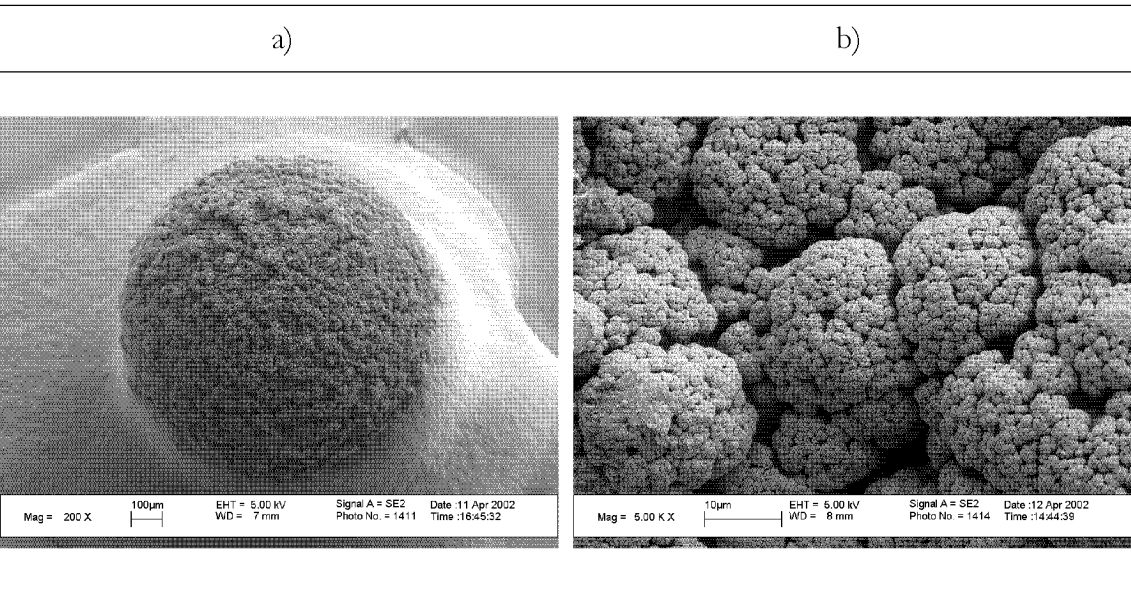
8.4 Conclusion

The mechanical strength of the electrodes made with metallic powder particles is generally weak without the use of a binding material. Therefore, two different types, RVC carbon and lanthanum phosphate bound *Raney* nickel electrodes were investigated. No real breakthrough could be achieved with these new types of electrodes. In all the cases the electrode stability could be increased, but the catalytic activity was much lower.

Although it was expected that a fixed bed electrode should perform better than the reactor concept employed until now, it must be conceded that this is not the case. However, the negative results are mostly based on the low performance of the electrode materials rather than on the reactor concept itself. Commercial extruded *Raney* catalysts have no or a very low hydrogenation capacity. The self-made electrodes are much more active, but the capacity is not high enough. In addition, it is well known that *Raney* nickel electrodes made by electrodeposition do not show a very long lifetime. By using fixed and fluidized bed electrodes their active period is even lower due to friction forces.

The electrocatalytic hydrogenation of vat dyes would be an attractive alternative for the reduction of vat dyes. However, the electrode stability is of paramount importance for an industrial application. Unfortunately, until now, it was not possible to find an electrode material with both high mechanical strength and high catalytic activity. Thus, more investigations have to be made in this field.

Electrocatalytic hydrogenation of vat dyes Part IV: Kinetics of hydrogen evolution and hydrogenation of the indigo on *Raney* nickel electrodes

9.1 Introduction

The specific focus of this study was to collect current voltage data on *Raney* nickel electrodes during the electrochemical evolution of hydrogen in the presence and the absence of indigo, to interpret the hydrogen evolution data using *Butler-Volmer* type current-voltage kinetic relationships and to compare measured indigo electrohydrogenation rates with those predicted from a kinetic model containing a chemical catalytic rate expression for the indigo reduction and the *Butler-Volmer* kinetic expressions. Therefore, the aim was to analyse whether the mechanism for the formation of leuco indigo with electro-generated atomic hydrogen on *Raney* nickel is identical to that for the catalytic hydrogenation with molecular hydrogen. For this reason, a study was carried out to address the question regarding a rate expression for the reduction of indigo on *Raney* nickel *via* catalytic hydrogenation.

The mechanism of surface catalysis is very complex. Fluid-phase reactions of this type are conceived to proceed according to at least the following five steps [229]:

- diffusion of the reacting molecules to the surface
- adsorption of the reactants at the surface
- reaction on the surface

- desorption of the products
- diffusion of the products into the fluid

A comprehensive kinetic description of the over-all five-step process is possible but yet not very helpful in evaluating the mechanism from kinetic data. Usually it is assumed that only one of the steps offers appreciable resistance to the reaction.

9.2 Experimental

9.2.1 Chemicals

All aqueous solutions were prepared with deionized water. Indigo was supplied from BASF, Ludwigshafen, Germany. Sodium hydroxide (*Fluka*, p.a.), *Raney* nickel (*Fluka*, 83440) and Argon 4.8 were used for experiments as reveived, without further purification.

9.2.2 Catalytic hydrogenation

According to a standard procedure, different amounts of catalyst and indigo were mixed in 1 M NaOH and degassed for 1 h before the hydrogenation was started [230].

Preliminary hydrogenation experiments at atmospheric pressure were carried out in a magnetically stirred 100 ml glass reactor. The kinetic study at higher pressure was carried out in a 100 ml stainless-steel autoclave. The reactor was stirred magnetically (1000 min^{-1}). The pressure was held at a constant value by a computerized constant-volume/constant-pressure equipment (*Büchi* BPC 9901). By monitoring the pressure in the vessel and with the injected pulses the hydrogen uptake could be measured [230].

9.2.3 Voltammetric experiments

A conventional two-compartment glass H-cell (each with a volume of 200 ml), separated by a Nafion-324 membrane (DuPont) was used both for voltammetry and small-scale preparative electrolysis. *Raney* nickel electrodes have been used as described in *chapter 6*. A computer-controlled potentiostat (*Radiometer Copenhagen* DEA 332) was used for the voltammetric experiments. Cells were connected to a thermostat (*Colora Messtechnik GmbH*).

Cathodic suspensions of indigo were composed of 1 M NaOH and about 10^{-3} M (0.262 g l^{-1}) of indigo. They were degassed during at least 2 h before the experiment and maintained under an argon atmosphere during the measurements. Anodic solutions consisted of 1 M NaOH. All reduction experiments were performed at 50°C. During a potential sweep the pH was not controlled because the increase of the pH value due to the production of hydroxyl ions during the experiment amounts to less than 0.1 pH unit.

9.3 Catalytic hydrogenation of indigo

9.3.1 Typical hydrogenation behaviour

The course of the reaction was followed by plotting the indigo concentration *vs.* the time of the reaction. In all the cases studied a zero-order kinetic law was observed due to the high and constant hydrogen pressure (*i.e.*, Θ_H = const.) until approximately 90% conversion (*Figure 9-1*). At higher conversions the linear behaviour changed into a curve. Interestingly the reaction still continues after the consumtion of a stoichiometric amount of hydrogen. This effect can be interpreted by an overreduction of indigo, which is a quite typical phenomenon for vat dyes (*Figure 9-2*).
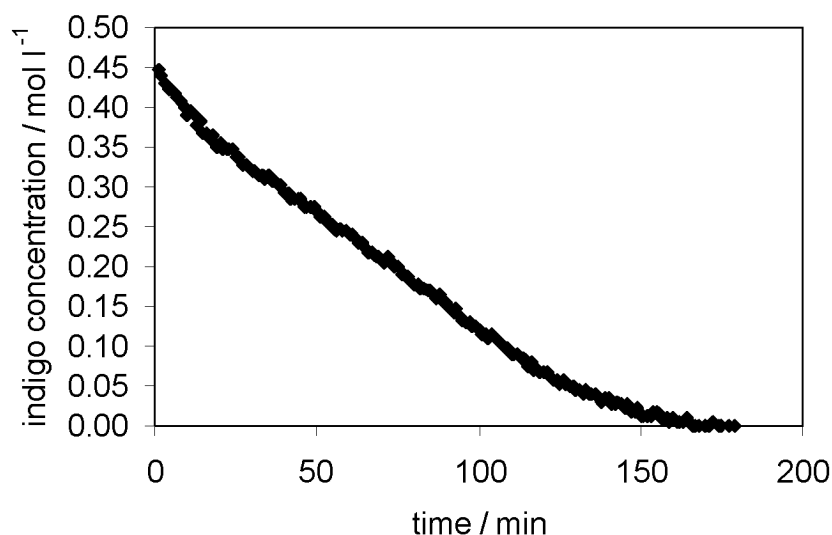
Fig. 9-1:   Typical hydrogenation run. System parameters: 1 M NaOH, 11.8 g l^{-1} indigo, hydrogen pressure 5 bar, 50°C, 1000 rpm, catalyst loading 10%.
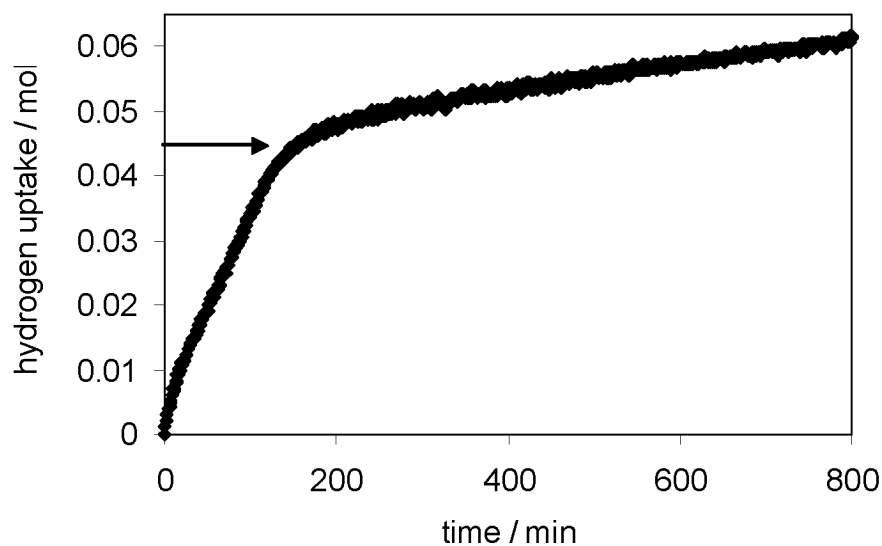
Fig. 9-2:   Stepwise hydrogen consumption curve. System parameters given in *Figure 9-1*.

9.3.2 Mass transfer effects

Hydrogenation runs made at various agitation regimes show that above 1000 rpm the rate is independent of the impeller speed (*Figure 9-3*). These results, together with those obtained at different catalyst loadings (*chapter 9.3.3*), indicate that in the range of the operating variables the system is probably controlled by the chemical reaction.
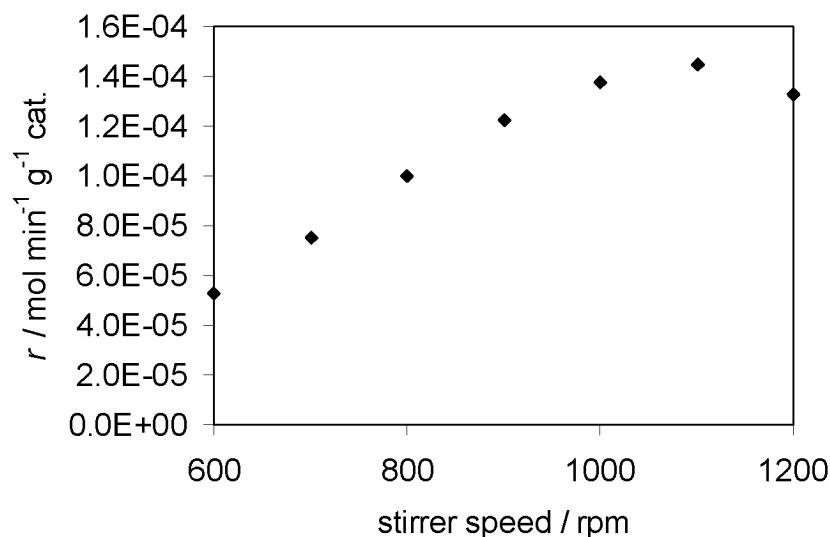
Fig. 9-3: Influence of stirring on the reaction rate r. System parameters: 1 M NaOH, 11.8 g l^{-1} indigo, hydrogen pressure 5 bar, 50°C, catalyst loading 10%.

9.3.3 Catalyst

Figure 9-4 indicates that there is an almost linear variation of the reaction rate with the catalyst concentration. As mentioned in *chapter 9.3.2*, these results indicate that in the range of the operating variables the system seems to be controlled by the chemical reaction.
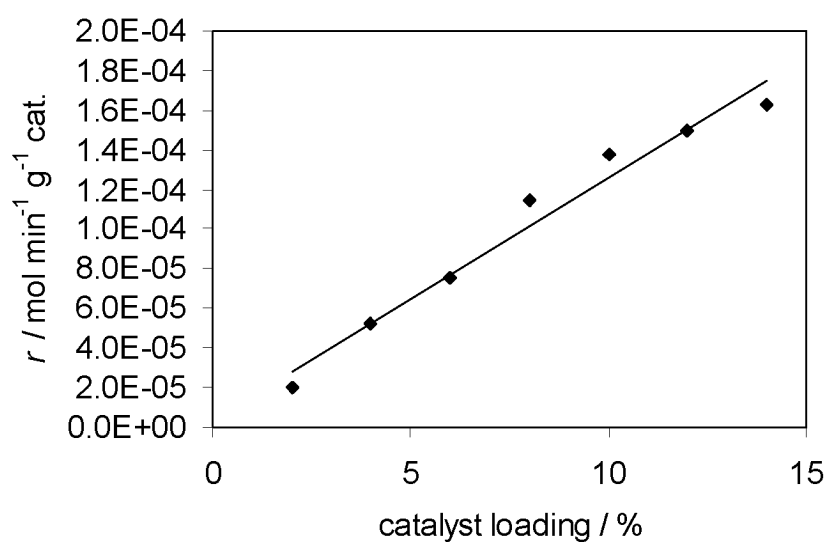
Fig. 9-4: Effect of catalyst loading on the reaction rate r. System parameters: 1 M NaOH, 11.8 g l^{-1} indigo, hydrogen pressure 5 bar, 50°C, 1000 rpm.

9.3.4 Pressure

The variantion of the reaction rate *vs.* the hydrogen pressure is shown in *Figure 9-5*. At low hydrogen pressure, the rate increases with increasing pressure of hydrogen, while at higher values the rate becomes more and more independent of the hydrogen pressure.
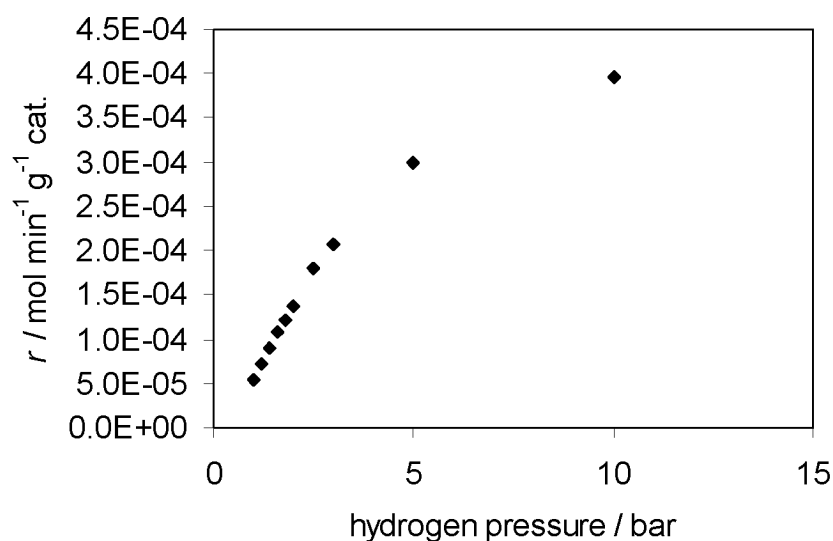
Fig. 9-5:   Effect of hydrogen pressure on the reaction rate *r*. System parameters: 1 M NaOH, 11.8 g l^{-1} indigo, 50°C, 1000 rpm, catalyst loading 10%.

9.3.5 Indigo concentration

Figure 9-6 indicates that there is an almost linear variation of the reaction rate with the indigo concentration.
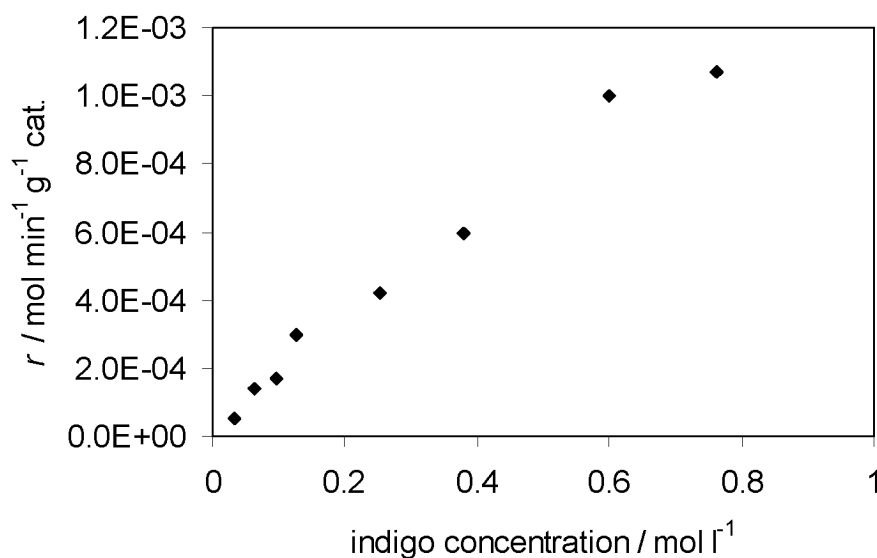
Fig. 9-6: Effect of the indigo concentration on the reaction rate r. System parameters: 1 M NaOH, hydrogen pressure 5 bar, 50°C, 1000 rpm, catalyst loading 10%.

9.3.6 Mechanism of the reaction

The values of the reaction rate r and the reaction constant (*Figure 9-4* - *Figure 9-5*) suggest the following conclusions:

- In the pressure range studied the gas phase is consisting essentially of hydrogen. Thus, its mass transfer resistance may be neglected. The solubility of hydrogen in the aqueous suspension will follow *Henry's* law and the pressure in the gas phase can be assumed to be directly proportional to the hydrogen concentration at the catalyst surface. In addition, it will be assumed that hydrogen is preferentially adsorbed in an atomic form.

- Mass transfer resistances in the liquid phase can be assumed to be negligible, based on the fact that the rate of reaction is independent of the agitation regime and is varying linearly with the loading of the catalyst. The controlling step can be then assumed to be a chemical reaction and the results can be further interpreted by microscopic kinetic models, such as those developed by *Langmuir-Hinshelwood*.

- The adsorption of hydrogen cannot control the rate of the process as this would require that the rate varies proportional to the hydrogen pressure and

inversely proportional to the reactant concentration. This requirement is not supported by the data illustrated in *Figure 9-1* and *Figure 9-5*.

- The adsorption of indigo (as particles and as single molecules) does not control the rate as this would require a decrease in rate with an increase in hydrogen pressure. *Figure 9-5* is contradicting this condition.

- The adsorption of the product cannot be rate-controlling as this would require the rate to increase up to a constant value when the hydrogen pressure and/or the concentration of the reacting dye are increased.

- The rate-controlling step is not the collision of one unadsorbed hydrogen atom on the adsorbed indigo (*Rideal*-mechanism). This would require that the rate be first order in the hydrogen pressure, which is not the case.

The *Langmuir-Hinshelwood* treatment limits then the possible mechanisms to those involving control by the surface reaction. For indigo it can be assumed that the controlling step is the reduction of the dye molecule to the radical species, because this soluble intermediate is very reactive and will be reduced much faster than indigo itself.

The rate equation is

$$
r = \frac{k' \cdot K_{H_2} \cdot K_{indigo} \cdot p_{H_2} \cdot c_{indigo}}{\left(1 + c_{radical} \cdot K_{radical} + c_{indigo} \cdot K_{indigo} + \sqrt{K_{H_2} \cdot p_{H_2}}\right)^2}
\qquad \text{(eq. 9.1)}
$$

Due to the fact that the rate increases linearly with increasing indigo concentration, we can assume that indigo is weakly adsorbed and neglect the respective terms in the denominator. In addition, the radical concentration is very low. Therefore, it is possible to write for the rate constant

$$
k_1 = \frac{k' \cdot K_{H_2} \cdot K_{indigo} \cdot p_{H_2}}{\left(1 + \sqrt{K_{H_2} \cdot p_{H_2}}\right)^2}
\qquad \text{(eq. 9.2)}
$$

The equation can be linearised as follows

$$\frac{1}{\sqrt{k_1}} = \frac{1}{\sqrt{K_{indigo} \cdot k'}} + \frac{1}{\sqrt{k' \cdot K_{H_2} \cdot K_{indigo}}} \cdot \frac{1}{\sqrt{p_{H_2}}}$$

(eq. 9.3)

The equation is a straight line and can be tested with the experimental data as shown in *Figure 9-7*. Obviously, there is a high degree of correlation between the model and the experimental data.
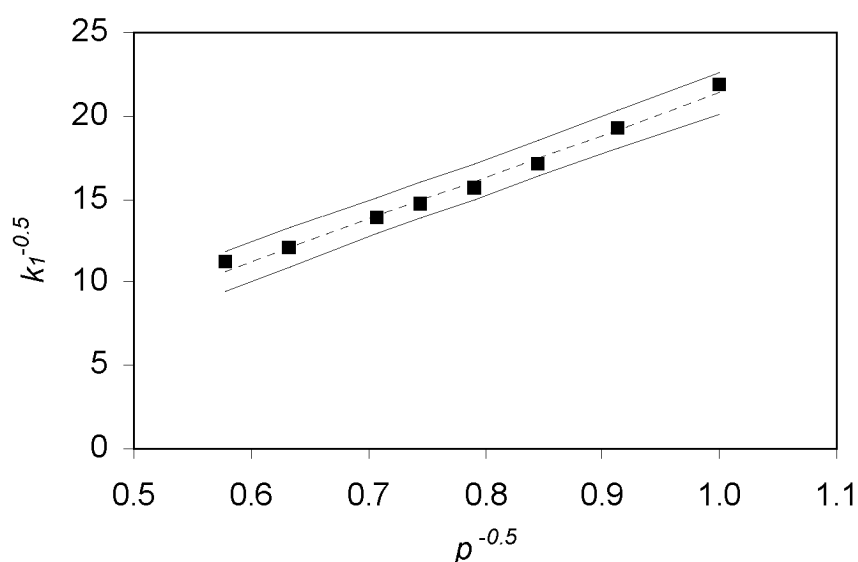
Fig. 9-7:   Test of the kinetic equation for the catalytic hydrogenation of indigo.

Estimates of the parameters can be obtained by nonlinear regression (using MATLAB[1]) (*Table 9-1*).

Table 9-1:   Results from nonlinear regression

	value	confidence intervall (95%)
k / $min^{-1} g\ cat.^{-1}$	3.52E-4	± 8.1E-5
K_{H2} / $cm^3 mol^{-1}$	0.066	± 0.006
K_{indigo} / $cm^3 mol^{-1}$	55.0	± 8.1

[1] MATLAB is a computer programme.

9.4 Electrochemical rate expression for the evolution of hydrogen on *Raney* nickel electrodes

9.4.1 Theory

Hydrogen evolution has been one of the most frequently studied electrode reactions due to its importance in water electrolyzers, fuel cells and chlor-alkali cells. The kinetics has been studied extensively on bulk flat sheet nickel, powdered nickel, *Raney* nickel powder and on activated *Raney*-type high-surface-area flat sheets, expanded grids and composite-coated electrodes [231]-[237].

The reaction sequence during the electrochemical reduction of water (in neutral pH or alkaline solutions) to form molecular hydrogen can be visualized by two elementary steps:

- The synthesis of adsorbed hydrogen in the *Volmer* or discharge step (*reaction 9.1*)

$$H_2O + e^- = H_{ads} + OH^- \tag{9.1}$$
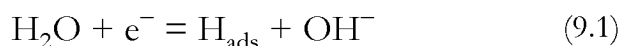
- The formation of molecular hydrogen either by the combination of two H_{ads} atoms (the *Tafel* or recombination step (*reaction 9.2*)) or by the reaction of H_{ads} with another water molecule (the *Heyrovský* or electrochemical desorption step (*reaction 9.3*))

$$2\,H_{ads} = H_2 \tag{9.2}$$
$$H_{ads} + H_2O + e^- = H_2 + OH^- \tag{9.3}$$
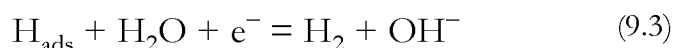
In the present study, both the *Volmer-Heyrovský* and *Volmer-Tafel* mechanisms were considered when analyzing the current-voltage data for the evolution of molecular hydrogen on *Raney* nickel. For the case where both steps are simultaneously rate-determining, the following current density/overpotential rate expressions were obtained [231]:

Volmer-Heyrovský rate expression

$$i = \frac{2i_{0,\,V}\exp\left(\dfrac{-(1-\alpha_V)F\eta}{RT}\right)\left[1 - \exp\left(\dfrac{2F\eta}{RT}\right)\right]}{M_1 + M_2}$$

(eq. 9.4)

where M_1 and M_2 are given by

$$M_1 = (1 - \Theta_H^0)\left[1 + \frac{i_{0,\,V}}{i_{0,\,Hy}}\exp\left(\frac{(1-\alpha_H+\alpha_V)F\eta}{RT}\right)\right]$$

$$M_2 = \Theta_H^0\exp\left(\frac{F\eta}{RT}\right)\left[1 + \frac{i_{0,\,V}}{i_{0,\,Hy}}\exp\left(\frac{-(1-\alpha_H+\alpha_V)F\eta}{RT}\right)\right]$$

α_V and α_H are the transfer coefficients for the *Volmer* and the *Heyrovský* reaction, respectively. With the simplification that $\alpha_H = \alpha_V$ and $(1 - \alpha_V) = \beta$ we can simplify *equation 9.4*:

$$i = \frac{2i_{0,\,V}\exp\left(\dfrac{-\beta F\eta}{RT}\right)\left[1 - \exp\left(\dfrac{2F\eta}{RT}\right)\right]}{(1 - \Theta^0_H)\left[1 + \dfrac{i_{0,\,V}}{i_{0,\,Hy}}\exp\left(\dfrac{F\eta}{RT}\right)\right] + \Theta^0_H\left[\dfrac{i_{0,\,V}}{i_{0,\,Hy}} + \exp\left(\dfrac{F\eta}{RT}\right)\right]}$$

(eq. 9.5)

The same is valid for the *Volmer-Tafel* rate expression

$$i = \frac{-L_2 + \sqrt{L_2^2 - 4L_1L_3}}{2L_1}$$

(eq. 9.6)

where L_1, L_2 and L_3 are given by

$$L_1 = i_{0,\,T}[(1 - \Theta_H^0)^2 - \Theta_H^0]\exp\left(\frac{2\beta F\eta}{RT}\right)$$

$$L_2 = 4i_{0,\,V}^2\left(-(\Theta_H^0)^2 - (1 - \Theta_H^0)^2\exp\left[\frac{2F\eta}{RT}\right]\right) - 4i_{0,\,V}^2\left(2\Theta_H^0(1 - \Theta_H^0)^2\exp\left[\frac{F\eta}{RT}\right]\right) -$$

$$- 4i_{0,\,V}^2\left((1 - \Theta_H^0)^2\frac{i_{0,\,T}}{i_{0,\,V}}\exp\left[\frac{\beta F\eta}{RT}\right]\right) + 4i_{0,\,V}^2\left(\Theta_H^0\frac{i_{0,\,T}}{i_{0,\,V}}\exp\left[\frac{(1+\beta)F\eta}{RT}\right]\right)$$

$$L_3 = 4i_{0,\,V}^2 i_{0,\,T}\left(1 - \exp\left[\frac{2F\eta}{RT}\right]\right)$$

In the above equations $i_{0,V}$, $i_{0,Hy}$ and $i_{0,T}$ are the exchange current densities for the *Volmer*, *Heyrovský* and *Tafel* reactions, respectively (in units of $A\ cm^{-2}$). Θ_H is the surface coverage of adsorbed atomic hydrogen, Θ_H^0 the equilibrium value (open-circuit) of the surface coverage of the adsorbed hydrogen, and η is the displacement of the cathode voltage away from its equilibrium (open-circuit) value.

The general rate expressions given above were modified in order to interpret the experimental current voltage data. In all hydrogen evolution experiments (with and without indigo) the bulk solution concentration of dissolved hydrogen gas was maintained at saturation so that $c_{H_2}^b = c^*_{H_2}$. In the analysis, the equilibrium surface coverage of atomic hydrogen (Θ_H^0) on the *Raney* nickel catalyst was set *a priori* at 0.05, in which case the above equations were simplified for the conditions $\Theta_H^0 \ll (1 - \Theta_H^0)$. The equilibrium surface coverage was not determined experimentally by transient polarization or ac-impedance[2] techniques because of the large variations in the reported values of Θ_H^0 (ranging from 0.03 to 0.07) [234], [235]. With the modifications and simplifications described above, the rate expression for the hydrogen evolution on *Raney* nickel according to *Volmer-Heyrovský* and the *Volmer-Tafel* mechanisms are:

Volmer-Heyrovský rate expression

$$i = \frac{2i_{0,V}\exp\left(\frac{-\beta F\eta}{RT}\right)\left[1 - \exp\left(\frac{2F\eta}{RT}\right)\right]}{(1 - \Theta_H^0)\left[1 + \frac{i_{0,V}}{i_{0,Hy}}\exp\left(\frac{F\eta}{RT}\right)\right]}$$

(eq. 9.7)

Volmer-Tafel rate expression

$$i = \frac{-L_5 + \sqrt{L_5^2 - 4L_4L_6}}{2L_4}$$

(eq. 9.8)

where L_4, L_5 and L_6 are given by

$$L_4 = i_{0,T}(1 - \Theta_H^0)^2\exp\left(\frac{2\beta F\eta}{RT}\right)$$

---

[2] ac = alternating current

$$L_5 = 4i_{0,V}^2\left(-(1 - \Theta_H^0)^2 \exp\left[\frac{2F\eta}{RT}\right]\right) - 4i_{0,V}^2\left((1 - \Theta_H^0)^2\frac{i_{0,T}}{i_{0,V}}\exp\left[\frac{\beta F\eta}{RT}\right]\right)$$

$$L_6 = 4i_{0,V}^2 i_{0,T}\left(1 - \exp\left[\frac{2F\eta}{RT}\right]\right)$$

The kinetic parameters for the hydrogen evolution to be determined from experimental current-voltage data on *Raney* nickel are the exchange current densities $i_{0,V}$, $i_{0,Hy}$ for the *Volmer-Heyrovský* rate equation or $i_{0,V}$, $i_{0,T}$ for the *Volmer-Tafel* mechanism and the transfer coefficient β for the *Volmer* reaction.

For the limiting case of large cathode overpotentials ($\eta << 0$), the atomic hydrogen production controls the molecular hydrogen evolution rate on *Raney* nickel. When $\eta << 0$, the terms containing $\exp((\beta F\eta)/(RT))$ in the equations given above are small. For this limiting overpotential regime, both the *Volmer-Heyrovský* and the *Volmer-Tafel* rate equations reduce to a single i-η relationship of the *Volmer* step (which is strictly applicable for $\Theta_H << 1$):

$$i = \frac{2i_{0,V}\exp\left(\frac{-\beta F\eta}{RT}\right)}{(1 - \Theta^0_H)} \qquad\qquad \text{(eq. 9.9)}$$

For the cathode overpotentials and the current densities near the equilibrium ($\eta \rightarrow 0$ and $i \rightarrow 0$), a linear increase ($\exp((\pm x) \approx 1 \pm x)$) in the hydrogen gas evolution current density with increasing overpotential is predicted. The corresponding straight line equations for the two mechanisms (for $\Theta_H << 1$) are:

Volmer-Heyrovský rate expression

$$i = \frac{\frac{-2i_{0,V}}{1 - \Theta_H^0}\left(\left(\frac{2F}{RT}\right)\eta\right)}{1 + \frac{i_{0,V}}{i_{0,Hy}}} \qquad\qquad \text{(eq. 9.10)}$$

Volmer-Tafel rate expression

$$i = \frac{\dfrac{-i_{0,V}}{1 - \Theta_H^0}\left(\dfrac{2F}{RT}\right)\eta}{1 + \dfrac{i_{0,V}}{i_{0,T}}}$$

(eq. 9.11)

9.4.2 Interpretation of the current-voltage data for the hydrogen evolution

The determination of the reaction mechanism and the kinetic parameters for the molecular hydrogen evolution on *Raney* nickel was performed in two parts. First, the hydrogen generation rates at high cathodic overpotentials ($\eta << 0$) were matched to the single limiting-case rate expression given by a logarithmic form of the *Butler-Volmer* equation (*equation 9.9*) and the kinetic parameters $i_{0,V}$ and β were determined. Subsequently, the calculated values of $i_{0,V}$ were used to assess the low-overpotential fit of i-η data to the special rate equation of the *Volmer-Heyrovský* mechanism and the equation of the *Volmer-Tafel* mechanism. The ratio of the exchange current densities (either $i_{0,V}/i_{0,Hy}$ or $i_{0,V}/i_{0,T}$) was used to fit the theory and the lower-overpotential data. From this match, the third kinetic parameter ($i_{0,V}$ or $i_{0,Hy}$) was determined. A careful comparison of the rate equations with the low-overvoltage data was used to decipher which of the two reaction steps (*Heyrovský* (*reaction 9.2*) or *Tafel* (*reaction 9.3*)) follow the *Volmer* reaction for the evolution of molecular hydrogen on *Raney* nickel.

Linear logarithmic fits of the high-overpotential hydrogen evolution data to the single i-η relationship (*equation 9.9*) (which is strictly applicable for $\Theta_H << 1$) are shown in *Figure 9-8*. It can be clearly seen that log i increases linearly with increasing cathode potential, and the experimental data were found to match the relationship in the range of 0.03 to -0.1 V. The *Volmer*-step exchange current density and the transfer coefficient were determined from the y-intercept, $(2i_{0,V})/(1 - \Theta_H^0)$, and the slope $(\beta F)/(2.303RT)$ of the linear current-overpotential regime. For the data in *Figure 9-8* the *Tafel* slope is 92.65

mV (which is slightly too low compared to the theoretical value of 120 mV). The exchange current density and the transfer coefficient were found to be 4.14 mA cm^{-2} and 0.55, respectively.
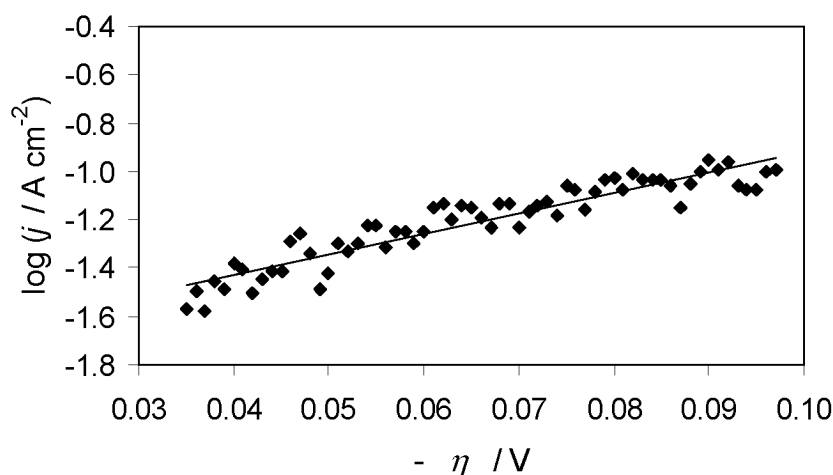
Fig. 9-8:   Linear logarithmic fit of high-overpotential current-voltage data for the evolution of hydrogen on *Raney* nickel electrodes in 1 M NaOH, 25°C to the *Volmer-Heyrovský* and *Volmer-Tafel* rate equations (E_{OCP} = -469 mV *vs.* Ag/AgCl, 3 M KCl).

Typical low-overpotential ($-0.02 \leq \eta \leq -0.01$ V) current-voltage data for the evolution of hydrogen are shown in *Figure 9-9*. An excellent match between the kinetic model (*equation 9.10* and *9.11*) and the experimental data was obtained for the *Volmer-Heyrovský* mechanism with $i_{0, V}/i_{0, Hy}$ = 0.45. In case of the *Volmer-Tafel* mechanism no value of $i_{0,V}/i_{0,T}$ could be found which reproduced the experimental current-voltage behaviour for $\eta \to 0$.

Such comparisons of the kinetic models with the linear data indicate clearly that molecular hydrogen evolution on *Raney* nickel proceeds *via* a *Volmer-Heyrovský* mechanism. For the current-voltage data in *Figure 9-9* the exchange current density was found to be 9.27 mA cm^{-2}. Although the magnitude of $i_{0,Hy}$ is larger than $i_{0,V}$, the difference is not large enough to make the *Volmer* step rate-limiting.
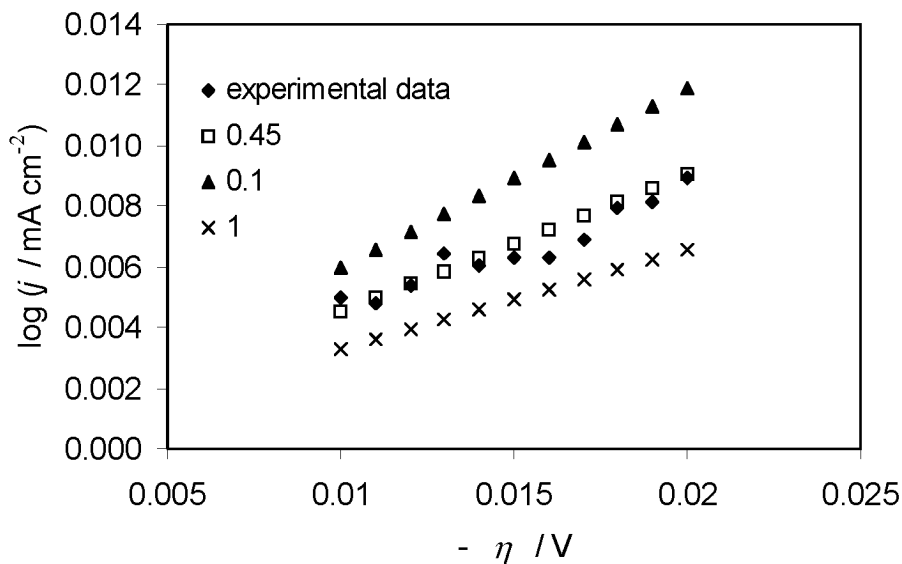
Fig. 9-9:   Linear fit of low-overpotential current-voltage data for the evolution of hydrogen on *Raney* nickel in 1 M NaOH, 25°C to the *Volmer-Heyrovský* and *Volmer-Tafel* rate equations (E_{OCP} = -469 mV *vs.* Ag/AgCl, 3 M KCl).

After the determination of the kinetic parameters, an overall fit of experimental data for the entire range of cathode overpotentials ($-0.01 \leq \eta \leq -0.1\,V$) to the rate equation of the *Volmer-Heyrovský* mechanism was examined. Such a model fit is shown in *Figure 9-10*. From this analysis it can be concluded that the *Volmer* reaction acts as the rate-determining step for the electrochemical hydrogen formation on *Raney* nickel at cathodic overpotentials more negative than -0.03 V. For η between 0.00 and -0.03 V, both the *Volmer* and *Heyrovský* steps are simultaneously controlling the overall hydrogen evolution rate (mixed control by two kinetic reactions), as evidenced by the ratio of the exchange current densities $i_{0,\,V}/i_{0,\,Hy}$ which is in the range of 0.45.
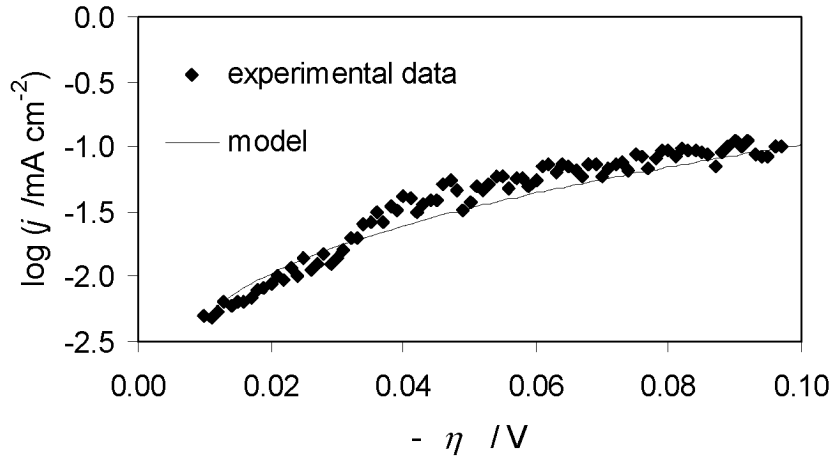
Fig. 9-10: Match of experimental current-overpotential data for the evolution of hydrogen on *Raney* nickel in 1 M NaOH, 25°C to the kinetic model, according to *Volmer-Heyrovský* (E_{OCP} = -469 mV *vs.* Ag/AgCl, 3 M KCl).

The *Volmer-Heyrovský* mechanism for the hydrogen evolution on *Raney* nickel differs somewhat from that found on flat-sheet nickel where the *Volmer* step had been determined to be rate-controlling. For composite-coated cathodes of *Raney* nickel (*Raney* nickel co-deposited with metallic nickel on a substrate) and phosphate-bound composite nickel electrodes the same results as presented in this study are published [234], [236].

9.4.3 Effect of temperature

The temperature dependence of $i_{0,V}$, $i_{0,Hy}$ and β for the hydrogen evolution on *Raney* nickel was investigated by performing potential-sweep experiments at four different solution temperatures (25, 50, 75, 100°C). For all experiments the experimentally determined charge-transfer coefficients were essentially constant over the entire temperature range, with an average value of 0.45, whereas both exchange current densities increase monotonically with increasing temperature. Using the classical *Arrhenius* temperature dependence:

$$i_{0,V} = P_{0,V}\exp\left[\frac{\Delta E_V}{RT}\right]$$
(eq. 9.12)

$$i_{0,Hy} = P_{0,Hy}\exp\left[\frac{\Delta E_{Hy}}{RT}\right]$$
(eq. 9.13)

The values of $P_{0,V}$ and $P_{0,Hy}$, the pre-exponential factors for the *Volmer* and *Heyrovský* reactions, and ΔE_V and ΔE_{Hy}, the activation energies for the exchange current densities, are listed in *Table 9-2*.
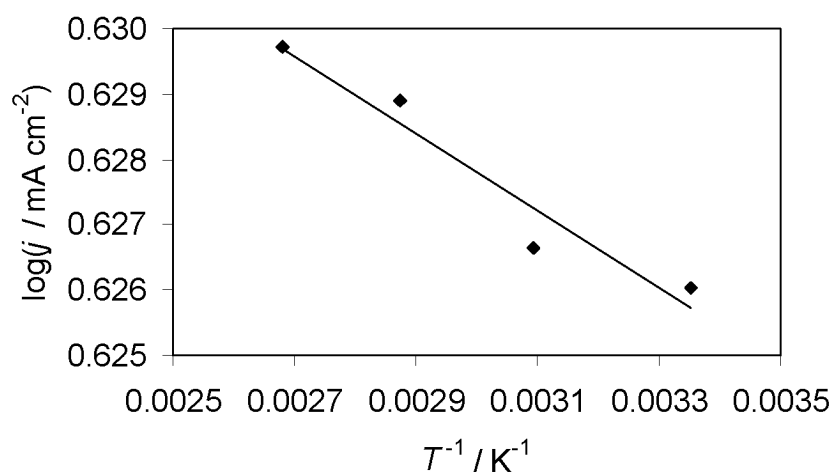
Fig. 9-11:   *Arrhenius* plot for the exchange current densities for the *Volmer* reaction in 1 M NaOH.
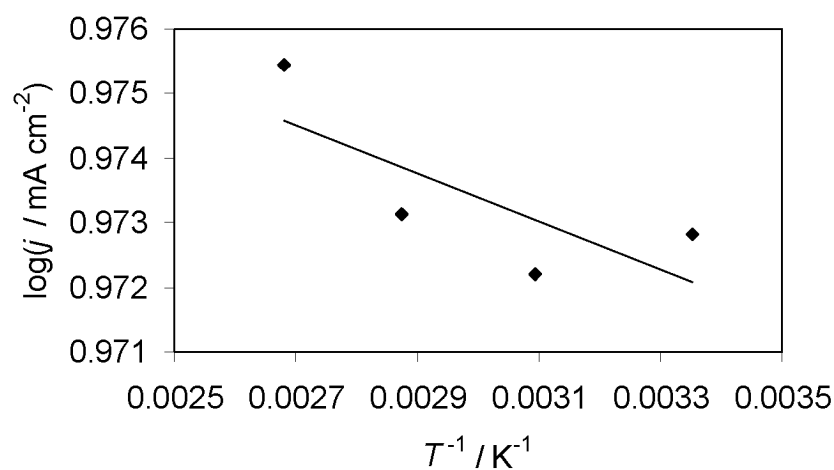
Fig. 9-12:   *Arrhenius* plot for the exchange current densities for the *Heyrovský* reaction in 1 M NaOH.

Table 9-2:   *Arrhenius* kinetic parameters for the hydrogen evolution on *Raney* nickel

$P_{0,V}$ / mA cm^{-2}	ΔE_V / J mol^{-1}	$P_{0,Hy}$ / mA cm^{-2}	ΔE_{Hy} / J mol^{-1}
5.9	48.9	3.7	30.7

9.5 Kinetic model for the simultaneous water reduction and indigo hydrogenation

9.5.1 Introduction

During the electrocatalytic hydrogenation of indigo on *Raney* nickel the *Volmer* and *Heyrovský* steps for the hydrogen evolution occur in conjunction with the catalytic reduction of indigo by electrogenerated H_{ads}.

$$H_2O + e^- = H_{ads} + OH^- \qquad (9.1)$$

$$H_{ads} + H_2O + e^- = H_2 + OH^- \qquad (9.3)$$

$$indigo + 2\,H_{ads} = leuco\ indigo \qquad (9.4)$$
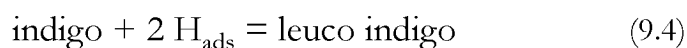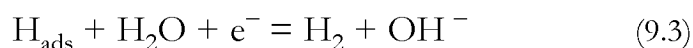
In the development of the model for the electrocatalytic hydrogenation the following assumptions were made:

- The reactions are not controlled by mass transfer or adsorption steps. However, until now the mechanism of the electrocatalytic hydrogenation process is not completely clear and it cannot be excluded that these steps are of importance for the reduction rate.

- The presence of indigo does not alter the mechanism of the hydrogen evolution on *Raney* nickel and the kinetic parameters are uneffected by either indigo, the radical or leuco indigo. The rate expressions for the generation of H_{ads} and the hydrogen evolution, however, have been modified to account for indigo adsorption, which reduced the number of sites on the surface of *Raney* nickel available for the equilibrium surface coverage of H_{ads}. However, indigo does not cause an anodic shift as observed in the case of other organic substrates (*e.g.* glucose), which indicates once more its weak adsorption.

- In parallel to the electrocatalytic hydrogenation also an electrochemical reduction by direct electron transfer can occur. The electrochemical reduction of mechanically attached vat dyes (*e.g.* indigo) has been analysed [5], [238]. Colloidal indigo may not interact with the electrode effectively, but this process cannot be excluded.

- Both hydrogenation steps (indigo to radical and radical to leuco dye) are assumed to be irreversible.

- In all electrocatalytic hydrogen evolution experiments (with and without indigo), the bulk solution concentration of dissolved hydrogen gas was maintained at saturation ($c_{H_2}^b = c^*_{H_2}$).

- The equilibrium surface coverage of atomic hydrogen (Θ_H^0) on the *Raney* nickel catalyst was set *a priori* at 0.05 [237].

- The electrochemical process from the dye pigment (D) *via* radical (R) to the leuco dye (L) can follow either a mechanism involving one step with two-electrons (*reaction 9.5*) or one involving two one-electron steps (*reaction 9.6*):

$$e^- + D = R \text{ and } R + e^- = L \qquad (9.5)$$
$$2\,e^- + D = L \qquad (9.6)$$
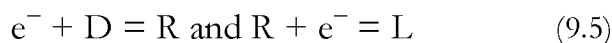
Based on the experimental results shown in *chapter 3* and reported by *Radugin*, a mechanism with two one-electron steps is assumed [238].

Although a good deal of practical experience has been collected, the theoretical understanding of indigo-voltammetry is still in its infancy. Thus, so far we can only speculate about the mechanism and the kinetics. *Figure 9-13* gives a simplified scheme of possible reaction pathways initiated by the application of a potential difference to the interface between electrode and solution. Dissolution of the solid reactant can take place as a result of the electrode reaction (α and γ) which converts a sparingly soluble reactant to a soluble one. A (parallel) slow dissolution of the reactant by the solvent may occur as well (β). The most intriguing question is how the electrode reaction might proceed. The electrode reaction can proceed at the interface between the solid reactant and the electrolyte (γ), but may occur also *via* a previously dissolved species (β–δ–λ). A direct electron transfer (α) can only occur at points where the three phases - electrode, solid reactant and electrolyte solution - are in contact with each other, because the electron transfer has to occur simultaneously with an ion transfer between the solid reactant and the electrolyte solution. Another possible reaction pathway includes the adsorption of the reactants and/or the products (β–ϵ–ζ). The model does not distinguish between adsorbed solid indigo

particles and dissolved indigo molecules. For the indigo reduction two views of the transfer mechanism are possible. Both, (A) dissolution and transport of indigo to the electrode surface followed by electron or hydride transfer and (B) electron or hydride hopping across the solid/solid boundary layer are plausible at a microscopic scale. The discussion seems to be the same as in the case of dyeing with disperse dyes. Either the solid material becomes adsorbed on the substrate surface or the dye is transferred by normal processes from the very dilute solution surrounding of the solid particles. *Vickerstaff* and *Waters* confirmed the secound possibility by successfully dyeing a cellophane sheet where the solid particles were kept isolated in a dialysis bag [239], [240]. However, in the case of the electrochemical reduction it was not possible to produce leuco indigo in the cathodic cell compartment where indigo was present in a dialysis bag.[3] Therefore, propably solid dye particles are the active species and solid/solid-contact controls the reaction.
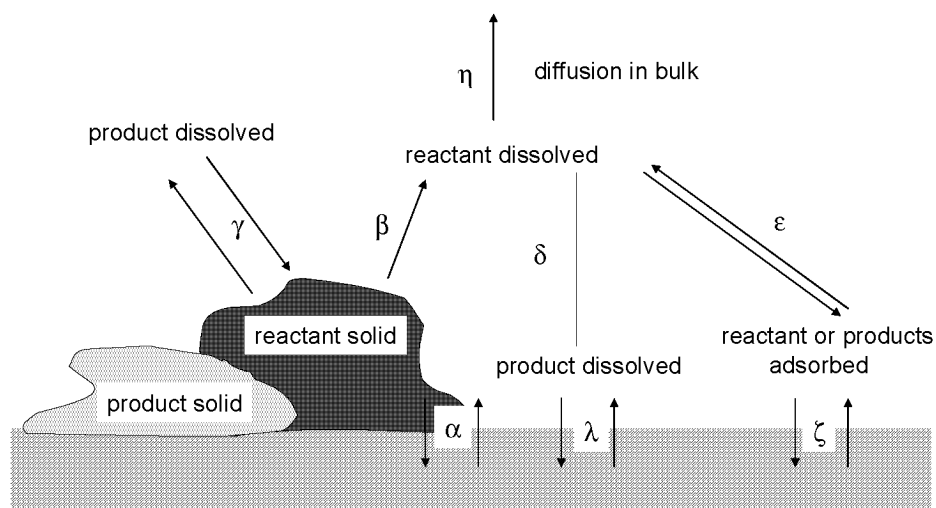
Fig. 9-13:   Scheme of possible reactions of solid compounds in electrochemical reactions. For an explanation see text [241].

---

[3] It was proved that leuco indigo can permeate the membrane.

Description of the whole process from the dye molecule (D) *via* the radical (R) to the leuco dye (L):

$$D + e^- + H^+ \underset{k_2}{\overset{k_1}{\rightleftharpoons}} R \qquad (9.7)$$

$$R + e^- + H^+ \underset{k_4}{\overset{k_3}{\rightleftharpoons}} L \qquad (9.8)$$

$$D + H_{ad} \underset{k_6}{\overset{k_5}{\rightleftharpoons}} R \qquad (9.9)$$

$$R + H_{ad} \underset{k_8}{\overset{k_7}{\rightleftharpoons}} L \qquad (9.10)$$

$$H_2O + e^- \underset{k_{10}}{\overset{k_9}{\rightleftharpoons}} H_{ad} + OH^- \qquad (9.11)$$

$$H_2O + e^- + H_{ad} \underset{k_{12}}{\overset{k_{11}}{\rightleftharpoons}} H_2 + OH^- \qquad (9.12)$$

$$D + L \underset{k_{14}}{\overset{k_{13}}{\rightleftharpoons}} 2\,R \qquad (9.13)$$
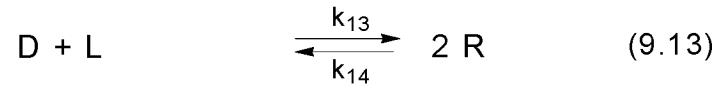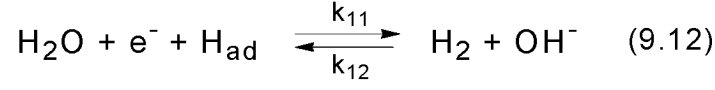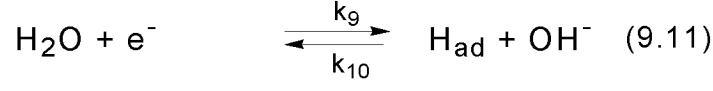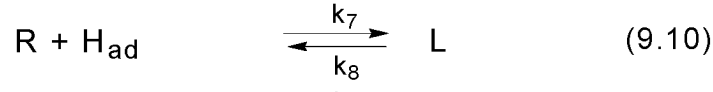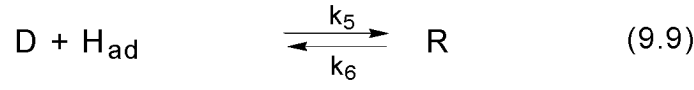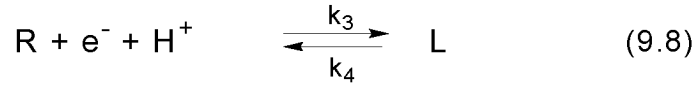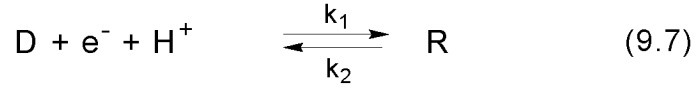
The rate of the process with respect to different reacting species can be given as

$$r_D = \frac{dc_D}{dt} = (-k_1\Theta_D + k_2\Theta_R - k_5\Theta_H\Theta_D + k_6\Theta_R)\sigma - k_{13}c_Dc_L + k_{14}c_R$$

$$r_R = \frac{dc_R}{dt} = k_1\Theta_D - k_2\Theta_R + k_5\Theta_H\Theta_D - k_6\Theta_R - k_3\Theta_R + k_4\Theta_L -$$
$$- k_7\Theta_R\Theta_H + k_8\Theta_L)\sigma + k_{13}c_Dc_L - k_{14}c_R$$

$$r_L = \frac{dc_L}{dt} = (k_3\Theta_R + k_7\Theta_H\Theta_R - k_8\Theta_L - k_6\Theta_L)\sigma - k_{13}c_Dc_L + k_{14}c_R$$

$$r_H = \frac{d\Theta_H}{dt} = (k_9(1 - \Theta_L - \Theta_R - \Theta_D - \Theta_H) - k_{10}\Theta_H + k_6\Theta_R - k_5\Theta_H\Theta_D -$$
$$- k_7\Theta_H\Theta_R + k_8\Theta_L - k_{11}\Theta_H + k_{12}(1 - \Theta_L - \Theta_R - \Theta_D - \Theta_H))\sigma$$

wherein $\sigma = 32\ cm^2$ (geometric electrode surface).

The surface coverage can be written in the following way for each component:

$$\Theta_D = \frac{K_D c_D}{(1 + K_D c_D + K_R c_R + K_L c_L + K_H c_{H_2})}$$

$$\Theta_R = \frac{K_R c_R}{(1 + K_D c_D + K_R c_R + K_L c_L + K_H c_{H_2})}$$

$$\Theta_L = \frac{K_L c_L}{(1 + K_D c_D + K_R c_R + K_L c_L + K_H c_{H_2})}$$

$$\Theta_H = \frac{K_H c_{H_2}}{(1 + K_D c_D + K_R c_R + K_L c_L + K_H c_{H_2})}$$

Thus, the term $K_H c_H$ can be substituted in all equations by

$$K_H c_{H_2} = \frac{\Theta_H(1 + K_D c_D + K_R c_R + K_L c_L)}{(1 - \Theta_H)}$$

Most of the kinetic constants given above can be written in a more comprehensive way:

$$k_1 = k_{0,1} \exp\left(\frac{\beta_1 F(E - E_{0,D})}{RT}\right)$$

$$k_2 = k_{0,1} \exp\left(\frac{-(1 - \beta_1)F(E - E_{0,D})}{RT}\right)$$

where $E_{0,D}$ = -700 mV $vs.$ Ag/AgCl, 3 M KCl.

$$k_3 = k_{0,2} \exp\left(\frac{\beta_2 F(E - E_{0,R})}{RT}\right)$$

$$k_4 = k_{0,2} \exp\left(\frac{-(1 - \beta_2)F(E - E_{0,R})}{RT}\right)$$

where $E_{0,R}$ = -1000 mV $vs.$ Ag/AgCl, 3 M KCl.

Some constants are already known:

$$k_9 = k_{0,3}\left(\frac{1 - \Theta_H - \Theta_L - \Theta_R - \Theta_D}{1 - \Theta_H^0}\right) \exp\left(\frac{\beta_3 F(E - E_{0,H})}{RT}\right)$$

$$k_{10} = k_{0,3}\left(\frac{\Theta_H}{\Theta_H^0}\right) \exp\left(\frac{-(1 - \beta_3)F(E - E_{0,H})}{RT}\right)$$

where

$$k_{0,3} = \frac{1}{F}[i_{0,V}] = \frac{1}{F}\left[P_{0,V}\exp\left(\frac{\Delta E_V}{RT}\right)\right]$$

and

$$k_{11} = k_{0,4}\left(\frac{\Theta_H}{\Theta_H^0}\right)\exp\left(\frac{-(1-\beta_4)F(E-E_{0,H})}{RT}\right)$$

$$k_{12} = k_{0,4}\left(\frac{1-\Theta_H-\Theta_L-\Theta_R-\Theta_D}{1-\Theta_H^0}\right)\exp\left(\frac{\beta_4 F(E-E_{0,H})}{RT}\right)$$

where

$$k_{0,4} = \frac{1}{F}[i_{0,Hy}] = \frac{1}{F}\left[P_{0,Hy}\exp\left(\frac{\Delta E_{Hy}}{RT}\right)\right]$$

and $E_{0,H} = -200$ mV $vs.$ Ag/AgCl, 3 M KCl.

The values of $P_{0,V}$ and $P_{0,Hy}$, the pre-exponential factors for the *Volmer* and *Heyrovský* reactions, and the two activation energies for the exchange-current density, are listed in *Table 9-2*.

In addition, *Jin* [277], [278] measured the kinetics of the comproportionation of indigo and leuco indigo by EPR-spectroscopy:

$$k_{13}\,(353\text{ K}) = 4.77 \cdot 10^2 \text{ cm}^3 \text{ mol}^{-1}\text{ s}^{-1}$$

The kinetic constant k_{14} can be calculated by using the equilibrium constant for the comproportionation of indigo and leuco indigo which has been estimated from standard reduction potential values for indigo and leuco indigo [277], [278]

$$K_{eq} = \frac{k_{13}}{k_{14}} = 3.36 \cdot 10^{26}$$

A kinetic rate equation for the catalytic hydrogenation of indigo was derived in *chapter 9.3.6*. The indigo hydrogenation rate per unit reactor volume

was converted into a surface reaction rate by dividing k by the surface area of catalyst per unit reactor volume (8900 cm^{-1} for *Raney* nickel powder catalyst with 10% loading [237]). The constant $k_5 = 6.59 \cdot 10^{-10}$ cm s^{-1} was used as a starting value for the simulation. In addition, the adsorption constant for indigo $K_D = 55$ cm^3 mol^{-1} (see *chapter 9.3.6*) was used as a starting value for the simulation.

In electrochemical reactions, the change of the amount of a compound can be determined from the measured current I which, according to the *Faraday* law, is always proportional to the rate of variation of the amount of the reaction products or initial compounds, *e.g.*, to the reaction rate:

$$\frac{dQ_i}{dt} = I = \sum_{i=1}^{k} z_i F(\pm v_i)$$

Here, the sign $\pm$ depends on the direction of the reaction, and Q_i is the amount of electricity consumed for the redox transformation. In our case, the current I is given by:

$$\frac{I}{96485} = k_1 \theta_D - k_2 \Theta_R + k_3 \Theta_R - k_4 \Theta_L + k_9 (1 - \Theta_L - \Theta_R - \Theta_D - \Theta_H) - k_{10} \Theta_H +$$

$$+ k_{11} \Theta_H - k_{12} (1 - \Theta_L - \Theta_R - \Theta_D - \Theta_H)$$

9.5.2 Simulation with Berkeley Madonna[4]

The mathematical simulation with the use of the equations given above can yield the profile of concentration *vs.* time and a theoretical dependence $I(\eta)$ with the parameters β_1, β_2, k_{01}, k_{02}, k_5, k_7, K_D, K_R, K_L by comparing the theoretical dependence with the experimental one. For this purpose, a nonlinear regression analysis of the experimental data by a *Newton* procedure was performed. The initial settings of the parameters were specified and the system of differential equations was solved by the *Runge-Kutta* method.

---

[4] Berkeley Madonna (version 8.0.1) is a computer programme.

A simulated concentration-time behaviour during the electrocatalytic hydrogenation process can be seen together with the experimental data in *Figure 9-14*. The fitting seems to be quite good and the constants of the model are summarized in *Table 9-3*.

Table 9-3: Summary of parameters in the kinetic model

β_1	β_2	k_{01}	k_{02}	k_5 / min^{-1} g cat.$^{-1}$	k_7 / min^{-1} g cat.$^{-1}$	K_D / cm^{3}mol^{-1}	K_R / cm^{3}mol^{-1}	K_L / cm^{3}mol^{-1}
0.4	0.55	3E-12	8E-10	1.1E-4	1.01	7 585	3 390	180

It is interesting to mention that the adsorption constant of indigo of 7585 cm^{3}mol^{-1} is much higher than in the case of the catalytic hydrogenation with molecular hydrogen (55 cm^3 mol^{-1}, *chapter 9.3.6*). This might be caused by the fact that the experimental data with planar porous electrode grids are compared with data based on powdered *Raney* nickel. Adsorption of indigo particles is probably much smaller in the case of a powdered catalyst. On the other hand, the adsorption constants evaluated by kinetic measurements does not represent real equilibrium constants. It is possible, that due to a fast subsequent consumption of the adsorped species, the surface coverage never reaches an equilibrium. In addition, in the kinetic model of the catalytic hydrogenation with molecular hydrogen the adsorption of the radical species and leuco indigo is neglected. Thus, a comparison between the two values is very difficult. Furthermore, it has to be mentioned that the presented simplified model assumes fast mass transfer or adsorption steps compared to the reaction rate. However, until now the mechanism of the electrocatalytic hydrogenation process is not completely clear and it cannot be excluded that these steps are rate determining.

Nevertheless, the rate constant k_7 for the radical hydrogenation is several orders of magnitude higher than that of indigo, suggesting that the rate-determining step in the hydrogenation process is the hydrogenation of the insoluble

indigo to the radical. Moreover, the estimated hydrogenation rate constant k_5 is in the same order of magnitude as in the case of the hydrogenation experiments with molecular hydrogen. Thus, it can be concluded that the reaction mechanism for the reduction of indigo on *Raney* nickel is probably unaffected by the source of adsorbed hydrogen, whether it be an external supply of pressurized gas or generated by the electrical discharge of water molecules.
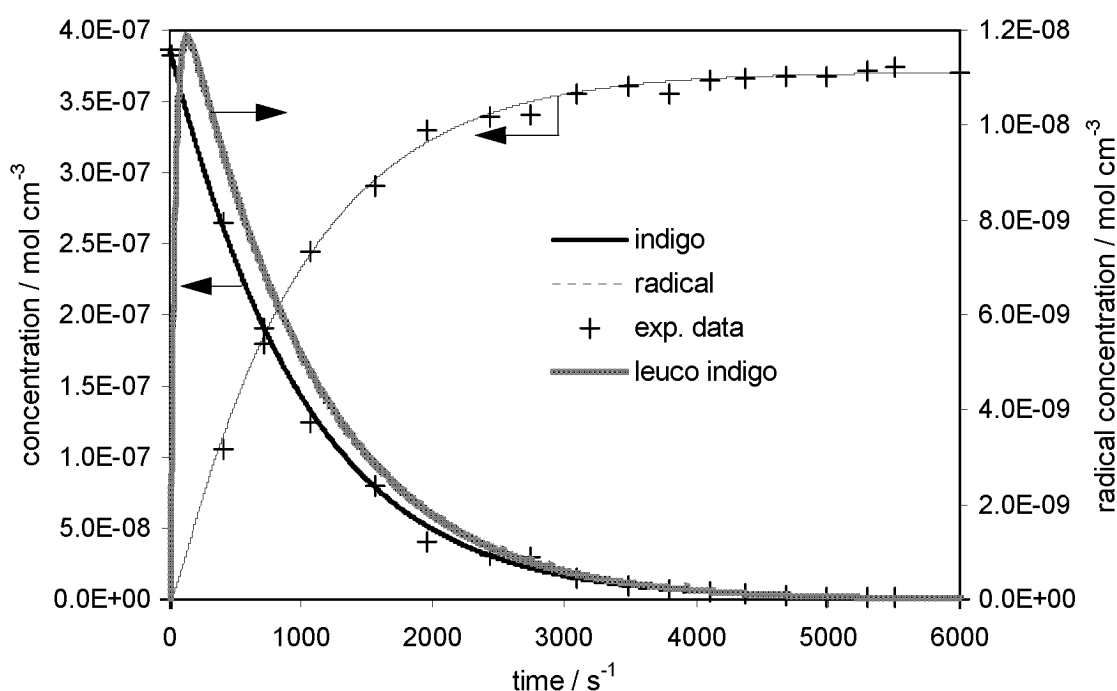
Fig. 9-14:   Match of the model profile of concentration *vs.* time to the experimental data on a *Raney* nickel electrode. System parameters: -900 mV (*vs.* Ag/AgCl, 3 M KCl), 1 M NaOH, 0.1 g l⁻¹ indigo, 50°C. E_{OCP} = -470 mV *vs.* Ag/AgCl, 3 M KCl. (+) experimental data.

The constants can be used to model also the current voltage data. A typical fit of the model with experimental current-voltage data is shown in *Figure 9-15*. Analysing the charge balance shows the influence of the current density on the process. The total current is the sum of the partial currents for the *Volmer* and *Heyrovský* step and the electrochemical reduction of the dye. Therefore, the current efficiency of the whole process can be split in two parts: the current efficiency of the electrochemical reduction and the current efficiency of the electrocatalytic hydrogenation process. The remaining part of the charge is used to produce molecular hydrogen. It is obvious from *Figure 9-16* that the amount of the electrochemical reduction of the dye is increasing at smaller val-

ues of the overpotential. The electrocatalytic hydrogenation process shows a maximum at a certain current density. This is in agreement with the experimental results and can be interpreted clearly. An increase of the current density favours the hydrogenation over the evolution of hydrogen which leads to an increase of the current efficiency. A further increase favours the hydrogen evolution over the hydrogenation, which ends up in a diminution of the current efficiency.
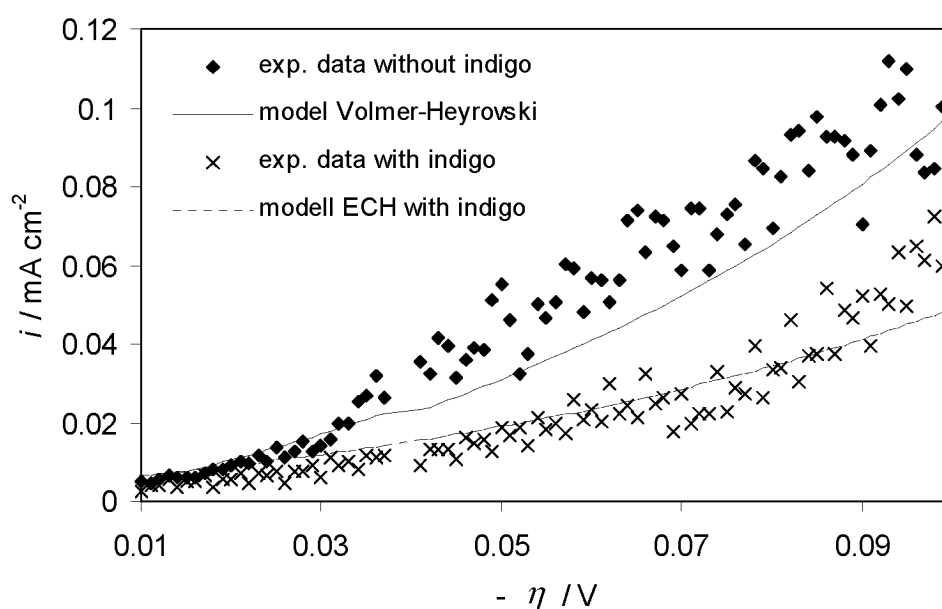
Fig. 9-15: Match of the model of hydrogen evolution/indigo reduction to experimental current-voltage data on a *Raney* nickel electrode. Same experimental parameters as in *Figure 9-14*.
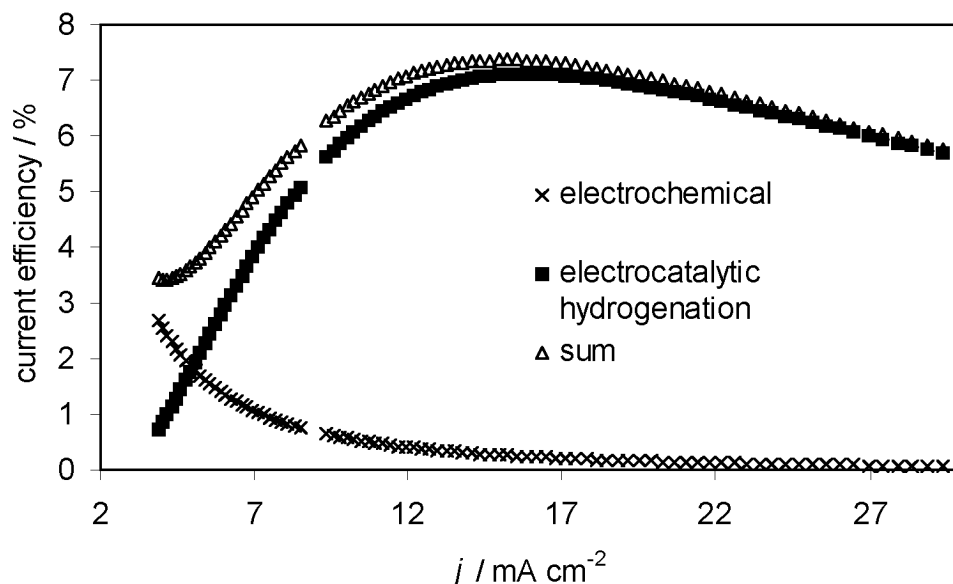
Fig. 9-16: Current efficiencies of the different processes on *Raney* nickel electrodes *vs.* current density *j*. Same experimental parameters as in *Figure 9-14*.

9.6 Conclusion

Kinetic models for the hydrogen evolution and the indigo reduction on *Raney* nickel electrodes have been proposed and tested. Both in the presence and the absence of indigo the hydrogen evolution is proceeding *via* a *Volmer-Heyrovský* mechanism. At low cathodic overpotentials, both steps control simultaneously the overall rate of the reaction, whereas at high cathodic overpotentials the generation of H_{ads} (*Volmer* reaction) is the rate-determining step. During the electrocatalytic hydrogenation of indigo the hydrogen evolution occurs in conjunction with the chemical catalytic hydrogenation of the organic substrate. A kinetic model for the prediction of the concentration *vs.* time and polarization curves was formulated. The model accurately predicted the experimental production rates of leuco dye. However, numerous assumptions were necessary to derive the kinetic equations and, therefore, the model is just a description of the behaviour, but not a kinetic law based on a detailed molecular theory.

Electrochemical reduction of indigo in fixed and fluidized beds of graphite

10.1 General Aspects

The direct electrochemical reduction of indigo would be an elegant vatting process, because it minimizes the consumptions of chemicals. Although it is not feasible to reduce indigo in an aqueous suspension on a planar electrode [4]-[20], it is possible to reduce indigo microcrystals after an immobilization on the surface of several electrode materials [5]. Thus, the limiting factor seems to be the poor contact between the indigo particles and the electrode, and it is desirable to develop a reduction process based on different reactor design which enables the intensification of the contact between the dye particles and the electrode.

Recently the so-called precoat-layer-cell has been presented as a solution (*chapter 2.4.3*), [151], [152], [276]. The severe drawback of this technique seems to be the large pressure drop built up during the filtration process and the persistent danger of blocking the reactor. Therefore, in the present thesis the industrial feasibility of the reduction of indigo in fixed and fluidized beds of graphite granules was investigated.

Graphite is a very cheap and stable material and the pressure drop caused by granular material is much lower than in the case of the fine powder of *Raney* nickel. Due to the high hydrogen overvoltage on graphite [252] under the applied conditions, no chemisorption or only very weak chemisorption of hydrogen is possible. Therefore, a normal electron transfer seems to be the relevant process for the reduction of indigo.

To optimize the operating conditions, a great deal of work focussed on the acceleration of the electron transfer reaction by modification of the graphite

surface by different pre-treatment methods as well as the modification of the electrode surface with quinones and anthraquinones. In addition, the influence of noble metals supported on the granules was studied.

10.2 Experimental

10.2.1 Chemicals

All aqueous solutions were prepared with deionized water. Indigo was supplied from BASF, Ludwigshafen, Germany. Remazol brilliant blue was received from DyStar Textilfarben, Frankfurt, Germany and Procion brilliant blue RS was supplied from BEZEMA AG, Montlingen, Switzerland. Sodium hydroxide (Fluka, p.a.), hexachloroplatinic(IV) acid hydrate (Fluka, purum), palladium chloride (Fluka, purum), potassium permanganate (Fluka, p.a.), potassium peroxodisulfate (Fluka, p.a.), potassium dichromate (Fluka, p.a.), hydrogen peroxide 30% (Fluka, p.a.), anhydrous sodium sulfate (Merck, p.a.), anthraquinone-2-carboxylic acid (Aldrich, 98%), 1-aminoanthraquinone (Fluka, techn.), 2-aminoanthraquinone (Fluka, techn.), acenaphthenequinone (Fluka, purum), N,N'-dicyclohexylcarbodiimide (Fluka, puriss.), sodium borohydride (Fluka, p.a.), p-benzoquinone (Fluka, puriss.), 1,4-naphthoquinone (Fluka, puriss.), 1,2,5,8-tetrahydroxyanthraquinone (Sigma-Aldrich), thionyl chloride (Fluka, puriss.) and Argon 4.8 were used as received. 5-Amino-acenaphthenequinone was synthesized from acenaphthenequinone by nitration [242] and subsequent reduction with hydrazine hydrate in the presence of an iron oxide hydroxide catalyst according to a reported general procedure [243].

10.2.2 Cells

A conventional laboratory flow-through H-cell was used in preliminary experiments designed to determine whether the crucial contact between indigo particles and the electrode could indeed be achieved. The results obtained after an optimization were then used as a guide in designing and operating a contin-

uous larger-scale flow cell to show the industrial feasibility at higher indigo concentrations.

a) Small-scale apparatus

A small flow channel with a packed or fluidized bed was used for the experiments. The working electrode consisted of a bed made up of 40 g of graphite granules (d = 2-3 mm). A stainless-steel wire (d = 1.5 mm) was located in the centre of the bed as current feeder. Ru/Ta was used as anode material, and the cell was divided into two compartments by a Nafion-324 membrane (DuPont). The set-up of this pilot plant used in the experiments is given in *Figure 4-1* and *Figure 4-2*. The flow circuit is described in detail in *chapter 4.2.2.* the current was supplied from a potentiostat (Radiometer Copenhagen DEA 332, Electrochemical Interface IMT102 and Software Voltamaster2).

b) Large-scale apparatus

The cell has a cylindrical concentric arrangement with a central position of the counter electrode (Pt/Ru), an outer position of the feeder (100 mesh stainless-steel grid (G. Bopp + Co. AG, Switzerland)) and with a ceramic separator (Alsint 99,7-tube, porous, d = 5 cm, FIRAG AG, Ebmatingen, Switzerland) between them (*Figure 10-3*). The working electrode consists of a bed electrode made up of 2 kg of graphite granules (d = 2-3 mm) with a bed depth of 5 cm and a height of 15 cm. The same electrolyte circuit was used as that for the small-scale reactor.
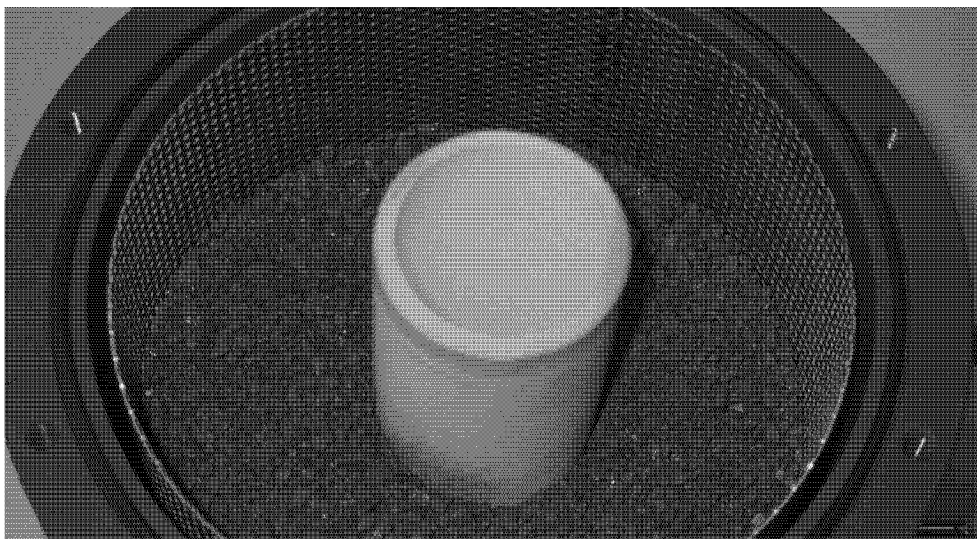
Fig. 10-1: Picture of the inner room of the large-scale apparatus.
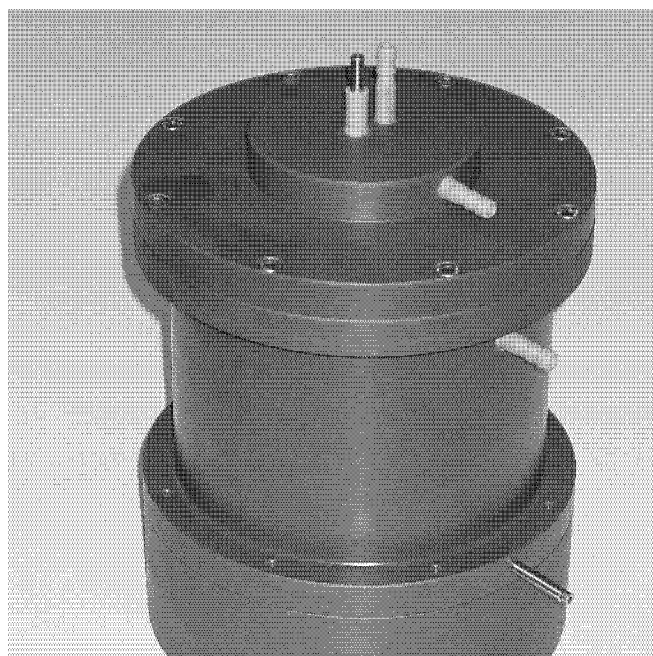
Fig. 10-2: Exterior view of the large-scale apparatus.
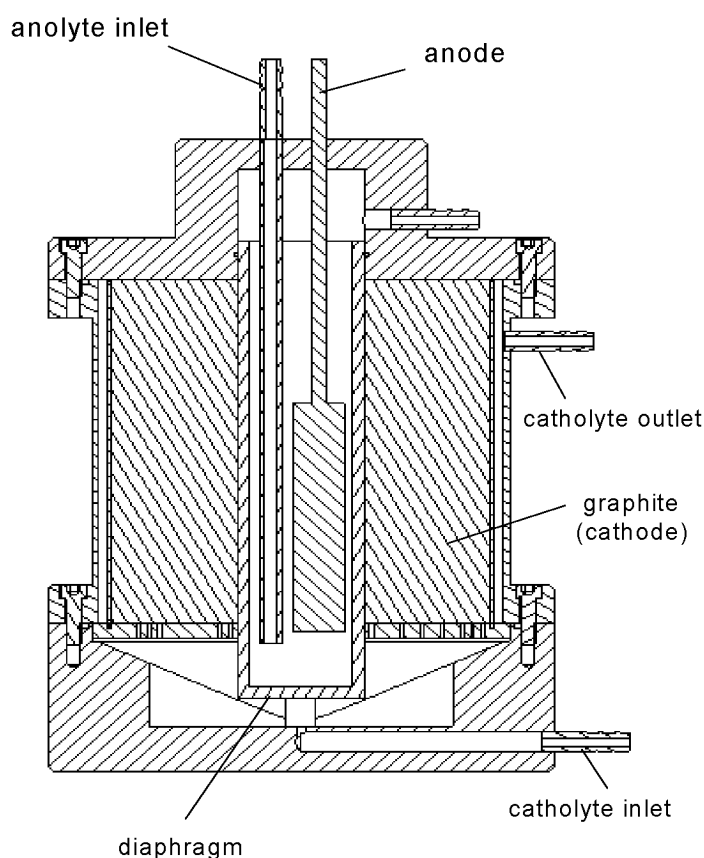
Fig. 10-3:   Schematic figure of the large-scale apparatus (by P. Trüssel, ICB workshop)

10.2.3 Electrode preparation

Four different commercial graphite granules were used after washing three times with distilled water and wetting overnight in 1 M NaOH: (A) enViro Gram, No. 00514, enViro Cell, Oberursel, Germany; (B) PMC, Sevierville, TN, USA, granular carbon, Lot. No. 2840; (C) TIMREX T1000-8000 graphite, Timcal group, Bodio, Switzerland; (D) Norit RX3 Extra, Lot. No. 510207, Norit Nederlands B.V., Amersfoord, Netherlands.

a) Noble metal deposition on graphite

Platinised graphite was prepared by impregnating it with a freshly prepared hexachloroplatinic solution, reduction with hydrazine and subsequent adsorp-

tion of the platinum particles on the graphite [244], [245]. Graphite, as a support for palladium, was prepared by impregnating it with a freshly prepared $PdCl_2$ solution in 0.1 M H_2SO_4, reduction with hydrazine and subsequent adsorption of the palladium particles on the graphite [244]. In addition, commercial carbon granules with 0.5 wt.% platinum were used as received (PMC, Sevierville, TN, USA, 0.5%Pt/#2840 granular carbon, Lot. No. 20617).

b) Oxidative pre-treatment

The graphite (en Viro cell) was treated with nitric acid under several conditions (*Table 10-1*). After the oxidation the samples were washed with distilled water and dried overnight at 110°C. In a second procedure the graphite was soaked with a 10^{-2} M solution of acidified (sulphuric acid to pH 2) potassium permanganate (1 g graphite per 10 ml of solution) for 5 h. After the oxidation the samples were washed with distilled water and dried overnight at 110°C. In a third method the graphite was soaked with a saturated solution of sodium peroxodisulfate $(Na_2S_2O_8)$ in 2 M H_2SO_4 (1 g graphite per 10 ml of solution) for 2 h. After the oxidation the samples were washed with distilled water and dried overnight at 110°C. Finally, in a fourth method, the graphite was kept in contact with an acidified (sulphuric acid to pH 2) 8% (w/w) solution of H_2O_2 (1 g graphite per 10 ml of solution) in a beaker until the gas evolution ceased (approx. 40 min). During this operation the temperature of the reaction mixture rose from room temperature to 45°C. After the oxidation the samples were washed with distilled water and dried overnight at 110°C.

c) Modification of the graphite granules with quinones and anthraquinones

To introduce various functional groups on the graphite surface, 10 g of graphite (enViro cell) were immersed in a 3:1 (by volume) mixture of H_2SO_4-HNO_3 at 100°C for 4 h. After cooling the graphite particles were filtered off and washed with distilled water. Subsequently, the graphite was treated with 100 ml of 5% NaOH to neutralise the excess acid present, followed by washing with distilled water. The granules became rather crumbly and were partly disintegrated during this procedure. Therefore, too small particles were removed by

sieving to guarantee a constant active surface of the electrode. The resulting oxidized graphite was dried over $CaCl_2$ for 24 h. The carboxylic groups formed were reduced to alcoholic or phenolic functional groups by reacting 10 g graphite with 20 g of $NaBH_4$ in 500 ml of distilled methanol. The reduction process was carried out for 12 h with constant stirring. Afterwards, the methanol was removed from the slurry and the reduced graphite washed with 500 ml of pure methanol. Benzoquinone and naphthoquinone were covalently attached to the pre-treated graphite by refluxing the graphite and the respective quinone with $ZnCl_2$ (1:1) in dry benzene for 78 h. The resulting material was soxhlet extracted for another 60 h with acetone as the solvent.

The covalent functionalization with anthraquinone was carried out according to a reported procedure [246], [247] (*Figure 10-4*). Anthraquinone carboxylic acid was first activated by stirring with N,N'-dicyclohexylcarbodiimide (DCC) in dry tetrahydrofuran for 24 h. The pre-treated reduced graphite was added to this solution for another 24 h. The resulting material was soxhlet extracted for 60 h with methanol as the solvent.

1,2,5,8-tetrahydroxyanthraquinone,   1-aminoanthraquinone,   2-aminoanthraquinone and 5-amino-acenaphthenequinone were immobilized by covalent modification of the graphite *via* the carboxylic groups at the surface. The pre-treated oxidized graphite was first activated by stirring it with N,N'-dicyclohexylcarbodiimide (DCC) in dry tetrahydrofuran for 24 h. The mediator molecule was added to this solution for another 24 h. The resulting material was soxhlet extracted for 60 h with methanol as the solvent.
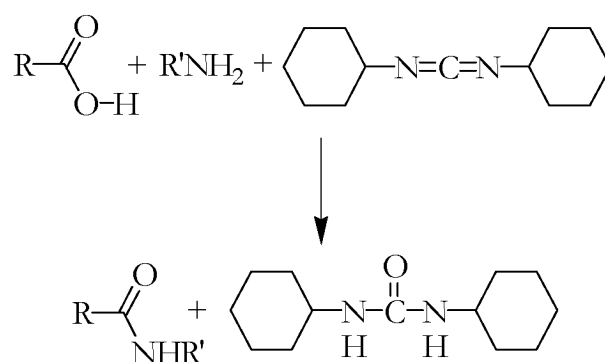
Fig. 10-4:   Method for forming peptide bonds [247].

In the case of the application of acid chloride groups, the oxidized en Viro cell graphite was treated with a solution (20% (v/v)) of $SOCl_2$ in dry benzene to acylate the carboxyl groups at the surface. After rinsing the graphite with dry benzene, the activated electrodes were rapidly transferred to benzene solutions of 5-amino-acenaphthenequinone and 1,8-dihydroxyanthraquinone where the coupling reaction between the acyl and amino as well as the hydroxyl groups occurred. A period of 24 h was allowed to complete the reaction, after which the electrodes were washed thouroughly with benzene and methanol. The resulting material was soxhlet extracted for 60 h with methanol as the solvent.

The graphite was modified by reactive dyes by treating the pre-treated reduced enViro cell graphite with an alkaline (0.1 M NaOH) solution of C.I. Reactive Blue 4 and C.I. Reactive Blue 4 for 2 h at 25°C. The resulting material was soxhlet extracted for 60 h with methanol as the solvent.

10.2.4 Procedure

Cathodic dispersions of indigo were usually composed of 0.1 g l^{-1} indigo (sieve fraction between 0.06 - 0.08 mm) in 1 M NaOH. In the large-scale cell concentrations up to 100 g l^{-1} were investigated. In all experiments the solutions were deoxygenated for at least 2 h before the experiment and maintained under a nitrogen atmosphere during the measurements. Anodic solutions consisted of 1 M NaOH. Usually the reduction experiments were performed at 50°C and a fluid flow velocity of 1.68 cm s^{-1}. In the case of different pH-values, the difference in ionic strength in comparison with a 1 M NaOH (pH = 14) was compensated by adding Na_2SO_4.

10.2.5 Redox titration

Before the titration experiments all quinones were reduced quantitatively with sodium borohydride to the hydroquinones as described in the literature [260], [261]. The unreacted borohydride was decomposed with sulfuric acid. Afterwards an aliquot part from the clear supernatant liquid was treated with an excess of a ferric(III) sulfate solution and the quantity of ferrous(II) sulfate

formed after equilibration was titrated with potassium bichromate [258], [262]. The solutions were protected against oxidation by dry ice (CO_2). Although this technique is cumbersome, with such a titration it is possible to have access to areas of the surface, such as the interior of pores, which are usually invisible to spectroscopic techniques such as XPS.

10.3 Results and discussion

From the graphite materials examined (enViro cell, Timcal, Norit, PMC), the granular material from enViro cell – which in contrast to the other cathode materials is rather exhibiting a coke-type structure (production at 1000°C instead of 2500°C) – proved to be the most active catalyst. Therefore, this material was used for further investigations. A series of galvanostatic runs was carried out in order to assess the effect of operating parameters such as the current density, the pH, the temperature, the indigo concentration and the flow rate of the catholyte on the electrochemical kinetics. Leuco indigo was produced – in contrast to the process based on the electrochemical reduction of the indigo radical (*chapters 3 - 5*) – directly from the indigo suspension and was identified by spectrophotometric analysis (λ_{max} = 410 nm). Thus, direct electron-transfer between indigo and the graphite seems to be the relevant process. However, it cannot be excluded that the electrochemical reduction of the soluble indigo radical is occurring similarly to the direct reduction of the indigo pigment. Certainly, the radical species (λ_{max} = 565 nm) was formed after some time by the comproportionation of indigo with leuco indigo. Nevertheless, it is not very probable that the radical-mechanism is significantly relevant for this process, as the concentration of the radical species is very low and, consequently, so is its reduction rate.

Laboratory dyeing experiments show a dyeing behavior of the electrochemically reduced indigo similar to that of conventional reduction methods. In addition, in the vast majority of cases a 95% mass balance for indigo was obtained after the experiment by reoxidation to the insoluble product and filtration of the electrolyte. Therefore, it is obvious that the reaction product is

stable under the conditions applied and no other products are formed (*e.g.* by overreduction). In all experiments an induction period between 30 and 60 min without formation of leuco indigo was observed. This is due to the remaining traces of dissolved oxygen which consume a certain amount of the leuco indigo generated. An increased stripping time with argon before the addition of indigo could reduce this period. However, in addition, the induction period could be reduced by the presence of indigo during the stripping time (*Figure 10-5*). Usually, indigo really adheres to the graphite surface, but in the case of a flow system, at the same time it might also be washed off. Therefore, it takes some time until a reactive layer of indigo is formed on the surface of the graphite granules. If this pre-filtration can take place during the stripping period, the reduction of indigo can start much earlier. However, the production rate of leuco indigo has never been influenced by the pre-filtration step.
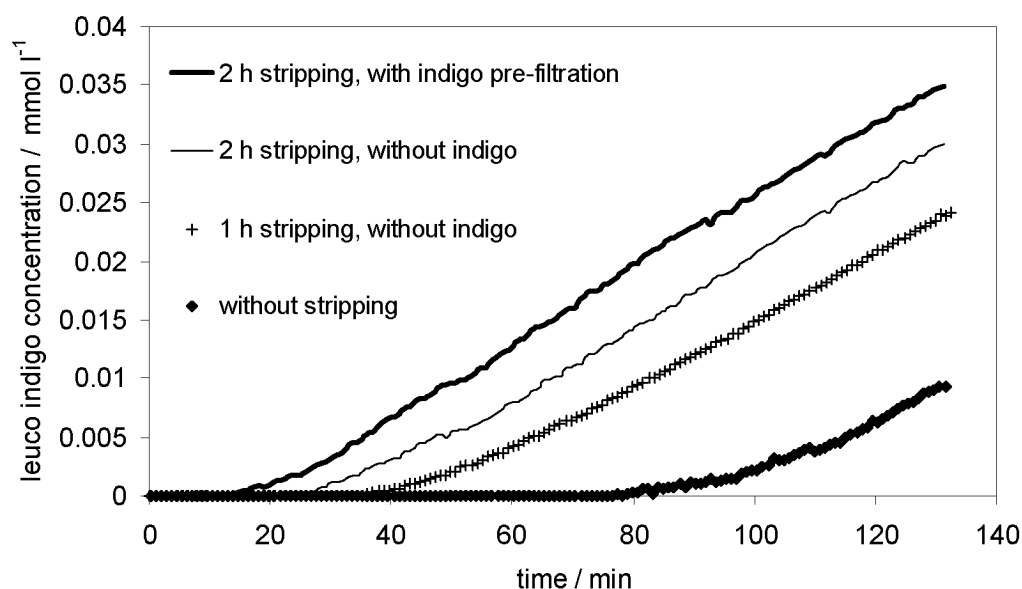
Fig. 10-5:   Influence of the stripping time and the presence of indigo before the experiment on the induction period. System parameters: enViro cell graphite granules, 1 M NaOH, 100 mg l^{-1} indigo, current density (related to the area of the membrane (5 cm^2)) 2 mA cm^{-2}, 50°C, fluid velocity 1.67 cm s^{-1}.

10.3.1 Influence of current density and temperature

The reaction rate as a function of the current density and the temperature is shown in *Figure 10-6*. At all temperatures the reduction rate passes a maxi-

mum with increasing current density and also increases with increasing temperature. In addition, the maxima are shifted to higher current values with increasing temperature. At 90°C the maximum reduction rate was approximately 40 nmol min^{-1} g^{-1} graphite.

A more profound understanding can be obtained by analysing the production rate as a function of electrode potential (*Figure 10-7*). The maximum is always reached at a potential of approximately -1200 mV *vs.* Ag/AgCl, 3 M KCl, which is close to the necessary value for the cathodic evolution of hydrogen. Therefore, at too high values of the current density indigo is removed from the electrode surface by gas evolution and the formation of the leuco dye is diminished. The slight shift of the maxima to a lower potential with increasing temperature can be attributed to the reduction in the overpotential.
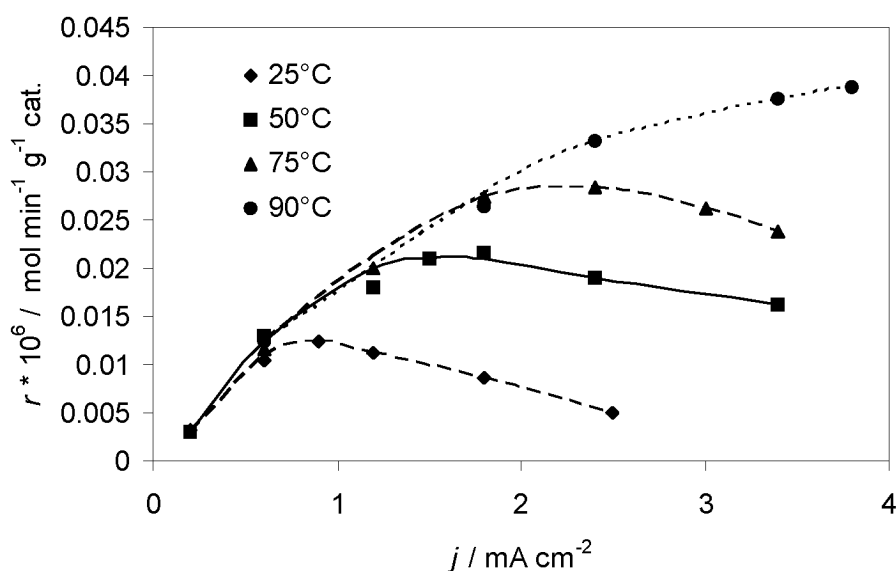
Fig. 10-6:   Influence of the current density *j* and temperature *T* on the production rate *r* for leuco indigo. System parameters: enViro cell graphite granules, 1 M NaOH, 100 mg l^{-1} indigo, fluid velocity 1.67 cm s^{-1}. The current density is related to the area of the membrane (5 cm^2).
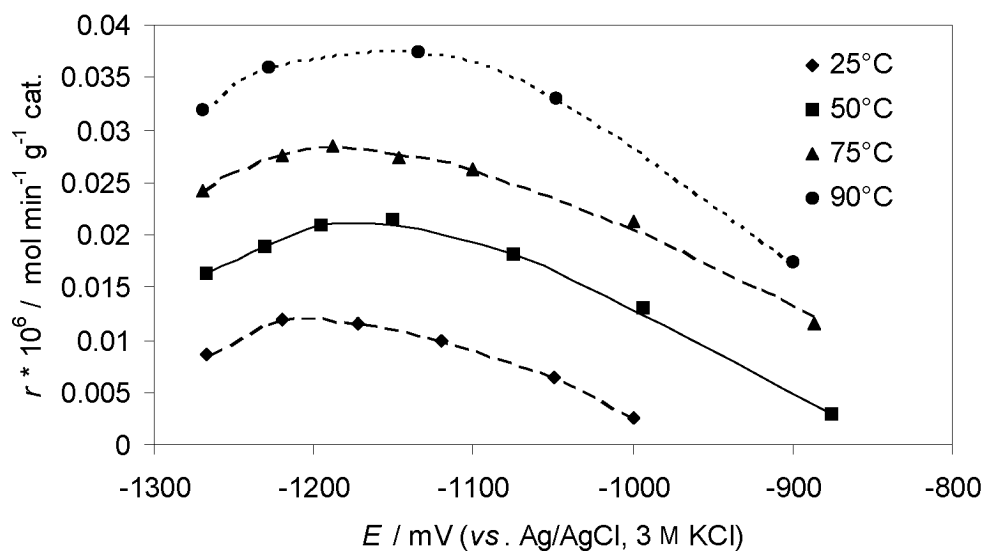
Fig. 10-7:   Influence of the cathode potential E and temperature T on the production rate r for leuco indigo. System parameters: enViro cell graphite granules, 1 M NaOH, 100 mg l^{-1} indigo, fluid velocity 1.67 cm s^{-1}. The current density is related to the area of the membrane (5 cm^2).

The current efficiency reaches a maximum of approximately 50% at a current density of 0.6 mA cm^{-2} (*Figure 10-8*). This observation is not in agreement with theory, according to which the current efficiency should increase steadily when the current density is reduced. However, at very small production rates the influence of oxygen present in the solution due to tightness problems becomes significant and may reduce the efficiency of the process.

The apparent activation energy of this electrode process was calculated from the relationship between the logarithm of the reduction rate *vs.* T^{-1} at a constant cathodic potential of -1.05 V *vs.* Ag/AgCl, 3 M KCl. The value is E_A = 11.4 ± 0.17 kJ mol^{-1} (95%, N = 3) (*Figure 10-9*).
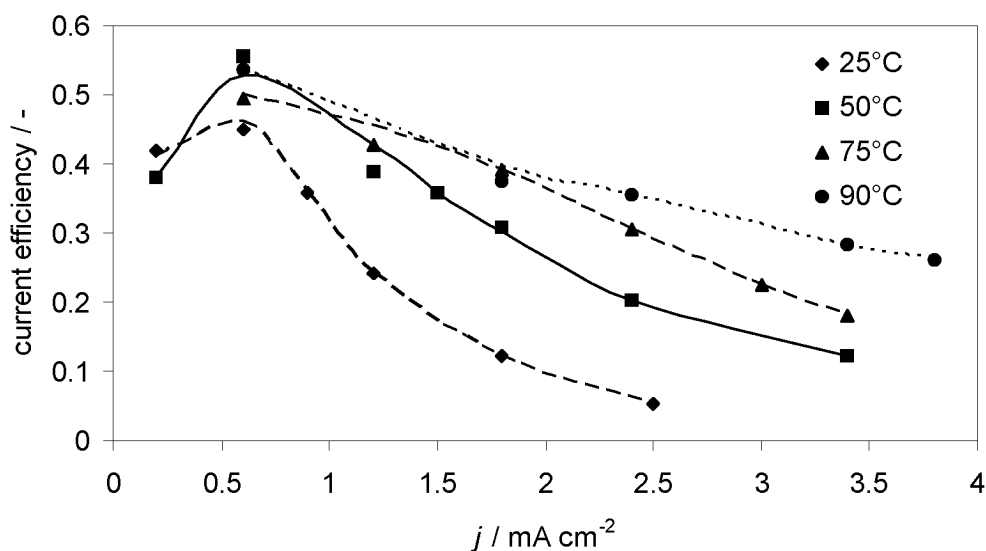
Fig. 10-8:   Influence of the current density j and temperature T on the current efficiency of the production rate r for leuco indigo. System parameters: enViro cell graphite granules, 1 M NaOH, 100 mg l^{-1} indigo, fluid velocity 1.67 cm s^{-1}. The current density is related to the area of the membrane (5 cm^2).
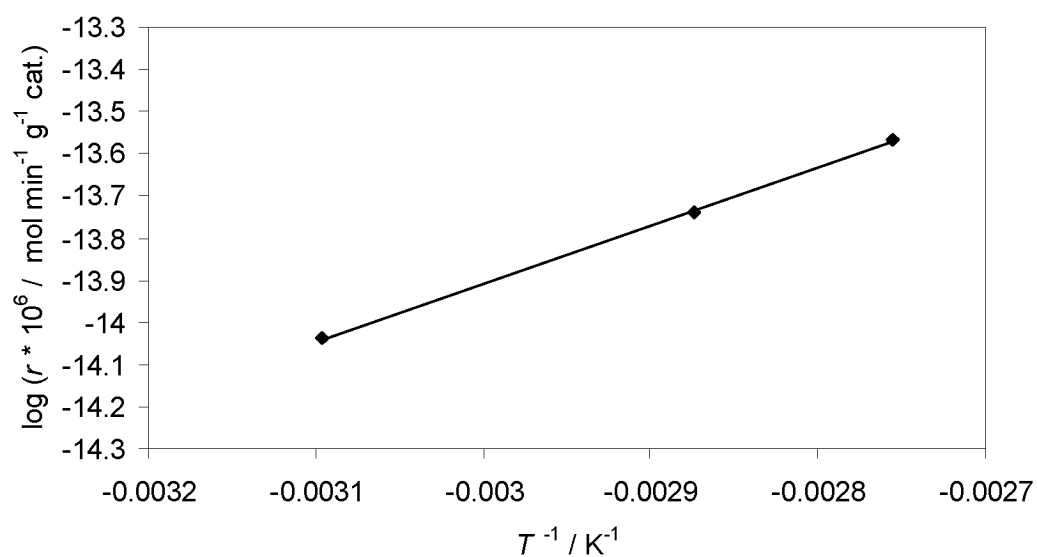
Fig. 10-9:   *Arrhenius* plot. System parameters: enViro cell graphite granules, 1 M NaOH, 100 mg l^{-1} indigo, measured at -1050 mV *vs.* Ag/AgCl, 3 M KCl, fluid velocity 1.67 cm s^{-1}.

10.3.2 Influence of the pH

It is obvious from the reaction mechanism of the evolution of hydrogen that hydroxide ions are produced at the surface of the cathode. Therefore, the pH near the surface is most probably higher than that in the bulk solution and the pH of an unbuffered electrolyte increases as the electrolysis proceeds (*e.g.*, in case of pH = 10 at the beginning of the electrolysis a final pH of 10.8 was reached). However, the effect of the initial pH of the bulk solution on the efficiency of the reduction was investigated, and the results are reported in *Figure 10-10*. Obviously, the conversion is clearly enhanced with increasing pH. This effect might be caused by the presence of the more soluble ionic forms of leuco indigo, because non-ionic or 'acid' forms of reduced indigo are poorly soluble in water [14]. On the other hand, it is possible that on graphite the positive effect of increasing the pH could be due in part to the decrease of the rate of the evolution of hydrogen competing with the reduction of indigo.
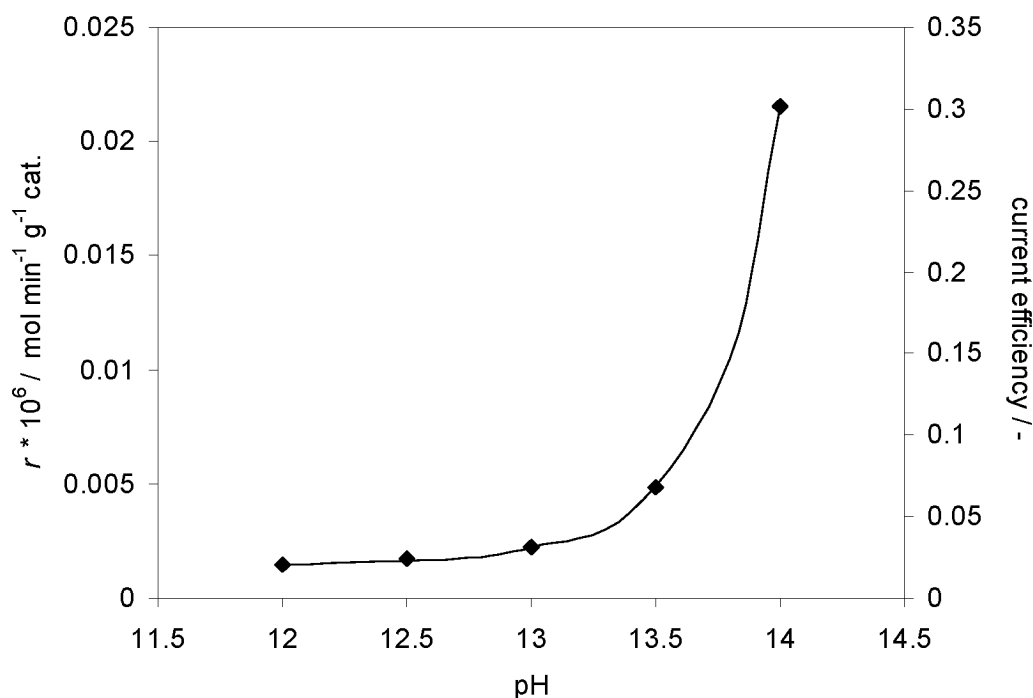
Fig. 10-10: Influence of the pH on the production rate r for leuco indigo and the current efficiency. System parameters: enViro cell graphite granules, 100 mg l^{-1} indigo, current density (related to the area of the membrane (5 cm^2)) 2 mA cm^{-2}, 50°C, fluid velocity 1.67 cm s^{-1}.

10.3.3 Influence of the fluid velocity

The influence of the fluid velocity was analysed during batch experiments at a constant potential of -1200 mV $vs.$ Ag/AgCl, 3 M KCl. *Figure 10-11* gives the relationship between the measured reduction rate and the flow rate, with an obvious peak near the fluidisation point. In the packed-bed region the rise in reduction rate is caused by the increase of the mass transfer coefficient and the increase in the pressure drop due to much more efficient filtration with increasing flow velocity. Thus, a maximum of 8.75 nmol min^{-1} g^{-1} graphite of the reduction rate was reached exactly at the fluidisation point ($u_c = 2.1$ cm s^{-1}), which has been determined by the *Richardson* and *Zaki* method (*chapter 4.3.6*) [182], [183]. Above the fluidisation point the expansion of the bed causes a sharp rise in the effective resistance of the particle phase. The associated ohmic drop leads to a sharp decrease of the macrokinetic current density and the fil-tration layer is destroyed. Therefore, it would be probably optimal to use a fixed-bed electrode which cannot expand (*e.g.*, flow operation in the downward direction to press the granules against a frit) at high fluid flow rates.
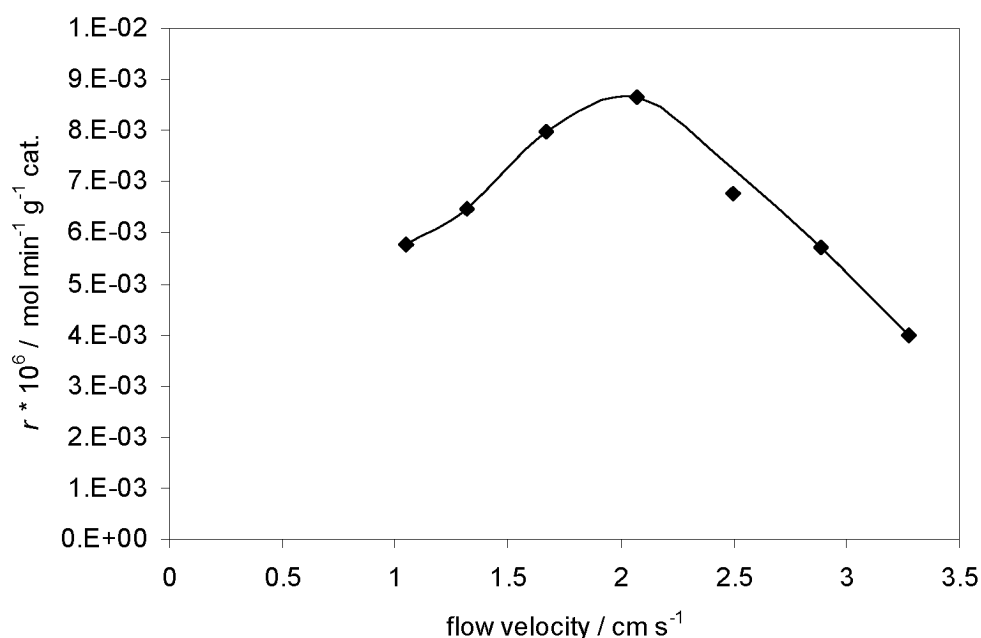
Fig. 10-11: Influence of the fluid velocity on the production rate r for leuco indigo. System parameters: enViro cell graphite granules, 1 M NaOH, 100 mg l^{-1} indigo, current density (re-lated to the area of the membrane (5 cm^2)) 2 mA cm^{-2}, 25°C.

10.3.4 Influence of the indigo concentration

It is obvious from *Figure 10-12* that an increasing indigo concentration can enhance the reaction rate. This effect is probably based on the better contact between the indigo particles and the graphite granules due to the higher probability of a collision between these two solid species. In addition, the adsorbed layer of indigo pigment will be stabilised by the increasing pressure drop over the fixed bed. However, it is important to mention that a blocking of the electrode was never observed during the experiments.
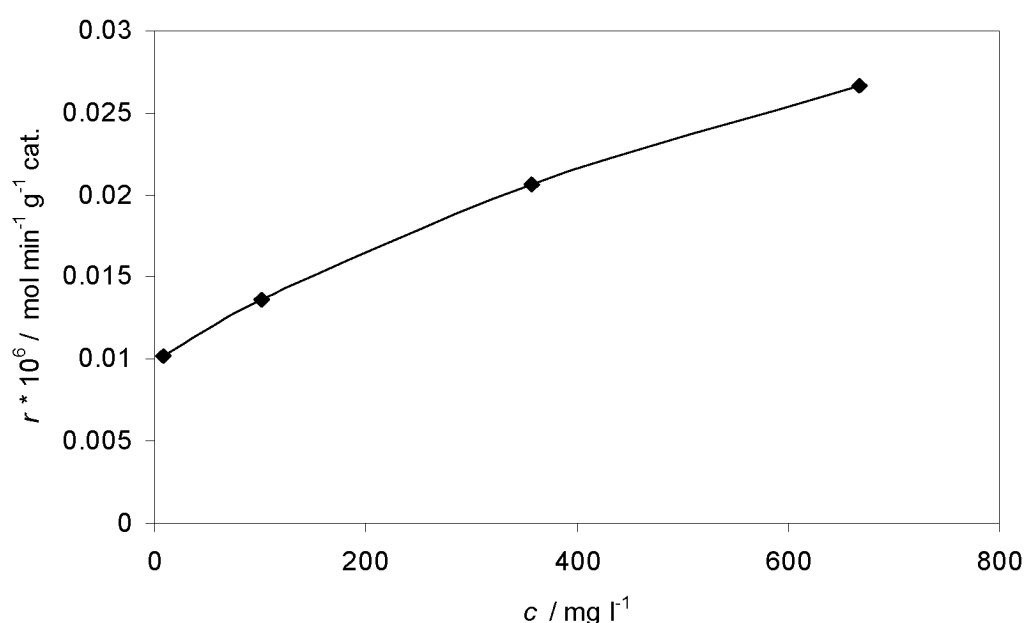
Fig. 10-12: Influence of the indigo concentration *c* on the production rate *r* for leuco indigo. System parameters: enViro cell graphite granules, 1 M NaOH, current density (related to the area of the membrane (5 cm^2)) 2 mA cm^{-2}, 50°C, fluid velocity 1.67 cm s^{-1}.

10.3.5 Influence of the oxidative pre-treatment of the graphite

At present, there is little doubt that much of the chemical activity of the carbon surface is connected with quinone and hydroquinone groups, whether directly attached to the carbon black surface or part of more complex structures (*Figure 10-13*), [248]-[252].

(a)   (b)   (c)   (d)   (e)
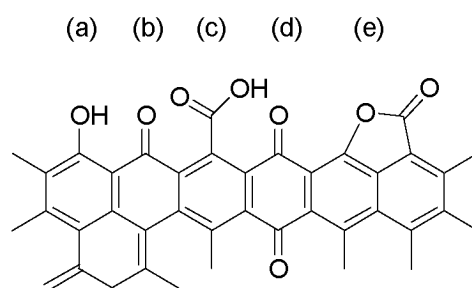
Fig. 10-13: Schematic representation of various oxygen functionalities at the carbon surface: (a) phenol; (b) carbonyl; (c) carboxy; (d) quinone; (e) lactone [252].

In addition, it is well known that an oxidative pre-treatment can increase the content of oxygen-containing groups on the surface of carbon [248]-[259]. Therefore, it should be possible to accelerate the electron transfer reaction by the selective generation of quinone-like functionalities on the surface of the graphite electrode.

In the first method, the graphite was treated with nitric acid under various conditions (*Table 10-1*). Obviously, after this pre-treatment no activity for indigo reduction could be observed. This effect might be based on the destructive reaction of nitric acid with graphite which was investigated by several workers [253]-[255]. In addition, the granules crumbled into small particles at too high concentrations of nitric acid.

Table 10-1: Influence of the oxidative pre-treatment of enViro cell granules with nitric acid under various conditions on the reduction rate of indigo

conditions	reduction rate $r^{1)}$ / nmol min^{-1} g^{-1}
untreated	20
boiled for 24 h with 1 M HNO_3	< 1
boiled for 2 h with conc. HNO_3	< 1
stirring at 25°C with 1 M HNO_3 for 1 h	< 1
stirring at 25°C with conc. HNO_3 for 1 h	< 1

[1)] System parameters: enViro cell graphite granules, 1 M NaOH, 100 mg l^{-1} indigo, current density (related to the area of the membrane (5 cm^2)) 2 mA cm^{-2}, 50°C, fluid velocity 1.67 cm s^{-1}.

In the second procedure, the graphite was soaked with a solution of acidified potassium permanganate. The observed decrease in reduction rate is probably based on the decomposition of the graphite with permanganate and the formation of MnO_2 on the carbon surface, which is described in the literature [255]-[257]. In the third method, the graphite was soaked with a saturated solution of sodium peroxodisulfate ($Na_2S_2O_8$), but this had no influence on the reduction rate. In the fourth method, the graphite was treated with acidified H_2O_2. The reduction rate could be approximately doubled to a value of 40 nmol min^{-1} g^{-1} graphite[1]. Simultaneously, an increase in redox capacity could be measured by redox titration. Thus, the increasing catalytic activity probably correlates with the formation of quinoid functional groups.

The surface modification of carbon electrodes by electrochemical pre-treatment had been the subject of many investigations, and several reviews are available [252], [263]-[265]. Thus, the influence of a pre-anodization step in 20% H_2SO_4 at 50°C and 0.3 A cm^{-2} (related to the area of the membrane (5 cm^2)) was also studied. The redox capacity and the reduction rate are plotted in *Figure 10-14* as a function of the charge consumed during the electrochemical oxidative pre-treatment. This figure shows that both the redox capacity and the reduction rate increase steadily when the charge used to electrochemically oxidize the graphite electrode in the pre-treatment procedure varies between 0 and 200 C g^{-1} graphite. An electrochemical oxidation extended to and beyond a charge of 200 C g^{-1} graphite does not yield any further change. However, it is possible to accelerate the reduction rate by a factor of three to 60 nmol min^{-1} g^{-1} graphite[1]. In addition, it was possible to activate also other graphite materials (*e.g.*, TIMREX T1000-8000 graphite, Timcal group, Bodio, Switzerland) which were inactive for the reduction of indigo without pre-treatment. Therefore, the electrochemical pre-anodization seems to be a very efficient technique for changing the electrochemical behaviour of graphite electrodes.

---

[1] System parameters: enViro cell graphite granules, 1 M NaOH, 100 mg l^{-1} indigo, current density (related to the area of the membrane (5 cm^2)) 1.5 mA cm^{-2}, 50°C, fluid velocity 2 cm s^{-1}.
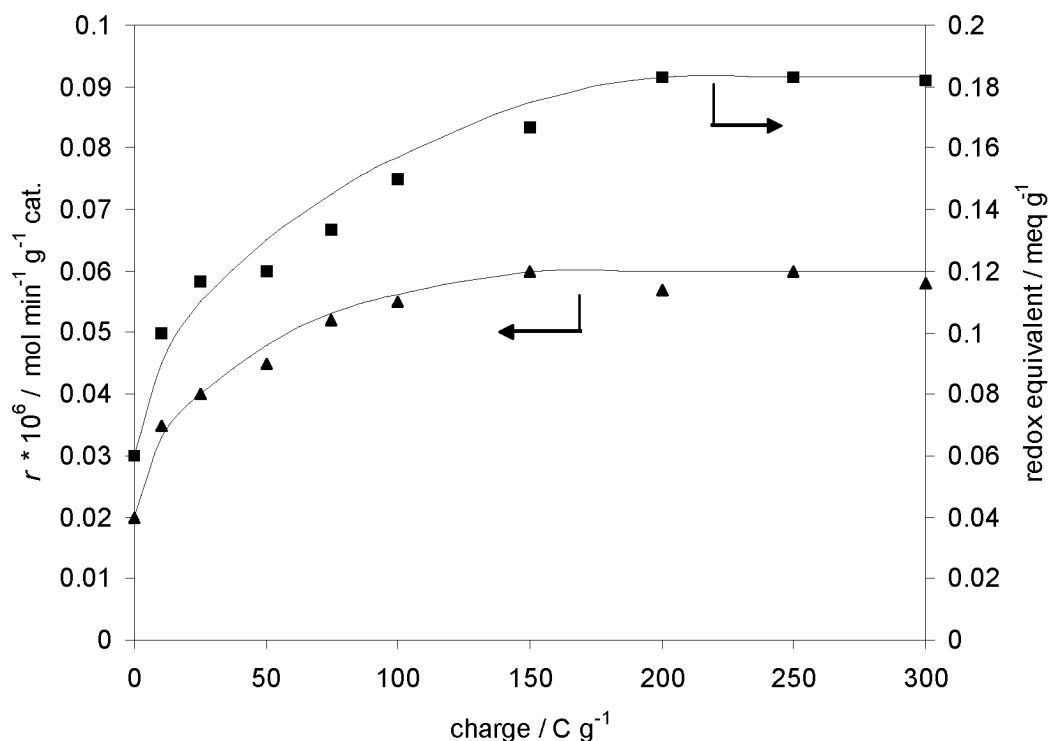
Fig. 10-14: Plot of the production rate r for leuco indigo and the redox equivalent of the graphite (enViro cell granules) as a function of the charge consumed during the electrochemical oxidation in 20% H_2SO_4 of a graphite electrode at 50°C and a current density of 50 mA cm^{-1} (related to the area of the membrane (5 cm^2)). System parameters: enViro cell graphite granules, 1 M NaOH, 100 mg l^{-1} indigo, current density (related to the area of the membrane (5 cm^2)) 2 mA cm^{-2}, 50°C, fluid velocity 1.67 cm s^{-1}.

10.3.6 Experiments with graphite granules modified by quinones

Another interesting approach to enhance the electrocatalytic properties of the graphite material is based on the covalent bonding of quinoid molecules to the graphite surface [246], [268]. By this, electron transfer mediators which can undergo fast electron transfer with the electrode (graphite) [246], [266], [267] and also with the substrate (indigo) are immobilized on the carbon electrode. Several immobilization methods are conceivable and a suitable one depends upon the substrate (*e.g.* graphite) and the mediator molecules. In the particular case of the reduction of indigo quinones and anthraquinones were used as redox-active molecules. These substances are already well known from the mediator process [269]. In addition, such species were used as catalysts for the

chemical vatting process [270]. Covalent functionalisation of graphite was carried out according to a reported procedure [246], [268]. *Figure 10-15* shows the possibility of immobilizing such species with an amine or hydroxyl functional group *via* the carboxylic groups on the surface. The quinone was modified according to *Figure 10-16*.
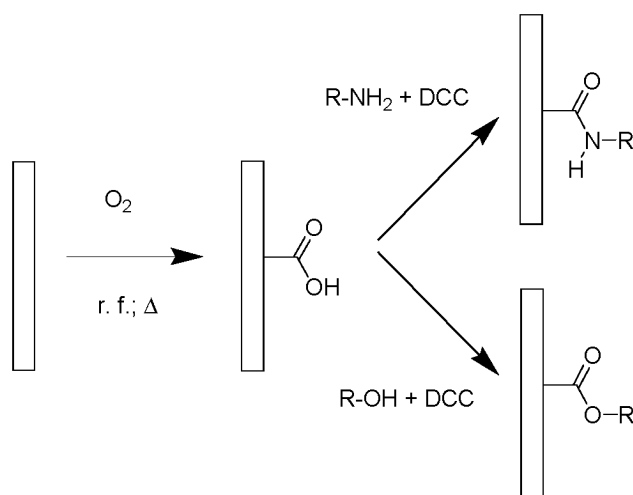
Fig. 10-15: Covalent modification *via* the carboxylic surface group on carbon. DCC = dicyclohexylcarbodiimide. r.f. = radio frequency plasma. Δ = thermal. R = *e.g.* anthraquinone.
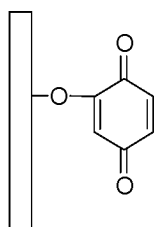
Fig. 10-16: Modification of the graphite with covalently bound quinone.

The modification usually takes place at the edge sites of the graphite and the physisorption preferentially occurs at the basal planes. Morphological studies by SEM showed that both orientations of the polyaromatic planes are present on the surface of the granules side by side (*Figure 10-17*). Thus, it is clear that the functionalized material may contain two types of quinone and anthraquinone species, one covalently attached to the graphite surface and the other physically adsorbed. In addition, it is well known that quinones strongly physisorb on graphite particles and even after 60 h of soxleth extraction some physisorbed molecules can be observed on the graphite [246], [271].
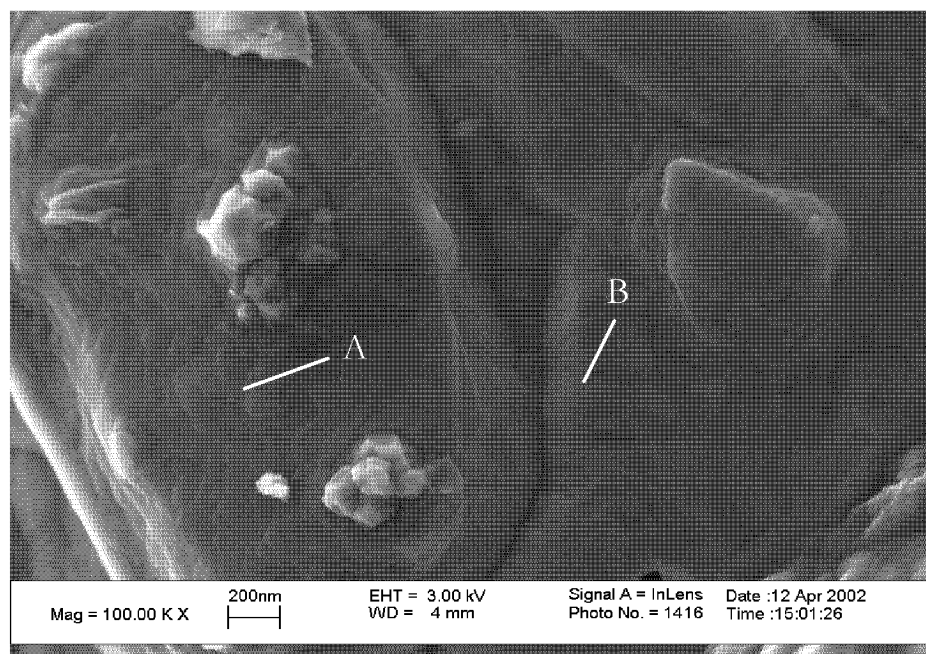
Fig. 10-17: SEM micrograph of a graphite granule (enViro cell). A: basal planes; B: edge sites.

Nevertheless, the catalytic activity of the electrodes modified by quinone and anthraquinone were demonstrated by carrying out preliminary studies on the reduction of indigo. The catalytic activity of the electrodes depends both on the amount or surface concentration and the nature of the attached species. Thus, the reduction rate was normalised by the redox capacity of the graphite, which correlates with the amount of quinoid functional groups (*Table 10-2*). 5-Amino-acenaphthenequinone and 1,8-dihydroxyanthraquinone proved to be the most active catalyst and it is possible to increase the normalised reduction rate compared to the unmodified reference material. All other immobilized species show lower activities than the reference graphite. In addition, it is somewhat surprising that 1-aminoanthraquinone is much more active than its isomer 2-aminoanthraquinone. Usually the redox reactions take place at similar potentials [272]. Probably the two isomers align in different orientations relative to the graphite surface. Thus, different electronic interactions have a bearing on the redox activity [272].

However, all modified electrodes exhibit a much lower reduction rate per gram material than the reference material. Therefore, the surface concentration

of the immobilized molecules should be increased by more efficient techniques. Preliminary experiments with acid chloride groups [268] instead of the carboxylic groups at the surface indicated a significantly higher catalytic activity of the electrode (*Table 10-3*). Unfortunately it was impossible to reach the level of the reference material (enViro cell graphite). Nevertheless, the normalised reduction rate remained more or less constant (*Table 10-2*). This is a kind of validation for the normalization procedure, which is obviously independent from the modification step.

Table 10-2: Influence of various immobilized quinoide and anthraquinoide molecules on the normalised reduction rate of indigo

immobilized mediator	reduction rate r_{norm} [4]/ nmol min^{-1} meq^{-1}
enViro cell graphite (reference)	347
before modifaction[1]	< 1
benzoquinone	25
naphthoquinone	58
1-aminoanthraquinone	231
2-aminoanthraquinone	150
anthraquinone-2-carboxylic acid	245
5-amino-acenaphthenequinone[2]	450
1,8-dihydroxyanthraquinone[2]	389
5-amino-acenaphthenequinone[3]	468
1,8-dihydroxyanthraquinone[3]	376

[1] enViro cell graphite after reaction with a H_2SO_4-HNO_3 mixture for 4 h at 100°C, a neutralisation step with NaOH and in some cases even after a reduction with $NaBH_4$.

[2] modification *via* the DCC-route and carboxylic groups at the surface.

[3] modification *via* the acylation of carboxylic groups at the surface with $SOCl_2$.

[4] System parameters: enViro cell graphite granules, 1 M NaOH, 100 mg l^{-1} indigo, current density (related to the area of the membrane (5 cm^2)) 1.5 mA cm^{-2}, 50°C, fluid velocity 2 cm s^{-1}.

In addition, dichlortriazine and β-sulphato-ethylsulphonyl reactive groups were used as anchor molecules reacting with amino or hydroxyl groups at the

graphite surface. The modification with C.I. Reactive Blue 19 (**9**) (Remazol brilliant blue R), which contains the sulfuric ester of a 2-hydroxyethyl sulfone ($-SO_2CH_2CH_2OSO_3H$) in the 3'-position of the aniline ring (*Figure 10-18*), yields reaction rates close to the reference material (*Table 10-3*). C.I. Reactive Blue 4 (**10**) (Procion brilliant blue RS), which contains a bifunctional dichlortriazine group, was even more effective (*Table 10-3*). Unfortunately, both covalent bonds are unstable under alkaline conditions [273], and after a few experiments the catalytic activity decreased to non-detectable values. Probably, detached redox-active molecules as dissolved mediator molecules had a positive influence on the reduction rate.

9:   X = $-SO_2CH_2CH_2OSO_3H$

10:   X =
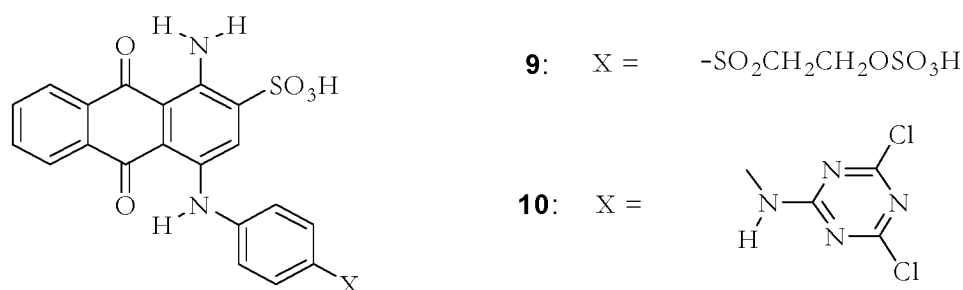
Fig. 10-18:   Basic structural formulas of the anthraquinone dyes employed. X = electrophilic reactive group [274].

10.3.7 Experiments with noble metals supported on the graphite

On the basis of recently presented experiments on the electrocatalytic hydrogenation (ECH) of indigo (*chapter 6 - 8*), it should be possible to improve the process by immobilizing noble metal particles on the surface of the graphite granules. Therefore, three different types of catalyst were investigated: on the one hand, carbon granules based on commercial crushed coconut shells with 0.5% (w/w) platinum (PMC, Sevierville, TN, USA) and on the other hand electrographite granules (enViro Cell, Oberursel, Germany) as a support for platinum and palladium. The latter material, especially with palladium as catalyst, showed a much higher activity for the reduction of indigo (*Figure 10-19*). However, the carbon granules based on coconut shells without platinum show - in contrast to the electrographite - no activity for the reduction of indigo. Therefore, the reduction activity can be correlated to the electrocatalytic

Table 10-3: Influence of several immobilized molecules on the reduction rate r of the indigo

immobilized mediator	reduction rate r [4]/ $\mu mol\ min^{-1}\ g^{-1}$ cat.
enViro cell graphite (reference)	0.021
before modification[1]	< 0.001
5-amino-acenaphthenequinone[2]	0.004
1,8-dihydroxyanthraquinone[2]	0.002
5-amino-acenaphthenequinone[3]	0.016
1,8-dihydroxyanthraquinone[3]	0.009
C.I. Reactive Blue 19 (**9**)[5]	0.019
C.I. Reactive Blue 4 (**10**)[5]	0.031

[1] enViro cell graphite after reaction with a H_2SO_4-HNO_3 mixture for 4 h at 100°C, a neutralisation step with NaOH and in some cases even after a reduction with $NaBH_4$.

[2] modification *via* the DCC-route and carboxylic groups at the surface.

[3] modification *via* the acylation of carboxylic groups at the surface with $SOCl_2$.

[4] System parameters: enViro cell graphite granules, 1 M NaOH, 100 mg l^{-1} indigo, current density (related to the area of the membrane (5 cm^2)) 1.5 mA cm^{-2}, 50°C, fluid velocity 2 cm s^{-1}.

[5] values of the 2nd experimental run.

hydrogenation process induced by the platinum content. In addition, the results indicate that the nature of the noble metal dispersed on the carbon has a determining effect on the efficiency of the reduction process based on the electrocatalytic hydrogenation. This might be due to the competition between the hydrogen evolution and the hydrogenation process. In case of the system Pt/C, the rate of hydrogen desorption, respectively the *Heyrovský* and *Tafel* steps of the hydrogen evolution, is much faster than that for the hydrogenolysis, which results in a poor efficiency of ECH. On the other hand, for the Pd/C catalyst, the hydrogenolysis and the hydrogen desorption have comparable rates, resulting in fair to good electrogenolysis efficiencies.
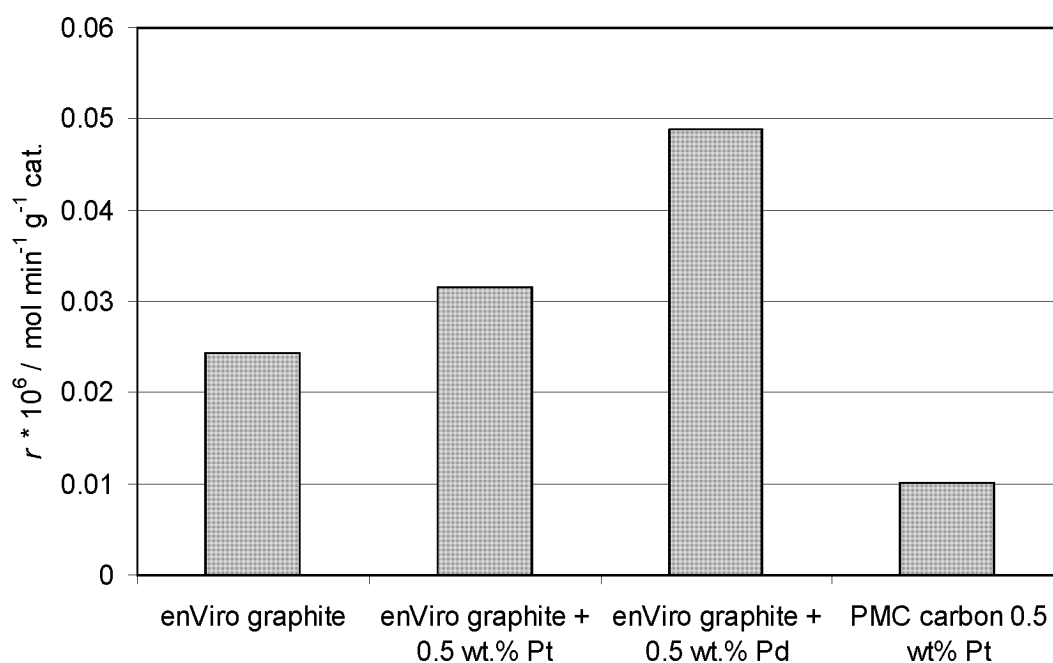
Fig. 10-19: Influence of different noble metals on the graphite as supporting material on the production rate r of leuco indigo. System parameters: enViro cell graphite granules, 1 M NaOH, 100 mg l^{-1} indigo, current density (related to the area of the membrane (5 cm^2)) 1.5 mA cm^{-2}, 50°C, fluid velocity 2 cm s^{-1}.

10.3.8 Results and discussion in the large-scale cell

According to the results achieved with the small-scale reactor, preliminary experiments were performed with pre-anodized graphite[2] at a pH of 14, a fluid flow of 2 cm s^{-1}, a diaphragm current density of 1 mA cm^{-2} (240 cm^2), 10 g l^{-1} indigo and 50°C. Under these conditions, the following results were obtained:

Current efficiency: 61%

Specific productivity: 10 mg min^{-1} kg^{-1} graphite

Mean voltage: 2.8 V

Power consumption: 1 kWh kg^{-1}

---

[2] System parameters: 20% H$_2$SO$_4$, current density (related to the area of the membrane (5 cm^2)) 50 mA cm^{-2}, 50°C, 2 cm s^{-1}, charge (Q) = 200 C^{-1} g^{-1}.

Although the scale of the reactor was increased by a factor of 30 and the experiments were performed at an indigo concentration up to 100 g l^{-1}, it was still possible to reduce indigo without blocking the reactor. Moreover, the current efficiency and the reduction rate were slightly enhanced to moderate values. Therefore, to achieve the common industrial production rates for leuco indigo of 200 g min^{-1} [275][3], a reactor size of approximately 20 m^3 of graphite would be necessary. However, no optimisation of the process was performed in the large-scale apparatus. This means that there is still potential for an improvement of the reduction rate.

10.4 Conclusions

Graphite granules were used as the electrode material in a fixed and fluidized bed reactor to address the question of the industrial feasibility of this novel direct electrochemical reduction method for vat dyes. Optimized conditions in the system were sought, and a scale-up in the indigo concentration to 10 g l^{-1} was achieved. Increasing the pH and the temperature can enhance the reduction rate, and a maximum conversion was found by optimising the current density and the flow velocity in the reactor. Special pre-treatments of the graphite (*e.g.*, soaking with hydrogen peroxide, pre-anodization, surface modification with quinones) can enhance the reduction rate by inducing the formation of quinoid functional groups. Immobilizing noble metal particles on the graphite surface can cause electrocatalytic hydrogenation in addition to the electron transfer process resulting in fair to good electrogenolysis efficiencies.

These results are a basis for the further development of a cheap, continuously and ecologically working cell for the direct electrochemical reduction of dispersed indigo and other vat dyes. Especially the introduction of surface functionalities by chemical reaction routes is an exciting research area at present. Hopefully the immobilization of redox-active substances (*e.g.*, metal

---

[3] Data based on the following assumptions: weight of the fabric 300 g m^{-1}; velocity of the fabric 40 m min^{-1}; shade 2 g per 100 g fabric; concentration 100 g l^{-1}.

complexes) will lead to even higher reduction rates. However, the next step will be trials on pilot plants after a scale-up procedure. Increasing the reactor size and the indigo concentration to more than 100 g l^{-1} may cause a blocking of the fixed bed. Therefore, the optimization of the cell design will be a necessary prerequisite for the successful realisation of this method.

Chapter 11

Conclusions and outlook

The current situation and suggested changes in the continuous vatting process are summarized in *Figure 11-1*. After several decades of research and development there is still no commercial reducing technology (including electrochemical processes) available today which can replace sodium dithionite in all areas of vat dye application. However, it is possible to diminish the consumption of sodium dithionite for stock vatting and for the stabilisation of the dye bath to a stoichiometrical minimum of 1.1 with state of the art technologies (*Figure 11-1, (a)*), (*chapter 2.3.1*). Such efforts result in significant money savings for the manufacturers, with an associated diminiution of the effluent load. Nevertheless, there is a continuing need for improving the eco-efficiency of this critical textile wet process. A further reduction of the necessary amount of reducing agent is only possible by the electrochemical vatting technique or by hydrogenation.

Catalytic hydrogenation seems to be an interesting solution (*Figure 11-1, (a, b)*), (*chapter 2.4.1*). Unfortunately, it is impossible to use this technique directly in the dye house due to the high explosion and fire risk (*Figure 11-1, (a)*). Therefore, dye suppliers offer concentrated pre-reduced leuco dye solutions for shipping to the dye house (*Figure 11-1, (b)*). However, the eco-efficiency of this process is negatively affected by the high water content of the product. In addition, the dye houses get completely reliant on the dye supplier, because at present only one company offers this technology.

Therefore, still the method of choice would be an electrochemical stock vatting technique (*Figure 11-1, (c)*). Various electrochemical reducing methods have been investigated in the last years. On the one hand, in a recent attempt the indirect electrochemical reduction employing a redox mediator was developed by *Bechtold et al.* (*chapter 2.4.2*). On the other hand, the work presented in this thesis clearly demonstrates the potential of three new alternatives: the

direct electrochemical reduction *via* the indigo radical as soluble intermediate (*chapters 3 - 5*), the electrocatalytic hydrogenation route (*chapters 6 - 9*) and the direct electrochemical reduction on graphite (*chapter 10*). Different aspects were investigated, including the influence of reaction parameters on the reaction rate and the influence of electrode material as well as the reactor design.

stock reduction on-site (dithionite, hydrogenation)

a)

bath stabilisation by dithionite

pre-reduced dye (hydrogenation)

b)

bath stabilisation by dithionite or electrochemical
reduction (mediator)

c)

electrochemical
reduction   bath stabilisation by dithionite
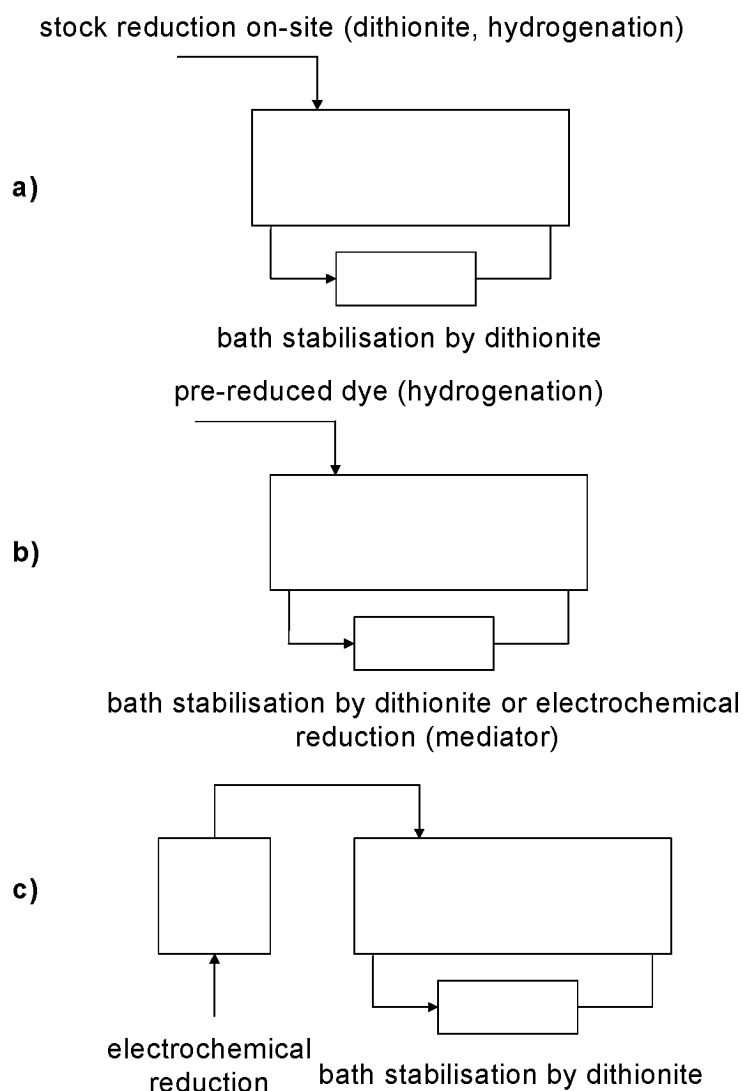
Fig. 11-1:   Implementation of electrochemistry in continuous vatting processes. (a) current situation; (b) pre-reduced dye; (c) electrochemical techniques.

All these methods offer tremendous environmental and economic benefits (*Table 11-1*), since they minimize the consumption of chemicals as well as the effluent load. From the point of stability, availability and the costs the latest development concerning the direct electrochemical reduction on graphite

Table 11-1: Comparison of costs in denim preparation and dyeing technique [258]

			stock solution and dye bath[6]		
			in practice	state of the art possibility[1]	electro-chemical[2]
stock solution	indigo (100 %)	g	1000	1000	1000
	dithionite (100%)[3]	g	-	-	-
	dithionite (90 %)[3]	g	1100	805	-
	caustic soda (50 %)[3]	g	1463	1043	455
	energy consumption[4]	kWh	-	-	1[7]
dye bath	dithionite (90 %)[3]	g	250	70	70
	caustic soda (50 %)[3]	g	230	64	64
total costs (without indigo)[5]		US$/kg	2.70	1.76	0.32
difference in costs		**US$/kg**	**0**	**-0.94**	**-2.38**

[1] Technology by Tex-A-Tec AG, Wattwil, Switzerland (*chapter 2.3.1*), [258].

[2] Direct electrochemical reduction in a fixed bed made of graphite granules (*chapter 10*).

[3] Product costs: sodium dithionite: 1.50 US$/kg, caustic soda: 0.40 US$/kg.

[4] Energy costs: 0.12 US$/kWh.

[5] Running or operating costs for vatting one kg of indigo.

[6] Dyestuff consumption in one line: 240 kg/d.

[7] *cf. chapter 10.*

granules (*chapter 10*) seems to be the most attractive process and the results are a promising basis for the further development of an electrochemical vatting technique. Until now, however, the electrochemical reactor performance is too low for the complete reduction of a stock solution in case of continuous dyeing. As a consequence, the operating costs and the return on investment (ROI) are not attractive enough for an application in the dyestuff industry. Therefore, in a particular embodiment of the dyeing process with pre-reduced dyes only the dye bath stabilization has been achieved by the electrochemical reduction in the presence of a mediator (*Figure 11-1, (b)*). By this, the dithionite is completely replaced. This process is close to commercialization by DyStar, but still numerous technical problems have to be solved. In addition, the disadvantages

of both the catalytic hydrogenation and the mediator technique are combined in one process.

On the other hand, an application of electrochemical vat dyeing in discontinuous exhaust dyeing processes might be possible, because the necessary reactor performance is much lower. Unfortunately, this concept is not suitable for indigo. Satisfying the needs of the customer (*i.e.* stone washed look [280], [281]) skin dyeing is still in progress, which can only be achieved in continuous processes. However, in the extensive range of vat dyes (*e.g.* indanthrene dyes) usually core dyeing is realised. Thus, the combination of an electrolyzer and a discontinuous yarn-dyeing machine is a conceivable variation for electrochemical vat dyeing. Moreover, in case of the mediator technique such a process is close to commercialization by DyStar with a yarn-dyeing machine (X-cones).

As most promising extensions of this work I would suggest the modification of several substrates (*e.g.*, graphite, conducting polymers) with redox-active functional groups (*e.g.*, metal complexes, quinones). There, the reactivity or stability of various functional groups under the reaction conditions is of main interest. In addition, investigations about the influence of different carbon materials can be envisaged. It can be speculated from the results presented in this thesis (*chapter 10*) that electrodes with a coke-type structure rather than a graphite structure are the most promising supporting materials. However, further work would be necessary to elucidate this aspect more in detail.

On the other hand, the versatility of this method has not been tested yet. This is a crucial point for an industrial application because indigo is only one product in a extensive range of vat dyes (*e.g.* indanthrene dyes). In addition, the reduction of mixed vat dyes (*e.g.* three dye components) should be investigated.

Further work aimed at exploring the scale-up procedure of the fixed bed reactor principle is of special interest. Special emphasis should be put on the danger of blocking the reactor and the intensification of the contact between the unsoluble dye particles and the electrode material. In addition, the influence of organic solvents, surfactants and dispersing agents on the electrochemical reduction on graphite should be analysed in detail.

Up to date, the theoretical understanding of the mechanism of the electrochemical indigo reduction is still in it's infancy. This knowledge is essential for

optimizing the reaction conditions and could be helpful in improving electro-chemical vat dyeing in general.

Finally, a completely different approach with pasty-like formulations could be tested. This could be a rewarding field of investigation, because the contact between the dye particles and the electrode could be maximized.

It is worth noting that all these extensions require numerous investigations. Nevertheless, in view of the successful development of several processes in the last years − especially during this thesis − it can be concluded that a good degree of progress in the right direction was made. The market introduction of the mediator process is imminent and the message is simple: 'electrochemistry in textile industry is coming our way'.

List of symbols

Abbreviations

ac	alternating current
CDx	cyclodextrin
C.I.	Colour index
CV	cyclic voltammogram
D	dye
ECH	electrocatalytic hydrogenation
EDX	energy dispersive X-ray analysis
EP	electronation-protonation
IR	ohmic drop
HV	high vacuum
L	leuco dye
R	dye radical species
RVC	reticulated vitreous carbon
SEM	scanning electron microscopy
Hydro	sodium dithionite

Latin symbols

a	-	index
d	m	diameter
c	mol m^{-3}	concentration
C	-	volumetric fractional concentration of solids
$c_{H_2}^b$	mol m^{-3}	bulk solution concentration of dissolved hydrogen gas

$c^*_{H_2}$	mol m^{-3}	concentration of dissolved hydrogen gas at saturation
CMC	mol l^{-1}	critical micellar concentration
D	m^2 s^{-1}	diffusion coefficient
E	V	electrode potential
E_A	J mol^{-1}	activation energy
E_P	V	peak potential
$E_{0,D}$	V	redox potential of the dye
$E_{0,R}$	V	redox potential of the dye radical
$E_{0,L}$	V	redox potential of the leuco dye
$E_{0,H}$	V	redox potential of hydrogen
F	As mol^{-1}	Faraday constant (= 96 485 As mol^{-1})
j	A m^{-2}	current density
j_L	A m^{-2}	limiting current density
j_{Ox}	A m^{-2}	peak current density for the oxidation reaction
j_P	A m^{-2}	peak current density
j_{Red}	A m^{-2}	peak current density for the reduction reaction
$i_{o,V}$	A m^{-2}	exchange current density for the *Volmer* reaction
$i_{o,H}$	A m^{-2}	exchange current density for the *Heyrovský* reaction
$i_{o,T}$	A m^{-2}	exchange current density for the *Tafel* reaction
k	min^{-1}	kinetic constant
K_i	cm^3 mol^{-1}	adsorption constant of species i
K_{eq}	-	equilibrium constant
n	mol	amount of moles
N	-	number of experiments
p	Pa	pressure
$P_{o,V}$	A m^{-2}	pre-exponential factor for the *Volmer* reaction
$P_{o,Hy}$	A m^{-2}	pre-exponential factor for the *Heyrovský* reaction
Q	m^3 s^{-1}	flow rate
Q	F mol^{-1}	charge
r	mol min^{-1}	reaction rate

r_{norm}	nmol min^{-1} meq^{-1}	normalized reaction rate
T	K or °C	temperature
u_C	cm s^{-1}	velocity of the empty tube fluidisation
u_i	cm s^{-1}	corresponding value at infinite dilution
v	mV s^{-1}	scan rate
w	rpm	rotation frequency
z	-	amount of electrons

Greek symbols

β	-	transfer coefficient
ε	-	voidage
ε_0	-	packed bed voidage
λ	nm	wavelength
λ_{max}	nm	absorption maximum
η	V	overvoltage
σ	m^2	electrode surface
Θ	-	surface coverage
Θ_H^0	-	equilibrium surface coverage of atomic hydrogen
ΔE_V	J mol^{-1}	exchange current density activation energy for the *Volmer* reaction
ΔE_{Hy}	J mol^{-1}	exchange current density activation energy for the *Heyrovský* reaction

References

[1]   E. Steingruber, 'Indigo and indigo colorants', Ullmann's Encyclopedia of Industrial Chemistry, 6th Ed., Online version, 2002.

[2]   H. Schlüter, 'Oekologische Anforderungen an Färbesysteme - Parameter für Küpenfärbesysteme', *Melliand Textilber.* **1995**, *76*, 143.

[3]   W. Schrott, P. Saling, 'Oekoeffizienz-Analyse - Produkte zum Kunden-nutzen auf dem Prüfstand', *Melliand Textilber.* **2000**, *81*, 190.

[4]   C.J. Grotthus, 'De l'influence de l'électricite galvanique sur les végétations métalliques', *Ann. chim. phys.* **1807**, *63*, 18.

[5]   A.M. Bond, F. Marken, E. Hill, R.G. Compton, H. Hügel, 'The electro-chemical reduction of indigo dissolved in organic solvents and as a solid mechanically attached to a basal plane pyrolytic graphite electrode immersed in aqeous electrolyte solution', *J. Chem. Soc., Perkin Trans. 2* **1997**, *9*, 1735.

[6]   S. Komorsky-Lovric, 'Square-wave voltammetry of an aqueous solution of indigo', *J. Electroanal. Chem.* **2000**, *482*, 222.

[7]   F. Goppelsroeder, 'Studien über die Anwendung der Elektrolyse zur Darstellung, zur Veränderung und zur Zerstörung der Farbstoffe, ohne oder in Gegenwart von vegetabilischen oder animalischen Fasern', Reichenberg, 1891.

[8]   F. Goppelsroeder, 'Über die Darstellung der Farbstoffe, sowie über deren gleichzeitige Bildung und Fixation auf der Faser mit Hilfe der Electrolyse', Reichenberg, 1885.

[9]   N.N., 'Société industrielle de Mulhouse', *Chem. Ztg.* **1884**, *8*, 361.

[10]   N.N., 'Société industrielle de Mulhouse', *Chem. Ztg.* **1884**, *8*, 1256.

[11]   F. Goppelsroeder, 'Neue Anwendung der Elektrolyse in der Färberei und Druckerei', *Dinglers polytech. J.* **1882**, *245*, 225.

[12]   F. Goppelsroeder, 'Anwendung der Elektrolyse zur Darstellung der In-digoküpe', *Dinglers polytech. J.* **1884**, *251*, 465.

[13]   F. Goppelsroeder, 'Anwendung der Elektrolyse zur Darstellung der In-
       digoküpe', *Dinglers polytech. J.* **1884**, *253*, 245.

[14]   F. Goppelsroeder, 'Ueber Bildung der Indigoküpe auf dem Zeuge selbst
       mit Hilfe des galvanischen Stromes und dadurch bewirkte Blaufärbung
       des Zeuges', *Dinglers polytech. J.* **1884**, *253*, 381.

[15]   F. Goppelsroeder, 'Über die Hydrogenation oder sogen. Reduction des
       Indigotins zu Indigweiss', *Chem. Ztg.* **1893**, *17*, 1633.

[16]   V. Wartha, 'Vorläufige Mitteilung über elektrische Küpen', *Chem. Ztg.* **1884**,
       8, 431.

[17]   J. Mullerus, 'Über die elektrolytische Reduktion von Indigo', *Chem. Ztg.*
       1893, *17*, 1454.

[18]   J. Nevyas, A. Lowy, 'The electrochemical reduction of indigo', *Trans. Am.
       Electrochem. Soc.* **1926**, *50*, 12.

[19]   F. Haber, 'Über die elektrische Reduktion von Nichtelektrolyten', *Zeitschr.
       physik. Chem.* **1900**, *32*, 258.

[20]   F. Haber, 'Bemerkungen zur Richtigstellung der Ausführungen des Herrn
       Binz', *J. Prakt. Chem.* **1901**, *64*, 289.

[21]   H. Chamaut, 'La réduction de l'indigo par voie électrolytique', Bull. Soc.
       Internat. Electriciens **1908**, *8*, 13.

[22]   H. Chaumat, 'Elektrode, bestehend aus einer Mischung von fein gepulver-
       tem Indigblau und einem fein gepulverten Leiter', DE223143, 1907.

[23]   D. Phillips, 'Environmentally friendly, productive and reliable: priorities
       for cotton dyes and dyeing processes', *J. Soc. Dyers Colour.* **1996**, *112*, 183.

[24]   M. Christen, G. Horstmann, 'Textilfarbstoffe im Spannungsfeld Qualität
       - Wirtschaftlichkeit', *Melliand Textilber.* **1987**, *68*, 50.

[25]   J.R. Aspland, 'A series on dyeing - chapter 3: Vat dyes and their applica-
       tion', *Textile Chem. Color* **1992**, *24*, 22.

[26]   H. Schlüter, 'Die Vorteile der Indanthren Farbstoffe als Kriterium für ihre
       segmentspezifische Anwendung', *Textilveredlung* **1990**, *25*, 218.

[27]   U. Baumgarte, 'Reduktions- und Oxidations-Prozesse beim Färben mit
       Küpenfarbstoffen', *Melliand Textilber.* **1987**, *68*, 189.

[28]   W. Schrott, 'Elektrochemisches Färben, Grundlagen und Perspektiven
       einer neuen Färbetechnologie zur Verbesserung von Produktionssicher-
       heit und Ökologie', Colloquium Produktionsintegrierte Wasser-/Abwas-
       sertechnik 2001, Nachhaltige Entwicklung in der Textilveredelung und
       Membrantechnik, 17 - 18 September, Bremen, Germany, A2-2, 2001.

[29] U. Baumgarte, 'Reduktions- und Oxidations-Prozesse beim Färben mit Küpenfarbstoffen', *Melliand Textilber.* **1987**, *68*, 276.

[30] U. Baumgarte, 'Developments in vat dyes and in their application 1974-1986', *Rev. Prog. Color. Relat. Top.* **1987**, *17*, 29.

[31] J.J. Porter, 'The mechanism of reduction of vat dye pigments in aqueous solutions', *Text. Res. J.* **1966**, *36*, 289.

[32] W.J. Marshall, R.H. Peters, 'The reduction properties of vat dyes, *J. Soc. Dyers Colour.* **1952**, *68*, 289.

[33] U. Baumgarte, 'Ueber den Chemismus der Reduktion von Küpenfarbstoffen', *Textilveredlung* **1969**, *4*, 821.

[34] U. Baumgarte, 'Ueber Reaktionen von Reduktionsmitteln bei der Küpenfärberei', *Textilveredlung* **1967**, *2*, 896.

[35] M. Jermini, 'α-Hydroxyketone als Reduktionsmittel für das Färben mit Küpenfarbstoffen', Ph.D. Dissertation, ETH Zurich, 1997.

[36] Yu. V. Polenov, V.A. Pushkina, V.V. Budanov, O.S. Khilinsakaya, 'Kinetics of heterogeneous reduction of Red-Brown Zh vat dyes with Rongalite in the absence of diffusion hindrance', *Russ. J. Appl. Chem.* **2001**, *74*, 1301.

[37] D. N. Epp. 'A world of color: Investigating the chemistry of vat dyes', *J. Chem. Educ.* **1995**, *72*, 726.

[38] M. Seefelder, 'Indigo in culture, science and technology', 2nd Ed., Landsberg, Ecomed, 1994.

[39] G. Grözinger, 'A century of the blues', *J. Soc. Dyers Colour.* **1996**, *112*, 220.

[40] A. Dutly, 'Geschichte des Indigos', *Chemie Plus* **1992**, *1*, 16.

[41] H. Essl, 'Jeans - das blaue Phänome Teil 1', *Textilveredlung* **1999**, *34*, 26.

[42] P. Roshan, R.N. Sandeep, 'Historical aspects of indigo dyeing', *Textile Dyer & Printer* **1997**, *30*, 13.

[43] P. Roshan, R.N. Sandeep, T. Jegadeesh, 'Denim series, part I, denim: The evergreen favorite', *Textile Dyer & Printer* **1996**, *29*, 15.

[44] P. F. Schatz, 'Indigo and Tyrian Purple - In nature and in the lab', *J. Chem. Educ.* **2001**, *78*, 1442.

[45] A. Bayer, 'Ueber die Reduktion des Indigblaus', *Ber. Dtsch. Chem. Ges.* **1868**, *1*, 17.

[46] P. Friedländer, *Fortschr. Teerfarbenfabr. Verw. Industriezweige* **1887-1890**, *2*, 100.

[47] K. Heumann, 'Neue Synthesen des Indigos und verwandter Farbstoffe', *Ber. Dtsch. Chem. Ges.* **1890**, *23*, 3043.

[48] P. Friedländer, *Fortschr. Teerfarbenfabr. Verw. Industriezweige* **1890-1894**, *3*, 281.

[49] K. Heumann, 'Neue Synthesen des Indigos und verwandter Farbstoffe', *Ber. Dtsch. Chem. Ges.* **1890**, *23*, 3431.

[50] A. S. Travis, 'Centenary year for the discovery of synthetic indigo', *Text. Chem. Color.* **1990**, *22*, 18.

[51] H. Schmidt, 'Indigo - 100 Jahre industrielle Synthese', *Chemie in unserer Zeit* **1997**, *31*, 121

[52] N.N., 'Am Montag wurde Blau gemacht', *Textilveredlung* **1990**, *25*, 246.

[53] K.G. Gilbert, D.T. Cooke, 'Dyes from plants: Past usage, present understanding and potential', *Plant Growth Regul.* **2001**, *34*, 57.

[54] D.J. Hill, 'Production of natural indigo in the United Kingdom', *Beiträge zur Waidtagung* **1992**, *4/5*, 23.

[55] A. Biertumpfel, G.W. Krause, B. Rudolph, A. Vetter, 'Variabilität von Färbewaid', Thüringer Landesanstalt für Landwirtschaft, Jena 106. VDLU-FA-Kongress 19-24 September, Darmstadt, Germany, p. 863, 1994.

[56] A. Vuorema, M. Keskitalo, 'Plant-derived indigo production from *Isatis tinctoria*', 9th International Conference on Dyes and Pigments, 12 - 16 May, Spindleruv Mlyn, Czech Republic, P 48, 2002.

[57] T. Bechtold, A. Turcanu, S. Geissler, E. Ganglberger, 'Process balance and product quality in the production of natural indigo from *Polygonum tinctorium Ait.* applying low-technology methods', *Bioresour. Technol.* **2002**, *81*, 171.

[58] T. Maugard, E. Enaud, A de La Sayette, P. Choisy, M.D. Legoy, 'β-Glucosidase-catalyszed hydrolysis of indican from leaves of *Polygonum tinctorium*', *Biotechnol. Prog.* **2002**, *18*, 1104.

[59] B.D. Ensley, D.T. Gibson, A.L. Laborde, 'Oxidation of naphthalene by a multicomponent enzyme system from *Pseudomonas sp.* strain NCIB 9816', *J. Bacteriol.* **1982**, *149*, 948.

[60] B.D. Ensley, B.J. Ratzkin, T.D. Osslund, M.J. Simon, L.P. Wackett, D.T. Gibson, 'Expression of napthalene oxidation genes in *Escherichia coli*, Results in the biosynthesis of indigo', *Science* **1983**, *222*, 167.

[61] J.W. Frost, K.M. Draths, 'Biocatalytic synthesis of aromatics from D-glucose: renewable microbial sources of aromatic compounds', *Annu. Rev. Microbiol.* **1995**, *49*, 557.

[62] J. W. Frost, J. C. Lievensem, 'Prospects for biocatalytic synthesis of aromatics in the 21st century', *New J. Chem.* **1994**, *18*, 341.

[63] A. Berry, T.C. Dodge, M. Pepsin, W. Weyler, 'Application of metabolic en-gineering to improve both the production and use of biotech indigo', *J. Ind. Microbiol & Biotechnol.* **2002**, *28*, 127.

[64] H. Bialy, 'Biotechnology, bioremediation, and blue genes', *Nature Biotechnology* **1997**, *15*, 110.

[65] A. Meyer, M. Würsten, A. Schmid, H.P.E. Kohler, B. Witholt, 'Hydroxyla-tion of indole by laboratory-evolved 2-Hydroxybiphenyl 3-Monooxygen-ase', *J. Biol. Chem.* **2002**, *277*, 34161.

[66] B. Bhushan, S.K. Samantha, R.K. Jain, 'Indigo production by naphtha-lene-degrading bacteria', *Lett. Appl. Microbiol.* **2000**, *31*, 5.

[67] K.E. O'Connor, S. Hartmans, 'Indigo formation by aromatic hydrocar-bon-degrading bacteria', *Biotechnol. Lett.* **1998**, *20*, 219.

[68] J. Shim, Y. Chang, S. Kim, 'Indigo and indirubin derivatives from indoles in *Polygonum tinctorium* tissue cultures', *Biotechnol. Lett.* **1998**, *20*, 1139.

[69] C. Young-Am, H. Yu, J. Song, H. Chun, S. Park, 'Indigo production in hairy root cultures of *Polygonum tinctorium Lour*', *Biotechnol. Lett.* **2000**, *22*, 1527.

[70] W. Lüttke, M. Klessinger, 'Infrarot- und Lichtabsorptionsspektren ein-facher Indigofarbstoffe', *Chem. Ber.* **1964**, *97*, 2342.

[71] M. Klessinger, W. Lüttke, 'Theoretical and spectroscopic investigations with indigo dyes. III. Effect of intermolecular hydrogen bonds on the spectra of indigo in the solid state', *Chem. Ber.* **1966**, *99*, 2136.

[72] E. Wille, W. Lüttke, 'Theoretical and spectroscopic studies on indigo dyes. 9. 4,4,4',4'-Tetramethyl-Δ2,2'-bipyrrolidine-3,3'-dione, a compound hav-ing the basic chromophore system of indigo', *Angew. Chem.* **1971**, *83*, 853.

[73] H. v. Eller, 'Crystal structure of indigo', *Bull. Soc. Chim. Fr.* **1955**, 1426.

[74] K.H. Ferber, 'Toxicology of indigo - a review', *JEPTO* **1978**, *7*, 73.

[75] J.N. Etters, 'Chemical conservation in denim manufacturing', *Text. Chem. Color.* **1999**, *31*, 32.

[76] G.M. Nabar, V.A. Shenai, 'Reduction potentials of vat dyes and their rela-tion to the ease of reduction and tendering behaviour', *Text. Res. J.* **1963**, 33, 471

[77] T.A. Ibidapo, 'Application of redox potentials in the selection of reducing agents for vat dyes', *Chem. Eng. J. + Biochem. Eng. J.* **1992**, *49*, 73.

[78] U. Keuser, 'Reduktionsmittel zum Färben mit Küpenfarbstoffen', *Melliand Textilber.* **1966**, *47*, 781.

[79] F. Widdel, 'Microbiology and ecology of sulfate- and sulfur-reducing bacteria', in 'Biology of anareobic microorganisms'; Ed. A.J.B. Zehnder, Wiley & Sons, New York, 1988, p. 469-586.

[80] R.C. Shah, S.V. Gokhale, 'Partial replacement of sodium hydrosulfite in continuous dyeing with vat dyes', *Text. Dyer & Printer* **1975**, *8*, 42.

[81] U. Baumgarte, 'Vat dyes and their application', *Rev. Prog. Color. Relat. Top.* **1974**, *5*, 17.

[82] J.N. Etters, 'Chemical Conservation in Denim Manufacturing', *Text. Chem. Color.* **1999**, *31*, 32.

[83] H. Ilg, V. Krenz, 'Ueber die Wirkung von Schwermetallkomplex-Verbindungen als Katalysator bei der Fixierung von Küpenfarbstoffen im Zweiphasendruck', *Melliand Textilber.* **1967**, *48*, 1341

[84] G. Zirker, G. Schulze, A. Blum, 'Redoxkatalysatoren im Küpendruck', *Melliand Textilber.* **1969**, *50*, 1096.

[85] Marte W., 'Biokompatible Denim Färbetechnologie', *Int. Text. Bull., ITB Veredlung* **1995**, *41*, 33.

[86] W. Marte, A. Marte, E. Marte, 'Process and apparatus for the preparation of a dyeing solution and their use in textile colouration', European Patent 0373119, 1990.

[87] F. Goavaert, E. Temmerman, P. Kiekens, 'Development of voltammetric sensors for the determination of sodium dithionite and indanthrene/indigo dyes in alkaline solutions', *Analytica Chimica Acta* **1999**, *385*, 307.

[88] J.T. Merritt III, K. R. Beck, C.B. Smith, P.J. Hauser, W.J. Jasper, 'Determination of indigo in dye baths by Flow Injection Analysis and redox titrations', *AATCC Review* **2001**, *1*, 41.

[89] J. N. Etters, 'Advances in indigo dyeing: Implications for the dyer, apparel manufacturer and environment', *Text. Chem. Color.* **1995**, *27*, 17.

[90] N.N., Sucker Müller, 'Kostengünstige Produktion auf Indigo-Färbeanlagen', *Melliand Textilber.* **1994**, *75*, 214.

[91] T. Bechtold, E. Burtscher, O. Bobleter, 'Konzentrationsbestimmung von Indigo in Ansatz- und Prozessbädern', *Textilpraxis International* **1992**, *47*, 44.

[92] J. N. Etters, 'pH-controlled indigo dyeing', *Amer. Dyestuff Rep.* **1998**, *87*, 15.

[93] K. Poulakis, E. Bach, D. Knittel, E. Schollmeyer, 'Einfluss von Ultraschall auf die Verküpungsgeschwindigkeit von Indigofarbstoffen mit α-Hydroxyaceton als Reduktionsmittel', *Textilveredlung* **1996**, *31*, 110.

[94] K. Schäfer, H. Höcker, 'Ultraschall-unterstütztes Färben von Textilien', *Textilveredlung* **2001**, *36*, 5.

[95] U. Baumgarte, 'Aktuelle Reduktionsmittelfragen bei den wichtigsten Verfahren der Küpenfärberei', *Melliand Textilber.* **1970**, *11*, 1332.

[96] S. Anders, W. Schindler, 'Vergleich von Reduktionsmitteln bei der reduktiven Reinigung von PES-Färbungen und Drucken', *Melliand Textilber.* **1997**, *78*, 85.

[97] M. Weiss, 'Thiourea dioxide: a safe alternative to hydrosulfite reduction. Part II', *Amer. Dyestuff Rep.* **1978**, *67*, 72.

[98] G.L. Medding, 'Vat dye reduction system', *Amer. Dyestuff Rep.* **1980**, *69*, 30, 77.

[99] G.P. Nair, R.C. Shah, 'Sodium borohydride in vat dyeing', *Text. Res. J.* **1970**, *40*, 303.

[100] U. Baumgarte, U. Keuser, 'Betrachtungen über den Einsatz von Natriumboranat in der Küpenfärberei', *Melliand Textilber.* **1966**, *47*, 286.

[101] R.B. Chavan, 'Environment-friendly dyeing processes for cotton', *Indian Journal of Fibre & Textile Research* **2001**, *26*, 93.

[102] R.B. Chavan, J.N. Chakraborty, 'Dyeing of cotton with indigo using iron(II) salt complexes' *Coloration Technology* **2001**, *117*, 88.

[103] M.R. Fox, J.H. Pierce, 'Indigo: Past and Present', *Text. Chem. Colorist* **1990**, *22*, 13.

[104] B. Semet, G.E. Grüninger, 'Eisen(II)-Salz-Komplexe als Alternative zu Hydrosulfit in der Küpenfärberei', *Melliand Textilber.* **1995**, *76*, 161.

[105] N.N. , 'Förderpreis der Stiftung Technopark an Walter Marte', *Textilveredlung* **1991**, *26*, 374.

[106] W. Marte, P. Rys, 'Verfahren zum Färben und Bedrucken von cellulosischen Fasermaterialien mit Küpenfarbstoffen', European Patent 0357 548, 1989.

[107] U. Baus, E. Beckmann, E. Kromm, H. Wagenmann, P. Rys, W. Marte, A.J. Klaus, U. Meyer, 'Accelerating dyeing and printing of cellulose textile with vat and/or sulphur dyes', German Patent 4338489, 1995.

[108] S. Ushida, M. Matsuo, 'Reduction of indigo by glucose', *Nippon Kasei Gakkaishi* **1991**, *42*, 61.

[109] A. Brochet, 'Manufacture of leuco derivatives of vat dyestuffs', U.S. Patent 1,247,927, 1917.

[110] G. Schnitzer, F. Suetsch, M. Schmitt, E. Kromm, H. Schlueter, R. Krueger, A. Weiper-Idelmann, 'Method of dyeing cellulose-containing textile material with hydrogenated indigo', World Patent 94/23114, 1994.

[111] E.H. Daruwalla, 'Dyeing with less chemicals', *Textile Asia* **1975**, *6*, 165.

[112] E.H. Daruwalla, S.D. Supanerkar, 'A vat dye reduction process', U.S. Patent 3953307, 1974.

[113] N.N., 'Einsparungsmöglichkeit in der Küpenfärberei', *Textil Praxis* **1975**, *30*, 381.

[114] N.N., 'Einsparungsmöglichkeit in der Küpenfärberei', *Textil Praxis* **1975**, *30*, 998.

[115] E.H. Daruwalla, 'Savings in the use of chemicals in dyeing', *International Dyer & Textile Printer* **1975**, *22*, 537.

[116] Farbwerke vorm. Meister Lucius & Brüning, 'Verfahren zur Reduktion von Indigo', German Patent 139567, 1902.

[117] C. Oloman, B. Lee, W. Leyton, 'Electrosynthesis of sodium dithionite in a Trickle-bed Reactor', *Can. J. Chem. Eng.* **1990**, *68*, 1004.

[118] D.W. Cawlfiled, R.E. Bolick, J.M. French, 'Electrochemical process for producing hydrosulphite solutions', European Patent 0257815, 1988.

[119] K.H. Kleifges, G. Kreysa, K. Jüttner, 'Electrochemical study of direct and indirect NO reduction with complexing agents and redox mediator', *J. Appl. Electrochem.* **1997**, *27*, 1012.

[120] T. Hemmingsen, 'The electrochemical reaction of sulphur-oxygen compounds-part I. A review of literature on the electrochemical properties of sulphur-oxygen compounds', *Electrochim. Acta* **1992**, *37*, 2775.

[121] T. Hemmingsen, 'The electrochemical reaction of sulphur-oxygen compounds-part II. Voltammetric investigation performed on platinum', *Electrochim. Acta* **1992**, *37*, 2785.

[122] E. Steckhan, 'Indirekte elektro-organische Synthesen - ein modernes Kapitel der organischen Elektrochemie', *Angew. Chem.* **1986**, *98*, 681.

[123] T. Bechtold, E. Burtscher, A. Amann, O. Bobleter, 'Reduktion von dispergiertem Indigo durch indirekte Elektrolyse', *Angew. Chem.* **1992**, *104*, 1046.

[124] T. Bechtold, E. Burtscher, O. Bobleter, 'Application of electrochemical processes and electroanalytical methods in textile chemistry', *Current Topics in Electrochemistry* **1998**, *6*, 97.

[125] T. Bechtold, E. Burtscher, O. Bobleter, 'Direct and indirect cathodic dyestuff reduction in textile dyeing', *Recent Res. Devel. in Electrochem.* **1998**, *1*, 245.

[126] T. Bechtold, E. Burtscher, A. Turcanu, O. Bobleter, 'The reduction of vat dyes by indirect electrolysis', *J. Soc. Dyers Colour.* **1994**, *110*, 14.

[127] T. Bechtold, E. Burtscher, O. Bobleter, 'Electrolytic cell with multiple partial electrodes and at least one antipolar counter electrode', World Patent 95/07374, 1995.

[128] W. Gerhardt, W. Gehlert, E. Glück, 'Electrolytic cell for treatment of metal ion containing industrial waste water', U.S. Patent 4,786,384, 1988.

[129] W. Blatt, L. Schneider, 'Electrolysis systems in the dyeing technology', *Melliand Textilber.* **1999**, 80, 624.

[130] W. Blatt, L. Schneider, 'Electrochemical cell for the indirect reduction of dyestuff', *Melliand Int.* **1999**, *80*, 240.

[131] J. Trauer, 'Anwendung der Ultrafiltration für das Schlichtemittel- und Indigo-Recycling', *Melliand Textilber.* **1993**, *74*, 559.

[132] S.P. Petrov, P.A. Stoychev, 'Ultrafiltration purification of dye wastewater', *Textilveredlung* **2002**, *37*, 10.

[133] N.N., 'Thies joins new yarn dyeing technology partnership', *International Dyer* **2000**, *185*, 4.

[134] N.N., 'Production trials for electrochemical dyeing', *International Dyer* **2002**, *187*, 6.

[135] T. Bechtold, E. Burtscher, S. Mohr, 'The electrochemical properties of alkali stable redox couples suited for indirect cathodic reduction of organic compounds', *Recent Res. Devel. Electrochem.* **1999**, *2*, 229.

[136] T. Bechtold, E. Burtscher, A. Amann, O. Bobleter, 'Alkali-stable iron complexes as mediators for the electrochemical reduction of dispersed organic dyestuffs', *J. Chem. Soc. Faraday Trans.* **1993**, *89*, 2451.

[137] T. Bechtold, E. Burtscher, D. Gmeiner, O. Bobleter, 'The redox-catalysed reduction of dispersed organic compunds, Investigations on the electrochemical reduction of insoluble organic compounds in aqueous systems' *J. Electroanal. Chem.* **1991**, *306*, 169.

[138] T. Bechtold, E. Burtscher, O. Bobleter, W. Blatt, L. Schneider, 'Optimization of multi-cathode membrane electrolysers for the indirect electrochemical reduction of indigo', *Chem. Eng. Techol.* **1998**, *21*, 11.

[139] T. Bechtold, E. Burtscher, O. Bobleter, W. Blatt, L. Schneider, 'Optimierung von Mehrkathoden-Membran-Elektrolysezellen zur indirekten elektrochemischen reduktion von Indigo', *Chem. Ing. Tech.* **1997**, *69*, 1453.

[140] T. Bechtold, E. Burtscher, G. Kühnel, O. Bobleter, 'Electrochemical reduction processes in indigo dyeing', *J. Soc. Dyers Colour.* **1997**, *113*, 135.

[141] T. Bechtold, E. Burtscher, A. Turcanu, O. Bobleter, 'Indirect electrochemical reduction of dispersed indigo dyestuff', *J. Electrochem. Soc.* **1996**, *143*, 2411.

[142] T. Bechtold, E. Burtscher, A. Turcanu, O. Bobleter, 'Dyeing behaviour of indigo reduced by indirect electrolysis', *Text. Res. J.* **1997**, *67*, 635.

[143] T. Bechtold, E. Burtscher, D. Gmeiner, O. Bobleter, 'Untersuchungen zur elektrochemischen Reduktion von Farbstoffen', *Melliand Textilber.* **1991**, *72*, 50.

[144] T. Bechtold, E. Burtscher, D. Gmeiner, O. Bobleter, 'Elektrochemische Untersuchungen und Verfahren in der Textilindustrie', *Textilveredlung* **1990**, *25*, 221.

[145] T. Bechtold, E. Burtscher, A. Turcanu, O. Bobleter, 'Multi-cathode cell with flow-through electrodes for the production of iron(II)-triethanolamine complexes', *J. Appl. Electrochem.* **1997**, *27*, 1021.

[146] T. Bechtold, E. Burtscher, A. Turcanu, F. Berktold, 'Elektrochemie in der Küpenfärberei und beim Färben mit Schwefelfarbstoffen', *Melliand Textilber.* **2000**, *81*, 195.

[147] T. Bechtold, E. Burtscher, 'Elektrochemie in der Textilveredelung', *International Textile Bulletin* **1998**, *44*, 64.

[148] S. Mohr, T. Bechtold, 'Electrochemical behaviour of iron-complexes in presence of competitive ligands: A strategy for optimization of current density', *J. Appl. Electrochem.* **2001**, *31*, 363

[149] T. Bechtold, E. Burtscher, A. Turcanu, 'Ca^{2+}-Fe^{3+}-D-gluconate-complexes in alkaline solution. Complex stabilities and electrochemical properties', *J. Chem. Soc., Dalton Trans.* **2002**, *13*, 2683.

[150] T. Bechtold, A. Turcanu, 'Electrochemical vat dyeing', *J. Electrochem. Soc.* **2002**, *149*, D7.

[151] T. Bechtold, E. Burtscher, D. Gmeiner, O. Bobleter, 'The redox-catalyzed reduction of dispersed organic compounds. Investigations on the electrochemical reduction of insoluble organic compounds in aqueous systems', *J. Electroanal. Chem.* **1991**, *306*, 169.

[152] Umweltbundesamt, Institut für Wasser-, Boden- und Lufthygiene, 'Dokumentation wassergefährdender Stoffe - Datenblattsammlung', S. Hirzel, Stuttgart, Datenblatt 201, 1997.

[153] C. Merk, J. Botzem, G. Huber, N. Grund, 'Method for electrochemical reduction of reducible dyes', World Patent 01/46497, 2001.

[154] C. Merk, G. Huber, A. Weiper-Idelmann, in Reactive Intermediates in Organic and Biological Electrochemistry, In Honor of the Late Professor Eberhard Steckhan, J. Yoshida, D. G. Peters, M. S. Workentin, Editors, PV 2001-14, The Electrochemical Society Proceedings Series, Washington, DC, p. 121, 2001.

[155] G. Horstmann, 'Dyeing as a new environmental challenge', *J. Soc. Dyers Colour.* **1995**, *111*, 182.

[156] D. Phillips, 'Environmentally friendly, productive and reliable: priorities for cotton dyes and dyeing processes', *J. Soc. Dyers Colour.* **1996**, *112*, 183.

[157] H. Schlüter, 'Oekologische Anforderungen an Färbesysteme - Parameter für Küpenfärbesysteme', *Melliand Textilber.* **1995**, *76*, 143.

[158] P. Saling, 'Eco-efficiency analysis for decision-making process in the chemical industry', Proc. Helsinki Symposium on Industrial Ecology and Materials Flows HelSIE, 30.08 - 03.09.2000, Porthania, University of Helsinki, Yliopistonkatu 3, p. 256., 2000.

[159] P. Saling, A. Kicherer, B. Dittrich-Krämer, R. Wittlinger, W. Zombik, I. Schmidt, W. Schrott, S. Schmidt, 'Eco-efficiency analysis by BASF: The method', *Int. J. LCA* **2002**, *7*, 203.

[160] F. Bruin, F.W. Heineken, M. Bruin, 'Narrow ESR hyperfine structure lines for a free radical dissolved in water', *J. Chem. Phys.* **1962**, *37*, 682.

[161] F. Bruin, F.W. Heineken, M. Bruin, 'Electron spin resonance spectra of the basic indigoid dye radical', *J. Org. Chem.* **1963**, *28*, 562.

[162] M. Bruin, F. Bruin, F.W. Heineken, 'ESR Study of Thio-indigo and related free radicals', *J. Chem. Phys.* **1962**, *37*, 135.

[163] G. A. Russell, E. G. Janzen, E. T. Strom, 'The Formation of radical-anions by electron transfer between anions and their unsatuirated analogs in dimethyl sulfoxide solution', *J. Am. Chem. Soc.* **1962**, *84*, 4155.

[164] G. A. Russell, E. G. Janzen, E. T. Strom, 'Electron-transfer processes. I. The scope of the reaction between carbanions or nitranions and unsaturated electron acceptors', *J. Am. Chem. Soc.* **1964**, *86*, 1807.

[165] G. A. Russell, R. Konoka, 'Radical anions derived from indigo and 2,2'-bibenzimidazole', *J. Org. Chem.* **1967**, *32*, 234.

[166] Y. Li, S. Dong, 'Indigo-carmine-modified polypyrrole film electrode', *J. Electroanal. Chemistry* **1993**, *348*, 181.

[167] G. Beggiato, G. Casalbore-Miceli, A. Geri, D. Pietrapaolo, 'Indigo-carmine: an electrochemical study', *Ann. Chim.* **1993**, *83*, 355.

[168] W. Marte, O. Dossenbach, U. Meyer, 'Method and apparatus for reducing vat and sulfur dyes during dyeing of textiles', World Patent 00/31334, 2000.

[169] X. Jin (ICB, ETH Zurich), personal communication, 2003.

[170] B. Milicevic, G. Eigenmann, 'Potentiometry, polarography, and electron spin resonance of alkaline solutions of sodium dithionite', *Helv. Chim. Acta* **1963**, *46*, 192.

[171] V. G. Levich, 'Physico-Chemical Hydrodynamics', Prentice-Hall, New Jersey, 1962.

[172] Y. V. Pleskov, V. Y Filipov, 'The Rotating Disc Electrode', Consultants Bureau (Plenum), New York, 1976.

[173] J. Heinze, 'Cyclovoltammetrie - die 'Spektroskopie' des Elektrochemikers', *Angew. Chem.* **1984**, *96*, 823.

[174] C.M.A. Brett, A.M.O. Brett, 'Electrochemistry: principles, methods and applications', Oxford University Press, 1993.

[175] A.J. Bard, L.R. Faulkner, 'Electrochemical methods', John Wiley & Sons, 1980.

[176] I.J. Brown, S. Sotiropoulos, 'Electrodeposition of Ni from a high internal phase emulsion (HIPE) template', *Electrochim. Acta* 2001, 46, 2711.

[177] A.N. Correia, S.A.S. Machado, 'Hydrogen evolution on electrodeposited Ni and Hg ultramicroelectrodes', *Electrochim. Acta* 1998, 43, 367.

[178] F. Hahn, B. Beden, M.J. Croissant, C. Lamy, 'In Situ UV Visible reflectance spectrocopic investigation of the nickel electrode-alkaline solution interface', *Electrochim. Acta* 1986, 31, 355.

[179] S.A.S. Machado, L.A. Avaca, 'The hydrogen evolution reaction on nickel surfaces stabilized by H-absorption', *Electrochim. Acta* **1994**, *39*, 1385.

[180] J. N. Etters, 'Indigo dyeing of cotton denim yarn: correlating theory with practice', *J. Soc. Dyers Colour.* **1993**, *109*, 251.

[181] J. Lindley, T.J. Mason and J.P. Lorimer, 'Sonochemically enhanced Ullmann reactions', *Ultrasonics* **1987**, *25*, 45.

[182] T.J. Mason and P. Lorimer, 'Sonochemistry', Ellis Horwood Ltd. (Wiley), Chichester GB, 1988.

[183] K.S. Suslick, D.J. Casadonte, M.L.H. Gren, M.E. Thompson, 'Effects of high intensity ultrasound on inorganic solids', *Ultrasonics* **1987**, *25*, 56.

[184] J.F. Richardson, W.N. Zaki, 'Sedimentation and fluidization part 1', *Trans. Inst. Chem. Eng.* **1954**, *32*, 35.

[185] J.M. Coulson, J.F. Richardson, Chemical Engineering, Vol. 2, Pergamon Press, Oxford, 1991.

[186] F. Coeuret, Le Goff, 'L'electrode poreuse percolante (EOPP) - II. Transfer de matiere en lit fixe ou fluidise de grains non-conducteurs', *Electrochim. Acta* **1976**, *21*, 195.

[187] A.T.S. Walker, A.A. Wragg, 'Mass transfer in fluidised bed electrochemical reactors', *Electrochim. Acta* **1980**, *25*, 323.

[188] Y. Inoue, Y. Yamamoto, H. Suzuki, 'Novel one-pot synthesis of indigo from indole and organic hydroperoxide', *Stud. Surf. Sci. Cat.* **1994**, *82*, 615.

[189] E. Steingruber, 'Indigo and indigo colorants', Ullmann's Encyclopedia of Industrial Chemistry, Vol. A 14, 6th Ed., 2001.

[190] G. Wenz, 'Cyclodextrins as synthons for supramolecular structures and functional units', *Angew. Chem. Int. Ed. English* **1994**, *33*, 803.

[191] A. Ueno, I. Suzuki, T. Osa, 'Association dimers, excimers, and inclusion complexes of pyrene-appended γ-cyclodextrins', *J. Amer. Chem. Soc.* **1989**, *111*, 6391.

[192] S. Okubayashi, A. Yamazaki, Y. Koide, H. Shosenji, 'Effects of cyclodextrin on the electrolytic reduction of an anthraquinone dye', *J. Soc. Dyers Colour.* **1999**, *115*, 31.

[193] H. Hirai, N. Toshima, S. Uenoyama, 'Inclusion complex formation of γ-cyclodextrin. One host-two guest complexation with water-soluble dyes in ground state', *Bull. Chem. Soc. Japan* **1985**, *58*, 1156.

[194] W. Marte (Tex-A-Tec AG, Wattwil, Switzerland), personal communication, 2001.

[195] W. Marte *et al.*, 'Analytik Manual zur Kontrolle des Indigofärbeprozesses', Tex-A-Tec AG, Wattwil, Switzerland.

[196] S. Heimann, 'Textile Auxiliaries: Dispersing Agents', *Rev. Prog. Coloration* **1981**, *11*, 1.

[197] N.N., 'Setamol WS', Technische Information TI/T 7022 d, BASF, Ludwigshafen, Germay, 1997.

[198] R.A. Mackay, J. Texter, Eds., 'Electrochemistry in Colloids and Dispersions', VCH, New York, Weinheim, 1992.

[199] J.F. Rusling, 'Controlling electrochemical catalysis with surfactant microstructures', *Acc. Chem. Res.* **1991**, *24*, 75.

[200] J. Lipowski, in B.E. Conway, J.O.M. Bockris, R.E. White, Eds., 'Modern Aspects of Electrochemistry', No. 23, Plenum Press, New York, 1992.

[201] K. Kosswig, H. Stache, 'Die Tenside', Carl Hanser Verlag, München, 1993.

[202] R.J. Williams, J.N. Phillips, K.J. Mysels, 'Critical micelle concentration of sodium dodecyl sulfate at 25°C', *Trans. Faraday Soc.* **1955**, *51*, 728.

[203] J.F. Rusling, in B.E. Conway, J.O.M. Bockris, R.E. White, Eds., 'Modern Aspects of Electrochemistry', No. 26, Plenum Press, New York, 1992.

[204] J.F. Rusling, in A.J. Bard, Ed., 'Electroanalytical Chemistry. A Series of Advances', Vol. 18, Marcel Dekker, New York, 1994.

[205] E.L. Gyenge, C.W. Oloman, ' Influence of surfactants on the electroreduction of oxygen to hydrogen peroxide in acid and alkaline electrolytes', *J. Appl. Electrochemistry* **2001**, *31*, 233.

[206] D. Myers, 'Surfactant Science and Technology', VCH, Weinheim, New York, 1988.

[207] M. J. Rosen, 'Surfactants and interfacial phenomena', John Wiley, New York, 1989.

[208] H.P. Cady, R. Taft, 'Electronation', *Science* **1925**, *62*, 403.

[209] J.M. Chapuzet, A. Lasia, J. Lessard, In: Lipkowski J, Ross PN, editor. 'Electrocatalysis', Wiley-VCH, 1998. p. 155-97.

[210] F. Beck, 'Electrochemical and catalytic hydrogenation: common features and differences', *Int. Chem. Eng.* **1979**, *19*,1.

[211] F. Beck, 'Elektrochemische und katalytische Hydrierungen, Gemeinsamkeiten und Spezifitäten', *Chem. Ing. Tech.* **1976**, *48*, 1096.

[212] J. Lessard, G. Belot, 'Electrode for catalytic electrohydrogenation of organic compounds', U.S. Patent 4,584,069, 1986.

[213] D. Robin, M. Comtois, A. Martel, R. Lemieux, A.K. Cheong, G. Belot, J. Lessard, 'The electrocatalytic hydrogenation of fused polycyclic aromatic compounds at *Raney* nickel electrodes: the influence of catalyst activation and electrolysis conditions', *Can. J. Chem.* **1990**, *68*, 1218.

[214] D. Pletcher, M. Razaq, 'The reduction of acetophenone to ethylbenzene at a platinised platinum electrode', *Electrochim. Acta* **1981**, *26*, 819.

[215] T. Nonaka, M. Takahashi, T. Fuchigami, 'Stereochemical studies of the electrolytic reactions of organic compounds. Part 18. Comparative study of hydrogenation on metal-black cathodes and catalysts', *Bull. Chem. Soc. Japan* **1983**, *56*, 2584.

[216] L.L. Miller, L. Christensen, 'Electrocatalytic hydrogenation of aromatic compounds', *J. Org. Chem.* **1978**, *43*, 2059.

[217] R.L. Augustine, 'Catalytic hydrogenation', New York, Marcel Dekker, 1965.

[218] X. De Hemptinne, J.C. Jungers, 'Sur le mécanisme de l'hydrogénation électrochimique', *Z. Phys. Chem. N. F.* **1958**, *15*, 138.

[219] F. Beck, H. Gerischer, 'Elektrochemische Gesichtspunkte zur katalytischen Hydrierung an Platinkontakten in gepufferten Lösungen', *Z. Elektrochemie* **1961**, *65*, 504.

[220] A. Lasia, A. Rami, 'Kinetics of hydrogen evolution on nickel electrodes', *J. Electroanal. Chem.* **1990**, *294*, 123.

[221] A. K. Cheong, A. Lasia, J. Lessard, 'Hydrogen evolution reaction at composite-coated Raney nickel electrodes in aqueous and aqueous-methanolic solutions', *J. Electrochem. Soc.* **1993**, *140*, 2721.

[222] J.M. Lalancette, E. Potvin, H. Ménard, 'Phosphate bonded composite electrodes', U.S. Patent 4, 886, 591, 1989.

[223] J. Wang, 'Reticulated vitreous carbon - a new versatile electrode material', *Electrochim. Acta* **1981**, *26*, 1721.

[224] A. Cyr, F. Chlitz, P. Jeanson, A. Martel, L. Brossard, J. Lessard, 'Electrocatalytic hydrogenation of lignin models at Raney nickel and palladium-based electrodes', *Can J. Chem.* **2000**, *78*, 307.

[225] P. Dabo, A. Cyr, J. Lessard, L. Brossard, J. Lessard, 'Electrocatalytic hydrogenation of 4-phenoxyphenol on active powders highly dispersed in a reticulated vitreous carbon electrode', *Can. J. Chem.* **1999**, *77*, 1225.

[226] A.N. Strohl, G.D. J. Curran, 'Reticulated vitreous carbon flow-through electrodes', *Anal. Chem.* **1979**, *51*, 353.

[227] P. Dabo, A. Cyr, J. Lessard, L. Brossard, H. Ménard, 'Electrocatalytic hydrogenation of 4-phenoxyphenol on active powders highly dispersed in a reticulated vitreous carbon electrode', *Can J. Chem.* **1999**, *77*, 1225.

[228] J. Fournier, P.K. Wrona, A. Lasia, R. Lacasse, J.M. Lalancette, L. Brossard, H. Ménard, 'Catalytic influence of commercial Ru, Rh, Pt and Pd intercalated in graphite on the hydrogen evolution', *J. Electrochem. Soc.* **1992**, *139*, 2372.

[229] H. Dumont, P. Los, A. Lasia, H. Ménard, 'Studies of the hydrogen evolution reaction on lanthanum phosphate-bonded composite nickel-ruthenium electrodes in 1 M alkaline solution', *J. Appl. Electrochem.* **1993**, *23*, 684.

[230] J. Fournier, L. Brossard, J-Y. Tilquin, R. Cote, J. P. Dodelet, D. Guay, H. Menard, 'Hydrogen evolution recation in alkaline solution', *J. Electrochem. Soc.* **1996**, *143*, 919.

[231] S.M. Walas, 'Reaction Kinetics for Chemical Engineers', Butterworth Reprint Series in Chemical Engineering, p. 149 ff, 1989.

[232] M. von Arx, T. Mallat, A. Baiker, 'A new reaction pathway in the enanti-oselective hydrogenation of activated ketones on cinchona-modified plat-inum', *J. Catalysis* **2001**, *202*, 169

[233] K.J. Vetter, 'Electrochemical Kinetics', Academic Press, Inc., New York, pp. 518-555, 1967.

[234] B.E. Conway, H. Angerstein-Kozlowska, M.A. Sattar, B.V. Tilak, 'Study of a decomposing hydride phase at nickel cathodes by measurement of open-circuit potential decay', *J. Electrochem. Soc.* **1983**, *130*, 1825.

[235] A. Rami, A. Lasia, 'Kinetics of hydrogen evolution on Ni-Al-alloy elec-trodes', *J. Appl. Electrochem.* **1992**, *22*, 376.

[236] Y. Choquette, L. Brossard, A. Lasia, H. Ménard, 'Study of the kinetics of hydrogen evolution reaction on Raney nickel composite-coated electrode by AC impedance technique', *J. Electrochem. Soc.* **1990**, *137*, 1723.

[237] A.K. Cheng, A. Lasia, J. Lessard, 'Hydrogen evolution reaction at com-posite-coated Raney nickel electrodes in aqueous and aqueous-methanolic solutions', *J. Electrochem. Soc.* **1993**, *140*, 2721.

[238] Y. Choquette, L. Brossard, A. Lasia, H. Ménard, 'Investigation of hydro-gen evolution on Raney-nickel composite-coated electrodes', *Electrochim. Acta* **1990**, *35*, 1251.

[239] V. Anantharaman, P.N. Pintauro, 'The electrocatalytic hydrogenation of glucose; part I. Kinetics of hydrogen evolution and glucose hydrogenation on Raney nickel powder', *J. Electrochem. Soc.* **1994**, *141*, 2729.

[240] M.V. Radugin, A.G. Zakharov, T.N. Lebedeva, V.V. Lebedev, 'Kinetics of oxidation-reduction of thioindigo red B according to cyclic voltamme-try', *Russ. J. Gen. Chem.* **1996**, *66*, 647.

[241] T. Vickerstaff, E. Waters, 'The dyeing of cellulose acetate rayon with dis-persed dyes', *J. Soc. Dyers Colour.* **1942**, *58*, 116.

[242] I.D. Rattee, M.M. Breuer, 'The pysical chemistry of dye adsorption', Aca-demic press London, chapter 7, p. 221 ff, 1974.

[243] F. Scholz, B. Lange, 'Abrasive stripping voltammetry - an electrochemical solid state spectroscopy of wide applicability', *TrAC Trends Anal. Chem.* **1992**, *11*, 359.

[244] M. Rowe, J.St.H. Davies, 'Studies in the acenaphthene series', *J. Chem. Soc.* **1920**, *117*, 1344.

[245] M. Lauwiner, P. Rys, J. Wissmann, 'Reduction of aromatic nitro compounds with hydrazine hydrate in the presence of an iron oxide hydroxide catalyst. I. The reduction of monosubstituted nitrobenzene with hydrazine hydrate in teh presence of ferrihydrite', *Appl. Catal., A* **1998**, *172*, 141.

[246] F. Atamny, A. Baiker, 'Platinum particles supported on carbon: Potential and limitations of characterization by STM', *Surf. Interface Anal.* **1999**, *27*, 512.

[247] H. Bönnemann, W. Brijoux, R. Brinkmann, E. Dinjus, T. Joussen, B. Korall, 'Erzeugung von kolloiden Uebergangsetallen in organischer Phase und ihre Anwendung in der Katalyse', *Angew. Chem.* **1991**, *103*, 1344.

[248] P. Ramesh, S. Sampath, 'Electrochemical and spectroscopic characterization of quinone functionalized exfoliated graphite', *Analyst* **2001**, *136*, 1872.

[249] J.C. Sheehan, G.P. Hess, 'A new method of forming peptide bonds', *J. Am. Chem. Soc.* **1955**, *77*, 1067.

[250] Y.G. Ryu, S.I. Pyun, C.S. Kim, D.R. Shin, 'A study on the formation of surface functional groups during oxygen reduction on a platinum-dispersed carbon electrode in an 85% H_3PO_4 solution at elevated temperature', *Carbon* **1998**, *36*, 293.

[251] B. Donnet, 'The chemical reactivity of carbons', *Carbon* **1968**, *6*, 161.

[252] V.A. Garten, D.E. Weiss, 'A new quinone-hydroquionone character of activated carbon and carbon black', *Aust. J. Chem.* **1957**, *10*, 309.

[253] V.A. Garten, D.E. Weiss, 'A new interpretation of the acidic and basic structures in carbons', *Aust. J. Chem.* **1955**, *8*, 68.

[254] K. Kinoshita, 'Carbon, electrochemical and physicochemical properties', John Wiley & Sons, New York, 1998.

[255] N.N. Nemerovets, V.F. Surovikin, S.V. Orekhov, G.V. Sazhin, N.G. Saovnichuk, 'Formation of surface oxygen-containing groupings in the oxidation of carbon black', *Solid Fuel Chemistry (Engl. Transl. of Khim. Tverd. Topl.)* **1980**, *14*, 104.

[256] L.P. Gilyazetdinov, V.I. Romanova, A.S. Lutokhina, É.I. Tsygankova, I.M. Safronova, 'Oxidative surface modification of carbon blacks', *J. Appl. Chem. USSR (Engl. Transl. of Zhurnal Prikladnoi Khimii)* **1976**, *49*, 420.

[257] M. Acedo-Ramos, V. Gomez-Serrano, C. Valenzuela-Calahorro, A.J. Lopez-Peinado, 'Oxidation of activated carbon in liquid phase by FTIR', *Spectrosc. Lett.* **1993**, *26*, 1117.

[258] A.V. Melezhik, L.V. Makarova, A.A. Chuiko, 'The reaction of graphite with peroxodisulphuric acid', *Russ. J. Inorg. Chem. (Engl. Transl. Zhurnal Neorganicheskoi Khimii)* **1989**, *34*, 196.

[259] A. Banerjee, B.K. Mazumdar, A. Lahiri, 'Action of permanganate on coal', *Nature* **1962**, *193*, 267.

[260] A. Voet, A.C. Teter, 'Oxidations and reductions at the carbon black particle surface', *Amer. Ink Maker* **1960**, *38*, 44.

[261] Y.P. Wu, C. Jiang, C. Wan, R. Holze, 'Effects of pretreatment of natural graphite by oxidative solutions on its electrochemical performance as anode material', *Electrochim. Acta* **2003**, *48*, 867.

[262] B. Lindberg, J. Paju, 'Studies on quinones and hydroquinones', *Svensk Kem. Tidskr.* **1953**, *65*, 9.

[263] M.L. Studebaker, E.W.D. Huffman, A.S. Wolfe, L.G. Nabors, 'Oxygen-containing groups on the surface of carbon black', *Ind. Eng. Chem.* **1966**, *48*, 162.

[264] G. Jander, K.F. Jahr, 'Massanalye', W. de Gruyter, Berlin, p. 172-176, 1989.

[265] R.J. Bowling, R.T. Packard, R.L. McCreery, 'Raman spectroscopy of carbon electrodes', *J. Am. Chem. Soc.* **1989**, *111*, 434.

[266] R.L. McCreery, 'Carbon electrodes: structural effects on electron transfer kinetics', *J. Electroanal. Chem.* **1990**, *17*, 221.

[267] R.C. Engstrom, 'Electrochemical pretreatment of glassy carbon electrodes', *Anal. Chem.* **1982**, *54*, 2310.

[268] K.F. Blurton, 'An electrochemical investigation of graphite surfaces', *Electrochim. Acta* **1973**, *18*, 869.

[269] V.A. Bogdanovskaya, M.R. Tarasevich, M.L. Khidekel, G.I. Kozub, S.B. Orlov, 'Electrochemical and Electrocatalytic characteristics of chemically modified carbon material', *Soviet Electrochemistry (Engl. Transl. of Élektrokhimiya)* **1984**, *20*, 153.

[270] J. Schreurs, E. Barendrecht, 'Surface-modified electrodes', *Recl. Trav. Chim. Pays-Bas.* **1984**, *103*, 205.

[271] T. Bechtold, E. Burtscher, A. Turcanu, 'Anthraquinones as mediators for the indirect cathodic reduction of dispersed organic dyestuffs', *J. Electroanal. Chem.* **1999**, *465*, 80.

[272] K.S. Tschyong, F.I. Sadow, 'Studium des Reduktionsvermögens und der Beständigkeit alkalischer Natriumborhydridlösungen unter den Bedingungen der Küpenfärberei', *Textil Praxis* **1969**, *24*, 454.

[273] A.P. Brown, F.C. Anson, 'Cyclic and differential pulse behaviour of reactants confined to the electrode surface', *Anal. Chem.* **1977**, *49*, 2589.

[274] M. Sharp, 'A possible orientation effect in redox reactions of molecules which are chemically bound to electrode surfaces', *Electrochim. Acta* **1978**, *23*, 287.

[275] P. Rys, O.A. Stamm, 'Zur Reaktion von Reaktivfarbstoffen mit Cellulose. V. Untersuchungen von Nebenprodukten bei der Applikation von Reaktivfarbstoffen', *Helv. Chim. Acta* **1966**, *49*, 2288.

[276] H. Zollinger, 'Color Chemistry', VCH, Weinheim, p. 136 ff and p. 170, 1987.

[277] W. Marte (Tex-A-Tec AG, Wattwil, Switzerland), personal communication, 2002.

[278] H. Pütter, C. Merk (BASF, Ludwigshafen, Germany), personal communication, 2001.

[279] X. Jin (ICB, ETH Zurich), personal communication, 2002.

[280] X. Jin, 'Studies on the reaction between indigo and leuco indigo', Internal report, ICB, ETH Zurich, **2002**.

[281] D. Crettenand, 'Verfahrens- und reaktionstechnische Analyse neuer, biokompatibler, elektrochemischer Verküpungsverfahren im Fest- und Wirbelbettreaktor', Diploma thesis, ICB, ETH Zurich, 2002.

[282] H. Essl, 'Jeans - das blaue Phänome Teil 2', *Textilveredlung* **2000**, *35*, 23.

[283] H. Essl, 'Jeans - das blaue Phänome Teil 3', *Textilveredlung* **2000**, *35*, 27.

List of publications and awards

The following list summarises publications which are based on this thesis. The pertinent chapters which are the source of the publications are given in brackets.

Publications

- A. Roessler, D. Crettenand, O. Dossenbach, W. Marte, P. Rys, 'Direct electrochemical reduction of indigo', *Electrochim. Acta* **2002**, *47*, 1989. (*chapter 3*)
- A. Roessler, O. Dossenbach, W. Marte, P. Rys, 'Direct electrochemical reduction of indigo: Process optimization and scale-up in a flow cell', *J. Appl. Electrochem.* **2002**, *32*, 647. (*chapter 4*)
- A. Roessler, O. Dossenbach, W. Marte, P. Rys, 'Electrocatalytic hydrogenation of vat dyes', *Dyes and Pigments* **2002**, *54*, 141. (*chapter 6*)
- A. Roessler, O. Dossenbach, P. Rys, 'Electrocatalytic hydrogenation of indigo: Process optimization and scale-up in a flow cell', *J. Electrochem. Soc.* **2002**, *150*, D1. (*chapter 7*)
- A. Roessler, D. Crettenand, O. Dossenbach, P. Rys, 'Electrochemical reduction of indigo in fixed and fluidized beds of graphite granules', *J. Appl. Electrochem.* **2003** (in press). (*chapter 10*)
- A. Roessler, P. Rys, 'Electrochemical methods in the application of vat dyes', *Adv. Colour Sci. Technol.* **2003**, *6*, (in press).
- A. Roessler, X. Jin, 'State of the art technologies and new electrochemical methods for the reduction of vat dyes', *Dyes and Pigments* **2003** (in press).

Varia

- A. Roessler, O. Dossenbach, U. Meyer, W. Marte, P. Rys, 'Direct electrochemical reduction of indigo', *Chimia* **2001**, *55*, 879. (*chapter 3*)

- B. Brauckmann, A. Roessler, O. Dossenbach, P. Rys, 'Färbung von Blue Jeans - ein Umweltproblem?', *Labor Flash* **2002**, *31*, 10.
- B. Brauckmann, A. Roessler, O. Dossenbach, P. Rys, 'Die Farbe der Blue Jeans', *Laborscope* **2003**, *30*, 4.
- B. Brauckmann, A. Roessler, O. Dossenbach, P. Rys, 'Inwieweit ist die Färbung von Blue Jeans mit Umweltproblemen behaftet?', *Chemie Plus* **2003**, *12*, 3.

Patents

- A. Roessler, W. Marte, O. Dossenbach, 'Verfahren und Apparatur zur elektrokatalytischen Hydrierung von Küpen- und Schwefelfarbstoffen', Swiss Patent Pending 2001, 2322/01.
- A. Roessler, P. Rys, D. Crettenand, 'Verfahren zur Reduktion von organischen Verbindungen mittels elektrochemisch beladener Kohle', Swiss Patent Pending 2002, 1299/02.
- A. Roessler, W. Marte, P. Rys, 'Verfahren zur elektrochemischen Reduktion von Küpen- und Schwefelfarbstoffen', Swiss Patent Pending 2002, 1863/02.

Conference Contributions

- <u>A. Roessler</u>, O. Dossenbach, P. Rys, 'Direct electrochemical reduction of indigo', 15th International Forum on Applied Electrochemistry, 11 - 15 November 2001, Sheraton Sand Key, Clearwater Beach, Florida, USA (poster).
- A. Roessler, 'Direct electrochemical reduction of indigo', COLORCHEM' 02, 9th International Conference on pigments and dyes, 12 - 16 Mai 2002, Harmony Club Hotel Spindleruv Mlyn, Czech Republic (poster).
- A. Roessler, 'Electrocatalytic hydrogenation of vat dyes', COLORCHEM' 02, 9th International Conference on pigments and dyes, 12 - 16 Mai 2002, Harmony Club Hotel Spindleruv Mlyn, Czech Republic (poster).
- A. Roessler, <u>P. Rys</u>, 'New electrochemical methods in the application of vat dyes', COLORCHEM' 02, 9th International Conference on pigments and

dyes, 12 - 16 Mai 2002, Harmony Club Hotel Spindleruv Mlyn, Czech Republic (oral presentation).

- A. Roessler, O. Dossenbach, P. Rys, 'Electrocatalytic hydrogenation of vat dyes', International Society of Electrochemistry, 53rd Annual Meeting, Düsseldorf, Germany, 15 - 20 September 2002 (oral presentation).

- A. Roessler, O. Dossenbach, P. Rys, 'Electrocatalytic hydrogenation of vat dyes', ELECTROCHEM 2002, University of Central Lancashire, Preston, UK, 02 - 05 September 2002 (oral presentation).

Awards

- COLORCHEM'02 Clariant innovation award to acknowledge the best scientific achievement presented at COLORCHEM'02, 9th International Conference on pigments and dyes, 12 - 16 Mai 2002, Harmony Club Hotel Spindleruv Mlyn, Czech Republic.

Curriculum vitae

name: Albert Roessler

date and place of birth: 23.05.1975 at Innsbruck, Austria

Citizen of: Austria

Education:

- 1981 - 1985   primary school in Innsbruck, Austria
- 1985 - 1990   secondary academic school, Innsbruck, Austria
- 1990 - 1995   secondary college of chemical engineering (HTL), Wels, Austria
- 1996 - 2000   diploma education in Chemical Engineering at the Swiss Federal Institute of Technology (ETH), Zurich
- 2000   diploma thesis in the field of Direct Methanol Fuel Cells at the Royal Institute of Technology, Stockholm
- 2000-2003   PhD thesis at the Institute for Chemical and Bioengineering, ETH Zurich, in the research group of Prof. P. Rys

Experience:

- 08/1992   Freudenthaler Umwelttechnik, Inzing, Austria
- 08/1993, 08-09/1994, 08-12/1995, 07-08/1997   assistant at the Institute of Hygiene, University Innsbruck, Austria
- 07-08/1998   Laboratory of the Department for Environmental Protection, Government of Tyrol, Innsbruck, Austria

- 01-07/1999   assistant at the Institute of Process Engineering, ETH Zurich , particle technology laboratory, Prof. S.E. Pratsinis
- 08/1999   R&D department for Materials Science, Swarovski & Co., Wattens, Austria

Teaching:

- WS 2001/02, WS 2002/03   Übungen, Allgemeine Chemie, Teil Anorganische Chemie I, Prof. R. Nesper
- SS 2001, SS 2002   Übungen, Allgemeine Chemie, Teil Anorganische Chemie II, Prof. R. Nesper, Prof. H. Grützmacher
- WS 2000/01   Übungen, Chemieingenieurwesen I, Prof. M. Morbidelli, O. Dossenbach, O.M. Kut
- SS 2002, SS 2003   Übungen, Chemieingenieurwesen, Prof. A. Baiker
- WS 2000, SS 2001, SS 2002   Praktikum Technische Chemie, Prof. G. Consiglio, Prof. R. Prins, Prof. P. Rys
- partly   Chemieingenieurthermodynamik and Strömungslehre und Wärmetausch, O. Dossenbach